Exploring biomarkars and predictive factors for outcomes in advanced pulmonary disease

Bodén, Embla

2024

Document Version:
Publisher's PDF, also known as Version of record

Exploring biomarkers and predictive factors
for outcomes in advanced pulmonary disease

Exploring biomarkers and predictive factors for outcomes in advanced pulmonary disease

Embla Bodén, MD

LUND
UNIVERSITY

DOCTORAL DISSERTATION

Doctoral dissertation for the degree of Doctor of Philosophy (PhD) at the Faculty of Medicine at Lund University to be publicly defended on 19th of December 2024 at 09.00 in Segerfalksalen, BMC A, Lund.

Faculty opponent
Assoc. Prof. **Dr. Irene Bello**, MD, PhD, Hospital Clínic de Barcelona

Organization: LUND UNIVERSITY

Document name: Doctoral Dissertation **Date of issue:**

Author(s): Embla Bodén, MD **Sponsoring organization:**

Title and subtitle: Exploring biomarkers and predictive factors for outcomes in advanced pulmonary disease

Abstract:

Pulmonary diseases including but not limited to lung cancer, chronic obstructive pulmonary disease (COPD), cystic fibrosis (CF) and pulmonary fibrosis (PF) are common causes of death, with acute hospital admissions due to respiratory pathology having increased by more than three-fold compared to other causes of hospitalization within the last decade. Treatment options are scarce, and survival rates are low, and identification of biomarkers for primary lung cancer and factors which influence mortality and morbidity following lung transplantation (LTx) are arguably some of the most central problems to tackle in the aims of prolonging survival for patients with advanced pulmonary disease.

The aims of the research included in this thesis were to identify biomarkers which can potentially aid in the diagnosis and monitoring of lung cancer, as well as tentatively predict prognosis for the affected patients. Furthermore, this work aims to clarify how different factors such as infectious diseases caused by fungi and severe acute respiratory syndrome coronavirus 2 (SARS-CoV-2) affect survival and the development of chronic lung allograft dysfunction (CLAD) after LTx.

The methods used in the five papers included in this thesis include collection of blood and exhaled breath particles (EBP) from patients with primary non-small cell lung cancer (NSCLC) and coronavirus disease 2019 (COVID-19), proteomic analysis of blood and EBP by proximity extension assay (PEA) and mass spectrometry (MS), and chart reviews of Scandinavian lung transplant recipients with fungal colonization or COVID-19.

The results of papers I and II revealed a number of proteins in blood and EBP respectively to be potential biomarkers for the diagnosis and prognosis of primary NSCLC. In paper III it was shown that a combination of proteins and analysis of protein concentration in exhaled air can likely serve as a biomarker panel of sorts to distinguish between patients with and without polymerase chain reaction (PCR) verified COVID-19. Paper IV suggested that fungal colonization following LTx does not negatively impact outcomes, irrespective of fungal genus, and paper V showed significantly decreased mortality after COVID-19 for vaccinated LTx recipients, as well as higher mortality rates for patients infected in early stages of the COVID-19 pandemic.

The work included in this thesis demonstrates the feasibility of using less invasive methods such as liquid biopsies in the form of blood, and EBP to explore potential biomarkers for advanced pulmonary disease. It also suggests several promising proteins for further exploration in this matter. Furthermore, we shed light on the actual impact of fungal colonization in LTx recipients, showing that this may not be a major cause for concern, as previously believed. Finally, we highlight the importance of vaccination against COVID-19 in LTx recipients and show the success of two different sociopolitical approaches taken during the pandemic.

Key words: lung cancer; lung transplantation; biomarkers; prognosis; chronic rejection; mortality

Language: English, Swedish **Number of pages**: 101

ISSN and key title: 1652-8220

ISBN: 978-91-8021-653-1

Recipient's notes Price Security classification

Exploring biomarkers and predictive factors for outcomes in advanced pulmonary disease

Embla Bodén, MD

Supervisor: Professor Dr. Sandra Lindstedt, MD, PhD

Co-supervisor: Dr. Franziska Olm, PhD

Co-supervisor: Dr. Jesper Magnusson, MD, PhD

Faculty of Medicine
Department of Clinical Sciences, Lund

ISBN 978-91-8021-653-1
ISSN 1652-8220

Printed in Sweden by Media-Tryck, Lund University
Lund 2024

Dedicated to women in science

Table of Contents

Abstract

Pulmonary diseases including but not limited to lung cancer, chronic obstructive pulmonary disease (COPD), cystic fibrosis (CF) and pulmonary fibrosis (PF) are common causes of death, with acute hospital admissions due to respiratory pathology having increased by more than three-fold compared to other causes of hospitalization within the last decade. Treatment options are scarce, and survival rates are low, and identification of biomarkers for primary lung cancer and factors which influence mortality and morbidity following lung transplantation (LTx) are arguably some of the most central problems to tackle in the aims of prolonging survival for patients with advanced pulmonary disease.

The aims of the research included in this thesis were to identify biomarkers which can potentially aid in the diagnosis and monitoring of lung cancer, as well as tentatively predict prognosis for the affected patients. Furthermore, this work aims to clarify how different factors such as infectious diseases caused by fungi and severe acute respiratory syndrome coronavirus 2 (SARS-CoV-2) affect survival and the development of chronic lung allograft dysfunction (CLAD) after LTx.

The methods used in the five papers included in this thesis include collection of blood and exhaled breath particles (EBP) from patients with primary non-small cell lung cancer (NSCLC) and coronavirus disease 2019 (COVID-19), proteomic analysis of blood and EBP by proximity extension assay (PEA) and mass spectrometry (MS), and chart reviews of Scandinavian lung transplant recipients with fungal colonization or COVID-19.

The results of papers I and II revealed several proteins in blood and EBP respectively to be potential biomarkers for the diagnosis and prognosis of primary NSCLC. In paper III it was shown that a combination of proteins and analysis of protein concentration in exhaled air can likely serve as a biomarker panel of sorts to distinguish between patients with and without polymerase chain reaction (PCR) verified COVID-19. Paper IV suggested that fungal colonization following LTx does not negatively impact outcomes, irrespective of fungal genus, and paper V showed significantly decreased mortality after COVID-19 for vaccinated LTx recipients, as well as higher mortality rates for patients infected in early stages of the COVID-19 pandemic.

The work included in this thesis demonstrates the feasibility of using less invasive methods such as liquid biopsies in the form of blood, and EBP to explore potential biomarkers for advanced pulmonary disease. It also suggests several promising proteins for further exploration in this matter. Furthermore, we shed light on the actual impact of fungal colonization in LTx recipients, showing that this may not be a major cause for concern, as previously believed. Finally, we highlight the importance of vaccination against COVID-19 in LTx recipients and show the success of two different sociopolitical approaches taken during the pandemic.

Populärvetenskaplig sammanfattning

Lungan är ett komplext organ, som skiljer sig från de flesta andra organ i kroppen genom att de står i direktkontakt med omgivningen genom andningen. Detta kan introducera skadliga ämnen och mikroorganismer som kan orsaka infektioner och skada i lungorna. Utöver det finns det även flera allvarliga lungsjukdomar som på sikt kan vara dödliga trots existerande behandlingsalternativ. Exempel på sådana sjukdomar innefattar lungcancer, som kan behandlas både medicinskt och kirurgiskt, samt kroniskt obstruktiv lungsjukdom (KOL) och cystisk fibros (CF), med flera, där det enda slutgiltiga behandlingsalternativet är lungtransplantation (LTx). Prognosen för långtidsöverlevnad efter både lungcancer och LTx är tyvärr dålig, varför det är viktigt att undersöka alternativa metoder för diagnosticering och behandling, samt vilka faktorer som kan tänkas påverka utfallet för dessa patienter.

Metoderna som i dagsläget används för att kliniskt diagnosticera och följa lungcancer är mer eller mindre invasiva och medför risk för skada och obehag hos patienterna. Det är därför av stor vikt att identifiera alternativa tillvägagångssätt för att upptäcka och uppskatta prognos för lungcancer, som till exempel genom minimalt invasiva blodprover eller icke-invasiva prover på utandningsluften. Genom att undersöka kompositionen av proteiner i sådana prover kan man utforska om det går att identifiera några nya så kallade biomarkörer som skulle kunna vara till nytta för tidigare detektion och/eller monitorering av sjukdomsförloppet vid primär lungcancer eller andra luftvägssjukdomar, till exempel coronavirussjukdom 2019 (COVID-19).

Liknande problematik finns inom fältet för LTx, med jämförelsevis mycket kort överlevnad hos dessa patienter i förhållande till medelöverlevnaden efter andra former av organtransplantation. De vanligaste komplikationerna efter LTx är olika former av akut och kronisk rejektion, infektioner, njursvikt samt utveckling av cancersjukdom. Särskilt problemen kronisk rejektion (CLAD) och infektiösa komplikationer är oerhört aktuella inom detta forskningsområde och det hade varit enormt fördelaktigt för både patienter och samhället i stort att lyckas öka kunskapen kring hur dessa företeelser påverkar utfallet efter LTx. Det är dessa ovan nämnda problem som denna avhandling syftar till att vidga kunskapen inom.

Delarbete I

I delarbete I utforskar vi användandet av blod som substrat för identifiering av nya potentiella biomarkörer. Genom insamling av blod från patienter med primär icke-småcellig lungcancer (NSCLC) vid tre separata tillfällen, ett före operation och två efter, kunde dynamiken i hur koncentrationen av olika proteiner i blodet förändrades analyseras. Vi fann här att proteinuttrycket av de två proteinerna ”major histocompatibility complex class 1 polypeptide-related sequence A/B” (MIC-A/B)

och ”tumor necrosis factor ligand superfamily 6” (FASLG) var signifikant stigande efter att man opererat bort patienternas lungcancer jämfört med innan operationen. Detta antyder att operationen har varit lyckad och att cancercellerna som innan operationen eventuellt undertryckte produktionen av dessa proteiner är borta. Dessutom visade sig proteinuttrycket av FASLG att vara signifikant lägre bland patienter som senare fick återfall i sin sjukdom eller gick bort. Detta stödjer det potentiella användandet av just proteinet FASLG som en biomarkör för att förutsäga prognosen för enskilda patienter med NSCLC. Vi såg också att proteinet ”hepatocyte growth factor” (HGF) hade en nedåtgående trend efter operationen, detta var dock inte signifikant. Resultaten validerades med hjälp av större studier på liknande material som finns att tillgå i ett genbibliotek online.

Delarbete II

I det andra arbetet fortsatte vi sökandet efter biomarkörer för NSCLC, men denna gång i utandningsluften. Här samlade vi in partiklar i utandningsluften (EBP) och mätte partikelflödet (PFR) hos patienter med och utan NSCLC för att sedan kunna jämföra grupperna. Resultaten visade att PFR hos patienter med NSCLC var signifikant högre än hos lungfriska kontrollpatienter. Analys av proteinuttrycket i EBP visade signifikant högre preoperativ koncentration av fem proteiner hos patienter med NSCLC jämfört med kontrollpatienter. Efter operationen visade sig tre av de fem proteinerna, ”microfibrillar-associated protein 5” (MFAP5), ”phospholipid transfer protein” (PLTP) och ”mesenchymal epithelial transition” (MET) ha en sjunkande trend hos cancerpatienterna och uttrycket var inte längre signifikant högre bland cancerpatienterna jämfört med kontrollpatienterna. Detta kan tyda på radikalt borttagande av cancern som tidigare ökade produktionen av dessa proteiner. För att validera resultaten analyserades även uttrycket av proteinet MET i blod och vi fann en tydlig korrelation mellan proteinuttrycket av just MET i EBP och blod, vilket styrker resultaten. Ytterligare validerades resultaten genom användning av större datasamlingar i en digital genbank.

Delarbete III

I delarbete III undersöker vi kompositionen av EBP hos patienter som har varit inlagda med verifierad coronavirussjukdom 2019 (COVID-19) med hjälp av masspektrometri och jämför denna med friska kontrollpatienter samt patienter som har luftvägssymptom men utan verifierad COVID-19. Här såg vi en markant ökning i mängden producerade partiklar per volym utandad luft (PEV) hos sjuka patienter jämfört med friska kontroller. Proteinuttrycket visade sig också skilja sig signifikant mellan de tre grupperna och proteiner som har sin verkan i inflammatoriska processer var uppreglerade bland de COVID-19 positiva patienterna. Med hjälp av

maskininlärning skapades en modell som med 92% säkerhet kunde bedöma om en patient var positiv för COVID-19 eller ej baserat på proteinuttrycket i EBP.

Delarbete IV

I detta fjärde delarbete valde vi att utforska hur kolonisering och infektion med svamp i luftvägarna påverkar överlevnaden och förekomsten av CLAD hos lungtransplanterade patienter. Här kunde vi visa att enbart kolonisering utan invasiv infektion inte påverkade vare sig överlevnaden eller utvecklingen av CLAD hos dessa patienter, oavsett om det gällde kolonisering innan eller efter LTx. Vi såg dock att den underliggande sjukdomen KOL visade sig vara en riskfaktor för utvecklandet av CLAD, samt att sjukdomen CF agerade som en skyddande faktor för död bland patienter med postoperativ svampkolonisering. Dessa fynd beror sannolikt till stor del på dessa patientgruppers underliggande hälsotillstånd och ålder. Vidare såg vi att invasiva svampinfektioner (IFI) utgjorde en signifikant ökad risk för patienterna att utveckla CLAD jämfört med enbart kolonisering, samt att saminfektion med bakterier och/eller virus vid tidpunkten för svampkolonisering inte påverkade något av utfallen.

Delarbete V

I det femte och sista delarbetet som ingår i denna avhandling fortsatte vi utforska hur infektionssjukdomar påverkar utfallet efter LTx. I och med den nyligen genomgångna pandemin fann vi det intressant att studera just COVID-19. Vi samlade in data från patientjournaler tillhörande lungtransplanterade patienter som alla hade genomgått minst en episod av COVID-19 vid ett av de tre universitetssjukhusen Lund (Skånes universitetssjukhus), Göteborg (Sahlgrenska universitetssjukhuset) eller Köpenhamn (Rigshospitalet). Resultaten visade att vaccination med minst två doser av ett vaccin mot COVID-19 signifikant minskar risken för dödlighet bland lungtransplanterade patienter som drabbas av sjukdomen. Vi såg även att infektion med den första varianten av viruset ”*Wuhan*” medförde en större risk för död jämfört med infektioner orsakade av den senaste varianten ”*Omicron*”. Gällande de substantiella skillnaderna i hur grannländerna Sverige och Danmark hanterade pandemin rent sociopolitiskt verkar detta inte ha påverkat utfallet för lungtransplanterade patienter, då ingen ökad risk för död eller CLAD sågs för något av de två länderna.

List of publications

Paper I

Bodén E, Andréasson J, Hirdman G, Malmsjö M, Lindstedt S. Quantitative proteomics indicate radical removal of non-small cell lung cancer and predict outcome.

Biomedicines. 2022 Oct 28;10(11):2738.

Paper II

Andréasson J, **Bodén E**, Fakhro M, von Wachter C, Olm F, Malmsjö M, Hallgren O, Lindstedt S. Exhaled phospholipid transfer protein and hepatocyte growth factor receptor in lung adenocarcinoma.

Respir Res. 2022 Dec 21;23(1):369.

Paper III

Hirdman G, **Bodén E**, Kjellström S, Fraenkel C, Olm F, Hallgren O, Lindstedt S. Proteomic characteristics and diagnostic potential of exhaled breath particles in patients with COVID-19.

Clin Proteomics. 2023 Mar 27;20(1):13.

Paper IV

Bodén E, Sveréus F, Niroomand A, Akbarshahi H, Ingemansson R, Larsson H, Lindstedt S, Olm F. Fungal colonization before or after lung transplantation has no negative impact on death or the development of chronic lung allograft dysfunction.

Manuscript.

Paper V

Bodén E, Perch M, Hertz Liebermann R, Søfteland J M, Magnusson J‡, Lindstedt S‡. Impact of COVID-19 after lung transplantation: a retrospective multi-center study on the influence of differing political and social approaches between two Scandinavian countries. ‡**Shared last authorship**.
Manuscript.

Abbreviations

A1AD	Alpha-1 antitrypsin deficiency
ACE2	Angiotensin-converting enzyme 2
BALF	Bronchoalveolar lavage fluid
BOS	Bronchiolitis obliterans syndrome
CCI	Charlson Comorbidity Index
CF	Cystic fibrosis
CI	Confidence interval
CLAD	Chronic lung allograft dysfunction
CO_2	Carbon dioxide
COPD	Chronic obstructive pulmonary disease
COVID-19	Coronavirus disease 2019
COV-NEG	Covid negative patient
COV-POS	Covid positive patient
CT	Computed tomography
DNA	Deoxyribonucleic acid
DPCC	Dipalmitoyl phosphatidylcholine
EBC	Exhaled breath condensate
EBP	Exhaled breath particles
ELISA	Enzyme-linked immunosorbent assay
EORTC	European Organization for Research and Treatment of Cancer
FDA	Food and Drug Administration
FDR	False discovery rate
FEV_1	Forced expiratory volume in one second
FVC	Forced vital capacity
GvHD	Graft versus host disease
H^+	Hydrogen ion
HCO	Healthy control patient
HCO_3^-	Bicarbonate
HEPA	High efficiency particulate air
H_2O	Water, dihydrogen monoxide
HPLC-MS/MS	High-performance liquid chromatography-mass spectrometry
HR	Hazard ratio
IASLC	International Association for the Study of Lung Cancer
IFI	Invasive fungal infection
IQR	Interquartile range
ISHLT	International Society for Heart and Lung Transplantation
KTx	Kidney transplantation
LFQ	Label free quantification
LOD	Limit of detection
LTx	Lung transplantation
LUAD	Lung adenocarcinoma

MET	Mesenchymal epithelial transition
MSGERC	Mycoses Study Group Education and Research Consortium
MV	Minute volume
n	Number of
NPI	Normalized probe intensity
NPX	Normalized protein expression
ns	Not significant
NSCLC	Non-small cell lung cancer
NYHA	New York Heart Association
O_2	Oxygen
OPC	Optical particle counter
PCR	Polymerase chain reaction
PET	Positron emission tomography
PEV	Particles per exhaled volume of air
PExA	Particles in exhaled air
PF	Pulmonary fibrosis
PFR	Particle flow rate
PFS	Progression-free survival
PFT	Pulmonary function test
PGD	Primary graft dysfunction
PH	Pulmonary hypertension
pH	Potential of hydrogen
PSW	propensity score weighting
pTNM	Pathological TNM
RAS	Restrictive allograft syndrome
RNA	Ribonucleic acid
RTLF	Respiratory tract lining fluid
SARS-CoV-2	Severe acute respiratory syndrome coronavirus 2
SCC	Squamous cell carcinoma
SOT	Solid organ transplantation
Spp.	Species
SUS	Skåne University Hospital
TNM	Tumor, Node, Metastasis
VOC	Volatile organic compounds
WHO	World Health Organization

Introduction

The respiratory system

The respiratory system is in a unique position together with the gastrointestinal tract, by standing in direct contact with the surrounding environment (1). With every breath, air is inhaled, heated, humidified and filtered from external particles and pathogens (2). As the air reaches the alveoli in the most distal parts of the airways, the gas exchange takes place across the epithelial-endothelial interface, and oxygen (O_2) enters the bloodstream while carbon dioxide (CO_2) exits it. In spite of mechanical barriers and several layers of immune mechanisms, pathogens manage to make their way into the airways on a daily basis, and sometimes these can cause pathological reactions in the host, leading to damaged lung tissue (3).

Architecture and physiology

The respiratory system is made up of the proximal and the distal airways, of which the distal airways are located within the thoracic cavity. The proximal airways are located outside of the thoracic cavity and are made up of the oral and nasal cavities, the pharynx, and the larynx, while the distal airways consist of the trachea, the bronchi, the bronchioles, the alveolar ducts, and the alveoli (Figure 1) (4). The respiratory tract is divided into 23 generations, as described by the Weibel classification in 1963. At each generation the airway is divided into two smaller airways, starting at generation zero, which is the trachea, and ending in the 23rd generation which is the alveolar sacs (5). The first approximately 15 generations, ending in the terminal bronchioles, make up the conducting zone of the airways, transporting, heating, and humidifying the air inhaled. This part of the airways is also known as the dead space, as no gas exchange takes place here. Generations 16 – 19 are sometimes referred to as the transitional zone, with the occasional alveolus along the walls of the respiratory bronchioles. The transitional zone merges with the respiratory and acinar zones, where alveolar ducts are completely covered by alveoli (generations 20 – 23). This is where the gas exchange takes place and what makes up the bulk of the pulmonary tissue (6). Alveoli are made up of different types of cells, the majority of which are type I pneumocytes which are squamous cells forming an interface with the microvasculature of the lung tissue, ideal for gas exchange. A small fraction of the alveolar surface is made up of type II

pneumocytes, which are cuboidal cells, responsible for the production of surfactant, and are able to self-renew and differentiate into type I pneumocytes (7). Other cells residing within the respiratory tract include basal cells, club cells, ciliated cells, goblet cells, and more. Basal cells are the stem cells of the airways, facilitating epithelial regeneration, while club cells secrete anti-inflammatory proteins and goblet cells secrete mucous. Throughout the respiratory tract, the ciliated cells are responsible for the mucociliary clearance, acting as miniscule brooms, sweeping unwanted microbes and particles in a peripheral direction to be expelled from the lungs through coughing or swallowing (Figure 1) (8).

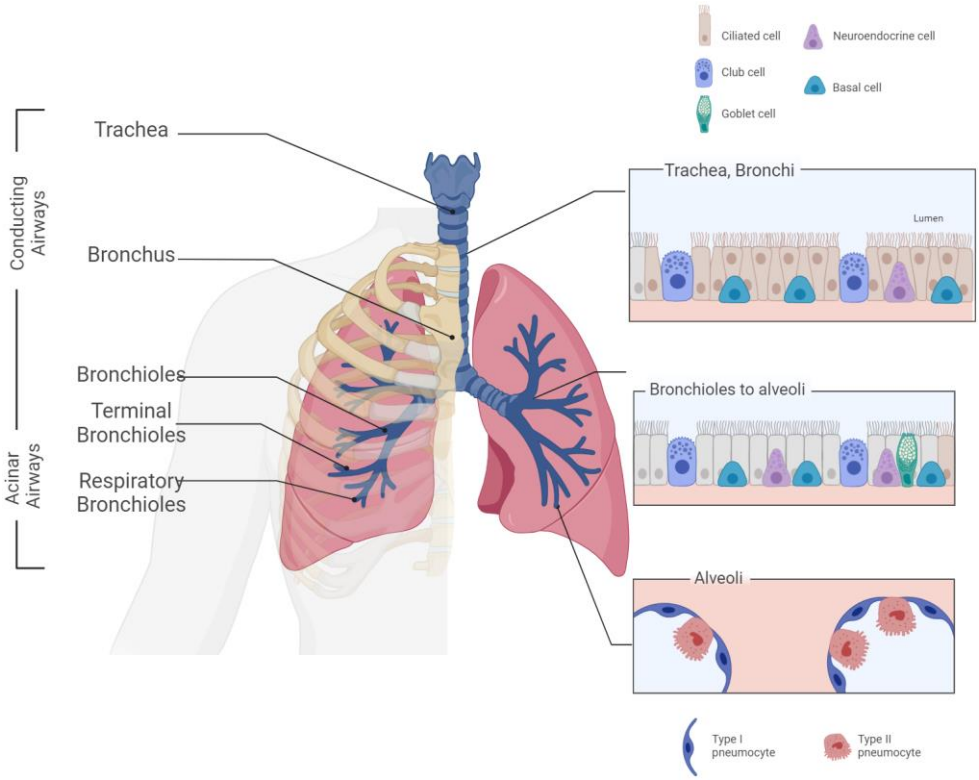

Figure 1: Macroscopic and microscopic anatomy of the airways. Anatomic overview of the proximal and distal airways, including major anatomical landmarks and cellular types of the different parts of the respiratory tract. Figure created in BioRender.com and used with permission.

Covering the inside of the airways is the respiratory tract lining fluid (RTLF), a layer of mucous, creating a protective barrier between the airway epithelial cells and the inhaled air. The RTLF consists of water, ions, macromolecules such as mucins, proteoglycans and lipids and surfactant (9). Surfactant is created by the type II pneumocytes and is an important component of the RTLF as it is responsible for lowering the surface tension in the airways, minimizing the force needed for each inhaled breath, and preventing the collapse of the alveoli upon exhalation (10, 11).

Surfactant is made up of approximately 90% lipids, the most abundant one in mammals being the phospholipid dipalmitoyl phosphatidylcholine (DPCC) (11).

Zooming out, each lung consists of lobes and anatomical segments, supplied with air from the terminal branches of the lobar bronchi, and blood from the pulmonary arteries (12). The right lung, being slightly larger than the left lung, consists of ten segments and three lobes (upper, middle, and lower) while the left lung consists of eight to nine segments and two lobes (upper and lower) (4, 13). Surrounding the lungs is the visceral pleura, which also creates the oblique and horizontal fissures separating the lobes of the lungs by invaginating upon itself. The visceral pleura transitions to the parietal pleura at the apex of the lungs, which then runs along the inside of the chest wall (14). The two pleural sheets create a small airtight space containing the serous pleural liquid, which lubricates and facilitates the movement of the lungs without friction (15). Further protecting the structures inside the chest cavity are 12 pairs of ribs, originating from the thoracic vertebrae and ending in the costal cartilage, adhering to the sternum (16). The diaphragm is the muscle that forms the convex base of the thoracic cavity and it is attached to the xiphoid portion of the sternum, the lower six ribs and the lumbar spine, separating the thorax from the abdomen and aiding the breathing process by expanding and compressing the lungs (13, 17-19).

Pulmonary function

Normal breathing is powered by several muscles, the primary one being the diaphragm. Contraction of the diaphragm generates negative intrathoracic pressure, drawing air into the lungs where gas exchange takes place. The lung function of a person depends on several factors, including sex, age, height and comorbidities. Lung capacity can be evaluated by pulmonary function tests (PFT) such as spirometry, which yields several measurements, amongst which are forced expiratory volume in one second (FEV_1), forced vital capacity (FVC), and FEV_1/FVC ratio (20). FEV1 measures how many liters of air a person can exhale forcefully in one second after full inhalation, while the FVC measures a person's total capacity for forced exhalation after a full inhalation, independent time (Figure 2). The ratio between the two reflects whether there are any air flow limitations, as is the case in patients with for example chronic obstructive pulmonary disease (COPD) (20, 21).

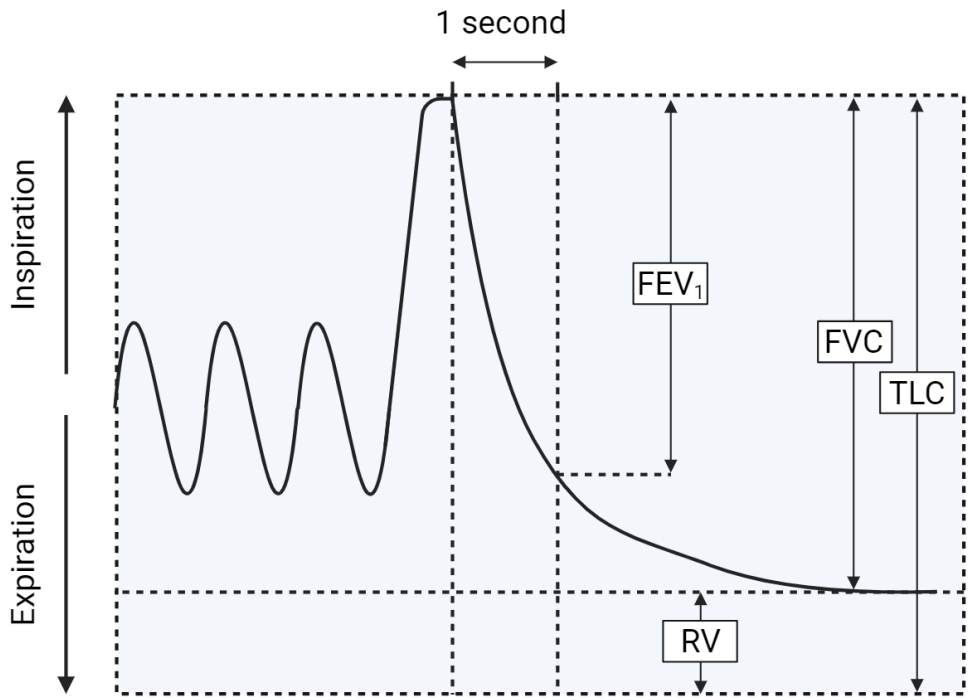

Figure 2: Example of spirometry maneuver. Diagram depicting a spirometry maneuver and different lung volumes. Figure created in BioRender.com. *FEV_1: forced expiratory volume in one second, FVC: forced vital capacity, TLC: total lung capacity, RV: residual volume.*

Cardiopulmonary circulation

The circulation is powered by the heart, acting as a pump to perfuse all organs with oxygenated blood. The pulmonary circulation is a low-pressure system, containing approximately 20% of the total blood volume at each point in time, pumped into the lungs via the pulmonary arteries, which originate from the right ventricle. The blood is then pumped back to the left atrium through the pulmonary veins, oxygenated and ready to be pumped out by the left ventricle into the rest of the body. The bronchial arteries, supplying the walls of the conducting airways with blood, receive less than 1% of the total pulmonary blood flow (22, 23). Within the lungs, the arteries closely follow the structure of the airways, reaching the alveoli where the arteries containing deoxygenated blood branch into arterioles which guide the blood into the capillary beds, where O_2 enters the bloodstream and CO_2 leaves it (23). After passing through the capillaries, oxygenated blood enters the venules and the pulmonary venous system and is led back to the left atrium of the heart (24).

Gas exchange and acid-base balance

The gas exchange between blood and air takes place in the capillary beds, surrounding the alveoli in the respiratory zone of the airways. The capillaries within the lungs have an average diameter of 6.3 µm and the total length of capillaries in the human lung has been estimated to be around 7 000 km, creating a very large alveolar surface area. The wall of each capillary is only a few cell layers thin, consisting of squamous epithelial cells. The thin cell walls of the capillaries lie against the alveolar walls which consist mainly of pneumocytes, with an interstitial compartment in between. These three components together make up the septal wall, over which the gas exchange takes place. The interstitial compartment contains a small volume of fluid which can increase in pathological states and create pulmonary oedema, limiting the gas exchange. There are also a variety of cell types within the interstitium, including macrophages, fibroblasts, mast cells and pericytes (24). The gas exchange itself is driven by passive diffusion due to differences in pressure gradients of both O_2 and CO_2 between blood and air, the rate of which is determined by the diffusion capacity, which in turn is dependent on the capillary surface area and septal wall thickness (25).

The acid-base balance of the body is upheld by the kidneys and the lungs, the kidneys having the capacity to regulate the blood potential of hydrogen (pH) slower and over longer time compared to the lungs which can alter the pH in a matter of minutes (26). The cells of the body produce CO_2, which is an acid, when performing cell respiration, which combines with water (H_2O) to create hydrogen ions (H^+) and bicarbonate (HCO_3^-) which lowers the blood pH. Thus, breathing can regulate the body's pH-balance by changing the frequency and volume of each breath. A higher minute volume (MV) results in larger amounts of CO_2 being expelled from the body, increasing the pH, while a lower MV leads to increased retainment of CO_2, lowering the pH (25).

Hydration and dehydration of CO_2:

$$CO_2 + H_2O \leftrightarrow H_2CO_3 \leftrightarrow H^+ + HCO_3^- \qquad (25)$$

Lung cancer

Cancers of the respiratory system, including the trachea, the bronchi and the lungs, are the fourth most common cause of death on a global level according to the World Health Organization (WHO) (27). Lung cancer is the most common form of malignancy in the population as a whole, causing over 1.3 million deaths annually, corresponding to almost 13% of all cancer-related deaths (28, 29). Approximately 85% of all lung cancer cases are caused by non-small cell lung cancer (NSCLC), a

type of cancer that encompasses several subtypes including lung adenocarcinoma (LUAD), squamous cell carcinoma (SCC) and large-cell carcinoma (30, 31). Out of the three subtypes LUAD makes up the greatest portion of NSCLC cases, accounting for approximately 40% of all lung cancer cases, while SCC is the type of NSCLC that is most often linked to a history of smoking (31, 32).

Diagnosis and prognosis

As of today, there are still no widely implemented screening methods for lung cancer, despite there being studies proving that screening with low-dose computed tomography (CT) reduces lung cancer mortality (33). Furthermore, lung cancer often presents without symptoms or with late onset of symptoms including but not limited to coughing, increased production of sputum, dyspnea and increased frequency of respiratory infections (30, 34). This often leads to late detection, and approximately 75% of patients have either locally advanced or metastasized disease at diagnosis (35). As a result of this, the survival rates for NSCLC remain devastatingly low with 5-year survival rates ranging from 67% for patients with Tumor, Node, Metastasis (TNM) stage I (T1 – T2, N0, M0), all the way down to less than 5% for patients with stage IIIB or higher (34).

Diagnosis and staging of lung cancer relies not only on imaging such as conventional x-rays, computed tomography (CT) and positron emission tomography (PET), but also on more invasive methods such as bronchoscopy and biopsies. These procedures are necessary to determine the type of lung cancer and whether there are any targetable genetic alterations present within the cells. However, these methods are potentially harmful to the patient and are costly (36). Alternative, less invasive means of diagnosing and monitoring NSCLC over time would therefore be beneficial for both patients and society.

Treatment options

Treatment of lung cancer can be divided into the categories surgery, chemotherapy, radiation, targeted therapies and immunotherapy. Surgical resection of the primary tumor is the most common choice of treatment for low stage (stage I – II) localized NSCLC. The preferred surgical approach is most often removal of the entire lobe in which the tumor resides, a so-called lobectomy, but depending on size and location of the tumor, the type of surgery can also be a lesser resection, a bilobectomy or even a pneumonectomy. Surgical treatment also involves exploration of lymph node stations, with removal of cancer affected nodes (37). Chemotherapy is used less frequently as a primary treatment option for NSCLC since the development of targeted therapies, but the use of cisplatin and carboplatin, typically in combination with other treatment methods, is still highly relevant. These drugs interfere with the deoxyribonucleic acid (DNA) repair system in the cancer cells, leading to DNA

damage and cell death. The use of targeted therapies is on the rise, with more and more genetic alterations being identified as potential targets. This enables more personalized care, based on the specific genetic characteristics of the cancer cells in each patient (38). Immunotherapy on the other hand, consists of antibodies that target ligands on the cancer cells, inhibiting the binding of the activating antigen, thus disturbing the cell cycle of the malignant cells (39). Lastly, radiotherapy is mostly used in conjunction with other treatment methods, to control local or regional advances of the disease, and to lessen symptoms for the patient (38, 40).

Lung transplantation

Solid organ transplantation (SOT) has been around as a method of treating critically ill patients for decades, with the first successful kidney transplant (KTx) being performed in 1954 in Boston, USA (41, 42). Since then, the field of SOT has been ever evolving, and in 1963 the first human lung transplant (LTx) took place. In 1971 the first successful single LTx could finally take place, extending the life of a patient by almost 11 months, and in 1988 the first successful double LTx was carried out (43). Undoubtedly, the discovery of the immunosuppressant cyclosporine A in the 1970's had a major role in this, being the first calcineurin inhibitor of its kind. Calcineurin inhibitors specifically inhibit a step in the proliferation process of T-cells, successfully acting as an immunosuppressant without unwanted cytostatic effects (44). Around the same time, Dr. Frank Veith discovered that the use of a shorter part of the donor bronchus minimized the risk of the otherwise common problem of ischemic complications to the bronchus of the transplanted lung, as the bronchial circulation is not re-anastomosed in LTx (43).

Surgical techniques

The mode of entry into the thoracic cavity has changed over the years, starting off as a midline sternotomy, which was later converted to bilateral anterior clamshell incisions and a transverse sternotomy in the late 1980´s. Nearing the 2000´s the bilateral anterolateral clamshell incisions without a sternotomy were introduced, which is now the standard approach used. The modern surgical technique of sequentially attaching each lung at the mainstem bronchus level was originally pioneered by Dr. Henri Metras in 1950, however it was only taken into regular use in 1990. In the four decades between those years, LTx was performed en bloc, which was later shown to cause higher rates of airway dehiscence (43).

Immunosuppression

The first ever LTx recipient was treated with a combination of steroids, azathioprine and cytoablative radiation of the thymus. The patient died from kidney failure after only 18 days but showed no signs of rejection of the lungs. Between 1963 and the discovery of cyclosporine A in the 1970's, not a single LTx recipient survived long enough to be discharged from the hospital. In 1983 cyclosporine A was approved for use by the Food and Drug Administration (FDA), after which it became a vital part of the standard immunosuppressive regimen in SOT recipients (43).

Outcomes

As of today, LTx is the standard treatment option for patients with end-stage pulmonary diseases of non-malignant etiologies, and more than 4 500 lung transplantations are now being performed annually around the globe (45). Underlying pulmonary diseases that may be cause for LTx in advanced stages include COPD, CF, pulmonary fibrosis (PF), pulmonary hypertension (PH), alpha-1 antitrypsin deficiency (A1AD) as well as less common diseases such as graft versus host disease (GvHD), and others (46). However, long-term survival of LTx recipients remains a pressing issue, with the median survival following LTx only reaching six years (47, 48). The most common complications following LTx are infections, malignancies, kidney failure and chronic rejection in the form of chronic lung allograft dysfunction (CLAD). CLAD affects up to 50% of all LTx recipients within five years of transplantation, and can be categorized as being either obstructive or restrictive, the obstructive form called bronchiolitis obliterans syndrome (BOS) being more common compared to the restrictive form restrictive allograft syndrome (RAS) (48).

Fungal infections

Pulmonary diseases affect the lung function in different ways, compromising the structural and immunological integrity of the lungs. This can predispose patients to infections caused by bacteria, viruses and fungi, which can be challenging to identify due to similar symptoms to the underlying pulmonary disease. LTx recipients especially are at risk for serious infections due to decreased mucociliary clearance and intense immunosuppressive regimens, which if undiagnosed can lead to more serious complications and poor outcomes in the form of rejection or death (49, 50). The most common fungi to infect and colonize LTx recipients are different subspecies of the mold *Aspergillus* species (spp.) and the yeast *Candida* spp., and the general consensus is that invasive fungal infections (IFI) caused by these microorganisms are associated with increased early mortality, partly because of the frequency with which IFI causes severe bacterial coinfections (51, 52). However,

the exact knowledge of how less aggressive fungal infections and fungal colonization affect LTx recipients remains lacking, with previous research suggesting different outcomes based on the infecting agent genus and the preventive measures taken (51, 53-55).

The most common fungal infectious agents are *Aspergillus fumigatus* and *Candida albicans*. The incidence of severe infections with the previously more common fungus *Pneumocystis jirovecii* has declined substantially due to prophylactic treatment (56, 57). The manifestations of infections caused by molds and yeasts differ slightly, with molds such as *Aspergillus* spp. being more likely to cause systemic engagement with multi organ disease and fungemia, while yeasts like *Candida* spp. often cause more localized complications like mediastinitis and infections of the pleural space (57). The spores of the strain *Aspergillus fumigatus* are comparatively small, and although the fungus is a facultative aerobe, it thrives in the hypoxic environment that it creates by microvascular invasion and thrombosis in the small airways, which also contributes to the inflammatory response which is an important part of the fungus' virulence (58). While the most common way of infection by *Aspergillus* spp. is through inhalation, respiratory infections caused by *Candida* spp. most often reach the lungs through hematological dissemination originating from the skin or the gastrointestinal tract, even though it is a natural part of the oropharyngeal flora (59).

Preoperative fungal colonization is common and can also cause overgrowth into the newly transplanted allograft. To limit the consequences of these opportunistic infections, prophylactic antifungal treatment is administered in varying intensities and durations after LTx depending on local clinical policies (60). There is however no widely accepted treatment protocol for antifungal prophylaxis, and several different regimens are applied using substances like triazoles, tetrazoles and amphotericin B (50). The use of these types of medications has limitations and can cause drug interactions, altering the concentrations of vital immunosuppressants like calcineurin inhibitors by competitive inhibition of the metabolizing enzyme family cytochrome P450 (CYP450) (61, 62).

COVID-19

The family of coronaviridae consisting of enveloped positive-sense, single-stranded ribonucleic acid (RNA) viruses has caused respiratory tract infections long before the emergence of the novel severe acute respiratory syndrome coronavirus 2 (SARS-CoV-2) back in December of 2019 (63, 64). It is estimated that approximately 2% of the globe's population are healthy carriers of coronaviridae, and that this family of viruses cause between 5 – 10% of all acute respiratory infections in humans. Infection with SARS-CoV-2 gives rise to the coronavirus disease 2019 (COVID-

19), which if symptomatic can cause a multitude of different symptoms, most often respiratory symptoms of pneumonia, coughing, shortness of breath, fevers, myalgia, headaches and gastrointestinal symptoms (65). The occurrence of ageusia and anosmia, the loss of the sense of taste and smell, which became recognized symptoms among the public, has been shown to vary between different populations (66). Severe infection with SARS-CoV-2 can manifest as acute respiratory distress syndrome (ARDS), septic shock with multi organ failure and death (67). By march 2020 the WHO declared the disease a global pandemic, and as of today there have been over 750 million confirmed cases and more than 7 million deaths caused by COVID-19 (65, 68).

COVID-19 has turned out to be highly contagious, and transmission of the virus happens both through direct droplet transmission, airborne aerosol generation and indirectly through contact with contaminated surfaces. Studies have shown alarmingly long survival times of the virus on non-porous surfaces like glass or steel of up to 28 days (65). Upon entering the body, the spike protein (S1) on the virus binds to the angiotensin-converting enzyme 2 (ACE2) receptor which is highly expressed on pulmonary epithelial cells, and is cleaved by the protease transmembrane protease serine 2 (TMPRSS2), which enables fusion between virion and host cell membranes (Figure 3) (69). Inside the host cells the virus replicates and synthesizes proteins, spreading through the body by way of infiltrating adjacent cells (70).

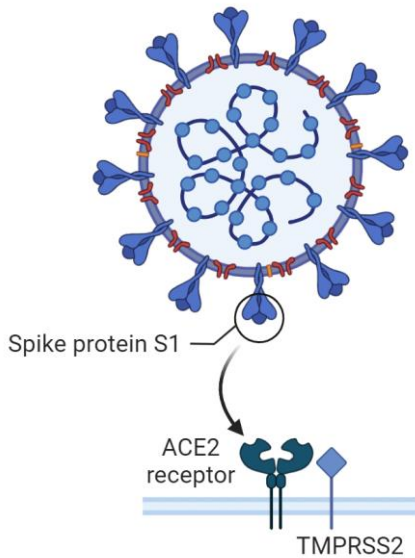

Figure 3: SARS-CoV-2 binding to human cells. Simplified image of the binding of a SARS-CoV-2 virion to a human cell by attachment of S1 to the ACE2 receptor and subsequent cleavage by TMPRSS2. Figure created in BioRender.com. *SARS-CoV-2: severe acute respiratory syndrome coronavirus 2, S1: spike protein 1. ACE2: angiotensin-converting enzyme 2, TMPRSS2: transmembrane protease serine 2.*

Factors influencing the severity of disease in infected individuals include viral load and degree of inflammation and immune response. The initial innate immune response results in a cytokine storm which in turn triggers the adaptive immune response. As the disease progresses, cells are damaged and die, which causes the formation of hyaline membranes and increased vascular permeability, contributing to the impaired oxygen diffusion and fatality of COVID-19. Impaired viral clearance is common in certain groups of individuals such as older persons and immunocompromised patients like LTx recipients (71-73).

Particles in exhaled air

Access to the distal airways is instrumental in the care of patients with advanced pulmonary disease. However, this is not always easy, and clinicians are mostly limited to strategies of varying invasiveness, like transthoracic biopsies or bronchoscopy, introducing a risk of complications at each performed procedure. Several alternative methods for sampling of the small airways have been suggested, including induced sputum, bronchoalveolar lavage fluid (BALF), exhaled breath condensate (EBC), and volatile organic compounds (VOC) (74-77). While there is research suggesting the usefulness of these methods in the exploration of changes within the diseased lungs, no clinically useful biomarkers have yet been discovered, and the methods are significantly limited by low specificity as well as salivary contamination, among other things (74, 76, 78, 79). Therefore, the emergence of the relatively new method for collection of particles in exhaled air (PExA), was a welcome addition to the repertoire of methods for detecting novel biomarkers in a patient's breath. The PExA method (Gothenburg, Sweden) was coined in 2004 and has since been applied to discover biomarkers for several different types of pulmonary diseases, including asthma, COPD, primary graft dysfunction (PGD) and lung cancer in both spontaneously breathing patients and in conjunction with mechanical ventilation (74, 80).

Within the PExA device there is an optical particle counter (OPC) and an inertial impactor, which each count and stratify the patient's exhaled particles by size, ranging from 0.33 – 4.55 µm in diameter (81). This renders both a particle flow rate (PFR), measured as particle flow per litre of exhaled air, and exhaled breath particles (EBP), which are collected onto a membrane that can be frozen at -80°C and analyzed at a later timepoint. These measurements are acquired by instructing the patient to follow a specific breathing maneuver, breathing into a mouthpiece which is attached to the device and contains a three-way valve. Air is inhaled through a filter, eliminating contamination from room air, and is exhaled into the machine (Figure 4) (74). By fully exhaling and inhaling into the device, the small airways open and close repeatedly, generating EBP from the RTLF, and the use of this method has been shown to produce samples which resemble the composition of

BALF, with particles predominantly originating from generations 14 – 17 of the small airways (81, 82).

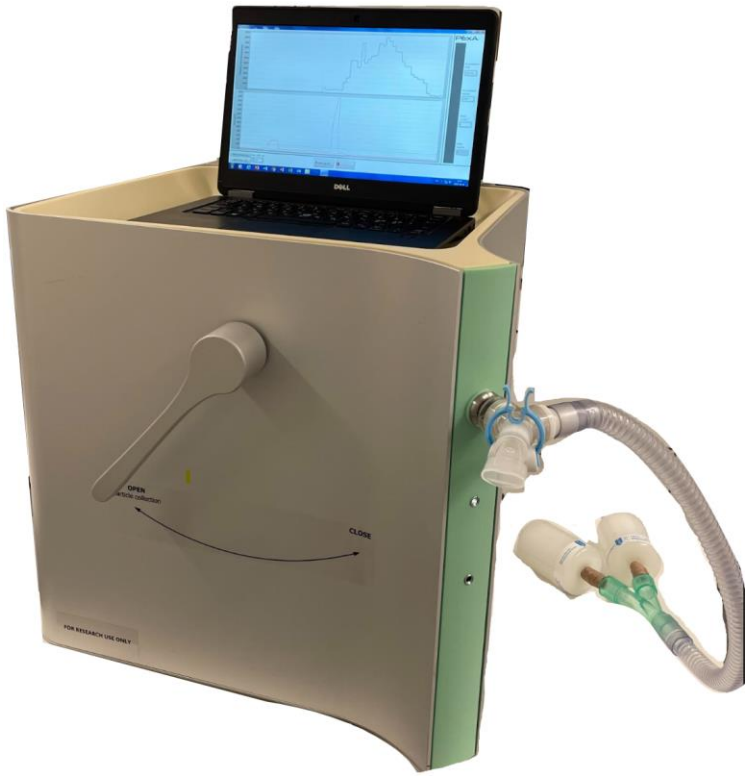

Figure 4: The PExA device. Image of the PExA device which was used to collect EBP and measure PFR in papers I – III. Mouthpiece with three-way valve and tube connected to HEPA-filter on the right side. © Embla Bodén. *PExA: particles in exhaled air, EBP: exhaled breath particles, PFR: particle flow rate, HEPA: high efficiency particulate air.*

Aims

Paper I

The aim of the first paper was to identify potential protein biomarkers in plasma from patients diagnosed with primary NSCLC, and to evaluate the biomarkers' potential for being used to clinically diagnose disease and evaluate surgical treatment of NSCLC.

Paper II

The aim of the second paper was to investigate the feasibility of using a device for collection of EBP and measurement of PFR to identify potential biomarkers for primary LUAD.

Paper III

The aim of the third paper was to explore the differences in particle production and proteomic composition of EBP between patients with PCR-verified COVID-19, patients with respiratory symptoms but no COVID-19, and healthy controls, to identify potential biomarkers for pulmonary disease.

Paper IV

The aim of the fourth paper was to shed light on the impact of fungal colonization of the respiratory tract within the first year after LTx on the two outcomes survival and development of chronic rejection of the lung allograft. We further aimed to explore what factors may potentially influence the outcomes in the setting of fungal colonization.

Paper V

The fifth and final paper aimed to elucidate what factors influence the outcomes following infection with COVID-19 in LTx recipients in the two neighboring

countries Sweden and Denmark in a setting of vastly differing sociopolitical approaches to the recent COVID-19 pandemic.

Material and methods

Study populations

Paper I

The first paper in this thesis includes a total of 29 patients with primary NSCLC, admitted to Skåne University Hospital (SUS), Lund for surgical resection of the tumour. The genotypes LUAD and SCC were included, and the stages of cancer in the included subjects ranged from IA – IIIA (T1a – T4, N0 – N2, M0), according to the International Association for the Study of Lung Cancer's (IASLC) TNM seventh edition staging system (83). Blood samples were collected at three timepoints, once before surgery and twice after, resulting in a total of 86 collected samples due to one patient not being available for sampling at the first timepoint following surgery. Exclusion criteria included symptoms of ischemic heart disease, any unstable medical condition such as heart failure New York Heart Association (NYHA) class III or IV, serum creatinine > 140 μmol/L, glycated haemoglobin (HbA1c) > 48.0 mmol/mol, as well as signs of liver cirrhosis, bleeding disorders or drug abuse (84). The follow-up time for survival was 3.5 years (Figure 5).

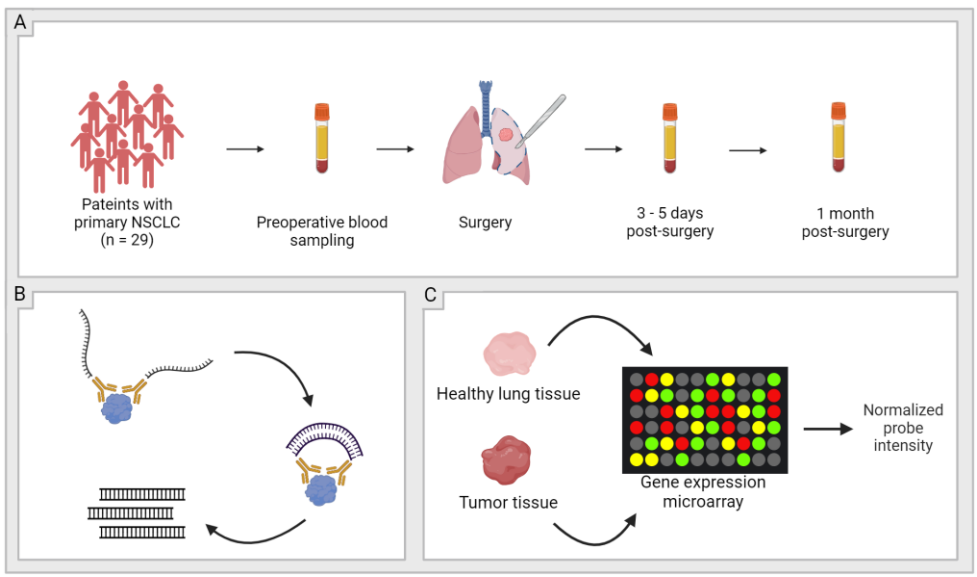

Figure 5: Schematic overview of paper I. Study overview of paper I. A: Twenty-nine patients with primary NSCLC were included. Blood samples were obtained before surgical resection of NSCLC, 3 – 5 days after surgery and one month after surgery. B: Proteomic analysis was performed using PEA technology. C: Protein expression patterns were validated in larger cohorts found in NCBI's GEO. Figure created in BioRender.com. *NSCLC: non-small cell lung cancer, PEA: proximity extension assay, NCBI: National Center for Biotechnology Information, GEO: gene expression omnibus.*

Paper II

This second paper includes patients with primary LUAD admitted for surgical resection at SUS, Lund, and control patients without any pulmonary disease who were admitted for other cardiothoracic surgical procedures. In total, thirty-five patients were included, of which 17 were LUAD patients and 18 were control patients. Cancer patients were included if the cancer stage was lower or equal to a pathological TNM (pTNM) of N2/IIIA according to the seventh edition of the IASLC's TNM staging criteria (83). Samples of exhaled breath were obtained at two timepoints for LUAD patients, once before surgery and once after. The control patients were only sampled once, prior to surgery. The follow-up time for survival was three years after surgery (Figure 6).

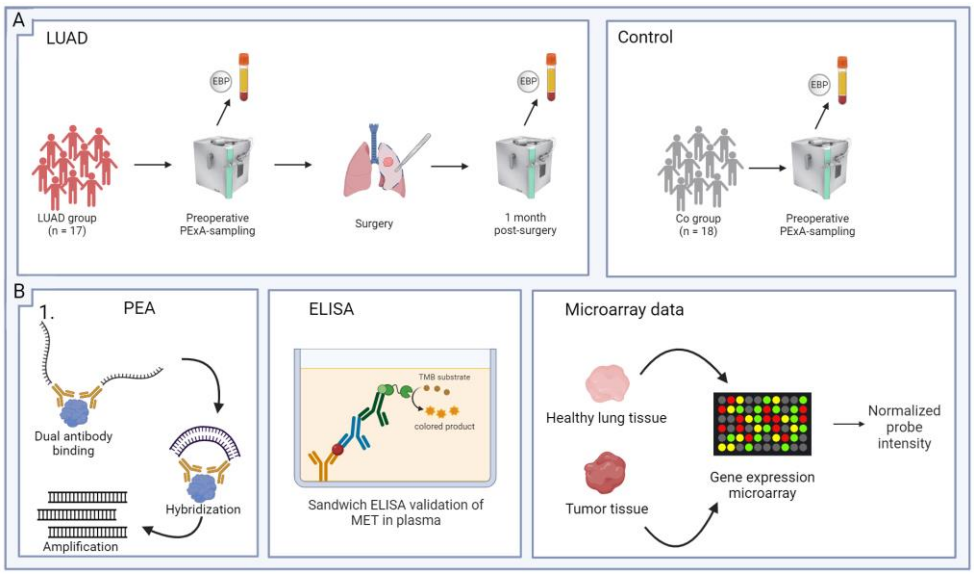

Figure 6: Schematic overview of paper II. Study overview of paper II. A: Seventeen patients with primary LUAD and 18 control patients were included. Samples of blood and EBP were collected prior to and one month after surgical resection of LUAD for cancer patients and before surgery for control patients. B: Proteomic analysis was performed using PEA technology. Protein expression patterns were validated in with an ELISA and by accessing larger cohorts in NCBI's GEO. Figure created in BioRender.com. *LUAD: lung adenocarcinoma, EBP: exhaled breath particles, PExA: particles in exhaled air, PEA: proximity extension assay, ELISA: enzyme-linked immunosorbents assay, MET: hepatocyte growth factor, NCBI: National Center for Biotechnology Information, GEO: gene expression omnibus.*

Paper III

The third paper is a prospective study in which patients with PCR-verified COVID-19, patients with respiratory symptoms but repeated negative PCR-tests for COVID-19, and voluntary healthy controls are included. All patients were recruited between May and November 2020. A total of 48 patients were included in the three subgroups, with 20 COVID-19 positive patients (COV-POS), 16 symptomatic but COVID-19 negative patients (COV-NEG), and 12 healthy controls (HCO) (Figure 7). All symptomatic patients were recruited either as inpatients from the infectious ward or directly from the emergency department at SUS, Lund. All patients gave samples of exhaled breath at one point in time. The study is registered at ClinicalTrials.gov with the trial register number NCT04503057.

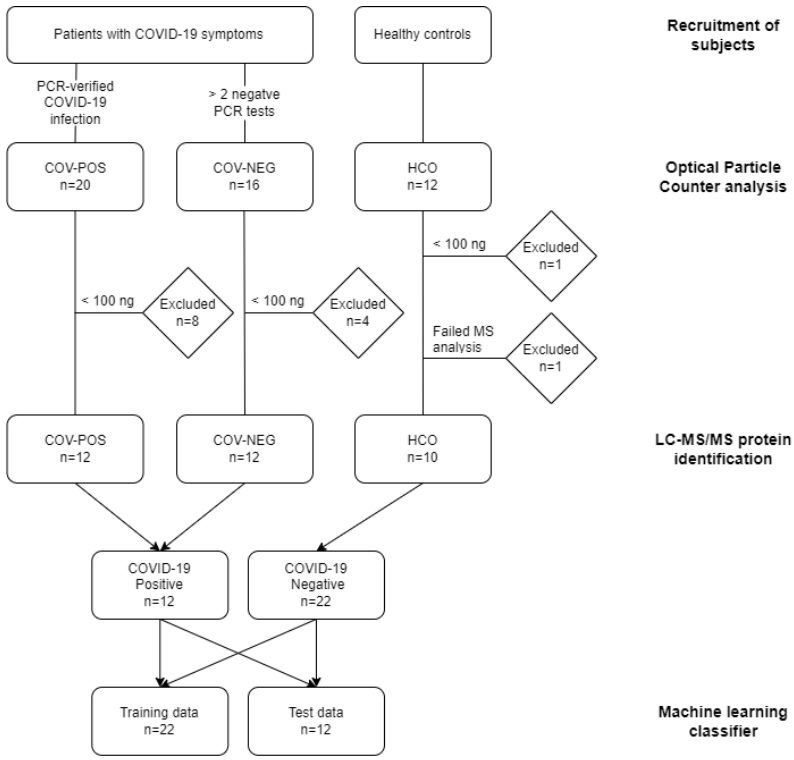

Figure 7: Flow chart of patient inclusion and sample exclusion. Forty-eight patients were recruited and divided into groups. Subsequently 13 samples were excluded due to collection of less than 100 ng of EBP. One sample in the HCO group was excluded due to technical issues in the MS analysis. *COVID-19: coronavirus disease 2019, PCR: polymerase chain reaction, COV-POS: COVID-19 positive, COV-NEG: COVID-19 negative, HCO: healthy controls, ng: nanograms, MS: mass spectrometry, EBP: exhaled breath particles.*

Paper IV

In the fourth paper, which uses chart reviews to investigate factors influencing outcomes after LTx, a total of 134 patients transplanted at SUS, Lund between the years 2011 – 2020 are included. Follow-up was terminated on 2023-06-01. Exclusion criteria included age below 18 years, death within 30 days of LTx, re-transplantation, and loss of follow-up due to the patient's home clinic being elsewhere in the country (Figure 8). Retrospective chart reviews were performed, extracting data from local medical records on fungal colonization and infection. Fungal colonization was defined according to the International Society for Heart and Lung Transplantation's (ISHLT) consensus guidelines (85). IFI was defined according to the European Organization for Research and Treatment of Cancer (EORTC), and the Mycoses Study Group Education and Research Consortium's (MSGERC) consensus guidelines (86). Fungal colonization either before LTx or during the first twelve months after LTx was recorded. The patients were divided into three subgroups: IFI, fungal colonization, and no fungal event. Patients with fungal colonization were further divided into subgroups depending on the genus of the colonizing agent.

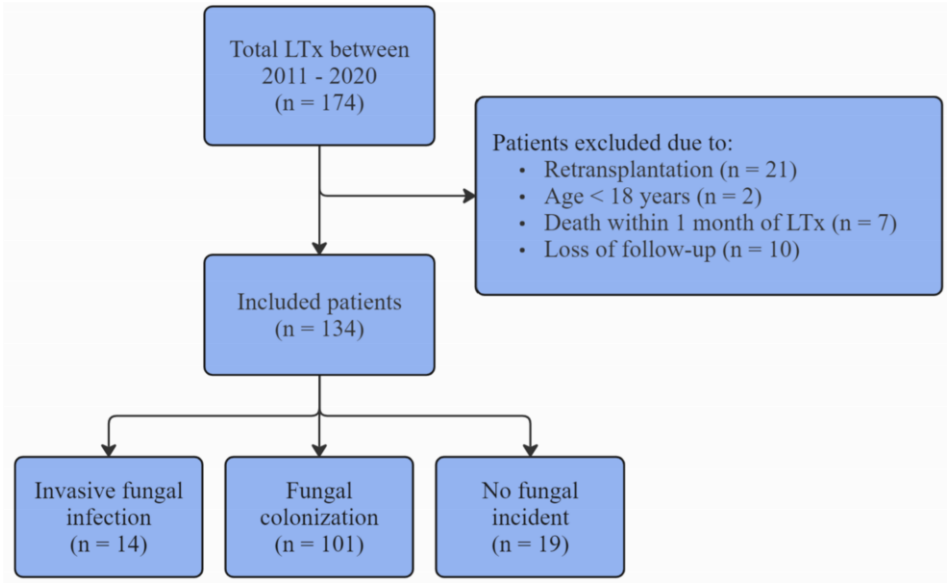

Figure 8: Flow chart of inclusion, and exclusion criteria in paper IV. A total of 174 transplantations between 2011 – 2020 resulted in the inclusion of 134 LTx recipients. The subjects were divided into the three subgroups IFI, fungal colonization, and no fungal incident. *LTx: lung transplantation, IFI: invasive fungal infection.*

Paper V

The fifth and final paper in this thesis includes a total of 318 LTx recipients from both Sweden and Denmark, transplanted between the years 1993 – 2023. All patients included have had at least one episode of PCR-verified COVID-19 after LTx and were alive at the start of the pandemic. All subjects were followed for one year (365 days) after the first positive PCR-test, or until death, whichever came first. All included patients were 18 years of age or older. The patients were divided into subgroups based on vaccination status at the time of infection (fully vaccinated, n = 282, unvaccinated, n = 36), country of residence (Sweden, n = 188, Denmark, n = 130) and dominant strain of SARS-CoV-2 at the time of infection (*Wuhan*, n = 29, *Alpha*, n = 31, *Delta*, n = 24, *Omicron*, n = 235), as demonstrated earlier by others (87). The periods of different dominating strains of SARS-CoV-2 were as follows: *Wuhan* (January 2020 – December 2020), *Alpha* (January 2021 – July 2021), *Delta* (August 2021 – December 2021) and *Omicron* (January 2022 – December 2023) (Figure 9). For the purposes of balancing the subgroups of patients, the strains of SARS-CoV-2 were further categorized as early (*Wuhan* and *Alpha*) or late (*Delta* and *Omicron*). Full vaccination against SARS-CoV-2 was defined as having received at least two doses of any vaccine against COVID-19.

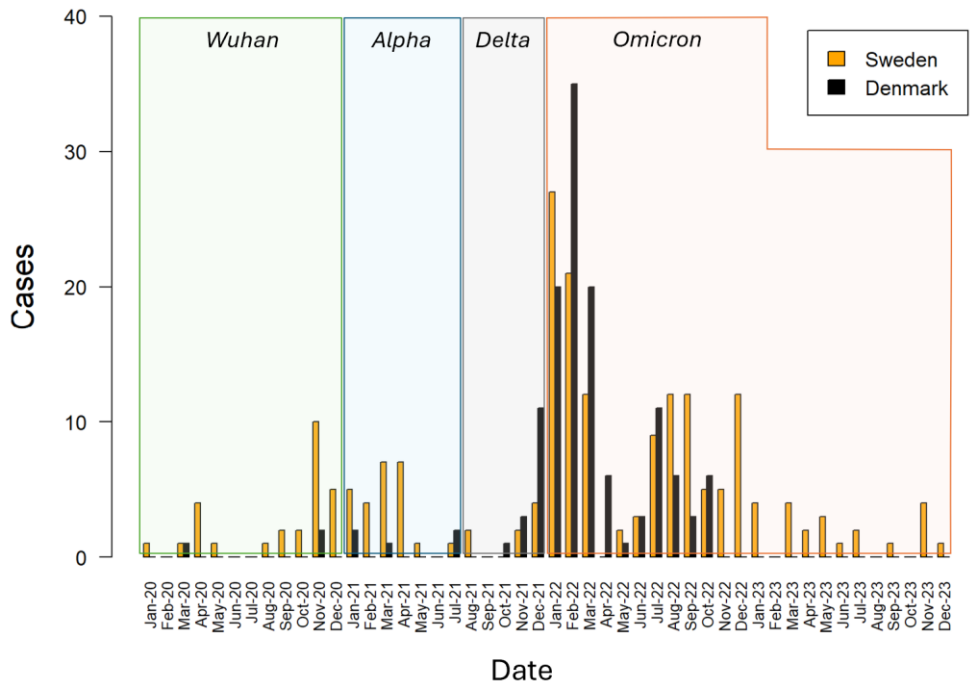

Figure 9: Overview of COVID-19 cases in Sweden and Denmark. Number of cases of COVID-19 in LTx recipients per month in the two neighboring countries Sweden and Denmark, divided by the dominant strain of SARS-CoV-2 at the time of infection. *COVID-19: coronavirus disease 2019, LTx: lung transplantation, SARS-CoV-2: severe acute respiratory sydrome coronavirus 2.*

Sample collection

In papers I – III samples in the form of blood and EBP are acquired and used for the purpose of proteomic analyses.

Blood sampling

Blood from patients with primary NSCLC in studies I and II was drawn at all timepoints. The blood samples were taken in lab with the use of BD Vacutainer Eclipse Signal Blood Collection Needle with Integrated Holder (22G x 1) (Becton, Dickinson and Company, Plymouth, UK) and K2E (EDTA) 6 mL blood collection tubes (Becton, Dickinson and Company, New Jersey, USA). Two tubes of blood were obtained from each patient at each timepoint. The blood was spun in the MPW-352R cooling centrifuge (Med.Instruments, Warsaw, Poland) for ten minutes at 5000 rounds per minute (rpm), at room temperature (22°C), within 30 minutes of collection, after which the plasma was aliquoted into 1.5 mL SafeSeal micro tubes (Sarstedt, Nümbrecht, Germany) and stored in freezers at −80°C until analysis.

Particles in exhaled air

The particles in exhaled air (PExA, Gothenburg, Sweden) method was used to collect EBP and measure PFR from patients in studies I – III. Here, the study subjects are instructed to breathe according to a special breathing maneuver into a mouthpiece which is attached to the device. The mouthpiece makes up a three-way valve, preventing the mixing of inhaled and exhaled air (Figure 4). The maneuver entails full exhalation, the holding of breath on emptied lungs for approximately five seconds, and full inhalation followed by a slow exhalation into the device (74, 88). The maneuver is repeated until a set amount of total accumulated EBP has been collected, typically between 100 – 300 ng. All breathing is done through the mouth, with the application of a nose clip, through a high efficiency particulate air (HEPA) filter to eliminate contamination from particles in the room air.

Within the machine there is an optical particle counter (OPC) and an inertial impactor, serving to quantify the EBP as well as stratify them into size bins depending on diameter, ranging from 0.33 – 4.55 µm. The device further measures the flow and volume of exhaled air, yielding the PFR. The machine is kept at body temperature to prevent condensation, and the EBP are collected onto LCR membrane filters (Hydrophilic polytetrafluoroethylene filter, 0.45 µm pore size, Millipore, Merck, Darmstadt, Germany) (89). The filters with the sample material on them are stored at -80°C until analysis.

Proteomic analyses

Different techniques for the analysis of the proteomic composition of blood and EBP respectively are used throughout studies I – III. A summary with explanations for the methods proximity extension assay (PEA), enzyme-linked immunosorbent assay (ELISA), and mass spectrometry (MS) follows below.

Proximity extension assay

The use of PEA is applied in papers I and II and is based on predetermined protein panels consisting of 92 unique proteins, created by the company Olink (Olink Proteomics AB, Uppsala, Sweden). Each of the available panels focuses on an area of research and cannot be changed upon request. In study I, the panel entitled "Target 96 Oncology II" was used. This panel is made up of proteins related to various forms of malignancies and was thus deemed relevant to the topic of lung cancer. In the second study the panel entitled "Target 96 Cardiometabolic" was used, due to it being the only available panel which did not require dilution of the samples which already held very small amounts of biological material.

The PEA analysis is an immunoassay which requires dual antibody recognition to yield a signal. For each protein in the chosen panel there is a matched antibody pair, carrying unique oligonucleotides, which hybridize when brought into proximity by binding to the same protein. The hybridized DNA-tags are then detected by the Fluidigm BioMark PCR system, resulting in cyclic amplification depending on the amount of the protein detected in each sample. The data output is presented as normalized protein expression (NPX), a relative means of quantification on a log2 scale for protein expression levels. A predetermined limit of detection (LOD) of 15% is used, excluding proteins with lower expression from further analysis. NPX values are relative and thus cannot be compared between proteins. For further information on detection limits, assay characteristics, assay performance, and validation is available on the manufacturer's webpage (90).

Mass spectrometry

In the third study, we used high-performance liquid chromatography-mass spectrometry (HPLC-MS/MS) to analyze the proteomic composition of EBP from patients with COVID-19, patients with respiratory symptoms, and healthy controls. The collected samples were incubated in 2% sodium dodecyl sulfate (Sigma-Aldrich, St. Louis, USA) in 50 millimolar (mM) triethylammonium bicarbonate (TEAB) (Thermo Fisher Scientific, Massachusetts, USA) at 37°C for two hours. After the first incubation 400 mM dithiothreitol (Sigma-Aldrich, St. Louis, USA) was added before another 45 minutes of incubation. The samples were alkylated in

darkness for 30 minutes with the addition of 800 mM iodoacetamide (Sigma-Aldrich, St. Louis, USA). Lastly, 12% aqueous phosphoric acid was added to a final concentration of 1.2%.

Next, the samples in 1.2% phosphoric acid were collected onto S-Trap columns (Protify, New York, USA) with 90% methanol and 100 mM TEAB. The proteins were later digested with MS-grade endoproteinase Lys-C (Lys-C) (Promega, Fitchburg, USA) during a two-hour incubation at 37°C. Following this incubation, a total amount of 1.45 µg of sequence grade trypsin (Promega, Fitchburg, USA) was added in two doses over the course of a night. Peptides were then eluted with 50 mM TEAB, 0.2% formic acid (Sigma-Aldrich, St. Louis, USA) and 50% acetonitrile (Sigma-Aldrich, St. Louis, USA) and dried in a vacuum concentrator (SpeedVac, Eppendorf, Hamburg, Germany) at 45°C and stored at -20°C for later analysis.

The digested peptides were separated with the use of nanoflow chromatography in a liquid chromatography (LC) system (Evosep One, Odense, Denmark). The standard 60 samples per day method with a gradient length of 21 minutes was used in conjunction with an Evosep column containing 1.5 µm ReproSil-Pur C18-AQ particles. The LC system was connected to a captive source using the timsTOF Pro mass spectrometer (Bruker Daltonics, Billerica, Massachusetts, USA). The instrument was set to the data-dependent acquisition parallel accumulation serial fragmentation (DDA-PASEF) mode with ten scans per cycle and accumulation and ramp times of 100 milliseconds each. Dynamic exclusion was activated at 0.4 minutes.

For analysis of the raw MS data the system MaxQuant version 2.0.20 (Max Planck Institute, Munich, Germany) was used, applying the Andromeda database search algorithm, and the files were searched against the UniProt human protein database as well as the UniProt SARS-CoV-2 proteome database (ID: UP000464024) (91). The false discovery rate (FDR) was set to 1% for protein- and peptide levels and the first pass (MS1) match tolerance was set at 20 and 40 parts per million (ppm) for the first and main search, respectively. Missed cleavages of two were allowed.

Machine learning

In paper III we applied a machine learning model to predict which patients were positive for COVID-19. The model was built in R, using RStudio version 4.2.0 (RStudio, Massachusetts, USA), with the CARET package (version 6.0-93). Imputation was used for missing values and was done in Perseus version 2.0.5.0 (Max Planck institute of biochemistry, Germany). Features included in the model were chosen based on analysis of variance (ANOVA) scores and number of missing values, resulting in the use of 11 proteins and the number of particles per exhaled

volume of air (PEV) (Table 1). The created biomarker panel was exported into R and the measurements were randomly divided into a training (n = 22) and a testing group (n = 12). The training set was used to train a random forest model with tenfold cross validation, using 100 repeats and 1000 trees. The optimal number of random candidate variables was decided through receiver operating characteristics (ROC), and was set at two, and the results were based on the model's application on the test set of the data. Results are reported as accuracy, sensitivity, specificity and area under the ROC curve (AUC-ROC).

Protein abbreviation	Full name of protein
ORM1	Orosomucoid 1
IGHG1	Immunoglobin heavy constant gamma 1
CAPN1	Calpain 1
CASP14	Caspase 14
IGLC6	Immunoglobin lambda constant 6
APOA1	Apolipoprotein A1
TF	Transferrin
IGKC	Immunoglobin kappa constant
EPPK1	Epiplakin 1
SFTPB	Surfactant protein B
IGHA1	Immunoglobin heavy constant alpha 1

Table 1: Proteins included in the biomarker panel. Abbreviation and full name of all proteins which were included in the biomarker panel used in the machine learning model in paper III.

Validation

Enzyme-linked immunosorbents assay

An ELISA was performed within the scope of paper II to confirm the results regarding the expression patterns of the protein MET in EBP. The analysis was performed on plasma from the included patients in the study, using the Ray Biotech Catalog ELH-HGFR kit (RayBiotech Incorporated, Georgia, USA) for human samples. The analysis was performed with the use of a 96-well microplate containing a known quantity of antigens, binding to the specific antibody that the kit is made for, enabling detection. The addition of a chromogenic substance to the wells in the plate results in a color change which can be read, quantifying the amount of the protein in each well (92).

Gene expression omnibus

To validate the findings of the proteomic analyses in papers I and II, we explored data from other researchers, deposited in the National Center for Biotechnology

Information's (NCBI) gene expression omnibus (GEO) (National Library of Medicine, Maryland, USA) (93). Here, data from larger cohorts were identified, and protein expression patterns were validated where possible. The datasets used contained information from proteomic analyses of NSCLC tissue and healthy lung tissue (GSE10072 and GSE1980).

Chart review

For papers IV and V, we conducted chart reviews of the included LTx recipients' medical records and extracted data from the local systems Melior (Sweden) (paper IV and V) and Sundhedsplatformen (Denmark) (paper V). Data regarding fungal infections, fungal colonization, antifungal treatment, demographics, and follow-up appointments, including data on PFT, histology, rejection and survival were collected within the scope of study IV. For paper V we similarly collected data regarding any episodes of COVID-19 in LTx recipients, the treatment thereof, demographics, vaccination status, PFT, and the outcomes survival and chronic rejection. Each patient's medical record was reviewed manually.

Statistical analysis

For all papers included in this thesis, statistical significance was defined as **** ($p < 0.0001$), *** ($p < 0.001$), ** ($p < 0.01$), * ($p < 0.05$), and not significant (ns) ($p > 0.05$).

Paper I

The descriptive statistics in paper I are presented as mean, range, number of subjects (n) and percentage. Statistical analyses were carried out by statisticians at Olink, using R, and in GraphPad Prism version 9.3.0 (GraphPad, California, USA). The data was analyzed through the fitting of a linear mixed-effects regression model. Subject ID and type of cancer were treated as random effects. Adjustments for multiple comparisons were made with the Benjamini-Hochberg approach and an FDR of 0.05, and Tukey's method. The emmeans package in R was used for Posthoc testing, comparing all timepoints in a pairwise manner. Additional comparisons of subgroups were made with the Mann-Whitney test.

Paper II

In paper II we performed an a priori power analysis with hedges g, based on results from an earlier publication (94). A statistical power of 87% and an effect size of 1.82 was reached. Descriptive statistics are presented as mean, range, standard error of the mean (SEM), n, and percentage. All analyses were performed in GraphPad Prism version 9.2.0. The statistical tests used include the student's t-test, simple linear regression and Pearsson's correlation.

Paper III

In paper III the data was normalized in the software NormalizerDe, using robust linear regression normalization (95). Protein expression was defined as a label free quantification value (LFQ). Further statistical analyses were performed in Perseus version 2.0.5.0 and RStudio version 2.4.0. Denoted decoy proteins and contaminants were removed, as were proteins detected in less than 45% of samples in one or more groups. Significant differences were identified with ANOVA and Posthoc testing was conducted with Tukey's method. Differentially expressed proteins were determined with an s0 of 0.1, and the FDR was set to 0.05. A heatmap of LFQ values was created using the R package pheatmap, using Euclidean clustering and showing protein expression as normalized z-scores. For analysis of protein – protein interactions and reactome pathways, the stringApp version 11.5 in the software Cytoscape version 3.9.1 (Cytoscape, California, USA) was used. Subcellular locations were determined with CellWhere version 1.1 (96).

Paper IV

All statistical analyses were performed in RStudio version 2023.12.1. Data were presented as mean, range, hazard ratio (HR) with 95% confidence intervals (CI), n, and percentage. Propensity score weighting (PSW) was used to achieve balance between subgroups, as calculated by linear regression. Survival and CLAD-free survival were visualized with Kaplan Meier curves. Censoring was used for patients with no event at the end of follow-up. Statistical risk was calculated with weighted cox proportional hazards models and results were presented as HR with 95% CI. Both univariate and multivariate analyses were carried out.

Paper V

Demographic data are presented as n, percentage, mean and range. Statistical calculations were conducted in RStudio, with R version 4.1.2. Subgroups were balanced through PSW, and propensity scores were calculated with a logistic regression model. Charlson comorbidity index (CCI) was calculated for each patient

according to the ICD-10 CCI algorithm (97). Survival and CLAD-free survival were visualized with Kaplan Meier curves, censoring subjects with no event at the end of follow-up. Statistical differences in risk were calculated with weighted cox proportional hazards models and the results were reported as HR with 95% CI. Both univariate and multivariate models were fitted to the data.

Results

Paper I

Descriptive results

A total of 29 patients with primary NSCLC were included. Blood samples were collected at three timepoints: before surgical resection (n = 29), within the first week after (n = 28), and at one month post resection (n = 29), resulting in a total of 86 blood samples. There was one missing sample at the second timepoint due to one patient no longer being admitted to the hospital at this time. The mean age in the cohort was 71 years (range 46 – 84 years), the number of male patients was 48 (48%), and the fractions of patients diagnosed with LUAD versus SCC were 0.72 and 0.28 respectively, which corresponds to numbers reported in other parts of the world (98).

Proteomic analysis

The predetermined protein panel entitled "Target 96 Oncology II" consisting of 92 unique proteins was used in paper I. Proteomic analysis of plasma could detect all 92 proteins in more than 75% of the samples. Sixty-three of the 92 proteins (68%) were revealed to be expressed in significantly differing levels between the three timepoints after adjusting for multiple testing. The 12 proteins with the lowest adjusted p-values were chosen for further literature review and analysis (Table 2).

Protein abbreviation	Full name of protein
IL-6	Interleukin-6
MUC-16	Mucin-16
Furin	Furin
TGFα	Protransforming growth factor alpha
HGF	Hepatocyte growth factor
VEGFA	Vascular endothelial growth factor A
MIC-A/B	MHC class 1 polypeptide-related sequence A/B
AREG	Amphiregulin
DLL1	Delta-like protein 1
FASLG	Tumor necrosis factor ligand superfamily member 6
GPNMB	Transmembrane glycoprotein NMB
TNFRSF6B	Tumor necrosis factor receptor superfamily member 6B

Table 2: Top 12 proteins chosen for further analysis. Abbreviation and full name of the top 12 proteins with the lowest adjusted p-values which were chosen for further review and analysis in paper I.

Pairwise comparisons of protein expression levels between all three timepoints: preoperative, one-week postoperative, and one-month postoperative, were done for each of the 12 proteins (Figure 10). These analyses revealed significantly elevated expression of the proteins AREG, DLL1, Furin, IL-6, TGFα, and TNFRSF6B at both postoperative timepoints compared to preoperative levels. A similar trend could be seen for the proteins MUC-16 and VEGFA, although statistical significance was not reached. Moreover, the levels of expressed MIC-A/B in plasma were also significantly higher at both postoperative timepoints compared to preoperative levels (preoperative NPX = 3.82 ± 0.70, one-week postoperative NPX = 4.20 ± 1.69 ($p < 0.0001$), one-month postoperative NPX = 4.00 ± 1.70 ($p = 0.0009$)). The results also showed a significant elevation in expression of the protein FASLG at the one-month postoperative timepoint compared to preoperative expression levels (preoperative NPX = 8.34 ± 0.45, one-month postoperative NPX = 8.63 ± 0.34 ($p < 0.0001$)). The same expression pattern could be identified for the protein GPNMB. Finally, the expression levels of the protein HGF were significantly elevated at the one-week postoperative timepoint compared to preoperative levels, however, there was a lowering trend between the two postoperative measurements (preoperative NPX = 8.04 ± 0.60, one-week postoperative NPX = 8.58 ± 0.58 ($p < 0.0001$), one-month postoperative NPX = 8.15 ± 0.45 ($p = 0.23$)) (Table 3).

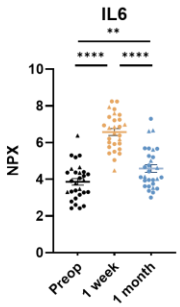
IL6
**
****
****
NPX
10
8
6
4
2
0
Preop
1 week
1 month

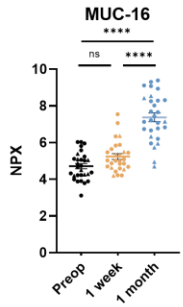
MUC-16
****
ns
****
NPX
10
8
6
4
2
0
Preop
1 week
1 month

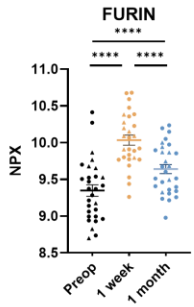
FURIN
****
****
****
NPX
11.0
10.5
10.0
9.5
9.0
8.5
Preop
1 week
1 month

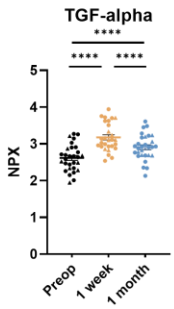
TGF-alpha
****
****
****
NPX
5
4
3
2
1
0
Preop
1 week
1 month

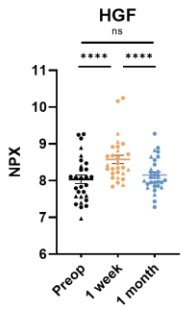
HGF
ns
****
****
NPX
11
10
9
8
7
6
Preop
1 week
1 month

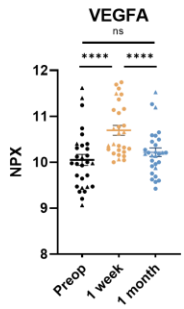
VEGFA
ns
****
****
NPX
12
11
10
9
8
Preop
1 week
1 month

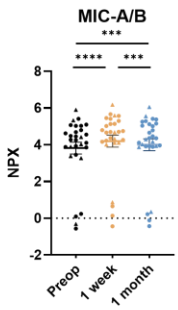
MIC-A/B
***
****
***
NPX
8
6
4
2
0
-2
Preop
1 week
1 month

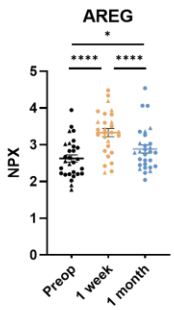
AREG
*
****
****
NPX
5
4
3
2
1
0
Preop
1 week
1 month

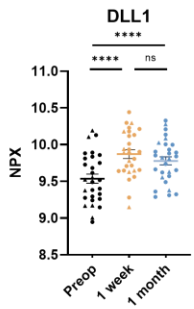
DLL1
****
****
ns
NPX
11.0
10.5
10.0
9.5
9.0
8.5
Preop
1 week
1 month

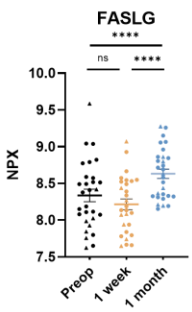
FASLG
****
ns
****
NPX
10.0
9.5
9.0
8.5
8.0
7.5
Preop
1 week
1 month

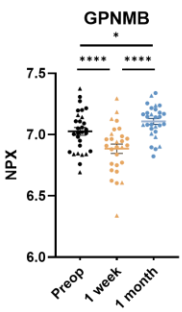
GPNMB
*
****
****
NPX
7.5
7.0
6.5
6.0
Preop
1 week
1 month

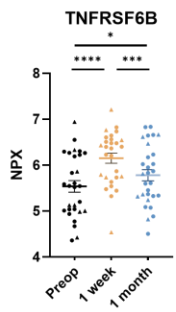
TNFRSF6B
*
****
***
NPX
8
7
6
5
4
Preop
1 week
1 month

Figure 10: Protein expression over time for the top 12 proteins in paper I. Protein expression compared between preoperative and postoperative samples depicted, expressed as NPX. *IL-6: interleukin-6, MUC-16: mucin-16, TGF-alpha: transforming growth factor alpha, HGF: hepatocyte growth factor, VEGFA: vascular endothelial growth factor A, MIC-A/B: MHC class I polypeptide-related sequence A/B, AREG: amphiregulin, DLL1: delta-like protein 1, FASLG: tumor necrosis factor ligand superfamily member 6, GPNMB: transmembrane glycoprotein NMB, TNFRSF6B: tumor necrosis factor receptor superfamily member 6B, NPX: normalized protein expression (NPX), ns: not significant.*

Protein Abbreviation	Protein	NPX Preop (Mean ± SD)	NPX 1 Week (Mean ± SD)	NPX 1 Month (Mean ± SD)	*p*-Value Preop vs. 1 Week	*p*-Value Preop vs. 1 Month	*p*-Value 1 Week vs. 1 Month
AREG	Amphiregulin	2.63 ± 0.51	3.33 ± 0.59	2.88 ± 0.58	$p < 0.0001$	$p = 0.0237$	$p < 0.0001$
DLL1	Delta-like protein 1	9.54 ± 0.33	9.87 ± 0.31	9.78 ± 0.29	$p < 0.0001$	$p < 0.0001$	ns
Furin	Protein furin	9.35 ± 0.41	10.03 ± 0.36	9.64 ± 0.33	$p < 0.0001$	$p < 0.0001$	$p < 0.0001$
IL-6	Interleukin-6	3.86 ± 0.95	6.57 ± 0.97	4.59 ± 1.09	$p < 0.0001$	$p = 0.0016$	$p < 0.0001$
MIC-A/B	MHC class 1 polypeptide-related sequence A/B	3.82 ± 0.70	4.20 ± 1.69	4.00 ± 1.70	$p < 0.0001$	$p = 0.0009$	$p = 0.0003$
MUC-16	Mucin-16	4.71 ± 0.74	5.24 ± 0.81	7.37 ± 1.26	ns	$p < 0.0001$	$p < 0.0001$
TGFα	Transforming growth factor alpha	2.62 ± 0.35	3.18 ± 0.37	2.91 ± 0.34	$p < 0.0001$	$p < 0.0001$	$p < 0.0001$
TNFRSF6B	Tumor necrosis factor receptor superfamily member 6B	5.54 ± 0.67	6.15 ± 0.57	5.78 ± 0.64	$p < 0.0001$	$p = 0.0214$	$p = 0.0003$
VEGFA	Vascular endothelial growth factor A	10.05 ± 0.63	10.69 ± 0.55	10.22 ± 0.49	$p < 0.0001$	ns	$p < 0.0001$
FASLG	Tumor necrosis factor ligand superfamily member 6	8.34 ± 0.45	8.22 ± 0.38	8.63 ± 0.34	ns	$p < 0.0001$	$p < 0.0001$
GPNMB	Transmembrane glycoprotein NMB	7.03 ± 0.17	6.89 ± 0.20	7.11 ± 0.13	$p < 0.0001$	$p = 0.0207$	$p < 0.0001$
HGF	Hepatocyte growth factor	8.04 ± 0.60	8.58 ± 0.58	8.15 ± 0.45	$p < 0.0001$	ns	$p < 0.0001$

Table 3: Top 12 proteins NPX values at all timepoints. Expression levels of each of the top 12 proteins in paper I, expressed as NPX ± SD. *NPX: normalized protein expression, SD: standard deviation, vs.: versus.*

Comparing protein expression between patients who died or experienced relapse and patients with progression-free survival

Of the 29 patients included in this study, four experienced relapse of NSCLC or died within the follow-up time. Proteomic analysis revealed consistently lower expression of the protein FASLG in these four patients, at all timepoints, compared to patients with progression-free survival (PFS). The largest difference was observed in preoperative values (dead/relapse NPX = 7.91 ± 0.11, PFS NPX = 8.40 ± 0.45 ($p < 0.05$)) (Figure 11). A cox proportional hazards model showed a negative parameter estimate of -3.126, indicating that a decrease in the predictor variable is associated with an increased hazard of the event ($p = 0.0672$). Larger numbers are likely needed to reach significance. Similar analyses were also performed for the

proteins HGF and MIC-A/B, however no associations between expression levels and specific outcomes could be seen.

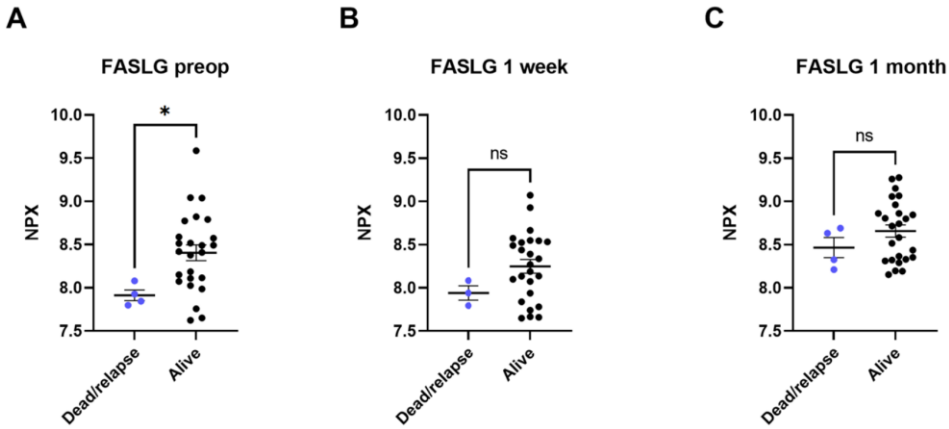

Figure 11: Expression of FASLG depending on outcome. Expression levels of the protein FASLG at all three timepoints, divided by outcome in the form of PFS or death/relapse of NSCLC. *FASLG: tumor necrosis factor ligand superfamily member 6, NPX: normalized protein expression, ns: not significant, PFS: progression-free survival.*

Validation

The NCBI's GEO was searched for relevant datasets, and two separate cohorts of NSCLC tissue were used for validation of the current study's findings. Gene expression is expressed as normalized probe intensity (NPI). One dataset (GSE10072) described the gene expression in LUAD tissue and healthy lung tissue from different individuals and showed a significantly higher expression of MIC-A (NM_000247) in healthy tissue compared to cancer tissue (NPI healthy controls = 8.18 ± 0.04, NPI cancer = 8.00 ± 0.03 ($p = 0.0044$)). Another dataset (GSE19804) described the gene expression in NSCLC tissue and adjacent healthy lung tissue in the same individuals. Here MIC-A (NM_000247) was also expressed in higher levels in healthy tissue (NPI healthy tissue = 8.19 ± 0.05, NPI NSCLC = 8.00 ± 0.06 ($p = 0.0166$)). The second dataset was also able to validate the present study's findings of higher expression of the protein FASLG (AF288573) in subjects with PFS, showing elevated expression in healthy lung tissue compared to NSCLC tissue (NPI healthy tissue = 4.56 ± 0.05, NPI NSCLC = 4.42 ± 0.04 ($p = 0.0239$)) (Table 4). The expression patterns for the proteins HGF and GPNMB could not be validated.

Protein	GenBank	GEO	Gene Expression Cancer	Gene Expression Control	Significance
MIC-A	NM_000247	GSE10072	8.00 ± 0.03	8.18 ± 0.04	$p = 0.0044$
MIC-A	NM_000247	GSE19804	8.00 ± 0.06	8.19 ± 0.05	$p = 0.0166$
FASLG	AF288573	GSE19804	4.42 ± 0.04	4.56 ± 0.05	$p = 0.0239$

Table 4: Gene expression of MIC-A and FASLG in tissue. Expression of the proteins MIC-A and FASLG in NSCLC tissue and healthy lung tissue, expressed as NPI, used for validation of findings in paper I. *MIC-A: MIC-A/B: MHC class I polypeptide-related sequence A, FASLG: tumor necrosis factor ligand superfamily member 6, NPI: normalized probe intensity, GEO: gene expression omnibus.*

Paper II

Descriptive results

Paper II includes a total of 35 patients, seventeen of whom had primary LUAD and 18 control patients without any pulmonary disease admitted for various cardiac procedures. Samples of EBP and PFR were collected at two timepoints for LUAD patients, once before surgical resection (n = 15) and once one month after surgery (n = 16). Control patients were only sampled preoperatively (n = 18). The mean age in the entire cohort was 70 years (range 43 – 83 years) and the number of male patients was 21 (60%). Survival of the LUAD patients was followed for three years. All patients but one were alive at the end of follow-up.

Elevated PFR in LUAD patients

When comparing the preoperative PFR between the healthy controls and the LUAD patients, a significantly higher value could be seen in the cancer patients (PFR LUAD = 18 490 ± 3 306, PFR control = 4 021 ± 899 ($p < 0.0001$)) (Figure 12). At the one-month follow-up appointment the PFR was still significantly elevated in LUAD patients compared to the preoperative samples from the control patients ($p = 0.0001$). There was no significant difference in PFR when comparing the LUAD group to themselves between the two timepoints (PFR preoperatively = 18 490 ± 3 306, PFR at follow-up = 30 210 ± 6 500 ($p = 0.1142$)).

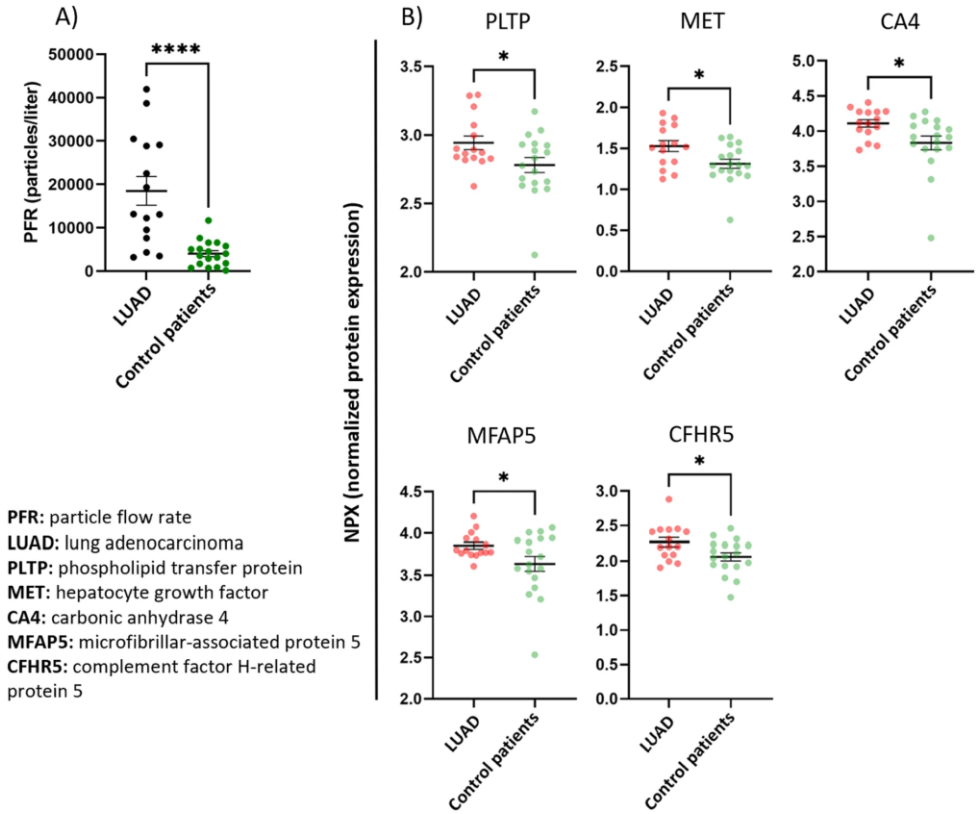

Figure 12: Differences in PFR and protein expression between LUAD and control patients. A: PFR from patients with primary LUAD compared to control patients prior to surgery. **B:** Protein expression patterns for the five investigated proteins in paper II compared between LUAD patients and control patients.

Proteomic analysis

Eighty-nine of the 92 proteins in Olink's "Target 96 Cardiometabolic" panel were found in more than 75% of the sent in EBP samples. Of these, five proteins were shown to be expressed in significantly higher concentrations in the preoperative samples of LUAD patients compared to control patients (Table 5). At the one-month postoperative measurement, the expression levels of the three proteins PLTP, MET and MFAP5 were no longer significantly elevated compared to the control patients (Figure 12).

Protein abbreviation	Full name of protein
CFHR5	Complement factor H-related protein 5
MFAP5	Microfibrillar-associated protein 5
PLTP	Phospholipid transfer protein
HGF-R/MET	Hepatocyte growth factor receptor/mesenchymal epithelial transition
CA4	Carbonic anhydrase 4

Table 5: The five proteins with increased expression in LUAD. Abbreviation and full name of the five proteins with significantly increased expression levels in patients with LUAD compared to healthy controls.

A heatmap of the five proteins was created, showing clustering of patients within their respective subgroups. The heatmap uses the standardized z-score for visualization of protein expression, with orange representing a lower expression, and blue indicating a higher expression (Figure 13).

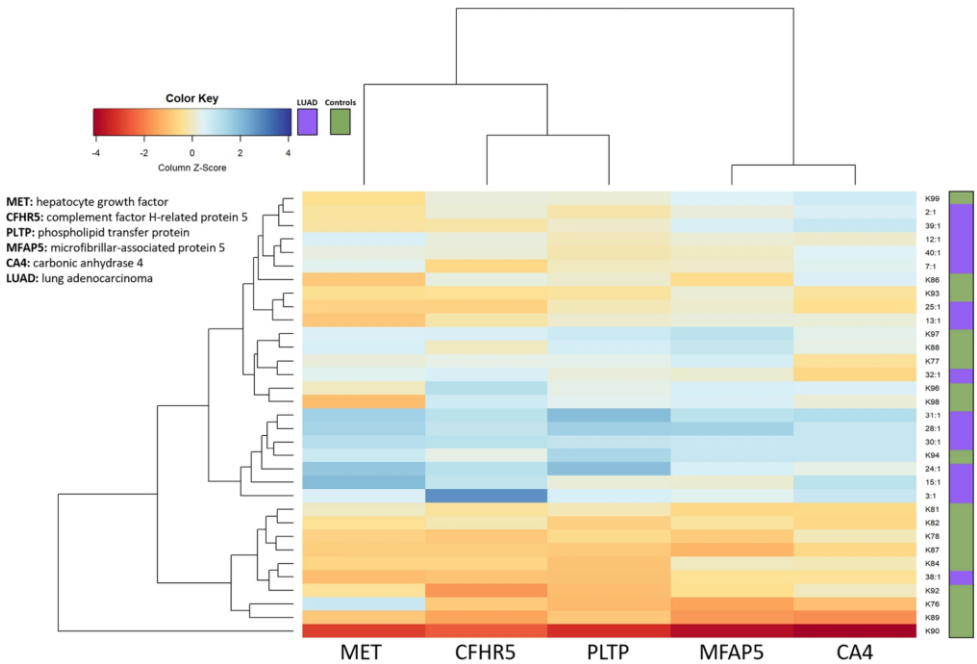

Figure 13: Heatmap of the five proteins of interest in paper II. Heatmap depicting relative protein expression of five proteins from paper II. Protein expression visualized as normalized z-score, with higher levels representing greater expression.

Validation

The findings of paper II were validated through analysis of the expression of MET in plasma from all patients included in this study, as well as by searching the NCBI's GEO for matching datasets.

The expression of MET was analysed in plasma with the use of an ELISA, which showed a significantly higher expression of the protein in LUAD patients before surgical resection compared to control patients (expression LUAD = 3 921 ± 144 pg/mL, expression control patients = 2 358 ± 161 pg/mL ($p < 0.0001$)). Furthermore, there was a significant correlation between the protein levels of MET in EBP and plasma when looking at all included patients (Figure 14).

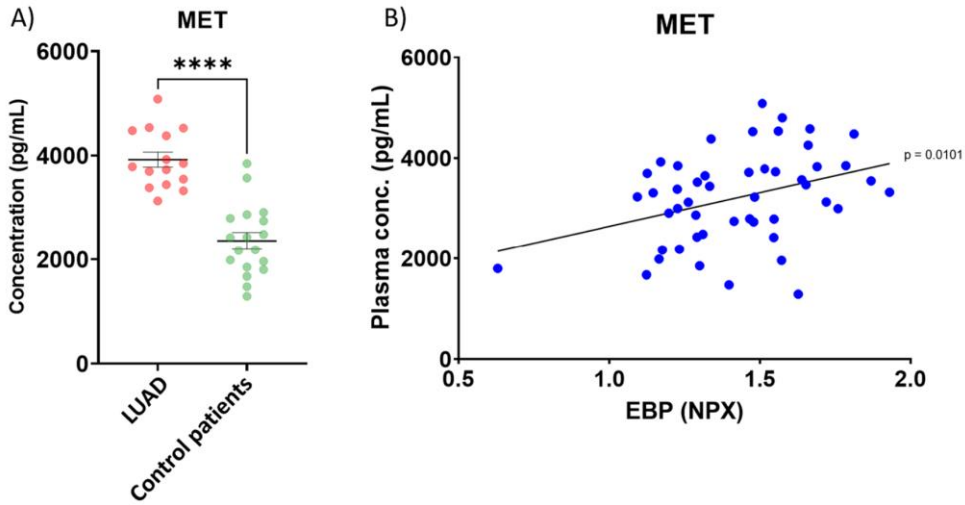

Figure 14: Concentration of MET in plasma and correlation between plasma and EBP levels. A: Preoperative expression of the protein MET in plasma from patients with LUAD and control patients. **B:** Correlation between MET expression in plasma and EBP from all patients included in the study. *MET: hepatocyte growth factor, LUAD: lung adenocarcinoma, EBP: exhaled breath particles, NPX: normalized proitein expression.*

The findings of the present study were also validated by searching the NCBI's GEO for datasets with matching characteristics to the current study. A dataset (GSE10072) describing the gene expression in LUAD tissue and healthy lung tissue from patients without cancer was used. Protein expression is expressed as NPI. The dataset revealed significantly elevated expression of the protein PLTP (NM_006227) in LUAD tissue compared to healthy lung tissue (NPI cancer = 9.99 ± 0.10, NPI healthy tissue = 9.29 ± 0.12 ($p = 0.008$)). The same results were seen for the protein MET (BG170541, BE870509), with significantly elevated expression in cancer tissue compared to healthy lung tissue (BG170541: NPI cancer = 9.52 ± 0.19, NPI healthy tissue = 8.79 ± 0.07 ($p = 0.0008$), BE870509: NPI cancer = 8.16 ± 0.07, NPI healthy tissue = 7.88 ± 0.03 ($p = 0.003$)) (Table 6).

Protein	GenBank	Gene expression cancer	Gene expression control	Significance
PLTP	NM_006227	9.66 ± 0.10	9.29 ± 0.12	p = 0.0080
MET	BG170541	9.52 ± 0.19	8.79 ± 0.07	p = 0.0008
MET	BE870509	8.16 ± 0.07	7.88 ± 0.03	p = 0.0030

Table 6: Validation of protein expression patterns. Expression of the proteins PLTP and MET in NSCLC tissue and healthy lung tissue, expressed as NPI, used for validation of findings in paper II. *PLTP: phospholipid transfer protein, MET: hepatocyte growth factor, NPI: normalized probe intensity.*

Paper III

Descriptive results

In this paper, a total of 48 patients with PCR-verified COVID-19 (COV-POS, n = 20), respiratory symptoms but no COVID-19 (COV-NEG, n = 16) and healthy controls (HCO, n = 12) were included. All patients gave samples of EBP at one timepoint, averaging seven days post the date of positive COVID-19 test (range 1 – 9 days). The median age with interquartile range (IQR) in each of the subgroups was; COV-POS 56 years (IQR: 53 – 64), COV-NEG 69 years (IQR: 53 – 80) and HCO 44 years (IQR: 29 – 46). The number of male subjects included in this study were 22 (46%). The incidences of obesity and a diagnosis of COPD or asthma were higher in the COV-POS subgroup compared to the COV-NEG and the HCO subgroups (obesity: COV-POS, n = 10 (50%), COV-NEG, n = 4 (25%), HCO, n = 1 (8.3%), COPD/asthma: COV-NEG, n = 4 (20%), COV-NEG, n = 1 (6.25%), HCO, n = 0 (0%)). Both the COV-POS and the COV-NEG subgroups exhibited similar symptomatology, although there was a higher incidence of dyspnoea in the COV-POS subgroup (COV-POS, n = 19 (95%), COV-NEG, n = 9 (56%), HCO, n = 0 (0%)).

Analysis of particle flow

The number of particles per exhaled volume of air (PEV) was calculated for each patient and was compared between subgroups. The results showed a significantly increased PEV in both COV-POS and COV-NEG patients compared to HCO (median PEV, COV-POS = 11 902 (IQR: 6 119 – 17 893), median PEV, COV-NEG = 8 159 (IQR: 5 406 – 12 000), median PEV, HCO = 3 622 (IQR: 2 506 – 5 790)). Further analyses revealed no significant correlations between PEV and age (r2 = 0.06954), or PEV and sex (p = 0.3254).

When looking at the particle distribution patterns in the three subgroups, the patients with symptoms (COV-POS and COV-NEG) revealed a trend of exhaling smaller particles compared to the HCO subgroup. Moreover, the HCO patients exhibited a bimodal particle size distribution curve, as opposed to the right skewed distribution curve of the symptomatic patients (Figure 15).

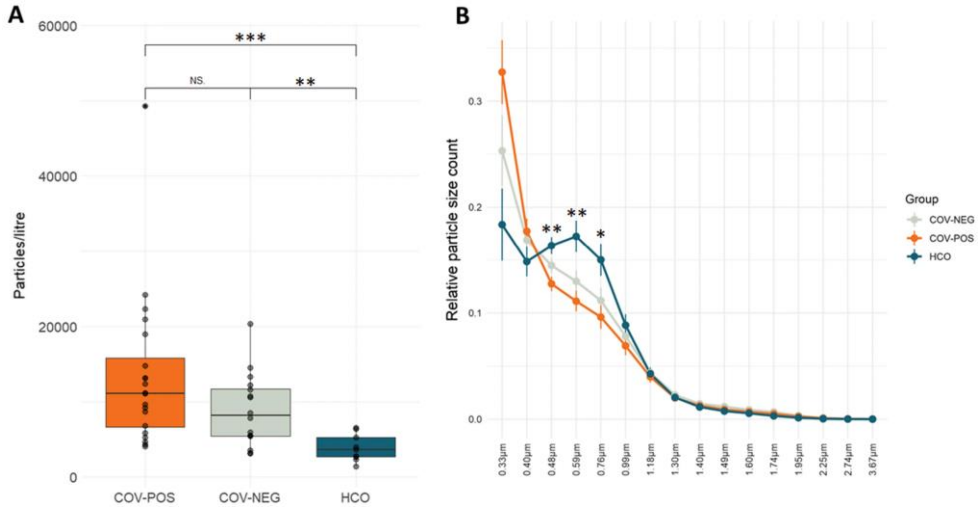

Figure 15: PEV and particle distribution pattern divided by subgroup. A: PEV in COV-POS, COV-NEG and HCO patients. **B:** Particle distribution pattern of EBP in COV-POS, COV-NEG and HCO patients. *COV-POS: COVID-19 positive, COV-NEG: COVID-19 negative, HCO: healthy control, PEV: particles per exhaled volume of air, ns: not significant, EBP: exhaled breath particles.*

Protein identification through LC-MS/MS

A total of 34 membranes (n COV-POS = 12, n COV-NEG = 12, n HCO = 10), all holding more than 100 ng of EBP were selected for proteomic analysis through LC-MS/MS. After exclusion of potential contaminants, the analysis identified 267 unique proteins across all three subgroups. Of these, 146 were present in over 45% of the samples in at least one of the three subgroups. One protein was found to be expressed exclusively in the COV-POS subgroup, namely immunoglobin heavy constant gamma 3 (IGHG33), and was seen in 50% of the COV-POS samples. The mean number of identified proteins in a single sample was 110.1 ± 15.8. No proteins related to the virus SARS-CoV-2 were reliably detected in any of the samples.

Quantitative proteomics

The proteins identified through LC-MS/MS were quantified, yielding LFQ-values. Twenty-six proteins were shown to differ significantly in expression levels between the three subgroups. These proteins were mostly related to extracellular processes but did include proteins which are naturally found in cell membranes, and intracellularly. Analysis of the reactome pathways revealed differences in expression levels of proteins related to the innate immune system and neutrophil

and platelet degranulation (Figure 16). A clustering analysis revealed three distinct subgroups, one of which was made up of eight of the COV-POS EBP samples (66.7%). The second and third clusters consisted of three COV-NEG EBP samples and the remaining 23 EBP samples respectively (Figure 17).

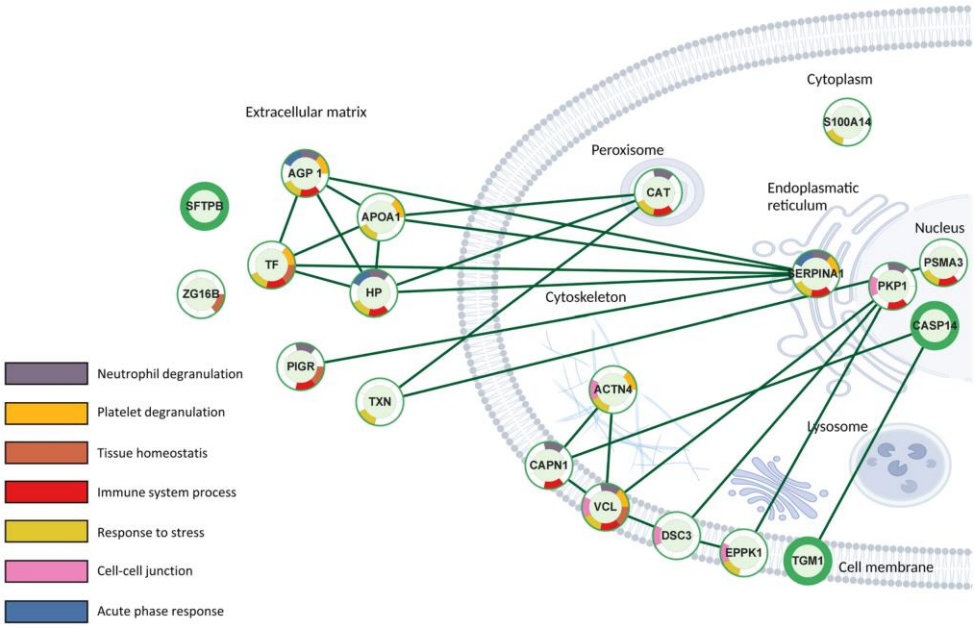

Figure 16: Reactome pathway analysis. Analysis of the reactome pathways of the proteins which were significantly differentially expressed in paper III. *See paper III for full names of proteins.*

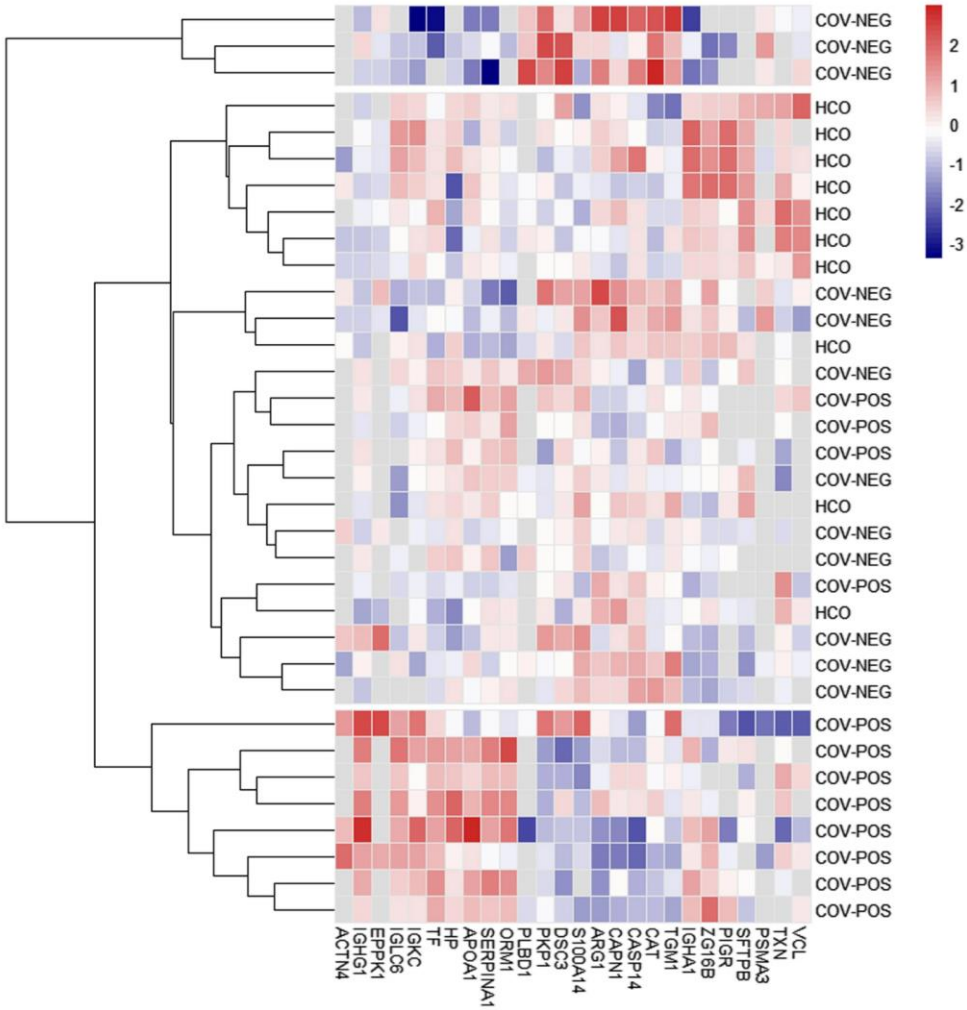

Figure 17: Clustering analysis of significantly differing proteins. A clustering analysis of the differentially expressed proteins in paper III was performed, revealing three distinct clusters of patients. *COV-POS: COVID-19 positive, COV-NEG: COVID-19 negative, HCO: healthy control, see paper III for full names of proteins.*

Nine of the identified proteins were significantly upregulated in COV-POS samples compared to COV-NEG and HCO samples, among which were three immunoglobins: immunoglobin kappa constant (IGKC), immunoglobin heavy constant gamma 1 (IGHG1) and immunoglobin lambda constant 3 (IGLC3), and one protein involved in wound healing, epiplakin (EPPK1). Five proteins of particular interest regarding COVID-19 were differentially expressed in COV-POS patients compared to the other two subgroups (Table 7). Furthermore, the expression of pulmonary surfactant-associated protein B (SFTPB) was significantly lower in both COV-POS and COV-NEG patients compared to the HCO subgroup. Eight

proteins were significantly downregulated in COV-NEG samples compared to HCO samples.

Protein abbreviation	Full name of protein
TF	Serotransferrin
APOA1	Apolipoprotein A-1
CASP14	Caspase-14
CAPN1	Calpain-1
ORM1	Alpha-1-acid glycoprotein 1

Table 7: Differentially expressed proteins of interest in COVID-19. Abbreviation and full name of the five proteins of specific interest in COVID-19 with significantly differing expression between the subgroups.

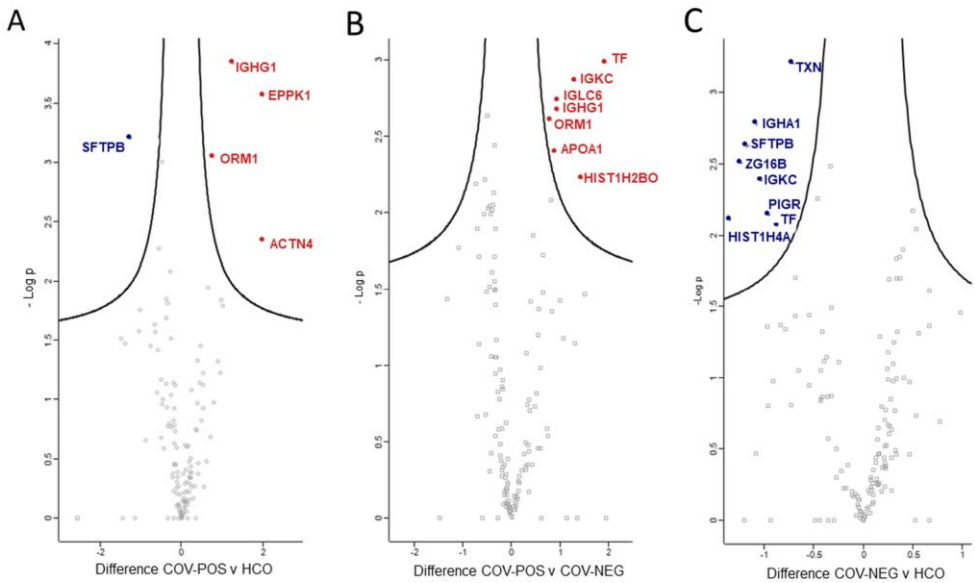

Figure 18: COV-POS patients showed significantly differentially expressed proteins in EBP. The x-axis show the difference in intensity, and the y-axis shows the negative log p-value. Significantly differentially expressed are highlighted in red (upregulated) and blue (downregulated). **A:** Comparison of COV-POS and HCO. **B:** Comparison of COV-POS and COV-NEG. **C:** Comparison of COV-NEG and HCO. *COV-POS: COVID-19 positive, COV-NEG: COVID-19 negative, HCO: healthy control, EBP: exhaled breath particles, see paper III for full names of proteins.*

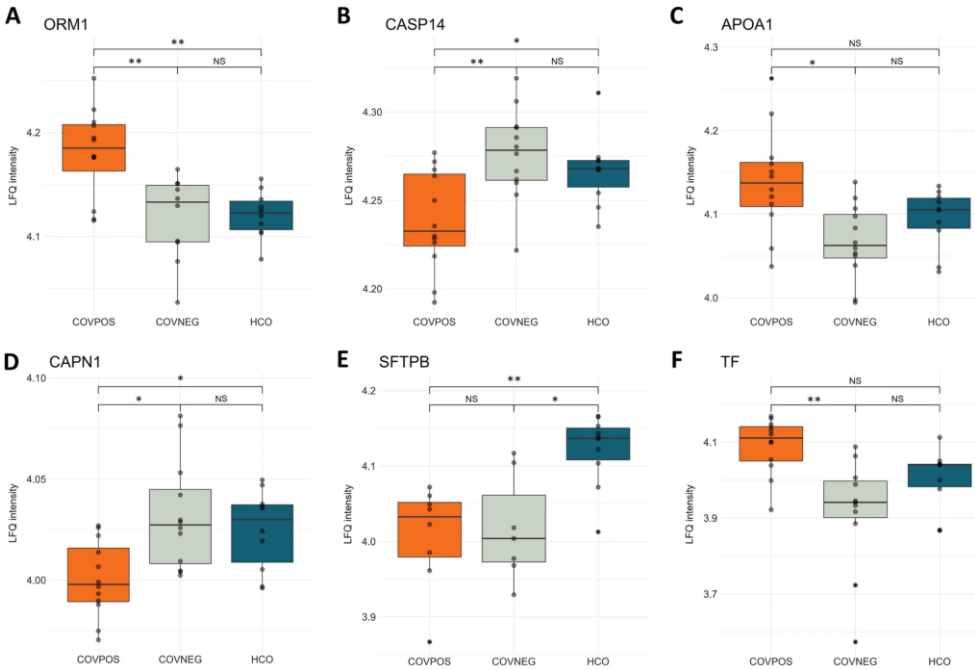

Figure 19: The six most abundant differentially expressed proteins. Differences in protein expression of the six most abundant proteins (**A – F**) compared between COV-POS, COV-NEG, and HCO. *ORM1: alpha-1-acid glycoprotein 1, CASP14: Caspase-14, APOA1: apolipoprotein 1, CAPN1: calpain 1, SFTPB: pulmonary surfactant associated protein B, TF: transferrin, COV-POS: COVID-19 positive, COV-NEG: COVID-19 negative, HCO: healthy control, LFQ: label free quantification.*

Machine learning classification

A biomarker panel consisting of 11 proteins and the PEV was used for building the random forest machine learning model (Table 8). The machine learning model was run on the training group, consisting of 22 randomly selected samples, and ranked the 12 factors in the biomarker panel according to importance. The model resulted in a ROC-AUC of 0.97 for the training dataset (95% CI: 0.88 – 1.06). Running of the model on the testing dataset (n = 12) yielded a ROC-AUC of 0.81 (95% CI: 0.52 – 1.1) and an accuracy of 0.92 (95% CI: 0.62 – 0.99), only misclassifying one COV-POS sample as being negative (Figure 20). The specific misclassified sample came from a 51-year-old female patient on day eight post positive PCR-test for COVID-19, and who was discharged the following day. The final machine learning model was determined to have a sensitivity of 75% and a specificity of 100%.

Biomarker abbreviation	Full name
PEV	Particles per exhaled volume of air
ORM1	Alpha-1-acid glycoprotein 1
IGHG1	Immunoglobin heavy constant gamma 1
CAPN1	Calpain-1
CASP14	Caspase-14
IGLC6	Immunoglobin lambda-6 chain C region
APOA1	Apolipoprotein A-1
TF	Serotransferrin
IGKC	Immunoglobin kappa constant
EPPK1	Epiplakin 1
SFTPB	Pulmonary surfactant associated protein B
IGHA1	Immunoglobin alpha-1 chain C region

Table 8: Proteins and markers included in the biomarker panel. Abbreviations and full names for all proteins included in the biomarker panel used for machine learning, plus PEV. *PEV: particles per exhaled volume of air.*

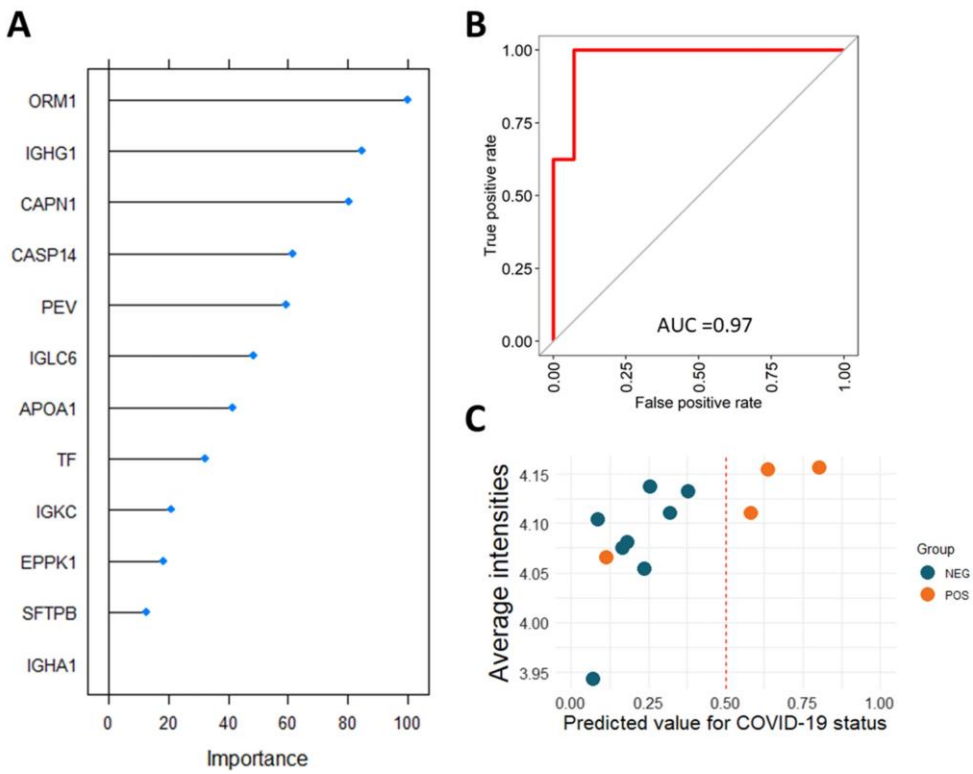

Figure 20: Biomarker panel used for machine learning, ROC-AUC, and classification of samples. **A:** Biomarkers included in the biomarker panel used for machine learning, ranked by estimated importance to the model. **B:** ROC-AUC for the training cohort. **C:** Classification of samples in the testing cohort by the machine model. *ROC-AUC: reciever operating characteristics area under the curve. COVID-19: coronavirus disease 2019, NEG: negative, POS: positive.*

Paper IV

Descriptive results

The fourth paper in this thesis includes 134 LTx recipients transplanted at SUS, Lund between 2011 – 2020. In total, 125 patients underwent double LTx (93.5%), seven patients underwent single LTx (5%), and two patients underwent heart- and lung transplantation (1.5%). The mean age in the study cohort was 52 years (range 19 – 68 years), and the number of male patients was 70 (52%). The mean follow-up time was 4.5 years (1 646 days, range 30 – 4 448 days). Nineteen of the included patients did not have any fungal colonization or infection after LTx, 14 patients had an IFI, and 101 patients were colonized by fungus post LTx. The infecting or colonizing agent was a yeast or a yeast-like fungus in 61 cases, referred to as candidal (*Candida* spp., *Saccharomyces* spp., *Pneumocystis jirovecii* or multiple spp.), and a mold in 54 cases, referred to as non-candidal (*Aspergillus* spp., *Paecilomyces* spp., *Rhizopus* spp. Or multiple spp.). The mean time from LTx to a positive culture for fungus was 2.1 months, with 64 patients (56%) being colonized or infected within one month of transplantation. Fungal colonization prior to LTx was present in 56 cases (42%), with eight patients subsequently developing postoperative IFI, 42 continuing to be colonized post LTx as well, and six having no fungal event after transplantation. Eighty-one patients (60%) died or developed graft failure leading to retransplantation within the follow-up time, and 41 patients (31%) developed CLAD.

Survival depending on fungal colonization

Patients who were colonized by fungus post LTx were compared to patients without a postoperative fungal event in the aspect of survival. Analyses revealed no statistically significant increase in the risk of death for colonized patients (HR = 1.06 (95% CI: 0.60 – 1.90), p = 0.832). Comparing all three subgroups (colonized, IFI, no event) showed consistent results, with no increased risk of death for either group (HR, colonized = 1.08 (95% CI: 0.57 – 2.06), p = 0.805, HR, IFI = 1.57 (95% CI: 0.63 – 3.93), p = 0.333) (Figure 21).

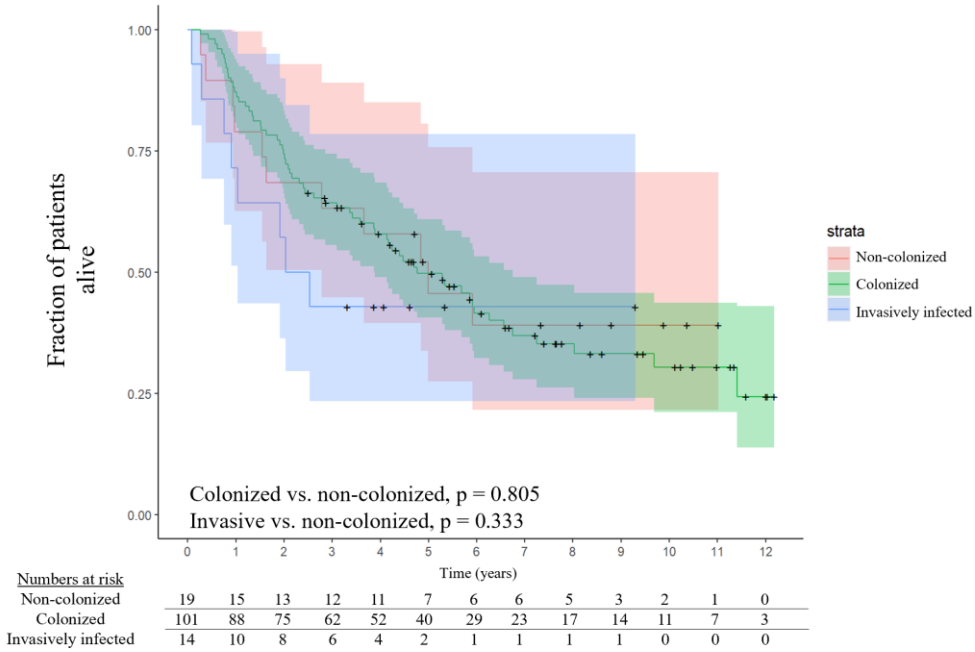

Figure 21: No significant difference in the risk of mortality between subgroups. Comparison of the risk of death with 95% CI between the three subgroups IFI, fungal colonization and, no fungal event. The risk of death was not increased in either subgroup. Numbers at risk table beneath indicates the number of patients alive at each time point. *CI: confidence interval, IFI: invaive fungal infection.*

The application of multivariate analyses, exploring the risk of death depending on postoperative fungal colonization, but including the factors preoperative colonization and underlying pulmonary disease, revealed consistent results, with no significantly increased risk of death for postoperatively colonized patients (HR = 1.37 (95% CI: 0.69 – 2.72), p = 0.370). However, the model did show that the underlying condition CF is a protective factor for the outcome death in LTx recipients (HR, CF = 0.30 (95% CI: 0.09 – 0.95), p = 0.041, HR, COPD = 1.65 (95% CI: 0.66 – 4.08), p = 0.282, HR, PF = 1.38 (95% CI: 0.45 – 4.29), p = 0.573, HR, A1AD = 0.76 (95% CI: 0.23 – 2.53), p = 0.654, HR, PH = 0.31 (95% CI: 0.06 – 1.54), p = 0.153, HR, preoperative fungal colonization = 1.65 (95% CI: 0.80 – 3.39), p = 0.173).

When comparing patients depending on fungal colonization prior to LTx, the results were similar, showing no significantly increased risk of death for colonized patients compared to non-colonized (HR = 1.50 (95% CI: 0.82 – 2.75), p = 0.186).

Development of CLAD depending on fungal colonization

Comparisons of CLAD-free survival, including survival free of CLAD progression, were made. The results showed no significantly increased risk of CLAD for

postoperatively colonized patients compared to patients with no fungal event (HR = 0.82 (95% CI: 0.38 – 1.77), p = 0.612). When comparing all three subgroups of patients (colonized, IFI, no event) there were still no significantly differing risks between the groups (HR, colonized = 1.04 (95% CI: 0.45 – 2.49), p = 0.932, HR, IFI = 1.01 (95% CI: 0.25 – 4.03), p = 0.994) (Figure 22).

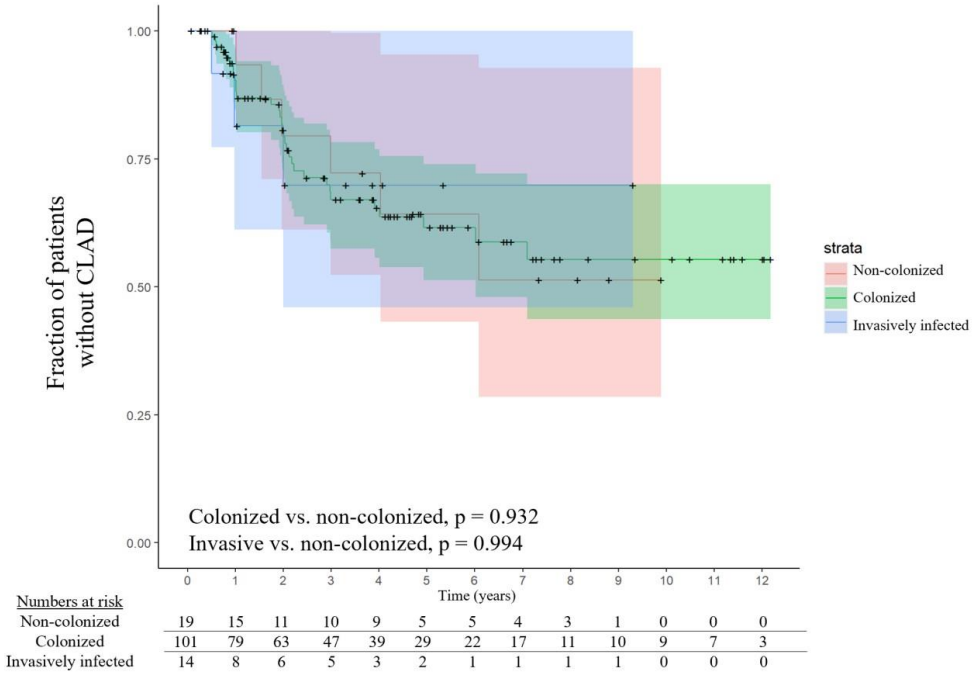

Figure 22: No significant difference in the risk of CLAD compared between subgroups. Comparison of the risk of developing CLAD with 95% CI between the three subgroups IFI, fungal colonization, and no fungal event. The risk of CLAD was not increased in either subgroup. Numbers at risk table beneath indicates the number of patients alive and without CLAD at each time point. *CLAD: chronic lung allograft dysfunction, CI: confidence interval, IFI: invasive fungal infection.*

A multivariate model was fitted to further explore the risk of developing CLAD depending on postoperative fungal colonization. This model included preoperative fungal colonization and underlying pulmonary condition. The results showed no significantly increased risk of CLAD development or progression for colonized patients (HR = 1.19 (95% CI: 0.61 – 2.31), p = 0.612), but did reveal the underlying disease COPD to be a significant risk factor for the development or progression of CLAD (HR, CF = 4.16 (95% CI: 0.68 – 25.54), p = 0.124, HR, COPD = 7.35 (95% CI: 1.11 – 48.88), p = 0.039, HR, PF = 2.47 (95% CI: 0.32 – 19.04), p = 0.386), HR, A1AD = 2.93 (95% CI: 0.38 – 22.89), p = 0.305, HR, PH = 5.08 (95% CI: 0.64 – 40.34), p = 0.124, HR, preoperative fungal colonization = 0.81 (95% CI: 0.30 – 2.22), p = 0.681).

When finally comparing the risk of CLAD depending on preoperative fungal colonization, the results were in line with the previous findings, showing no significantly increased risk of developing CLAD for preoperatively colonized patients (HR = 1.19 (95% CI: 0.61 – 2.31), p = 0.612).

Invasive fungal infection increases the risk of CLAD

When comparing the outcomes of patients with postoperative fungal colonization and IFI, there was no statistically increased risk of death for invasively infected patients (HR = 1.17 (95% CI: 0.36 – 3.79), p = 0.791). There was however a significantly increased risk of developing CLAD for the patients with IFI compared to only colonized patients (HR = 2.57 (95% CI: 1.32 – 5.02), p = 0.006).

The effect of fungal genus

Due to existing literature suggesting there to be a difference in outcomes after IFI based on what type of fungus is causing the infection, we investigated whether this would be true for fungal colonization alone. The analysis showed no such correlation. There was no significant increase in the risk of neither death nor CLAD development for patients colonized with non-candidal fungi compared to patients colonized with candidal fungi (HR, mortality = 1.53 (95% CI: 0.91 – 2.55), p = 0.106, HR, CLAD = 0.99 (95% CI: 0.48 – 2.03), p = 0.982).

Bacterial and viral coinfections

Bacterial coinfections were present at the time of positive fungal cultures or within the first year after LTx in the cases of no fungal event in 84 of all included patients (63%). Viral coinfections were present in 36 patients (27%). In the subgroup of patients with postoperative fungal colonization 55 patients (54%) had bacterial coinfections and 22 had viral coinfections (22%). In the subgroup with postoperative IFI these numbers were ten (71%) and five (36%) respectively. Of the patients with no fungal event after LTx, all had positive bacterial cultures at some point during the first year after LTx, and 14 (74%) had positive viral cultures. When looking into the risks of death and CLAD development, and factoring in coinfections, no significant impact was found.

Paper V

Descriptive results

Paper V includes a total of 318 LTx recipients who were transplanted at one of the three Scandinavian LTx centres Lund, Sweden (n = 56), Gothenburg, Sweden (n = 132) or Copenhagen, Denmark (n = 130). All patients had at least one episode of PCR-verified COVID-19 post LTx, and the follow-up was 365 days after verified

COVID-19. Of all included patients, a total of 31 (10%) underwent single LTx, 253 (79%) underwent double LTx, 10 (3%) underwent heart- and lung transplantation, and the remaining 24 patients (8%) underwent retransplantation. The mean age in the cohort was 55 years (range 18 – 78 years) and the number of male patients included was 155 (49%). The mean time elapsed from LTx to date of positive PCR test for COVID-19 was 7.1 years (2 607 days, range 1 – 10 613 days), the mean time from LTx to the end of follow-up was 7.9 years (2 889 days, range 283 – 10 978 days), and the mean time from positive PCR test for COVID-19 to end of follow-up was 338 days (range 2 – 265 days). Within the follow-up time of one year, a total of 33 patients dies (10%), a low death rate compared to global numbers (99). Thirty-six patients (11%) developed CLAD or experienced progression of a pre-existing CLAD diagnosis within the follow-up period.

The patients were divided into subgroups depending on country of residence (Sweden, n = 188 and Denmark, n = 130), vaccination status at date of positive PCR-test for COVID-19 (fully vaccinated, n = 282 and unvaccinated, n = 36), and time of infection (early, n = 83 and late, n = 235).

Outcome depending on country of residence

Comparison of the survival between patients from Sweden and Denmark revealed no statistically increased risk of death for either country (HR, Sweden = 1.49 (95% CI: 0.68 – 3.26), p = 0.314) (Figure 23). The same was true for the risk of developing CLAD or experiencing progression to a higher grade of CLAD (HR, Sweden = 0.63 (95% CI: 0.32 – 1.25), p = 0.187) (Figure 24).

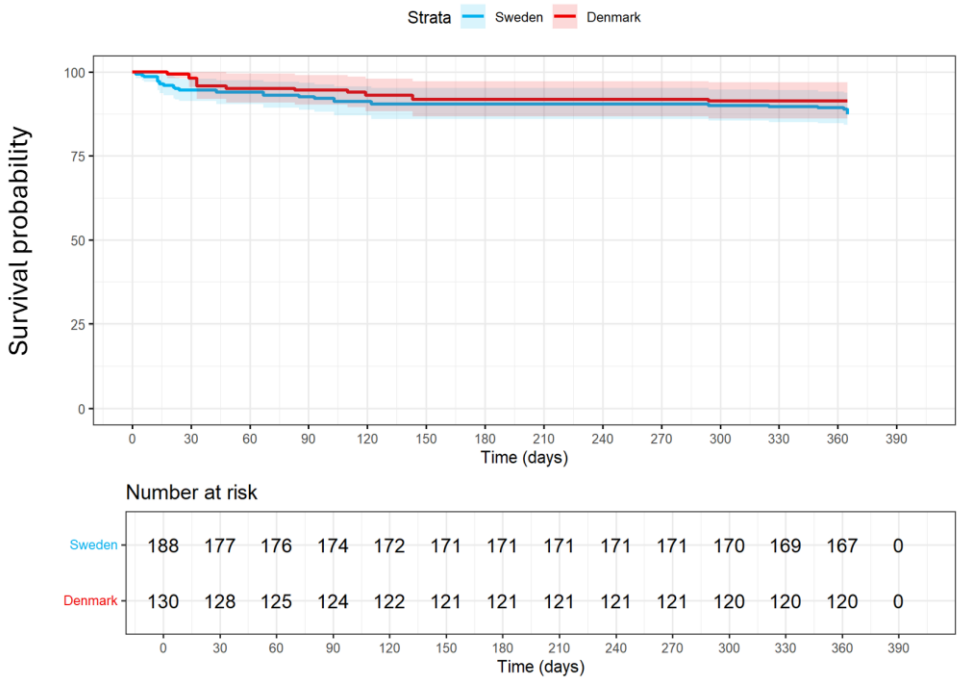

Figure 23: Survival compared between Sweden and Denmark. Kaplan Meier curve showing survival analysis, with no significant difference in the risk of death between the two countries.

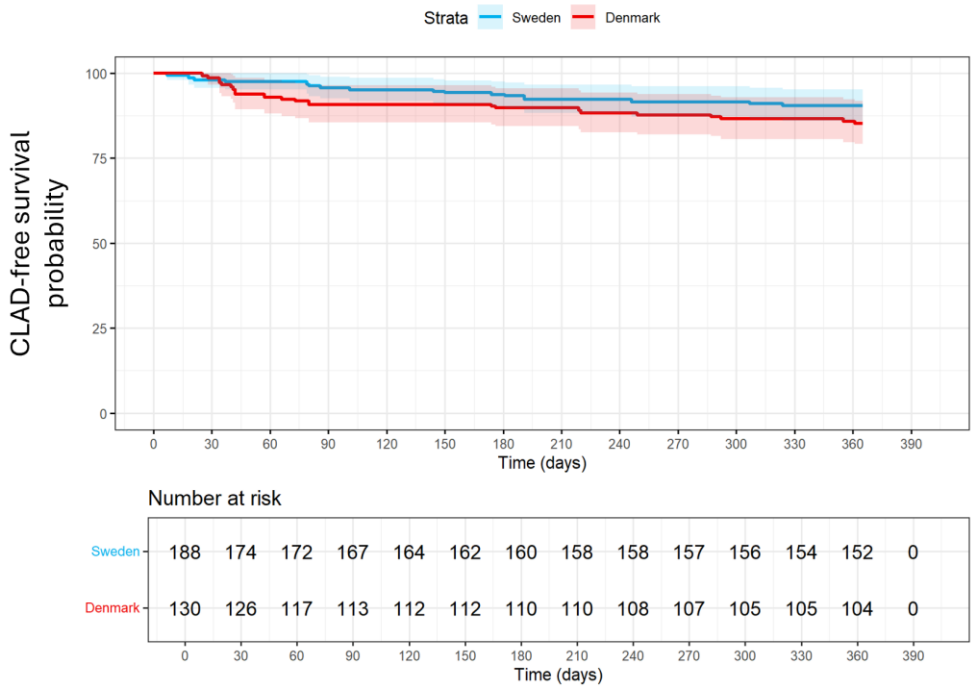

Figure 24: CLAD-free survival compared between Sweden and Denmark. Kaplan Meier curve showing survival analysis, with no significant difference in the risk of CLAD development or progression between the two countries. *CLAD: chronic lung allograft dysfunction.*

Outcome depending on infecting strain of SARS-CoV-2

When comparing survival between patients who were infected by the four different strains of SARS-CoV-2 which were dominant during different periods of the pandemic, a significantly increased risk of death for patients infected with the early strain *Wuhan* could be seen compared to patients infected with the late strain *Omicron* (HR, *Wuhan* = 3.59 (95% CI: 1.53 – 8.44), p = 0.003). The risk of developing CLAD or progressing to a higher grade of CLAD was shown not to differ significantly between any of the strains of the virus.

Outcome depending on vaccination status

Analysis of the risks of death and CLAD development or progression depending on the patients' vaccination status were also carried out. The results showed a significantly increased risk of death for unvaccinated patients compared to fully vaccinated patients (HR, unvaccinated = 3.49 (95% CI: 1.46 – 8.34), p = 0.005) (Figure 25). These results remained consistent when further dividing the patients by country of residence, showing an increased risk of death for Swedish unvaccinated patients compared to both Swedish vaccinated (HR unvaccinated = 3.55 (95% CI: 1.54 – 8.22), p = 0.003) and Danish vaccinated patients (HR unvaccinated = 4.56 (95% CI: 1.81 – 11.46), p = 0.001).

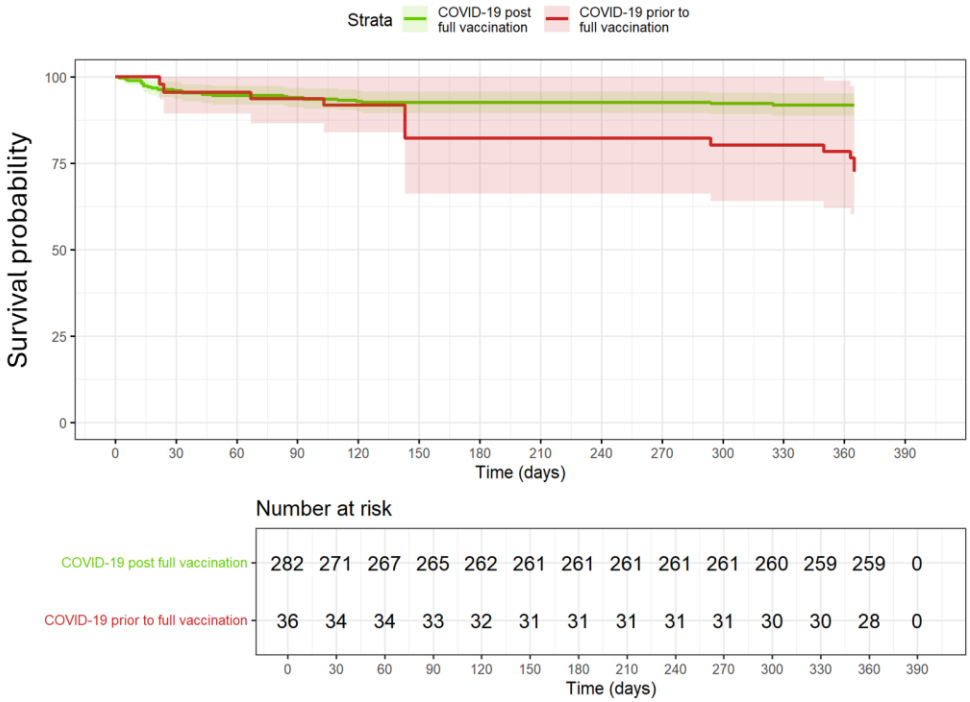

Figure 25: Survival compared between vaccinated and unvaccinated patients. Kaplan Meier curve showing survival analysis, with no significant difference in the risk of death between fully vaccinated patients and unvaccinated patients. *COVID-19: coronavirus disease 2019.*

When assessing the risk of CLAD development or progression between unvaccinated and fully vaccinated patients, no significant differences in risk could be found (HR, unvaccinated = 1.87 (95% CI: 0.57 – 6.11), p = 0.303) (Figure 26). Moreover, an analysis of survival compared between patients with and without development or progression of CLAD was done, showing no significantly increased risk of death for patients who developed CLAD or experienced progression of a pre-existing CLAD diagnosis (HR, development or progression of CLAD = 1.20 (95% CI: 0.41 – 3.47), p = 0.740).

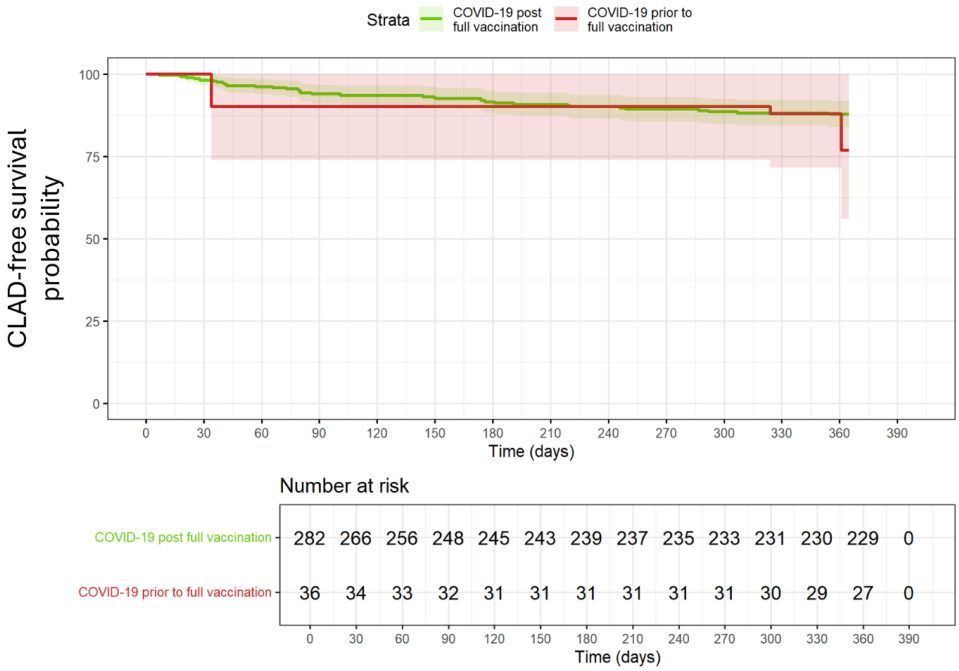

Figure 26: CLAD-free survival compared between vaccinated and unvaccinated patients. Kaplan Meier curve showing survival analysis, with no significant difference in the risk of CLAD development or progression between patients with full vaccination and unvaccinated patients. *CLAD: chronic lung allograft dysfunction, COVID-19: coronavirus disease 2019.*

Discussion

Paper I

With cancers of the respiratory tract being the fourth most common cause of death on a global level, it is arguably one of the more pressing areas of research. The non-small cell category of lung cancer, mainly made up of cases of LUAD and SCC, is challenging to diagnose in early stages, partly due to discrete symptoms, and poor outcomes are all too common (100, 101). Earlier publications have shown reduced mortality rates in primary lung cancer by screening of at-risk patients with low-dose CT (102). Despite this, no screening protocol is widely accepted, due to hesitations regarding the handling of false-positive findings as well as logistical and economic issues. The development of more cost efficient and less invasive methods would be an invaluable addition to the field.

In paper I liquid biopsies in the form of plasma were used for the exploration of potential biomarkers for primary NSCLC. Blood samples were collected once prior to surgical resection of the tumor, and twice after. All patients served as their own internal controls to minimize bias from inherently differing protein expression patterns between individuals. Proteomic composition of the samples was analysed with PEA technology, and significant differences in protein expression were identified in 63 proteins. The twelve proteins with the lowest overall p-values were further explored.

Despite previously published results suggesting that MIC-A/B could not be used to differentiate between different types of pulmonary diseases, they were among the top twelve chosen proteins in paper I (103). These proteins function as ligands to several different immune cells and are involved in antitumoral responses of the immune system. These proteins are naturally expressed in various forms of cancer, including NSCLC. However, the production of tumour-related proteases by the malignant cells has been shown to induce shedding of MIC-A/B, permitting the cancer cells to remain undetected by immune cells (104, 105). High levels of expressed MIC-A/B have also been suggested to be a positive prognostic factor for patients undergoing primary resection for NSCLC (106, 107). The findings of paper I, showing significantly increased expression of MIC-A/B after surgery, indicates radical removal of the NSCLC, previously suppressing expression. This was also validated by larger datasets from the NCBI's GEO.

Another one of the twelve proteins investigated in depth in paper I is the protein FASLG, which is activated by binding of the ligand, FAS, and is involved in the initiation of different forms of induced cell death. The signalling pathways in which FASLG is active also has a role in apoptotic cell death of damaged cells like cancer cells (108). The results of paper I showed significantly increased expression of FASLG one month after resection of the cancer, which is corroborated by a study by Ali *et al.*, demonstrating that FASLG is naturally expressed to a higher degree in healthy tissues, as well as the previously mentioned online GEO (109). The effects of FASLG are inhibited by another protein called TNFRSF6B, which was also among the twelve investigated proteins in paper I (110, 111). In the data collected for paper I, the expression of TNFRSF6B was not higher prior to surgical resection of the cancer compared to postoperative expression levels, although previous research has been able to demonstrate this (108, 110, 111). Interestingly, the levels of FASLG expressed in patients with poor outcomes, defined as recurrence of tumour burden or death, were consistently lower at all three timepoints compared to patients still alive and in remission at the end of follow-up. This suggests a usefulness of FASLG as a promising prognostic biomarker for NSCLC.

A protein called HGF, produced by fibroblasts in the lungs, was also among the more significant proteins in this paper. It is a proto-oncogene which stimulates cell motility, invasion, and morphogenesis. It also acts as a mitogen for both healthy and damaged cells (112). Earlier studies have showed increased levels of HGF in tumour tissue from patients with NSCLC, and increased levels of HGF in plasma have been suggested to correlate with poorer survival (113). In paper I, the plasma levels of HGF showed a decreasing trend between the two postoperative timepoints, and it is likely that with more time the difference would have become more evident (Figure 10).

Among the 12 proteins chosen for detailed literature review was also GPNMB. This is a glycoprotein, involved in the inhibition of T-cell activation, and it has been proven to be overexpressed in several human cancers, including NSCLC (114, 115). Moreover, overexpression of GPNMB has been linked to the potential of metastasis in malignant tumours (116). In this paper, the expression of GPNMB was significantly decreased at the first timepoint after surgical resection of NSCLC, and then significantly increased again at the second postoperative timepoint.

The eight proteins AREG, DLL1, furin, IL-6, MUC-16, TGFα, TNFRSF6B, and VEGFA were all significantly elevated at both postoperative timepoints, approximately one week and one month after surgery, respectively. This may be due to a general inflammatory response caused by the surgical procedure. In conjunction with surgery, inflammatory cells are recruited and activated, releasing substances like bradykinin, which can in turn lead to increased levels of the protein AREG (117, 118). The elevated plasma levels of IL-6, TGFα and DLL1 can likely be explained by these proteins' prominent role in the inflammatory response (119-123). In the process of wound healing and tissue remodelling, the proteins VEGFA and furin are

important, and MUC-16 is an important protein in maintaining the barrier function of the airway mucosa (124-129).

This paper has shown promising results, especially regarding the proteins MIC-A/B and FASLG. Of note though, the substrate used is plasma, introducing a risk of systemic contamination of samples. Further research on larger cohorts and with longer follow-up times would be beneficial. In conclusion, all 12 investigated proteins in paper I have either been previously shown to be elevated in states of inflammation and wound healing, or have a correlation with NSCLC, confirming the value of further research on their potential use as biomarkers for primary NSCLC.

Paper II

In continuation of paper I, this second paper explores the potential for using exhaled air and the particles originating from the distal airways (EBP) as a source for biomarkers. Here, patients with primary LUAD and control patients gave samples of EBP which were analysed with PEA technology. Due to very small sample sizes, in the range of nanograms, the panel applied for proteomic analysis was chosen based on not needing to dilute the samples ("Target 96 Cardiometabolic" panel).

The finding of significantly increased PFR in the group of patients with LUAD compared to control patients indicates the potential of this method to be used in the process of screening at-risk patients in the future. Additionally, the downwards trend of PFR in the month following surgical resection for the cancer patients suggests a potential for monitoring of disease progression as well.

In paper II the cancer patients had significantly higher preoperative levels of the proteins PLTP, CA4, CFHR5, MFAP5, and MET in exhaled breath compared to control patients. However, at the second sampling for the patients with LUAD, one month after surgical resection of the tumour, the expression levels of the proteins PLTP, MFAP5, and MET were lower to the point where they were no longer significantly elevated compared to the control patients. This could potentially be due to radical removal of the suppressant, in this case the cancer.

The protein PLTP is a glycoprotein regulating the transportation of phospholipids, and it is naturally expressed in the pulmonary epithelium. It has also been shown to have a significant involvement in the development of cancer and has been suggested to hold anti-inflammatory properties (130). In paper II, the expression of PLTP showed changes between preoperative and postoperative samples from cancer patients, indicating a potential for use in the evaluation of surgical treatment of LUAD.

Another protein which was found to differ significantly between patients with and without LUAD was CA4, a protein involved in the local pH-regulation within the lungs. It has also been demonstrated that low expression of CA4 is linked to LUAD, and poor outcomes in the form of metastasis and shorter survival (131-133). In the second paper of this thesis, the expression levels of CA4 were surprisingly elevated in LUAD patients at both timepoints compared to control patients, suggesting that this may not be an optimal protein for further exploration as a biomarker in EBP for LUAD.

The protein family CFHR 1 – 5 are proteins involved in the complement system, binding to complement factors. Defective variants of CFHR5 have previously been shown to be involved in the pathological process of hemolytic uremic syndrome. However, the expression of the protein CFHR1 has been demonstrated to be suppressed in LUAD and has been linked to poorer survival (134). Unfortunately, CFHR1 was not part of the protein panel, which was used in paper II, why there are no results on the expression pattern of this specific protein.

The extracellular protein MFAP5 is commonly upregulated in cancer-associated fibroblasts, which is also the case in NSCLC (135, 136). The protein is involved in the differentiation of these cells and has a role in the process of epithelial mesenchymal transition, which is central to cancer metastasis (136-139). In this project, the levels of MFAP5 in EBP were initially expressed in significantly higher levels in LUAD patients prior to surgery, compared to control patients, but one month later this difference was no longer significant. This shows the potential for this protein to be used as a biomarker for LUAD, or to be included in a future biomarker panel.

Finally, the protein MET was also found to be one of three proteins with a trend of lowering expression levels in EBP of cancer patients after surgical resection of a primary LUAD. This is the first time MET is identified as a potential biomarker for LUAD in EBP, and the results are promising, standing in line with previous findings (140). This protein acts as a receptor for the protein HGF, and is involved in cellular migration, proliferation, morphogenesis, and survival. Previous research has shown that mutations in the gene coding for the production of MET are associated with several types of cancer, including NSCLC, and elevated expression of MET in tumour cells has been correlated with a negative impact on survival in LUAD patients (141, 142). The results of paper II were validated both through an ELISA of soluble MET in plasma, and through the use of NCBI's GEO.

Paper III

The massive impact of the COVID-19 pandemic on health care systems all around the world was a major reason for the creation of paper III. Utilizing similar, but even

more advanced methods as in papers I and II, this project aimed to identify biomarkers for COVID-19. In paper III, samples of EBP were collected from patients with PCR-verified COVID-19, patients with respiratory symptoms but no verified COVID-19, and healthy controls. By using LC-MS/MS, an average of 110 proteins were detected in each sample of EBP, something that has not been possible to achieve with other methods like the analysis of EBC (143, 144). The proteins discovered in the collected samples of this project are involved in immune activation, blood coagulation, the acute phase response and cell adhesion among other things and are known to be found in RTLF. The additional analysis of exhaled particle patterns adds depth to the results of paper III, and this has previously been suggested to reflect pulmonary health (145).

The results of this project showed an increase in the accumulated amount of particles exhaled from patients with respiratory symptoms, a phenomena that has been previously established (145-147). When looking at the subgroups of patients in this study, the COV-POS patients demonstrated a significant increase in particle production, with a somewhat skewed distribution pattern towards the smaller particle sizes. Similarly, the COV-NEG patients also had an increase in particle production, although not as pronounced as the COV-POS patients. Suggesting disease-dependent variation between samples. This validates the previous findings of EBP being a suitable means of monitoring pulmonary diseases (148, 149).

An increased understanding of how changes to the RTLF affect its properties, and how different respiratory diseases impacts the proteomic environment in the lungs would be of great value. With the methods used in this part of my thesis work, a new dimension to the processes of diagnosing and monitoring pulmonary disease is added. While bronchoscopy samples of BALF provide vast amounts of information, this is an invasive method which comes with risks for the patient. The analysis of EBP in the current paper provided findings that were well aligned with previous studies, showing overexpression of several proteins of interest (150). The three proteins ORM1, alpha-1 antitrypsin, and haptoglobin are all involved in the body's response to inflammation and were found to be expressed at significantly higher levels in the COV-POS patients compared to HCO and COV-NEG patients.

The protein ORM1, which was identified in almost all analysed samples, is excreted from hepatic cells as a response to stress but has also been suggested to be produced by alveolar cells in similar situations (151). Additionally, increased expression of this protein has been implicated in COVID-19 previously, through studies of patient plasma, also showing correlation with disease severity (150).

Another protein by the name APOA1 was also significantly elevated in EBP from COV-POS patients compared to COV-NEG patients. This is a protein which is expressed in the pulmonary epithelium, and earlier publications have shown involvement of APOA1 in antioxidative and antiviral processes (152-155). Contrary to the findings in paper III, others have demonstrated decreased levels of APOA1 in

plasma of patients with COVID-19 (156, 157). However, there is literature supporting the current findings, with results of correlating APOA1 expression levels and lymphocyte infiltration in the lungs, such as in lung injury (158, 159). This suggests local origin of the increased expression of APOA1, making it a suitable biomarker for lung injury and COVID-19.

The glycoprotein TF, which is secreted from pulmonary epithelial cells and alveolar macrophages, is also involved in the bodily reaction to stress (160). This protein is known for having iron binding properties, but has also been implicated in the coagulation cascade, leading to a state of increased coagulation, something that is also seen in patients with COVID-19 (161). Interestingly, earlier research has been able to show a specific increase in levels of TF in BALF, with plasma levels showing opposite changes with lowered levels of the protein in patients with ARDS, presenting it as an interesting biomarker for disease processes specific to the lungs (162). In addition to this, the levels of TF in EBP from COV-NEG patients were downregulated compared to HCO, indicating that this biomarker could potentially be disease specific for COVID-19.

It would be of immense value to identify methods for continuous evaluation of pulmonary health. In the setting of COVID-19, the virus SARS-CoV-2 induces apoptosis of infected cells, leading to lower production of surfactant (163). Reduced expression of the protein SFTPB has also been demonstrated to precede clinical signs of ARDS (164, 165). This was also reflected in the proteomic composition of the samples in paper III, revealing lowered levels of SFTPB in symptomatic patients, possibly offering a way of identifying varying degrees of pulmonary damage in real time, something that is not possible in the clinic as of today.

Somewhat surprisingly, no proteins related directly to the SARS-CoV-2 virus were identified in the EBP samples. This has also been the case in another study, utilizing PCR analysis to analyse EBP, identifying viral proteins in only 12% of the samples (166). On the other hand, studies using material from the nasopharyngeal region have been successful in isolating proteins directly related to the virus (167, 168). The reason for not detecting such proteins in the current project may be the origin of the samples.

For validating the potential of the proposed biomarkers in this project, a biomarker panel consisting of 11 proteins and PEV values was applied to a random forest machine learning model, which was in turn used to try to differentiate between COVID-19 positive and negative EBP samples. The model achieved an accuracy of 92%, adding to our conviction that this type of biomarker panel can in fact be useful in the diagnosis of COVID-19.

The results of this paper are promising; however, the sample size is relatively small, necessitating more studies like this one before conclusions are drawn. This also introduces a level of uncertainty regarding the sensitivity and specificity of the

machine learning model, and further interesting differences in protein expression levels may have been detected with a larger cohort.

Paper IV

For patients with end-stage pulmonary diseases like COPD, CF or PF, the only definitive treatment option is LTx. However, survival is short, and there are several pressing problems which need to be tackled to improve the outcomes for LTx recipients. One such problem is the frequency of postoperative infections, which together with rejection are one of the leading causes of death after LTx. In fact, both bacterial and viral infections post transplantation have been shown to negatively impact outcomes (57, 169, 170). In addition to this, a considerable proportion of LTx recipients are colonized by fungus either prior to or after transplantation, although the knowledge of how this affects this category of patients over time is sparse. Different studies have resulted in different results, with some suggesting a connection between fungal infections and poor outcomes, and others not showing such a correlation (57, 171-176).

In paper IV we investigated the impact of fungal colonization on the outcomes survival and CLAD-free survival in LTx recipients. In this cohort 42% of the patients were colonized by fungus prior to LTx, and 87% of the patients were colonized after. Over 50% of the included patients presented with positive fungal cultures within one month of LTx. Despite high numbers of colonized patients, the results showed no significant impact on neither death nor CLAD development. They did however reveal a significant negative impact of IFI on the risk of developing CLAD compared to fungal colonization alone. Of the patients with IFI after LTx, approximately 50% were colonized by fungus before transplantation.

On the topic of IFI, a smaller study by Chong *et al.*, including 91 LTx recipients with IFI caused by yeasts or molds, showed an increased mortality rate in infected patients compared to non-infected patients (170). Two other larger studies, including patients infected only by molds, showed three-month and one-year mortality rates of 22% and 44% respectively (177, 178). In paper IV, the mean follow-up time was 4.5 years, and the one-year mortality rate was only 16%. When looking solely at the colonized patients, this number was even lower at 11%, highlighting the importance of separating fungal colonization and IFI as two different entities.

In support of the results mentioned above, two retrospective studies including 191 and 161 LTx recipients respectively showed a connection between IFI caused by both molds and yeasts and poor outcomes (179, 180). There are very few studies though, which investigate the impact of fungal colonization alone, and these are limited by the exclusion of yeasts and yeast-like fungi like *Candida* spp. And

Pneumocystis jirovecii. Moreover, the results have been incohesive, with some studies suggesting a negative impact of fungal colonization, and others not (172, 176, 181-183).

There is ongoing discussion on the topic of infection severity depending on the type of infecting fungus, with some believing that infections caused by the likes of *Aspergillus* spp. and other molds are more difficult to manage and constitute a greater risk compared to yeasts like *Candida* spp. (169, 184, 185). On the other hand, the significant dangers of candidemia have led to other researchers advocating the inclusion of yeasts in studies of fungal infections (186). The results of paper IV showed no significantly increased risk of neither death nor CLAD development for patients colonized with non-candidal fungi compared to patients colonized with candidal spp. of fungi. These results are corroborated by a large multi-centre study by Law *et al.*, showing a lack of association between airway colonization of *Aspergillus* spp. and the development of BOS (176).

Naturally there are many factors influencing the outcomes after LTx, including bacterial and viral coinfections, single LTx and preoperative fungal colonization of the diseased lungs (169, 187-189). In this fourth project, multivariate analysis including the abovementioned factors showed no association with poor outcomes in the form of death or CLAD development. They did however reveal the underlying condition CF to act as a protective factor for the risk of death, something that is likely explained by the low age and lack of comorbidities in this subgroup of LTx recipients (190). On a similar note, the emergence of COPD as a significant risk factor for the development of CLAD may be explained by greater age and poorer health status of these patients (191).

Although the results of paper IV differ somewhat from the majority of previous findings, they also add a new layer to the matter, showing that fungal colonization by fungi of any genus does not negatively impact the outcomes after LTx. This has to our knowledge not been demonstrated before. Furthermore, there are natural explanations to the difference in results, the most important ones being the inclusion of both yeasts and molds, and the separation of colonization and IFI in the current paper. The relatively small sample sizes in some of the subgroups in paper IV does introduce some uncertainty, and further studies on multiple centres and larger cohorts should be encouraged.

Paper V

During the COVID-19 pandemic the LTx recipients were a group of patients especially at risk, in part due to the high doses of immunosuppressive drugs required to prevent rejection (192, 193). Despite the close proximity and many similarities between Sweden and Denmark, the two Scandinavian countries opted for vastly

differing approaches to the pandemic. Many European countries, including Denmark, opted for a stricter approach with mandatory restrictions, while Sweden kept society mostly open and used recommendations rather than restrictions. This has led to a lot of discourse, with some claiming that Sweden failed in their handling of the pandemic, while others have suggested similar effects on the limiting of social contacts regardless of whether the restrictions were obligatory or voluntary (194-197). Furthermore, there has been an increase in the measured sense of loneliness among people living in more restrictive countries during the pandemic (198, 199).

In paper V we evaluate the effects of PCR-verified COVID-19 on the outcomes for LTx recipients in Scandinavia. The current cohort shows a cumulative mortality rate of 10%, which is among the lowest numbers reported in this type of research, with previous studies reporting mortality rates between 8 – 55% in LTx recipients specifically (200-202). The current results also reveal that there does not seem to be any significant differences in the outcomes death and CLAD development between patients from Sweden and Denmark.

Due to antigenic drift there were several different strains of the SARS-CoV-2 virus which circulated and dominated in different time periods during the pandemic (203). When comparing survival and CLAD-free survival between patients infected with the different strains of SARS-CoV-2, the results revealed a significantly increased risk of death for patients infected early in the pandemic compared to patients who were infected at later stages. These results are in line with previous publications, which also show that the late strain *Omicron* causes less severe infections compared to earlier strains (194, 204). Other factors which are likely to have impacted the decreasing mortality of the virus over time include vaccine availability and clinical experience (194). No differences in the risk of CLAD development or progression were found when comparing patients infected with the different strains of SARS-CoV-2.

The fast development and distribution of the mRNA vaccines against COVID-19 undoubtedly played a significant role in curbing the spread of the virus during the pandemic. Interestingly though, LTx recipients have been shown to exhibit lower humoral response rates compared to non-transplant recipients, with response rates after two doses of a vaccine below 40% (192, 193). This is likely due to the treatment of LTx recipients with anti-metabolites like mycophenolic acid (205). Moreover, the antibody titres following vaccination of LTx recipients decline faster over time. This can and has in part been combatted by third and fourth booster doses (192). In paper V, we investigate the impact of two or more doses of any vaccine against COVID-19 on outcomes. The results showed a significantly reduced risk of death for vaccinated patients compared to unvaccinated patients, but there was no difference in the risk of developing or progressing in a pre-existing CLAD diagnosis. This further strengthens the claim that vaccination against COVID-19 is effective in reducing the risk of death in infected patients. This is in line with previous publications (206).

The risk of decreases in pulmonary function following respiratory tract infections in LTx recipients is well established, and a persistent decline in FEV1 which cannot be explained by other aetiologies constitutes a CLAD diagnosis, a complication previously suggested to be linked to COVID-19 (207-209). In the current cohort, only 11% of the included patients developed CLAD or experienced progression to a greater CLAD grade within the first twelve months post COVID-19. These numbers are lower than the estimated one-year CLAD incidence in Scandinavia, possibly due to the general decline in transmission of other respiratory viruses during the pandemic (210, 211). The high CLAD-free survival rates in the current study support the findings that COVID-19 in LTx recipients does not negatively affect graft function within the first year after infection, a fact that has also been shown by others (208, 212).

This project showed no significant differences in outcomes between Swedish and Danish LTx recipients with COVID-19, despite major differences in sociopolitical approach to the pandemic. However, patients in both countries have likely practiced varying degrees of self-isolation regardless of legal reinforcements. Going forward it would be beneficial to conduct similar studies with longer follow-up times to expand the understanding of how coronaviridae affect the long-term outcomes of LTx recipients.

Ethical aspects

All papers included in this thesis are conducted in accordance with the declaration of Helsinki and are approved by local ethical review boards.

Ethical statements

- **Paper I:** The study is performed in accordance with the declaration of Helsinki and approved by the Swedish Ethical Review Authority with Dnr: 2017/519. All patients signed written and informed consents prior to enrollment.

- **Paper II:** The study is conducted in accordance with the declaration of Helsinki and is approved by the Swedish Ethical Review Authority with Dnr: 2017/519. All included patients signed a written, informed consent prior to enrollment.

- **Paper III:** The study is approved by the Swedish Ethical Review Authority with Dnr: 2018/129, 2020–018640427. All patients signed an informed consent form before taking part in the study.

- **Paper IV:** The study was conducted in accordance with the declaration of Helsinki and is approved by the Swedish Ethical Review Authority with Dnr: 2020-07115 and 2020-01864.

- **Paper V:** The study is conducted in accordance with the declaration of Helsinki and is approved by the Swedish Ethical Review Authority with Dnr: 2020-02153 and 2020-01771.

Ethical considerations

Before conducting any research, which involves humans or animals, the added value of the information which stands to be potentially gained should always be weighed against the risks of inflicting mental or physical harm. Below follow some specific considerations which I have reflected upon in the process of working with the projects included in my thesis.

White coat syndrome

As with all medical research including patients and patient samples, one must be careful not to push the subjects in a way that introduces discomfort or suffering. Research is and should be based on voluntary contributions, but due to the inherent power imbalance between a physician and their patient, the line between free will and the feeling of owing something to the person that helps you can become blurred.

The patients included in papers I – III all signed written and informed consent forms prior to giving blood- and/or EBP samples. To reduce the pressure a patient may feel to agree to being in a study, I made a point of always leaving the room for an amount of time before asking the patient to finally sign the consent form. By doing this, I hope that each person had time to read and consider the implications of joining a study without the pressure of onlooking eyes. However, this issue will always be present, and it is important that each researcher takes steps to mitigate the effects of white coat syndrome.

Sensitive patient information

All papers included in this thesis include patient information acquired from personal medical charts, especially papers IV and V. Therefore, all patient information is presented on group levels, and all personal data is stored in a coded manner, with the code corresponding to each individual being physically locked in with limited access. All biological material is also stored with each person's corresponding code in biobanks and will be kept in accordance with the local laws regulating human biobanks.

Conclusions

Paper I

The first study to be included in this thesis shows that the use of quantitative proteomics offers information on molecular interactions, signaling pathways, and biomarker identification by providing the relative protein abundance in select samples. Using plasma as a proteomic source from patients with NSCLC, this study implies that the three proteins MIC-A/B, FASLG, and HGF are valuable biomarkers and may not only be used as indicators of radical removal of NSCLC but also to predict outcomes for these patients.

Paper II

In this paper, PFR and EBP were used to analyze the proteomic data from patients with primary LUAD for the first time. The significant difference in PFR between patients with and without a cancer diagnosis is a potentially useful distinguishing factor between these patient categories. Analysis of the EBPs revealed the two proteins PLTP and MET to be significantly elevated in patients with LUAD, which was further validated with microarray data from a separate cohort. PLTP and MET are thus potential biomarkers for the diagnosis and evaluation of surgical resection of primary LUAD.

Paper III

In this paper, we showed that mass spectrometry based proteomic analysis of EBPs enables new possibilities for diagnostics of pulmonary diseases and detection of biomarkers. The number of particles produced is indicative of pulmonary disease status, and the protein composition differs significantly between healthy persons and patients infected with SARS-CoV-2. Potential biomarkers in EBP include extracellular acute-phase proteins, surfactant-associated proteins, and intracellular proteins. The potential for the use of an EBP biomarker panel in combination with analyses of particle concentration for the diagnosis of COVID-19 is promising.

Paper IV

In this fourth paper of my thesis work, chart reviews of local medical records were performed to shed light on the impact of fungal colonization post LTx on survival and the risk of CLAD development. The results show that fungal colonization alone does not negatively impact neither survival nor the risk of CLAD development, while patients with IFI showed an increased risk of developing CLAD. Further analyses revealed the underlying pulmonary condition COPD to be a risk factor for CLAD development in patients with postoperative fungal colonization, and CF to be a protective factor for death in this same group of patients. Coinfection with either bacteria or viruses did not have any impact on the outcomes.

Paper V

The fifth and final paper included in this thesis explores how COVID-19 affects Scandinavian LTx recipients, and what factors impact these effects. The results clearly demonstrate the efficiency of two or more doses of a vaccine against COVID-19, with a significantly higher risk of death for unvaccinated compared to vaccinated patients. Furthermore, we saw an increased risk of poor outcomes after COVID-19 for patients infected with the earliest strain of SARS-CoV-2 (*Wuhan*) compared to patients who were infected later in the pandemic (*Omicron*). Lastly, we also compared the outcomes between patients from Sweden and Denmark, two neighboring Scandinavian countries with vastly differing sociopolitical approach to the pandemic. Here we saw no difference in the outcomes of Swedish versus Danish patients.

Future perspectives

The research which has led to the creation of the five papers included in this thesis spans the exploration of minimally invasive methods for biomarker detection and factors which influence the two outcomes death and CLAD development after LTx. It identifies several promising proteins for further investigation as potential biomarkers for primary NSCLC. It also offers clarity to largely unknown effects of fungal colonization on LTx outcomes, as well as sheds light on the results of two vastly differing sociopolitical strategies to the recent COVID-19 pandemic. A natural next step would be the continuation of the work, which is started in papers I and II, by performing larger studies, including more subjects and several centres, to deepen the understanding of what role the proteins MET, HGF, FASLG, MIC-A/B, and PLTP play in the pathogenesis of primary NSCLC. Additional measurements and follow-up appointments, and assays performed on other substrates such as tumour tissue, would add a lot of value to the field. Furthermore, additional proteomic analyses of the first two papers' material by using MS would increase the robustness of the results, and potentially identify more interesting biomarkers.

The theory of a biomarker panel, which is discussed in paper III, is highly relevant, and it would be interesting to explore the potential for creating such a panel for other diseases than COVID-19, namely NSCLC, but perhaps also other infectious diseases such as fungal infections.

The work performed in paper IV introduces an argument for evaluating the use of prophylactic antifungal treatment in LTx recipients. The use of such medications is not without complications, and it would be interesting to perform additional chart reviews, looking at the antifungal treatment of LTx recipients with fungal colonization in more depth. Collaborations with other LTx centres would also add value. On a similar note, it would be interesting to expand the scope of paper V, looking at LTx centres outside of Scandinavia as well. The COVID-19 pandemic was likely not the last pandemic this world will see, and more research on which preventive strategies work, and how to best handle fragile patient populations in the future is highly relevant.

Acknowledgements

I want to express my immense gratitude to my people, my colleagues, my community, my friends, my loved ones. This work has been such a journey, with both highs and lows, and I couldn't have done it without the help and support of others. Thank you for being here.

Firstly, a heartfelt thank you to my main supervisor and source of inspiration – **Sandra Lindstedt**. I can't thank you enough for picking me up and taking me on back in my fifth semester of medical school. You saw something in me I didn't know was there. You have believed in me through it all, even when I didn't do so myself. Without you I would not be where I am today. I have learned so much.

To my co-supervisor, **Franziska Olm**, thank you, thank you, thank you. For putting up with me, for always being there to answer my stupid questions, for helping me look for things that are right in front of my nose, for discussing progress, results and possibilities. For always listening. I truly admire you and all the time and energy you put into your own work and others'. I'm so fortunate to call you a friend.

To my second co-supervisor, **Jesper Magnusson**, thank you for being so welcoming on my many data collection trips up to Sahlgrenska in Gothenburg. You have been such a great source of help and inspiration, even before you were officially my supervisor. For this I am very grateful.

To my **family** – mamma, pappa, Otto, Hampus, mormor, morfar, Jens, Kat, Linus, Olga, Villum. The list could go on. How would I ever have done this without you? I have struggled a lot throughout this process and have leaned heavily on you, especially you, världens bästa **mamma**. I love you all so much and am so blessed to have had you by my side from the beginning until now, as well as in my future endeavors. You hold a very big piece of my heart.

Anna Niroomand, I know it sounds cliché, but honestly, what would I do without you? Since we first peeped each other back when you came for your first project, I have grown so attached to you. I fear you will never get rid of me. The same goes for you **Margareta Mittendorfer**, I love you and you are forever my most trusted goose and hype-man. I think I'll always think of you when I boop a snoot.

To the lab mates turned friends, who made going to work fun. **Evamarie Braf, Lotta Looström** and **Fanny Sveréus**, you made this lab a happy place. I've had so

much fun with you and am so grateful for the time we have spent together. I can't wait to cheer you on going forward.

To all my co-authors, but especially to **Jesper Andréasson** and **Gabriel Hirdman**, thank you for being such easy-going and kindhearted souls, it has been a pleasure to work so closely with you. I admire your skill sets immensely.

To my friends, **Ylva**, **Agnès**, **Seda**, **Ebba** – I dare say you know how hard it has been for me at times. I value your friendship more than you probably think and am thankful that you stuck with me even when I was a bit of a bore. I'm happy to say that I have found people who are equally as weird and unapologetically opinionated as me.

To all my colleagues who have made these years into something I will never forget. There are no better people to spend your time at work with (days and nights), I am sure of it. It's said that it takes a village, and boy am I happy that I landed in this one. Firstly, to **Leif Pierre**, you are a very dear friend to me, and it pains me so much that you will no longer be around to give a hug or sit for a supportive chat. I don't know anyone who knows as much as you, whatever the question was we could always turn to you because "Leif will know a guy". I miss you and I wish you were here today. And to **Haider Ghaidan**, who is like you? Always happy, positive, encouraging. You once called me a diamond star and that's stuck with me ever since. You may just be the sweetest man on earth. To **Snejana Hyllén**, thank you for being such a boss lady, I really admire that. At first when I met you, I found you a little intimidating, but as I got to know you, I learned what a wonderfully nice and funny person and teacher you are. To **Dag Edström**, **Martin Stenlo**, **Tibor Huzevka** and **Theo Manolopoulos**, I am grateful for the chats, the laughs and the teaching moments in which you have let me try my hand at various procedures I was probably very likely to mess up (and sometimes did, I'm sure).

I also want to thank my more recent colleagues which I have grown to be very fond of. **Qi Wang**, **Nicholas Bèchet**, **Runchuan Gu**, **Sujeeth Prithiviraj, Niklas Sterner** and **Gunilla Kjellberg**, thank you for this time, and good luck with all your future endeavors.

To the PhD-students that came before me: Mohammed Fakhro, Ellen Broberg, Martin Stenlo, Haider Ghaidan, Anna Niroomand and more, thank you for paving the way and for lending your help where needed. Had I not had your work to read and be inspired by this monstrous task would have been much more difficult.

To my past teachers and inspirations, especially **Mads**, without you I would not be who I am today. Thank you for seeing me and for pushing me, for being there and supporting me when I felt lonely. I often think of you.

Thank you to all the staff working in the wards and the operating rooms, for always being accommodating and for lending a helping hand even though I rarely had good timing in asking.

Finally, I want to thank all research participants, both human and animal. Without you this would not have been possible. I admire your courage and will forever be grateful.

References

1. Olivieri, D, Scoditti, E. 2005. *Impact of environmental factors on lung defences*. European Respiratory Review;14(95):51.
2. Shelly, MP, Lloyd, GM, Park, GR. 1988. *A review of the mechanisms and methods of humidification of inspired gases*. Intensive Care Med;14(1):1-9.
3. Bustamante-Marin, XM, Ostrowski, LE. 2017. *Cilia and Mucociliary Clearance*. Cold Spring Harb Perspect Biol;9(4).
4. Chaudhry, R, Bordoni, B; 2024. *Anatomy, Thorax, Lungs*. StatPearls. Treasure Island (FL) ineligible companies. Disclosure: Bruno Bordoni declares no relevant financial relationships with ineligible companies.: StatPearls Publishing

5. Weibel, ER, Gomez, DM. 1962. *Architecture of the human lung. Use of quantitative methods establishes fundamental relations between size and number of lung structures*. Science;137(3530):577-85.
6. Patwa, A, Shah, A. 2015. *Anatomy and physiology of respiratory system relevant to anaesthesia*. Indian J Anaesth;59(9):533-41.
7. Chen, Q, Hirai, H, Chan, M, Zhang, J, Cho, M, Randell, SH, et al. 2024. *Characterization of perivascular alveolar epithelial stem cells and their niche in lung homeostasis and cancer*. Stem Cell Reports.
8. Davis, JD, Wypych, TP. 2021. *Cellular and functional heterogeneity of the airway epithelium*. Mucosal Immunology;14(5):978-90.
9. Lillehoj, EP, Kim, KC. 2002. *Airway mucus: its components and function*. Archives of Pharmacal Research;25(6):770-80.
10. Czechtizky, W, Su, W, Ripa, L, Schiesser, S, Höijer, A, Cox, RJ; 2022. *Chapter Two - Advances in the design of new types of inhaled medicines*. In: Witty DR, Cox B, editors. Progress in Medicinal Chemistry. 61: Elsevier. p. 93-162.
11. Parra, E, Pérez-Gil, J. 2015. *Composition, structure and mechanical properties define performance of pulmonary surfactant membranes and films*. Chemistry and Physics of Lipids;185:153-75.
12. Chamarthy, MR, Kandathil, A, Kalva, SP. 2018. *Pulmonary vascular pathophysiology*. Cardiovasc Diagn Ther;8(3):208-13.
13. Ugalde, P, Miro, S, Fréchette, E, Deslauriers, J. 2007. *Correlative anatomy for thoracic inlet; glottis and subglottis; trachea, carina, and main bronchi; lobes, fissures, and segments; hilum and pulmonary vascular system; bronchial arteries and lymphatics*. Thorac Surg Clin;17(4):639-59.

14. Liang, C, Shuang, L, Wei, L, Bolduc, JP, Deslauriers, J. 2011. *Correlative anatomy of the pleura and pleural spaces*. Thorac Surg Clin;21(2):177-82, vii-viii.
15. Karpathiou, G, Peoc'h, M. 2019. *Pleura revisited: From histology and pathophysiology to pathology and molecular biology*. Clin Respir J;13(1):3-13.
16. Safarini, OA, Bordoni, B; 2024. *Anatomy, Thorax, Ribs*. StatPearls. Treasure Island (FL) ineligible companies. Disclosure: Bruno Bordoni declares no relevant financial relationships with ineligible companies.: StatPearls Publishing

17. Smith, SE, Darling, GE. 2011. *Surface Anatomy and Surface Landmarks for Thoracic Surgery: Part II*. Thoracic Surgery Clinics;21(2):139-55.
18. Downey, R. 2011. *Anatomy of the Normal Diaphragm*. Thoracic Surgery Clinics;21(2):273-9.
19. Dianbo, C, Wei, L, Bolduc, J-P, Deslauriers, J. 2011. *Correlative Anatomy of the Diaphragm*. Thoracic Surgery Clinics;21(2):281-7.
20. Lynch, HN, Goodman, JE, Bachman, AN. 2021. *Lung physiology and controlled exposure study design*. Journal of Pharmacological and Toxicological Methods;112:107106.
21. Bhatt, SP, Nakhmani, A, Fortis, S, Strand, MJ, Silverman, EK, Sciurba, FC, et al. 2023. *FEV(1)/FVC Severity Stages for Chronic Obstructive Pulmonary Disease*. Am J Respir Crit Care Med;208(6):676-84.
22. Marshall, R. 1958. *The physiology and pharmacology of the pulmonary circulation*. Progress in Cardiovascular Diseases;1(4):341-55.
23. Suresh, K, Shimoda, LA. 2016. *Lung Circulation*. Compr Physiol;6(2):897-943.
24. Townsley, MI. 2012. *Structure and Composition of Pulmonary Arteries, Capillaries, and Veins*. Comprehensive Physiology.
25. Stickland, MK, Lindinger, MI, Olfert, IM, Heigenhauser, GJ, Hopkins, SR. 2013. *Pulmonary gas exchange and acid-base balance during exercise*. Compr Physiol;3(2):693-739.
26. Hamm, LL, Nakhoul, N, Hering-Smith, KS. 2015. *Acid-Base Homeostasis*. Clin J Am Soc Nephrol;10(12):2232-42.
27. World Health Organization. *The top 10 causes of death* 2020 [updated 2020-12-09; cited 2024 Jul 11]. Available from: https://www.who.int/news-room/fact-sheets/detail/the-top-10-causes-of-death.
28. World Cancer Research Fund International. *Worldwide cancer data* [cited 2024 Jul 11]. Available from: https://www.wcrf.org/cancer-trends/worldwide-cancer-data/.
29. Neal, JW, Dahlberg, SE, Wakelee, HA, Aisner, SC, Bowden, M, Huang, Y, et al. 2016. *Erlotinib, cabozantinib, or erlotinib plus cabozantinib as second-line or third-line treatment of patients with EGFR wild-type advanced non-small-cell lung cancer (ECOG-ACRIN 1512): a randomised, controlled, open-label, multicentre, phase 2 trial*. The Lancet Oncology;17(12):1661-71.

30. Molina, JR, Yang, P, Cassivi, SD, Schild, SE, Adjei, AA. 2008. *Non-Small Cell Lung Cancer: Epidemiology, Risk Factors, Treatment, and Survivorship*. Mayo Clinic Proceedings;83(5):584-94.
31. Herbst, RS, Heymach, JV, Lippman, SM. 2008. *Lung cancer*. N Engl J Med;359(13):1367-80.
32. National Cancer Institute. *Non-Small Cell Lung Cancer Treatment (PDQ®)–Health Professional Version* 2024 [updated 2024-06-25; cited 2024 Jul 11]. Available from: https://www.cancer.gov/types/lung/hp/non-small-cell-lung-treatment-pdq.
33. De Koning, HJ, Van Der Aalst, CM, De Jong, PA, Scholten, ET, Nackaerts, K, Heuvelmans, MA, et al. 2020. *Reduced Lung-Cancer Mortality with Volume CT Screening in a Randomized Trial*. New England Journal of Medicine;382(6):503-13.
34. Hoffman, PC, Mauer, AM, Vokes, EE. 2000. *Lung cancer*. Lancet;355(9202):479-85.
35. Arrieta, O, Cruz-Rico, G, Soto-Perez-De-Celis, E, Ramírez-Tirado, L-A, Caballe-Perez, E, Martínez-Hernández, J-N, et al. 2016. *Reduction in Hepatocyte Growth Factor Serum Levels is Associated with Improved Prognosis in Advanced Lung Adenocarcinoma Patients Treated with Afatinib: a Phase II Trial*. Targeted Oncology;11(5):619-29.
36. Medford, ARL, Agrawal, S, Free, CM, Bennett, JA. 2010. *A Prospective Study of Conventional Transbronchial Needle Aspiration: Performance and Cost Utility*. Respiration;79(6):482-9.
37. Lackey, A, Donington, JS. 2013. *Surgical management of lung cancer*. Semin Intervent Radiol;30(2):133-40.
38. Guo, Q, Liu, L, Chen, Z, Fan, Y, Zhou, Y, Yuan, Z, et al. 2022. *Current treatments for non-small cell lung cancer*. Front Oncol;12:945102.
39. Mamdani, H, Matosevic, S, Khalid, AB, Durm, G, Jalal, SI. 2022. *Immunotherapy in Lung Cancer: Current Landscape and Future Directions*. Frontiers in Immunology;13.
40. Uzel, EK, Figen, M, Uzel, Ö. 2019. *Radiotherapy in Lung Cancer: Current and Future Role*. Sisli Etfal Hastan Tip Bul;53(4):353-60.
41. Primc, D, Rački, S, Arnol, M, Marinović, M, Fućak-Primc, A, Muzur, A, et al. 2020. *The Beginnings of Kidney Transplantation in South-East Europe*. Acta Clin Croat;59(1):135-40.
42. Nordham, KD, Ninokawa, S. 2022. *The history of organ transplantation*. Proc (Bayl Univ Med Cent);35(1):124-8.
43. Panchabhai, TS, Chaddha, U, McCurry, KR, Bremner, RM, Mehta, AC. 2018. *Historical perspectives of lung transplantation: connecting the dots*. Journal of Thoracic Disease;10(7):4516-31.
44. Colombo, D, Ammirati, E. 2011. *Cyclosporine in transplantation - a history of converging timelines*. J Biol Regul Homeost Agents;25(4):493-504.
45. Kotloff, RM, Thabut, G. 2011. *Lung Transplantation*. American Journal of Respiratory and Critical Care Medicine;184(2):159-71.
46. Rampolla, R. 2014. *Lung transplantation: an overview of candidacy and outcomes*. Ochsner J;14(4):641-8.

47. Piechura, LM, Yazdchi, F, Harloff, MT, Shim, H, Sharma, NS, Keshk, M, et al. 2021. *Factors Associated with Very Long-Term Survival for Lung Transplant Recipients*. The Journal of Heart and Lung Transplantation;40(4):S159.
48. Bos, S, Vos, R, Van Raemdonck, DE, Verleden, GM. 2020. *Survival in adult lung transplantation: where are we in 2020?* Curr Opin Organ Transplant;25(3):268-73.
49. Iadarola, P, D'Amato, M, Grignano, MA, Viglio, S. 2024. *Sputum proteomics in lung disorders*. Adv Clin Chem;122:171-208.
50. Pennington, KM, Yost, KJ, Escalante, P, Razonable, RR, Kennedy, CC. 2019. *Antifungal prophylaxis in lung transplant: A survey of United States' transplant centers*. Clin Transplant;33(7):e13630.
51. Doğan Kaya, S, Uygun Kızmaz, Y, Türkmen Karaağaç, A. 2024. *Invasive Pulmonary Aspergillosis in Lung Transplant Recipients: Retrospective Clinical Analysis from a Tertiary Transplant Center*. Ann Ital Chir;95(3):294-8.
52. Villalobos, AP-C, Husain, S. 2020. *Infection prophylaxis and management of fungal infections in lung transplant*. Annals of Translational Medicine;8(6):414.
53. Umemura, K, Katada, Y, Nakagawa, S, Hira, D, Yutaka, Y, Tanaka, S, et al. 2024. *Comparison of the safety and cost-effectiveness of nebulized liposomal amphotericin B and amphotericin B deoxycholate for antifungal prophylaxis after lung transplantation*. Journal of Infection and Chemotherapy.
54. Permpalung, N, Liang, T, Gopinath, S, Bazemore, K, Mathew, J, Ostrander, D, et al. 2023. *Invasive fungal infections after respiratory viral infections in lung transplant recipients are associated with lung allograft failure and chronic lung allograft dysfunction within 1 year*. J Heart Lung Transplant;42(7):953-63.
55. Law, N, Hamandi, B, Fegbeutel, C, Silveira, FP, Verschuuren, EA, Ussetti, P, et al. 2019. *Lack of association of Aspergillus colonization with the development of bronchiolitis obliterans syndrome in lung transplant recipients: An international cohort study*. J Heart Lung Transplant;38(9):963-71.
56. Baek, YJ, Cho, YS, Kim, MH, Hyun, JH, Sohn, YJ, Kim, SY, et al. 2021. *The Prediction and Prognosis of Fungal Infection in Lung Transplant Recipients-A Retrospective Cohort Study in South Korea*. J Fungi (Basel);7(8).
57. Kennedy, CC, Razonable, RR. 2017. *Fungal Infections After Lung Transplantation*. Clin Chest Med;38(3):511-20.
58. Pasupneti, S, Manouvakhova, O, Nicolls, M, Hsu, J. 2017. *Aspergillus-related pulmonary diseases in lung transplantation*. Medical Mycology;55(1):96-102.
59. Shweihat, Y, Perry, J, 3rd, Shah, D. 2015. *Isolated Candida infection of the lung*. Respir Med Case Rep;16:18-9.
60. De Mol, W, Bos, S, Beeckmans, H, Lagrou, K, Spriet, I, Verleden, GM, et al. 2021. *Antifungal Prophylaxis After Lung Transplantation: Where Are We Now?* Transplantation;105(12):2538-45.
61. Shitrit, D, Ollech, JE, Ollech, A, Bakal, I, Saute, M, Sahar, G, et al. 2005. *Itraconazole Prophylaxis in Lung Transplant Recipients Receiving Tacrolimus (FK*

506): Efficacy and Drug Interaction. The Journal of Heart and Lung Transplantation;24(12):2148-52.
62. Chang, H-H, Lee, N-Y, Ko, W-C, Lee, H-C, Yang, Y-HK, Wu, C-J, et al. 2010. *Voriconazole inhibition of tacrolimus metabolism in a kidney transplant recipient with fluconazole-resistant cryptococcal meningitis*. International Journal of Infectious Diseases;14(4):e348-e50.
63. 2012. *Family - Coronaviridae*. In: King AMQ, Adams MJ, Carstens EB, Lefkowitz EJ, editors. Virus Taxonomy. San Diego: Elsevier. p. 806-28.
64. Li, H, Liu, SM, Yu, XH, Tang, SL, Tang, CK. 2020. *Coronavirus disease 2019 (COVID-19): current status and future perspectives*. Int J Antimicrob Agents;55(5):105951.
65. Cascella, M, Rajnik, M, Aleem, A, Dulebohn, SC, Di Napoli, R; 2024. *Features, Evaluation, and Treatment of Coronavirus (COVID-19)*. StatPearls. Treasure Island (FL) ineligible companies.: StatPearls Publishing

66. Moraschini, V, Reis, D, Sacco, R, Calasans-Maia, MD. 2022. *Prevalence of anosmia and ageusia symptoms among long-term effects of COVID-19*. Oral Dis;28 Suppl 2:2533-7.
67. Piluso, M, Ferrari, C, Pagani, S, Usai, P, Raschi, S, Parachini, L, et al. 2023. *COVID-19 Acute Respiratory Distress Syndrome: Treatment with Helmet CPAP in Respiratory Intermediate Care Unit by Pulmonologists in the Three Italian Pandemic Waves*. Adv Respir Med;91(5):383-96.
68. World Health Organization. *WHO Coronavirus (COVID-19) dashboard > Deaths [Dashboard]* data.who.int [cited 2024 Sept 18]. Available from: https://data.who.int/dashboards/covid19/deaths.
69. Metzdorf, K, Jacobsen, H, Greweling-Pils, MC, Hoffmann, M, Lüddecke, T, Miller, F, et al. 2023. *TMPRSS2 Is Essential for SARS-CoV-2 Beta and Omicron Infection*. Viruses;15(2).
70. Parasher, A. 2021. *COVID-19: Current understanding of its Pathophysiology, Clinical presentation and Treatment*. Postgraduate Medical Journal;97(1147):312-20.
71. Zhu, Y, Sharma, L, Chang, D. 2023. *Pathophysiology and clinical management of coronavirus disease (COVID-19): a mini-review*. Front Immunol;14:1116131.
72. Azer, SA. 2020. *COVID-19: pathophysiology, diagnosis, complications and investigational therapeutics*. New Microbes and New Infections;37:100738.
73. Lamers, MM, Haagmans, BL. 2022. *SARS-CoV-2 pathogenesis*. Nature Reviews Microbiology;20(5):270-84.
74. Roe, T, Silveira, S, Luo, Z, Osborne, EL, Senthil Murugan, G, Grocott, MPW, et al. 2024. *Particles in Exhaled Air (PExA): Clinical Uses and Future Implications*. Diagnostics;14(10):972.
75. Kita, K, Gawinowska, M, Chełmińska, M, Niedoszytko, M. 2024. *The Role of Exhaled Breath Condensate in Chronic Inflammatory and Neoplastic Diseases of the Respiratory Tract*. Int J Mol Sci;25(13).

76. Little, LD, Barnett, SE, Issitt, T, Bonsall, S, Carolan, VA, Allen, E, et al. 2024. *Volatile organic compound analysis of malignant pleural mesothelioma chorioallantoic membrane xenografts*. Journal of Breath Research;18(4):046010.
77. Amann, A, Costello, BDL, Miekisch, W, Schubert, J, Buszewski, B, Pleil, J, et al. 2014. *The human volatilome: volatile organic compounds (VOCs) in exhaled breath, skin emanations, urine, feces and saliva*. Journal of Breath Research;8(3):034001.
78. Zhang, VRY, Ramachandran, GK, Loo, EXL, Soh, AYS, Yong, WP, Siah, KTH. 2023. *Volatile organic compounds as potential biomarkers of irritable bowel syndrome: A systematic review*. Neurogastroenterology & Motility;35(7).
79. Griese, M, Noss, J, Bredow, CV. 2002. *Protein pattern of exhaled breath condensate and saliva*. PROTEOMICS;2(6):690-6.
80. Broberg, E, Pierre, L, Fakhro, M, Malmsjö, M, Lindstedt, S, Hyllén, S. 2023. *Releasing high positive end-expiratory pressure to a low level generates a pronounced increase in particle flow from the airways*. Intensive Care Medicine Experimental;11(1).
81. Larsson, P, Mirgorodskaya, E, Samuelsson, L, Bake, B, Almstrand, A-C, Bredberg, A, et al. 2012. *Surfactant protein A and albumin in particles in exhaled air*. Respiratory Medicine;106(2):197-204.
82. Behndig, AF, Mirgorodskaya, E, Blomberg, A, Olin, A-C. 2019. *Surfactant Protein A in particles in exhaled air (PExA), bronchial lavage and bronchial wash - a methodological comparison*. Respiratory Research;20(1).
83. Goldstraw, P, Crowley, J, Chansky, K, Giroux, DJ, Groome, PA, Rami-Porta, R, et al. 2007. *The IASLC Lung Cancer Staging Project: proposals for the revision of the TNM stage groupings in the forthcoming (seventh) edition of the TNM Classification of malignant tumours*. J Thorac Oncol;2(8):706-14.
84. Zhang, R, Ma, S, Shanahan, L, Munroe, J, Horn, S, Speedie, S. 2018. *Discovering and identifying New York heart association classification from electronic health records*. BMC Med Inform Decis Mak;18(Suppl 2):48.
85. Husain, S, Sole, A, Alexander, BD, Aslam, S, Avery, R, Benden, C, et al. 2016. *The 2015 International Society for Heart and Lung Transplantation Guidelines for the management of fungal infections in mechanical circulatory support and cardiothoracic organ transplant recipients: Executive summary*. J Heart Lung Transplant;35(3):261-82.
86. Donnelly, JP, Chen, SC, Kauffman, CA, Steinbach, WJ, Baddley, JW, Verweij, PE, et al. 2020. *Revision and Update of the Consensus Definitions of Invasive Fungal Disease From the European Organization for Research and Treatment of Cancer and the Mycoses Study Group Education and Research Consortium*. Clinical Infectious Diseases;71(6):1367-76.
87. Watanabe, T, Hirama, T, Akiba, M, Watanabe, T, Watanabe, Y, Oishi, H, et al. 2024. *COVID-19 pneumonia in lung transplant recipients: understanding risk factors and treatment outcomes in Japan*. Clin Exp Med;24(1):123.
88. Schwarz, K, Biller, H, Windt, H, Koch, W, Hohlfeld, JM. 2010. *Characterization of exhaled particles from the healthy human lung--a systematic analysis in relation to pulmonary function variables*. J Aerosol Med Pulm Drug Deliv;23(6):371-9.

89. Almstrand, A-C, Bake, B, Ljungström, E, Larsson, P, Bredberg, A, Mirgorodskaya, E, et al. 2010. *Effect of airway opening on production of exhaled particles*. Journal of Applied Physiology;108(3):584-8.
90. Olink. *What is PEA?* [cited 2024 Oct 2]. Available from: https://olink.com/technology/what-is-pea.
91. Tyanova, S, Temu, T, Cox, J. 2016. *The MaxQuant computational platform for mass spectrometry-based shotgun proteomics*. Nat Protoc;11(12):2301-19.
92. Gan, SD, Patel, KR. 2013. *Enzyme Immunoassay and Enzyme-Linked Immunosorbent Assay*. Journal of Investigative Dermatology;133(9):1-3.
93. National Library of Medicine. *GEO DataSets* [cited 2024 Oct 3]. Available from: https://www.ncbi.nlm.nih.gov/gds.
94. Broberg, E, Andreasson, J, Fakhro, M, Olin, A-C, Wagner, D, Hyllén, S, et al. 2020. *Mechanically ventilated patients exhibit decreased particle flow in exhaled breath as compared to normal breathing patients*. ERJ Open Research;6(1):00198-2019.
95. Willforss, J, Chawade, A, Levander, F. 2019. *NormalyzerDE: Online Tool for Improved Normalization of Omics Expression Data and High-Sensitivity Differential Expression Analysis*. J Proteome Res;18(2):732-40.
96. Zhu, L, Malatras, A, Thorley, M, Aghoghogbe, I, Mer, A, Duguez, S, et al. 2015. *CellWhere: graphical display of interaction networks organized on subcellular localizations*. Nucleic Acids Res;43(W1):W571-5.
97. Quan, H, Li, B, Couris, CM, Fushimi, K, Graham, P, Hider, P, et al. 2011. *Updating and validating the Charlson comorbidity index and score for risk adjustment in hospital discharge abstracts using data from 6 countries*. Am J Epidemiol;173(6):676-82.
98. Wang, W, Liu, H, Li, G. 2022. *What's the difference between lung adenocarcinoma and lung squamous cell carcinoma? Evidence from a retrospective analysis in a cohort of Chinese patients*. Front Endocrinol (Lausanne);13:947443.
99. Chambers, DC, Cherikh, WS, Harhay, MO, Hayes, D, Jr., Hsich, E, Khush, KK, et al. 2019. *The International Thoracic Organ Transplant Registry of the International Society for Heart and Lung Transplantation: Thirty-sixth adult lung and heart-lung transplantation Report-2019; Focus theme: Donor and recipient size match*. J Heart Lung Transplant;38(10):1042-55.
100. Cagle, PT, Allen, TC, Olsen, RJ. 2013. *Lung cancer biomarkers: present status and future developments*. Arch Pathol Lab Med;137(9):1191-8.
101. American Cancer Society. *Cancer Facts & Figures 2015* [cited 2024 Oct 11]. Available from: https://www.cancer.org/research/cancer-facts-statistics/all-cancer-facts-figures/cancer-facts-figures-2015.html.
102. Field, JK, Vulkan, D, Davies, MPA, Baldwin, DR, Brain, KE, Devaraj, A, et al. 2021. *Lung cancer mortality reduction by LDCT screening: UKLS randomised trial results and international meta-analysis*. Lancet Reg Health Eur;10:100179.
103. Djureinovic, D, Pontén, V, Landelius, P, Al Sayegh, S, Kappert, K, Kamali-Moghaddam, M, et al. 2019. *Multiplex plasma protein profiling identifies novel*

markers to discriminate patients with adenocarcinoma of the lung. BMC Cancer;19(1):741.
104. Ghadially, H, Brown, L, Lloyd, C, Lewis, L, Lewis, A, Dillon, J, et al. 2017. *MHC class I chain-related protein A and B (MICA and MICB) are predominantly expressed intracellularly in tumour and normal tissue*. Br J Cancer;116(9):1208-17.
105. . 2018. *Blocking MICA/MICB Shedding Reactivates Antitumor Immunity*. Cancer Discovery;8(6):OF20-OF.
106. Zhao, Y, Chen, N, Yu, Y, Zhou, L, Niu, C, Liu, Y, et al. 2017. *Prognostic value of MICA/B in cancers: a systematic review and meta-analysis*. Oncotarget;8(56):96384-95.
107. Okita, R, Yukawa, T, Nojima, Y, Maeda, A, Saisho, S, Shimizu, K, et al. 2016. *MHC class I chain-related molecule A and B expression is upregulated by cisplatin and associated with good prognosis in patients with non-small cell lung cancer*. Cancer Immunol Immunother;65(5):499-509.
108. Liu, W, Ramagopal, U, Cheng, H, Bonanno, JB, Toro, R, Bhosle, R, et al. 2016. *Crystal Structure of the Complex of Human FasL and Its Decoy Receptor DcR3*. Structure;24(11):2016-23.
109. Ali, AS, Perren, A, Lindskog, C, Welin, S, Sorbye, H, Grönberg, M, et al. 2020. *Candidate protein biomarkers in pancreatic neuroendocrine neoplasms grade 3*. Sci Rep;10(1):10639.
110. Bai, C, Connolly, B, Metzker, ML, Hilliard, CA, Liu, X, Sandig, V, et al. 2000. *Overexpression of M68/DcR3 in human gastrointestinal tract tumors independent of gene amplification and its location in a four-gene cluster*. Proc Natl Acad Sci U S A;97(3):1230-5.
111. Pitti, RM, Marsters, SA, Lawrence, DA, Roy, M, Kischkel, FC, Dowd, P, et al. 1998. *Genomic amplification of a decoy receptor for Fas ligand in lung and colon cancer*. Nature;396(6712):699-703.
112. Tsao, MS, Liu, N, Chen, JR, Pappas, J, Ho, J, To, C, et al. 1998. *Differential expression of Met/hepatocyte growth factor receptor in subtypes of non-small cell lung cancers*. Lung Cancer;20(1):1-16.
113. Siegfried, JM, Weissfeld, LA, Singh-Kaw, P, Weyant, RJ, Testa, JR, Landreneau, RJ. 1997. *Association of immunoreactive hepatocyte growth factor with poor survival in resectable non-small cell lung cancer*. Cancer Res;57(3):433-9.
114. Ott, PA, Pavlick, AC, Johnson, DB, Hart, LL, Infante, JR, Luke, JJ, et al. 2019. *A phase 2 study of glembatumumab vedotin, an antibody-drug conjugate targeting glycoprotein NMB, in patients with advanced melanoma*. Cancer;125(7):1113-23.
115. Funk, T, Fuchs, AR, Altdörfer, VS, Klein, R, Autenrieth, SE, Müller, MR, et al. 2020. *Monocyte-derived dendritic cells display a highly activated phenotype and altered function in patients with familial Mediterranean fever*. Clin Exp Immunol;201(1):1-11.
116. Li, YN, Zhang, L, Li, XL, Cui, DJ, Zheng, HD, Yang, SY, et al. 2014. *Glycoprotein nonmetastatic B as a prognostic indicator in small cell lung cancer*. Apmis;122(2):140-6.

117. Deacon, K, Knox, AJ. 2015. *Human airway smooth muscle cells secrete amphiregulin via bradykinin/COX-2/PGE2, inducing COX-2, CXCL8, and VEGF expression in airway epithelial cells*. Am J Physiol Lung Cell Mol Physiol;309(3):L237-49.
118. Zaiss, DMW, Gause, WC, Osborne, LC, Artis, D. 2015. *Emerging functions of amphiregulin in orchestrating immunity, inflammation, and tissue repair*. Immunity;42(2):216-26.
119. Sakamoto, K, Arakawa, H, Mita, S, Ishiko, T, Ikei, S, Egami, H, et al. 1994. *Elevation of circulating interleukin 6 after surgery: factors influencing the serum level*. Cytokine;6(2):181-6.
120. Jones, SA, Jenkins, BJ. 2018. *Recent insights into targeting the IL-6 cytokine family in inflammatory diseases and cancer*. Nat Rev Immunol;18(12):773-89.
121. Akira, S, Hirano, T, Taga, T, Kishimoto, T. 1990. *Biology of multifunctional cytokines: IL 6 and related molecules (IL 1 and TNF)*. Faseb j;4(11):2860-7.
122. Keewan, E, Naser, SA. 2020. *The Role of Notch Signaling in Macrophages during Inflammation and Infection: Implication in Rheumatoid Arthritis?* Cells;9(1).
123. Kimball, AS, Joshi, AD, Boniakowski, AE, Schaller, M, Chung, J, Allen, R, et al. 2017. *Notch Regulates Macrophage-Mediated Inflammation in Diabetic Wound Healing*. Front Immunol;8:635.
124. Belizon, A, Balik, E, Feingold, DL, Bessler, M, Arnell, TD, Forde, KA, et al. 2006. *Major abdominal surgery increases plasma levels of vascular endothelial growth factor: open more so than minimally invasive methods*. Ann Surg;244(5):792-8.
125. Pei, D, Weiss, SJ. 1995. *Furin-dependent intracellular activation of the human stromelysin-3 zymogen*. Nature;375(6528):244-7.
126. Guo, C, Jiang, J, Elliott, JM, Piacentini, L. 2005. *Paradigmatic identification of MMP-2 and MT1-MMP activation systems in cardiac fibroblasts cultured as a monolayer*. J Cell Biochem;94(3):446-59.
127. Cordova, ZM, Grönholm, A, Kytölä, V, Taverniti, V, Hämäläinen, S, Aittomäki, S, et al. 2016. *Myeloid cell expressed proprotein convertase FURIN attenuates inflammation*. Oncotarget;7(34):54392-404.
128. Haridas, D, Ponnusamy, MP, Chugh, S, Lakshmanan, I, Seshacharyulu, P, Batra, SK. 2014. *MUC16: molecular analysis and its functional implications in benign and malignant conditions*. Faseb j;28(10):4183-99.
129. Kesimer, M, Scull, M, Brighton, B, DeMaria, G, Burns, K, O'Neal, W, et al. 2009. *Characterization of exosome-like vesicles released from human tracheobronchial ciliated epithelium: a possible role in innate defense*. Faseb j;23(6):1858-68.
130. Albers, JJ, Vuletic, S, Cheung, MC. 2012. *Role of plasma phospholipid transfer protein in lipid and lipoprotein metabolism*. Biochim Biophys Acta;1821(3):345-57.
131. Xu, Y, Xu, WH, Shi, SN, Yang, XL, Ren, YR, Zhuang, XY, et al. 2020. *Carbonic Anhydrase 4 serves as a Clinicopathological Biomarker for Outcomes and*

Immune Infiltration in Renal Cell Carcinoma, Lower Grade Glioma, Lung Adenocarcinoma and Uveal Melanoma. J Cancer;11(20):6101-13.
132. Yu, DH, Huang, JY, Liu, XP, Ruan, XL, Chen, C, Hu, WD, et al. 2020. *Effects of hub genes on the clinicopathological and prognostic features of lung adenocarcinoma*. Oncol Lett;19(2):1203-14.
133. Chen, J, Hu, L, Zhang, F, Wang, J, Chen, J, Wang, Y. 2017. *Downregulation of carbonic anhydrase IV contributes to promotion of cell proliferation and is associated with poor prognosis in non-small cell lung cancer*. Oncol Lett;14(4):5046-50.
134. Wu, G, Yan, Y, Wang, X, Ren, X, Chen, X, Zeng, S, et al. 2019. *CFHR1 is a potentially downregulated gene in lung adenocarcinoma*. Mol Med Rep;20(4):3642-8.
135. Yeung, TL, Leung, CS, Yip, KP, Sheng, J, Vien, L, Bover, LC, et al. 2019. *Anticancer Immunotherapy by MFAP5 Blockade Inhibits Fibrosis and Enhances Chemosensitivity in Ovarian and Pancreatic Cancer*. Clin Cancer Res;25(21):6417-28.
136. Navab, R, Strumpf, D, Bandarchi, B, Zhu, CQ, Pintilie, M, Ramnarine, VR, et al. 2011. *Prognostic gene-expression signature of carcinoma-associated fibroblasts in non-small cell lung cancer*. Proc Natl Acad Sci U S A;108(17):7160-5.
137. Yuan, X, Wu, H, Han, N, Xu, H, Chu, Q, Yu, S, et al. 2014. *Notch signaling and EMT in non-small cell lung cancer: biological significance and therapeutic application*. J Hematol Oncol;7:87.
138. Sharif, A, Shaji, A, Chammaa, M, Pawlik, E, Fernandez-Valdivia, R. 2020. *Notch Transduction in Non-Small Cell Lung Cancer*. Int J Mol Sci;21(16).
139. Database, GTHG. MFAP5 Gene Protein Coding GeneCards The Human Gene Database [cited 2021 28/7]. Available from: https://www.genecards.org/cgi-bin/carddisp.pl?gene=MFAP5.
140. Lv, H, Shan, B, Tian, Z, Li, Y, Zhang, Y, Wen, S. 2015. *Soluble c-Met is a reliable and sensitive marker to detect c-Met expression level in lung cancer*. Biomed Res Int;2015:626578.
141. Matsumoto, K, Umitsu, M, De Silva, DM, Roy, A, Bottaro, DP. 2017. *Hepatocyte growth factor/MET in cancer progression and biomarker discovery*. Cancer Sci;108(3):296-307.
142. Masuya, D, Huang, C, Liu, D, Nakashima, T, Kameyama, K, Haba, R, et al. 2004. *The tumour-stromal interaction between intratumoral c-Met and stromal hepatocyte growth factor associated with tumour growth and prognosis in non-small-cell lung cancer patients*. Br J Cancer;90(8):1555-62.
143. Lacombe, M, Marie-Desvergne, C, Combes, F, Kraut, A, Bruley, C, Vandenbrouck, Y, et al. 2018. *Proteomic characterization of human exhaled breath condensate*. J Breath Res;12(2):021001.
144. Muccilli, V, Saletti, R, Cunsolo, V, Ho, J, Gili, E, Conte, E, et al. 2015. *Protein profile of exhaled breath condensate determined by high resolution mass spectrometry*. J Pharm Biomed Anal;105:134-49.
145. Stenlo, M, Hyllén, S, Silva, IAN, Bölükbas, DA, Pierre, L, Hallgren, O, et al. 2020. *Increased particle flow rate from airways precedes clinical signs of ARDS*

in a porcine model of LPS-induced acute lung injury. Am J Physiol Lung Cell Mol Physiol;318(3):L510-l7.
146. Stenlo, M, Silva, IAN, Hyllén, S, Bölükbas, DA, Niroomand, A, Grins, E, et al. 2021. *Monitoring lung injury with particle flow rate in LPS- and COVID-19-induced ARDS*. Physiol Rep;9(13):e14802.
147. Edwards, DA, Ausiello, D, Salzman, J, Devlin, T, Langer, R, Beddingfield, BJ, et al. 2021. *Exhaled aerosol increases with COVID-19 infection, age, and obesity*. Proc Natl Acad Sci U S A;118(8).
148. Hallgren, F, Stenlo, M, Niroomand, A, Broberg, E, Hyllén, S, Malmsjö, M, et al. 2021. *Particle flow rate from the airways as fingerprint diagnostics in mechanical ventilation in the intensive care unit: a randomised controlled study*. ERJ Open Res;7(3).
149. Broberg, E, Wlosinska, M, Algotsson, L, Olin, AC, Wagner, D, Pierre, L, et al. 2018. *A new way of monitoring mechanical ventilation by measurement of particle flow from the airways using Pexa method in vivo and during ex vivo lung perfusion in DCD lung transplantation*. Intensive Care Med Exp;6(1):18.
150. Shu, T, Ning, W, Wu, D, Xu, J, Han, Q, Huang, M, et al. 2020. *Plasma Proteomics Identify Biomarkers and Pathogenesis of COVID-19*. Immunity;53(5):1108-22.e5.
151. Crestani, B, Rolland, C, Lardeux, B, Fournier, T, Bernuau, D, Poüs, C, et al. 1998. *Inducible expression of the alpha1-acid glycoprotein by rat and human type II alveolar epithelial cells*. J Immunol;160(9):4596-605.
152. Gordon, SM, Hofmann, S, Askew, DS, Davidson, WS. 2011. *High density lipoprotein: it's not just about lipid transport anymore*. Trends Endocrinol Metab;22(1):9-15.
153. Georgila, K, Vyrla, D, Drakos, E. 2019. *Apolipoprotein A-I (ApoA-I), Immunity, Inflammation and Cancer*. Cancers (Basel);11(8).
154. Catapano, AL, Pirillo, A, Bonacina, F, Norata, GD. 2014. *HDL in innate and adaptive immunity*. Cardiovasc Res;103(3):372-83.
155. Lee, E, Lee, EJ, Kim, H, Jang, A, Koh, E, Uh, ST, et al. 2013. *Overexpression of apolipoprotein A1 in the lung abrogates fibrosis in experimental silicosis*. PLoS One;8(2):e55827.
156. Shen, B, Yi, X, Sun, Y, Bi, X, Du, J, Zhang, C, et al. 2020. *Proteomic and Metabolomic Characterization of COVID-19 Patient Sera*. Cell;182(1):59-72.e15.
157. Schmelter, F, Föh, B, Mallagaray, A, Rahmöller, J, Ehlers, M, Lehrian, S, et al. 2021. *Metabolic and Lipidomic Markers Differentiate COVID-19 From Non-Hospitalized and Other Intensive Care Patients*. Front Mol Biosci;8:737039.
158. Nukui, Y, Miyazaki, Y, Suhara, K, Okamoto, T, Furusawa, H, Inase, N. 2018. *Identification of apolipoprotein A-I in BALF as a biomarker of sarcoidosis*. Sarcoidosis Vasc Diffuse Lung Dis;35(1):5-15.
159. Mehrani, H, Ghanei, M, Aslani, J, Golmanesh, L. 2009. *Bronchoalveolar lavage fluid proteomic patterns of sulfur mustard-exposed patients*. Proteomics Clin Appl;3(10):1191-200.
160. Yang, F, Friedrichs, WE, Coalson, JJ. 1997. *Regulation of transferrin gene expression during lung development and injury*. Am J Physiol;273(2 Pt 1):L417-26.

161. Tang, X, Zhang, Z, Fang, M, Han, Y, Wang, G, Wang, S, et al. 2020. *Transferrin plays a central role in coagulation balance by interacting with clotting factors*. Cell Res;30(2):119-32.
162. Krsek-Staples, JA, Kew, RR, Webster, RO. 1992. *Ceruloplasmin and transferrin levels are altered in serum and bronchoalveolar lavage fluid of patients with the adult respiratory distress syndrome*. Am Rev Respir Dis;145(5):1009-15.
163. Xu, Z, Shi, L, Wang, Y, Zhang, J, Huang, L, Zhang, C, et al. 2020. *Pathological findings of COVID-19 associated with acute respiratory distress syndrome*. Lancet Respir Med;8(4):420-2.
164. Rühl, N, Lopez-Rodriguez, E, Albert, K, Smith, BJ, Weaver, TE, Ochs, M, et al. 2019. *Surfactant Protein B Deficiency Induced High Surface Tension: Relationship between Alveolar Micromechanics, Alveolar Fluid Properties and Alveolar Epithelial Cell Injury*. Int J Mol Sci;20(17).
165. Oratis, AT, Bush, JWM, Stone, HA, Bird, JC. 2020. *A new wrinkle on liquid sheets: Turning the mechanism of viscous bubble collapse upside down*. Science;369(6504):685-8.
166. Viklund, E, Kokelj, S, Larsson, P, Nordén, R, Andersson, M, Beck, O, et al. 2022. *Severe acute respiratory syndrome coronavirus 2 can be detected in exhaled aerosol sampled during a few minutes of breathing or coughing*. Influenza Other Respir Viruses;16(3):402-10.
167. Ihling, C, Tänzler, D, Hagemann, S, Kehlen, A, Hüttelmaier, S, Arlt, C, et al. 2020. *Mass Spectrometric Identification of SARS-CoV-2 Proteins from Gargle Solution Samples of COVID-19 Patients*. J Proteome Res;19(11):4389-92.
168. Zakharova, N, Kozyr, A, Ryabokon, AM, Indeykina, M, Strelnikova, P, Bugrova, A, et al. 2021. *Mass spectrometry based proteome profiling of the exhaled breath condensate for lung cancer biomarkers search*. Expert Rev Proteomics;18(8):637-42.
169. Samanta, P, Clancy, CJ, Nguyen, MH. 2021. *Fungal infections in lung transplantation*. Journal of Thoracic Disease;13(11):6695-707.
170. Chong, PP, Kennedy, CC, Hathcock, MA, Kremers, WK, Razonable, RR. 2015. *Epidemiology of invasive fungal infections in lung transplant recipients on long-term azole antifungal prophylaxis*. Clinical Transplantation;29(4):311-8.
171. Solé, A, Salavert, M. 2008. *Fungal infections after lung transplantation*. Transplantation Reviews;22(2):89-104.
172. Weigt, SS, Copeland, CF, Derhovanessian, A, Shino, MY, Davis, WA, Snyder, LD, et al. 2013. *Colonization With Small Conidia Aspergillus Species Is Associated With Bronchiolitis Obliterans Syndrome: A Two-Center Validation Study*. American Journal of Transplantation;13(4):919-27.
173. Arthurs, SK, Eid, AJ, Deziel, PJ, Marshall, WF, Cassivi, SD, Walker, RC, et al. 2010. *The impact of invasive fungal diseases on survival after lung transplantation*. Clinical Transplantation;24(3):341-8.
174. Nicod, LP, Pache, JC, Howarth, N. 2001. *Fungal infections in transplant recipients*. European Respiratory Journal;17(1):133-40.

175. Boutin, CA, Desjardins, M, Luong, ML. 2022. *Fungal infection and chronic lung allograft dysfunction: A dangerous combination*. Transplant Infectious Disease;24(6).
176. Law, N, Hamandi, B, Fegbeutel, C, Silveira, FP, Verschuuren, EA, Ussetti, P, et al. 2019. *Lack of association of Aspergillus colonization with the development of bronchiolitis obliterans syndrome in lung transplant recipients: An international cohort study*. The Journal of Heart and Lung Transplantation;38(9):963-71.
177. Doligalski, CT, Benedict, K, Cleveland, AA, Park, B, Derado, G, Pappas, PG, et al. 2014. *Epidemiology of Invasive Mold Infections in Lung Transplant Recipients*. American Journal of Transplantation;14(6):1328-33.
178. Vazquez, R, Vazquez-Guillamet, MC, Suarez, J, Mooney, J, Montoya, JG, Dhillon, GS. 2015. *Invasive mold infections in lung and heart-lung transplant recipients: Stanford University experience*. Transplant Infectious Disease;17(2):259-66.
179. Le Pavec, J, Pradère, P, Gigandon, A, Dauriat, G, Dureault, A, Aguilar, C, et al. 2021. *Risk of Lung Allograft Dysfunction Associated With Aspergillus Infection*. Transplant Direct;7(3):e675.
180. Valentine, VG, Gupta, MR, Walker, JE, Jr., Seoane, L, Bonvillain, RW, Lombard, GA, et al. 2009. *Effect of etiology and timing of respiratory tract infections on development of bronchiolitis obliterans syndrome*. J Heart Lung Transplant;28(2):163-9.
181. Weight, SS, Elashoff, RM, Huang, C, Ardehali, A, Gregson, AL, Kubak, B, et al. 2009. *Aspergillus Colonization of the Lung Allograft Is a Risk Factor for Bronchiolitis Obliterans Syndrome*. American Journal of Transplantation;9(8):1903-11.
182. Atchade, E, Desmard, M, Kantor, E, Genève, C, Tebano, G, De Tymowski, C, et al. 2020. *Fungal Isolation in Respiratory Tract After Lung Transplantation: Epidemiology, Clinical Consequences, and Associated Factors*. Transplant Proc;52(1):326-32.
183. Peghin, M, Monforte, V, Martin-Gomez, M-T, Ruiz-Camps, I, Berastegui, C, Saez, B, et al. 2016. *10 years of prophylaxis with nebulized liposomal amphotericin B and the changing epidemiology ofAspergillusspp. infection in lung transplantation*. Transplant International;29(1):51-62.
184. Saral, R. 1991. *Candida and Aspergillus infections in immunocompromised patients: an overview*. Rev Infect Dis;13(3):487-92.
185. Escamilla, JE, January, SE, Vazquez Guillamet, R. 2023. *Diagnosis and Treatment of Fungal Infections in Lung Transplant Recipients*. Pathogens;12(5):694.
186. Marinelli, T, Pennington, KM, Hamandi, B, Donahoe, L, Rotstein, C, Martinu, T, et al. 2022. *Epidemiology of candidemia in lung transplant recipients and risk factors for candidemia in the early posttransplant period in the absence of universal antifungal prophylaxis*. Transpl Infect Dis;24(2):e13812.
187. Dettori, M, Riccardi, N, Canetti, D, Antonello, RM, Piana, AF, Palmieri, A, et al. 2024. *Infections in lung transplanted patients: A review*. Pulmonology;30(3):287-304.

188. Phoompoung, P, Villalobos, APC, Jain, S, Foroutan, F, Orchanian-Cheff, A, Husain, S. 2022. *Risk factors of invasive fungal infections in lung transplant recipients: A systematic review and meta-analysis.* J Heart Lung Transplant;41(2):255-62.
189. Vadnerkar, A, Clancy, CJ, Celik, U, Yousem, SA, Mitsani, D, Toyoda, Y, et al. 2010. *Impact of Mold Infections in Explanted Lungs on Outcomes of Lung Transplantation*. Transplantation;89(2):253-60.
190. Urlik, M, Stącel, T, Latos, M, Nęcki, M, Zawadzki, F, Pasek, P, et al. 2022. *Results of Lung Transplantations Among Cystic Fibrosis Patients: A Single-Center Study*. Transplantation Proceedings;54(4):1082-5.
191. Verleden, GM, Gottlieb, J. 2023. *Lung transplantation for COPD/pulmonary emphysema*. Eur Respir Rev;32(167).
192. Kawana, S, Sugimoto, S, Matsubara, K, Choshi, H, Tanaka, S, Ishihara, M, et al. 2024. *Augmented humoral response to third and fourth dose of SARS-CoV-2 mRNA vaccines in lung transplant recipients*. Respir Investig;62(5):804-10.
193. Razia, D, Sindu, D, Cherrier, L, Grief, K, Walia, R, Tokman, S. 2024. *Remdesivir and molnupiravir had comparable efficacy in lung transplant recipients with mild-to-moderate COVID-19: a single center experience*. Frontiers in Transplantation;3.
194. El-Shabasy, RM, Nayel, MA, Taher, MM, Abdelmonem, R, Shoueir, KR, Kenawy, ER. 2022. *Three waves changes, new variant strains, and vaccination effect against COVID-19 pandemic*. Int J Biol Macromol;204:161-8.
195. Claeson, M, Hanson, S. 2021. *The Swedish COVID-19 strategy revisited*. The Lancet;397(10285):1619.
196. Scheel-Hincke, LL, Connolly, FF, Olofsson, J, Andersen-Ranberg, K; 2023. *Social, health, and economic impacts of the COVID-19 pandemic and the epidemiological control measures*

27 Two Nordic countries with different approaches to handling the COVID-19 pandemic: A comparison of Sweden and Denmark. In: Börsch-Supan A, Abramowska-Kmon A, Andersen-Ranberg K, Brugiavini A, Chłoń-Domińczak A, Jusot F, et al., editors. First results from SHARE Corona Waves 1 and 2: De Gruyter. p. 281-90.
197. Mishra, S, Scott, JA, Laydon, DJ, Flaxman, S, Gandy, A, Mellan, TA, et al. 2021. *Comparing the responses of the UK, Sweden and Denmark to COVID-19 using counterfactual modelling*. Scientific Reports;11(1).
198. Wester, CT, Bovil, T, Scheel-Hincke, LL, Ahrenfeldt, LJ, Möller, S, Andersen-Ranberg, K. 2022. *Longitudinal changes in mental health following the COVID-19 lockdown: Results from the Survey of Health, Ageing, and Retirement in Europe*. Annals of Epidemiology;74:21-30.
199. Ludvigsson, J, Von Herrath, MG, Mallone, R, Buschard, K, Cilio, C, Craig, M, et al. 2020. *Corona Pandemic: Assisted Isolation and Care to Protect Vulnerable Populations May Allow Us to Shorten the Universal Lock-Down and Gradually Re-open Society*. Frontiers in Public Health;8.
200. Roosma, E, Van Gemert, JP, De Zwart, AES, Van Leer-Buter, CC, Hellemons, ME, Berg, EM, et al. 2022. *The effect of COVID-19 on transplant function and development of CLAD in lung transplant patients: A multicenter experience*. The Journal of Heart and Lung Transplantation;41(9):1237-47.

201. Myers, CN, Scott, JH, Criner, GJ, Cordova, FC, Mamary, AJ, Marchetti, N, et al. 2020. *COVID-19 in lung transplant recipients*. Transplant Infectious Disease;22(6).
202. Aversa, M, Benvenuto, L, Anderson, M, Shah, L, Robbins, H, Pereira, M, et al. 2020. *COVID-19 in lung transplant recipients: A single center case series from New York City*. Am J Transplant;20(11):3072-80.
203. Yewdell, JW. 2021. *Antigenic drift: Understanding COVID-19.* Immunity;54(12):2681-7.
204. Arabi, M, Al-Najjar, Y, Mhaimeed, N, Salameh, MA, Paul, P, AlAnni, J, et al. 2023. *Severity of the Omicron SARS-CoV-2 variant compared with the previous lineages: A systematic review*. J Cell Mol Med;27(11):1443-64.
205. Altneu, E, Mishkin, A. 2022. *COVID-19 Vaccination in Lung Transplant Recipients*. Indian Journal of Thoracic and Cardiovascular Surgery;38(S2):347-53.
206. Moghadas, SM, Vilches, TN, Zhang, K, Wells, CR, Shoukat, A, Singer, BH, et al. 2021. *The Impact of Vaccination on Coronavirus Disease 2019 (COVID-19) Outbreaks in the United States*. Clinical Infectious Diseases;73(12):2257-64.
207. Pêgo-Fernandes, PM, Abrão, FC, Fernandes, FL, Caramori, ML, Samano, MN, Jatene, FB. 2009. *Spirometric assessment of lung transplant patients: one year follow-up*. Clinics (Sao Paulo);64(6):519-25.
208. Hage, R, Schuurmans, MM. COVID-Related Chronic Allograft Dysfunction in Lung Transplant Recipients: Long-Term Follow-up Results from Infections Occurring in the Pre-vaccination Era. Transplantology [Internet]. 2022; 3(4):[275-82 pp.].
209. Mohanka, MR, Mahan, LD, Joerns, J, Lawrence, A, Bollineni, S, Kaza, V, et al. 2021. *Clinical characteristics, management practices, and outcomes among lung transplant patients with COVID-19*. J Heart Lung Transplant;40(9):936-47.
210. Nykänen, A, Raivio, P, Peräkylä, L, Stark, C, Huuskonen, A, Lemström, K, et al. 2020. *Incidence and impact of chronic lung allograft dysfunction after lung transplantation – single-center 14-year experience*. Scandinavian Cardiovascular Journal;54(3):192-9.
211. de Zwart, AES, Riezebos-Brilman, A, Lunter, GA, Neerken, ECU, van Leer-Buter, CC, Alffenaar, JC, et al. 2022. *Impact of COVID-19 social distancing measures on lung transplant recipients: decline in overall respiratory virus infections is associated with stabilisation of lung function*. Eur Respir J;60(5).
212. Trindade, AJ, Chapin, KC, Gannon, WD, Hoy, H, Demarest, CT, Lambright, ES, et al. 2022. *Clinical course of SARS-CoV-2 infection and recovery in lung transplant recipients*. Transpl Infect Dis;24(6):e13967.

biomedicines

MDPI

Article

Quantitative Proteomics Indicate Radical Removal of Non-Small Cell Lung Cancer and Predict Outcome

Embla Bodén [1,2,3], Jesper Andreasson [1,4], Gabriel Hirdman [1,2,3], Malin Malmsjö [1] and Sandra Lindstedt [1,2,3,4,*]

1 Department of Clinical Sciences, Lund University, 22362 Lund, Sweden
2 Wallenberg Center for Molecular Medicine, Lund University, 22363 Lund, Sweden
3 Lund Stem Cell Center, Lund University, 22362 Lund, Sweden
4 Department of Cardiothoracic Surgery and Transplantation, Skåne University Hospital, 22242 Lund, Sweden
* Correspondence: sandra.lindstedt_ingemansson@med.lu.se

Abstract: Non-small cell lung cancer (NSCLC) is associated with low survival rates, often due to late diagnosis and lack of personalized medicine. Diagnosing and monitoring NSCLC using blood samples has lately gained interest due to its less invasive nature. In the present study, plasma was collected at three timepoints and analyzed using proximity extension assay technology and quantitative real-time polymerase chain reaction in patients with primary NSCLC stages IA–IIIA undergoing surgery. Results were adjusted for patient demographics, tumor, node, metastasis (TNM) stage, and multiple testing. Major histocompatibility (MHC) class 1 polypeptide-related sequence A/B (MIC-A/B) and tumor necrosis factor ligand superfamily member 6 (FASLG) were significantly increased post-surgery, suggesting radical removal of cancerous cells. Levels of hepatocyte growth factor (HGF) initially increased postoperatively but were later lowered, potentially indicating radical removal of malignant cells. The levels of FASLG in patients who later died or had a relapse of NSCLC were lower at all three timepoints compared to surviving patients without relapse, indicating that FASLG may be used as a prognostic biomarker. The biomarkers were confirmed using microarray data. In conclusion, quantitative proteomics could be used for NSCLC identification but may also provide information on radical surgical removal of NSCLC and post-surgical prognosis.

Keywords: non-small cell lung cancer; biomarkers; proteomics

Citation: Bodén, E.; Andreasson, J.; Hirdman, G.; Malmsjö, M.; Lindstedt, S. Quantitative Proteomics Indicate Radical Removal of Non-Small Cell Lung Cancer and Predict Outcome. *Biomedicines* **2022**, *10*, 2738. https://doi.org/10.3390/biomedicines10112738

Academic Editors: Alberto Ricci and Randolph C. Elble

Received: 28 August 2022
Accepted: 25 October 2022
Published: 28 October 2022

1. Introduction

Lung cancer is the number one cause of cancer-related deaths globally, causing around 1.8 million deaths annually [1,2]. Non-small cell lung cancer (NSCLC) accounts for approximately 85% of lung cancer cases, with lung adenocarcinoma (LUAD) and squamous cell carcinoma of the lung (SCC) being the most common forms [3,4]. The aim of this study was to identify protein biomarkers in the plasma of patients with primary NSCLC and to evaluate their potential usefulness in diagnosing and evaluating surgical resection of NSCLC. In this study, the tumor, node, and metastasis (TNM) 7th edition for lung cancer were used [5]. The methods used in the clinic to detect, diagnose, histologically subtype, and monitor lung cancer are mainly chest X-ray, bronchoscopy, and biopsy. An X-ray has a relatively low sensitivity and small tumors or tumors that are overshadowed by boney structures run a high risk of evading detection [6]. Furthermore, repeated radiographies in the form of a chest X-ray, computed tomography (CT), and positron emission tomography (PET), in lung cancer patients lead to radiation exposure levels exceeding recommended rates [7]. Bronchoscopy is time-consuming, costly, and invasive and comes with a risk of complications [8–10].

Next generation sequencing (NGS) is commonly used for guiding the choice of post-surgical treatment. NGS allows detection of changes such as substitutions, indels and rearrangements in, for example, proto-oncogenes in the tumor tissue [11]. Surgical removal

of the tumor mass is a widely used treatment option for the early stages of NSCLC and is the form of treatment with the highest success rate [12–16]. Treatment of NSCLC can induce remission, but the majority of patients experience relapse and disease progression [17,18]. Unfortunately, this high recurrence rate of NSCLC is also responsible for the high mortality rate [19,20]. The survival rates for lung cancer overall and, specifically for NSCLC, are low, ranging from 15–19% 1 year survival for stage IV to 81–85% 1 year survival for stage I [4,21–23]. Yet another hindrance to the long-term survival of NSCLC patients is failure to diagnose the cancer at an early stage [1,24]. Earlier diagnosis leads to better survival rates, fewer treatment-associated comorbidities, lower health care costs, and early identification. Surgical removal of low stage NSCLC has been shown to generate 5-year survival rates as high as 70% [1,21,25]. Despite this, screening of at-risk populations for lung cancer is only commonplace in certain parts of the world [26,27]. The Dutch–Belgian Randomized Lung Cancer Screening Trial (NELSON) study, a randomized controlled trial of current and former smokers using low dose radiation CT, without contrast, revealed increased numbers of non-symptomatic NSCLC patients in early stages eligible for surgery, along with lower mortality in the screened cohort [28]. The national lung screening trial (NLST) in Sweden also showed a significantly lower mortality among screened patients but was not able to show any differences between low-dose CT and conventional chest X-ray as a screening method [29].

The search for biomarkers in cancer is an ongoing hot topic. Proteins may potentially be used for monitoring, predicting prognosis, measuring response to treatment, and detecting relapse [30]. Unfortunately, there are few known prognostic biomarkers for lung cancer in clinical use [31,32]. Discovering candidate biomarkers in blood has emerged as an attractive alternative to conventional techniques due to its minimally invasive nature, it does not require elaborate preparation, and allows for repeated sampling with ease and minimal risk for the patient. In the current study, we explored potential biomarkers in blood drawn before and after surgical resection of NSCLC.

2. Materials and Methods

The current study is a clinical study, performed in accordance with the Declaration of Helsinki and approved by the local ethics committee (Dnr: 2017/519). All patients signed written and informed consent forms prior to enrollment.

2.1. Study Population

A total of 29 patients undergoing surgery for resection of primary NSCLC (LUAD or SCC), stages IA–IIIA (T1a–T4, N0–N2, M0), according to the International Association for the Study of Lung Cancer's (IASLC) TNM 7th edition, were included (Table 1) [5]. A total of 86 blood samples were collected; of these, 29 samples were preoperative, 28 were obtained 3–5 days post-surgery, and 29 were obtained 1 month after surgery (Figure 1). Timepoints for sampling were chosen based on the expected postoperative inflammation approximately 1 week post-surgery and the presumed downregulation of inflammation by 1 month post-surgery. It has previously been suggested that inflammation post-operation should be monitored for the first 4–7 days [33]. Exclusion criteria were chosen to minimize the risk of pathological processes other than NSCLC affecting the results of the proteomic analysis. Exclusion criteria include symptoms of ischemic heart disease, any unstable medical disorder, heart failure NYHA class III or IV, serum creatinine >140 µmol/L, diabetic subjects with glycated hemoglobin (HbA1c) > 48.0, as well as signs of liver cirrhosis, bleeding disorder or drug abuse. All patients were followed in regard to survival over 3.5 years after surgery.

Table 1. Patient characteristics. Descriptive statistics are presented as mean, range, number of patients, and percentage. Total number of patients is n = 29. *WHO* = World Health Organization, *R0* = macroscopically and microscopically radical, *R1* = macroscopically but not microscopically radical.

	***n* = 29**
Sex, *n* (%)	
Male	14 (48)
Female	15 (52)
Age, years	
Mean (range)	71 (46–84)
Mortality, *n* (%)	
Alive	26 (90)
Deceased	3 (10)
Time from diagnosis to death, days	
Mean (range)	603 (264–786)
Time from surgery to death, days	
Mean (range)	551 (211–736)
Comorbidities, *n* (%)	
None known	17 (59)
Coronary artery disease	2 (7)
Diabetes mellitus	3 (10)
Hypertension	10 (34)
Arrhythmias	1 (3)
WHO performance status prior to surgery, *n* (%)	
0	15 (52)
1	14 (48)
Smoking history, *n* (%)	
Current	4 (14)
Former (> 6 weeks)	21 (72)
Never	4 (14)
Histopathological classification, *n* (%)	
Adenocarcinoma	21 (72)
Squamous cell carcinoma	8 (28)
Tumor stage, *n* (%)	
IA	13 (45)
IB	8 (28)
IIA	3 (10)
IIB	2 (7)
IIIA	3 (10)
Lung resection, *n* (%)	
Wedge resection	2 (7)
Segmental resection	2 (7)
Lobectomy	23 (79)
Bilobectomy	1 (3)
Pneumonectomy	1 (3)
Radicality, *n* (%)	
R0	26 (90)
R1	3 (10)
Neoadjuvant therapy, *n* (%)	
Combined chemotherapy and radiotherapy	2 (7)
Adjuvant therapy, *n* (%)	
Single therapy, chemotherapy	6 (21)
Combined chemotherapy and radiotherapy	1 (3)

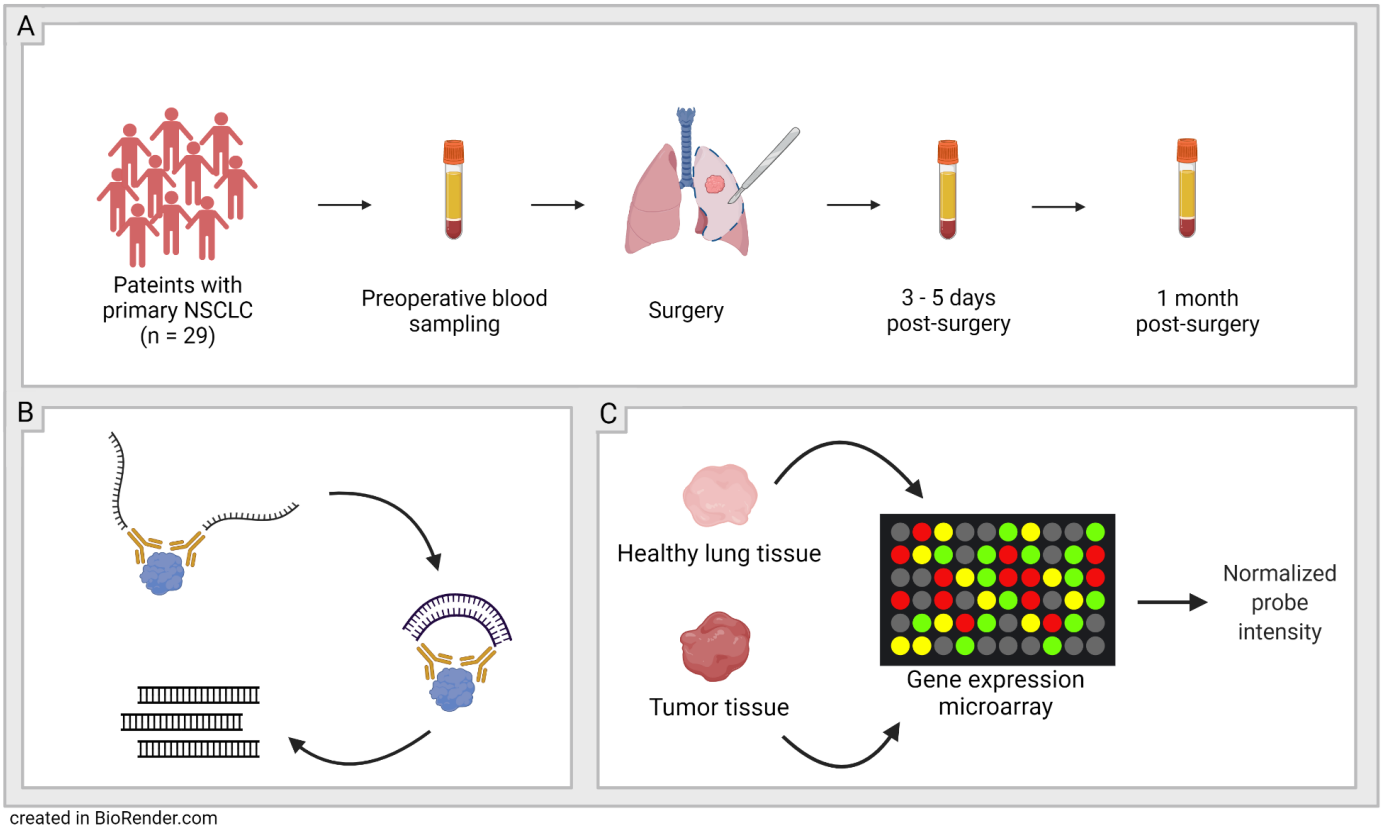

Figure 1. Schematic figure of study workflow. (**A**): Sampling-29 patients with primary non-small cell lung cancer (NSCLC) were included and blood plasma was sampled at three timepoints; before surgery, 3–5 days post-surgery, and 1 month post-surgery. (**B**): Olink's proximity extension assay (PEA) technology was used to quantify the proteins in the plasma samples. (**C**): Validation-Protein expression patterns in plasma were validated with microarray data from NCBI's GEO DataSets website.

2.2. Olink-Proximity Extension Assay (PEA)

A total of 92 proteins were analyzed using Olink's Target 96 Oncology II panel (Olink, Uppsala, Sweden). The Target 96 Oncology II panel consists of pre-determined proteins. The panel was chosen based on proteins related to lung cancer. For more information on this panel, see the manufacturer's webpage (https://www.olink.com/products-services/target/oncology-ii-panel/, accessed date on 27 August 2022).

The PEA analysis is a dual-recognition immunoassay that can be performed on very small plasma or serum samples down to 1.0 µL. The small amount of biospecimen needed is enough because of the exponential amplification that happens later on in the process. For every protein in the panel, there is a matched pair of antibodies that each carry a unique DNA tag (oligonucleotide). The oligonucleotides hybridize when brought into proximity due to the binding of the antibody pair to the same protein. Dual antibody binding is required which ensures a high specificity. Non-matched binding of antibodies to a protein does not yield a signal. The hybridized DNA tags include unique barcodes that can be detected by the system Fluidigm BioMark^{TM} HD standard real-time quantitative PCR. The oligonucleotides are then amplified in the presence of DNA polymerase, the number of cycles being determined by the protein concentration in each sample. Olink adds specially tailored blocking reagents to the analysis to reduce sample matrix interference. The qPCR is performed on eighty-eight customer samples and eight control samples that are assayed against the chosen panel of ninety-two proteins. This generates more than 8000 data points.

The PCR technique used by Olink allows for the readout of 96 protein assays in 96 samples simultaneously. The data are presented as normalized protein expression (NPX), a relative protein quantification unit on a $\log_2$ scale, for each protein biomarker in each

sample. This allows for the identification of changes in individual protein levels across the sample set. A high NPX value equals a high protein concentration. Olink's built-in quality control system uses three internal controls in each of the 96 wells of the sample plate. Additional sample controls for estimation of precision by intra- and inter-CVs (coefficients of variance), negative controls for the setting of the background levels for each protein, to calculate the limit of detection (LOD), and plate controls to compensate for potential variation between run plates are added.

Proteins with less than 15% detectability, i.e., proteins found in less than 15% of samples, according to Olink's predetermined LOD were removed from the analysis. All 92 proteins in the Olink Target 96 Oncology II panel remained in the analysis. All samples were analyzed simultaneously. Further information on detection limits, assay characteristics, assay performance, and validation for each protein is available on the manufacturer's webpage (http://www.olink.com, accessed date on 27 August 2022).

2.3. Confirmation of the Findings in Larger Cohorts

Microarray data from larger cohorts of subjects with NSCLC as well as healthy lung tissue were accessed through the NCBI's GEO DataSets website (https://www.ncbi.nlm.nih.gov/gds, accessed date on 23 September 2022) (National Library of Medicine, Rockville Pike, Bethesda, MD, USA). In the current study dataset GEO: GSE10072 describing gene expression in NSCLC tumor tissue and healthy lung tissue from separate controls, and dataset GEO: GSE19804 describing paired NSCLC tumor tissue and adjacent healthy lung tissue were used to validate the patterns of protein expression found in plasma.

2.4. Statistical Analysis

Descriptive statistics are presented in the form of mean, range, subject number (n), and percentage of subjects. Statistical analyses were carried out by Olink through their offered statistical analysis services and in GraphPad Prism version 9.3.0 (GraphPad Software, San Diego, CA, USA). Olink analyses the data by fitting a linear mixed-effects regression model with each patient and cancer type considered as random effects. p-values are adjusted for multiple testing using the Benjamini–Hochberg approach with a false discovery rate (FDR) set to 0.05. Posthoc testing of the significant proteins is performed by calculating estimated marginal means, comparing the timepoints in a pairwise manner. p-values generated by the posthoc test were adjusted for multiple comparisons with Tukey's method. Comparisons of smaller groups of samples were performed with the Mann–Whitney test. A cox proportional hazards model was performed in GraphPad Prism. Statistical significance was defined as **** ($p < 0.0001$), *** ($p < 0.001$), ** ($p < 0.01$), * ($p < 0.05$) and ns ($p > 0.05$).

3. Results

3.1. Proteomic Analysis

All 92 unique proteins in the Olink Target 96 Oncology II panel were detected in more than 75% of the samples. Of the 92 proteins, 63 (68%) were found to have a significant difference between the three timepoints after adjusting the p-values for multiple testing. The 12 proteins with the lowest adjusted overall p-values generated by a linear mixed-effects regression model were interleukin-6 (IL-6), mucin-16 (MUC-16), furin, protransforming growth factor alpha (TGFα), hepatocyte growth factor (HGF), vascular endothelial growth factor A (VEGFA), MHC class 1 polypeptide-related sequence A/B (MIC-A/B), amphiregulin (AREG), delta-like protein 1 (DLL1), tumor necrosis factor ligand superfamily member 6 (FASLG), transmembrane glycoprotein NMB (GPNMB), and tumor necrosis factor receptor superfamily member 6B (TNFRSF6B) (Table 2).

Table 2. Protein levels of the twelve proteins with the lowest overall *p*-values. Protein levels preoperatively, 1 week post-surgery (3–5 days post-surgery), and 1 month post-surgery. Protein levels are expressed as normalized protein expression (NPX), a relative protein quantification unit on a $\log_2$ scale. Statistical significance is listed in the table, ns was defined as ($p > 0.05$).

Protein Abbreviation	Protein	NPX Preop (Mean ± SD)	NPX 1 Week (Mean ± SD)	NPX 1 Month (Mean ± SD)	*p*-Value Preop vs. 1 Week	*p*-Value Preop vs. 1 Month	*p*-Value 1 Week vs. 1 Month
AREG	Amphiregulin	2.63 ± 0.51	3.33 ± 0.59	2.88 ± 0.58	$p < 0.0001$	$p = 0.0237$	$p < 0.0001$
DLL1	Delta-like protein 1	9.54 ± 0.33	9.87 ± 0.31	9.78 ± 0.29	$p < 0.0001$	$p < 0.0001$	ns
Furin	Protein furin	9.35 ± 0.41	10.03 ± 0.36	9.64 ± 0.33	$p < 0.0001$	$p < 0.0001$	$p < 0.0001$
IL-6	Interleukin-6	3.86 ± 0.95	6.57 ± 0.97	4.59 ± 1.09	$p < 0.0001$	$p = 0.0016$	$p < 0.0001$
MIC-A/B	MHC class 1 polypeptide-related sequence A/B	3.82 ± 0.70	4.20 ± 1.69	4.00 ± 1.70	$p < 0.0001$	$p = 0.0009$	$p = 0.0003$
MUC-16	Mucin-16	4.71 ± 0.74	5.24 ± 0.81	7.37 ± 1.26	ns	$p < 0.0001$	$p < 0.0001$
TGFα	Transforming growth factor alpha	2.62 ± 0.35	3.18 ± 0.37	2.91 ± 0.34	$p < 0.0001$	$p < 0.0001$	$p < 0.0001$
TNFRSF6B	Tumor necrosis factor receptor superfamily member 6B	5.54 ± 0.67	6.15 ± 0.57	5.78 ± 0.64	$p < 0.0001$	$p = 0.0214$	$p = 0.0003$
VEGFA	Vascular endothelial growth factor A	10.05 ± 0.63	10.69 ± 0.55	10.22 ± 0.49	$p < 0.0001$	ns	$p < 0.0001$
FASLG	Tumor necrosis factor ligand superfamily member 6	8.34 ± 0.45	8.22 ± 0.38	8.63 ± 0.34	ns	$p < 0.0001$	$p < 0.0001$
GPNMB	Transmembrane glycoprotein NMB	7.03 ± 0.17	6.89 ± 0.20	7.11 ± 0.13	$p < 0.0001$	$p = 0.0207$	$p < 0.0001$
HGF	Hepatocyte growth factor	8.04 ± 0.60	8.58 ± 0.58	8.15 ± 0.45	$p < 0.0001$	ns	$p < 0.0001$

3.2. Comparing Three Timepoints: Pre-Op vs. 3–5 Days Post-Op vs. 1 Month Post-Op

Pairwise comparisons of preoperative, 3–5 days post-surgery, and 1 month post-surgery samples for every protein in the assay revealed significantly elevated plasma levels of six proteins (AREG, DLL1, furin, IL-6, TGFα, and TNFRSF6B) in both the 3–5 days post-surgery and the 1 month post-surgery samples compared to the preoperative samples. Furthermore, the plasma levels of the proteins MUC-16 and VEGFA were also elevated but did not reach significant levels compared to samples preoperatively vs. 3–5 days for MUC-16 and preoperatively vs. 1 month for VEGFA (Table 2).

The levels of MIC-A/B were significantly increased 3–5 days post-surgery compared to pre-operative levels (pre-op 3.82 ± 0.70 NPX, 3–5 days post-op 4.20 ± 1.69 NPX [$p < 0.0001$]) as well as levels 1 month post-surgery (pre-op 3.82 ± 0.70 NPX, 1 month post-op 4.00 ± 1.70 NPX [$p = 0.0009$]) (Figure 2, Table 2).

Plasma levels of FASLG were significantly higher at 1 month post-surgery compared to pre-operative levels (pre-op 8.34 ± 0.45 NPX, 1 month post-op 8.63 ± 0.34 NPX [$p < 0.0001$]) (Figure 2, Table 2). GPNMB followed the same pattern as FASLG (Figure 2, Table 2).

Plasma levels of HGF were significantly higher 3–5 days post-surgery compared to pre-operative levels (pre-op 8.04 ± 0.60 NPX, 3–5 days post-op 8.58 ± 0.58 NPX [$p < 0.0001$]) and decreased back to preoperative levels 1 month post-surgery (pre-op 8.04 ± 0.60 NPX, 1 month post-op 8.15 ± 0.45 NPX [$p = 0.23$]) (Figure 2, Table 2).

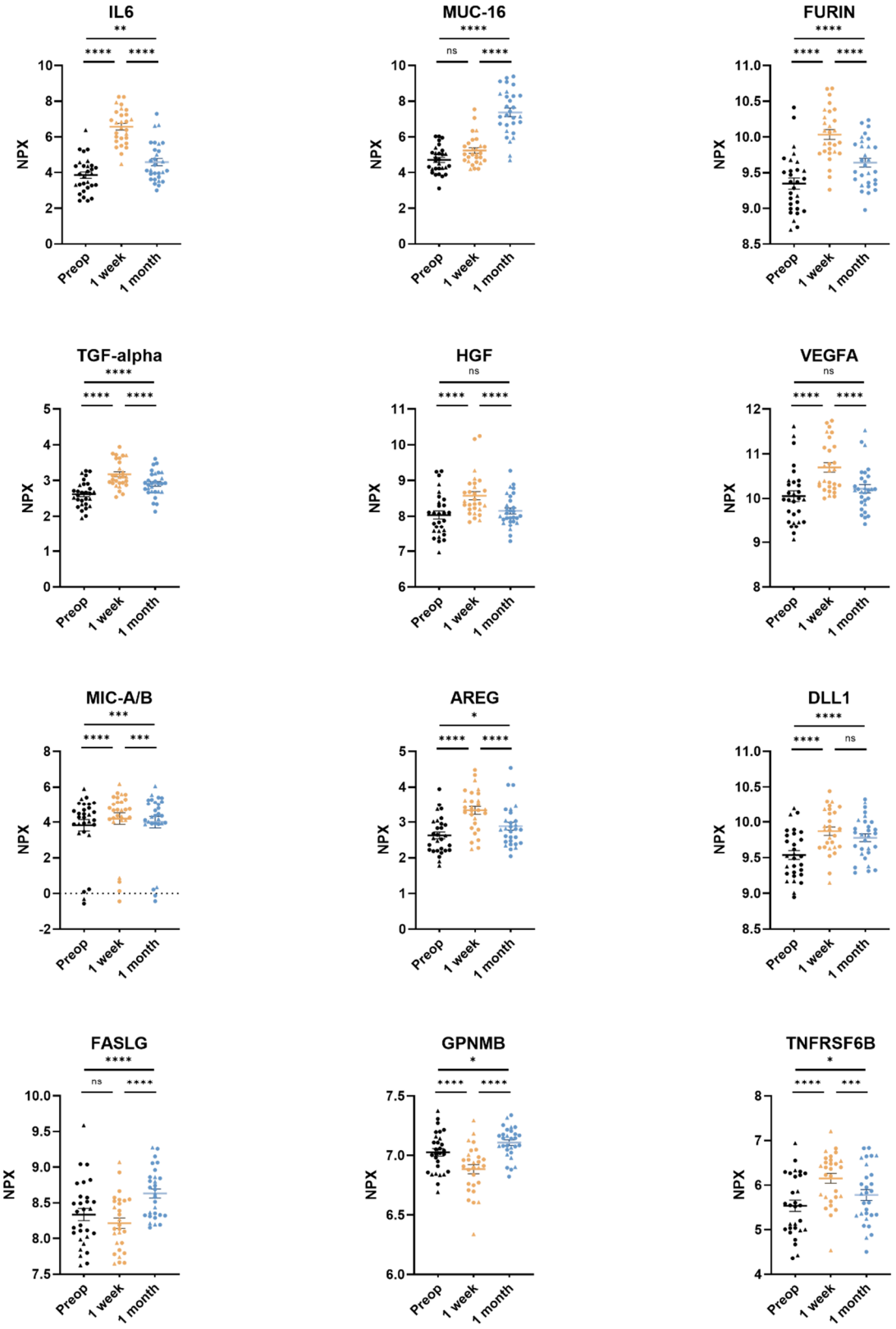

Figure 2. The twelve most significantly differing proteins in plasma from non-small cell lung cancer (NSCLC) patients. Adenocarcinoma datapoints are portrayed as circles and squamous cell carcinoma datapoints are portrayed as triangles. Plasma samples were taken preoperatively, 3–5 days post-surgery, and 1 month post-surgery. Protein levels pictured for interleukin-6 (IL6), mucin-16 (MUC-16), protein furin, transforming growth factor alpha (TGF-alpha), hepatocyte growth factor (HGF), vascular

endothelial growth factor A (VEGFA), MHC class I polypeptide-related sequence A/B (MIC-A/B), amphiregulin (AREG), delta-like protein 1 (DLL1), tumor necrosis factor ligand superfamily member 6 (FASLG), transmembrane glycoprotein NMB (GPNMB), and tumor necrosis factor receptor superfamily member 6B (TNFRSF6B). Protein levels are expressed as normalized protein expression (NPX), a relative protein quantification unit on a log2 scale. Statistical significance was defined as **** ($p < 0.0001$), *** ($p < 0.001$), ** ($p < 0.01$), * ($p < 0.05$) and ns ($p > 0.05$).

3.3. Comparison of Dead or Relapsed NSCLC to Survivors without Relapse

Four of the twenty-nine patients included in this study died or had recurring NSCLC within the follow-up time of 3.5 years. In these patients, lower levels of FASLG were seen at all three timepoints compared to the survivors without relapse. The most significant difference was found between preoperative FASLG levels in patients who died or in patients with a relapse of NSCLC compared to survivors with no relapse (dead or relapsed patients' pre-operative levels 7.91 ± 0.11 NPX, survivors' pre-operative levels 8.40 ± 0.45 NPX [$p < 0.05$]) (Figure 3). A Cox Proportional-Hazards Model was performed and showed a parameter estimate for preoperative NPX-values of FASLG of -3.126. A negative parameter estimate indicates a decrease in the examined predictor variable (in this case NPX levels) which increases the hazard for the event (death or relapse) (p-value of 0.0672). Due to the low mortality and recurrence rate ($n = 4$), a bigger cohort might be needed to show such significance.

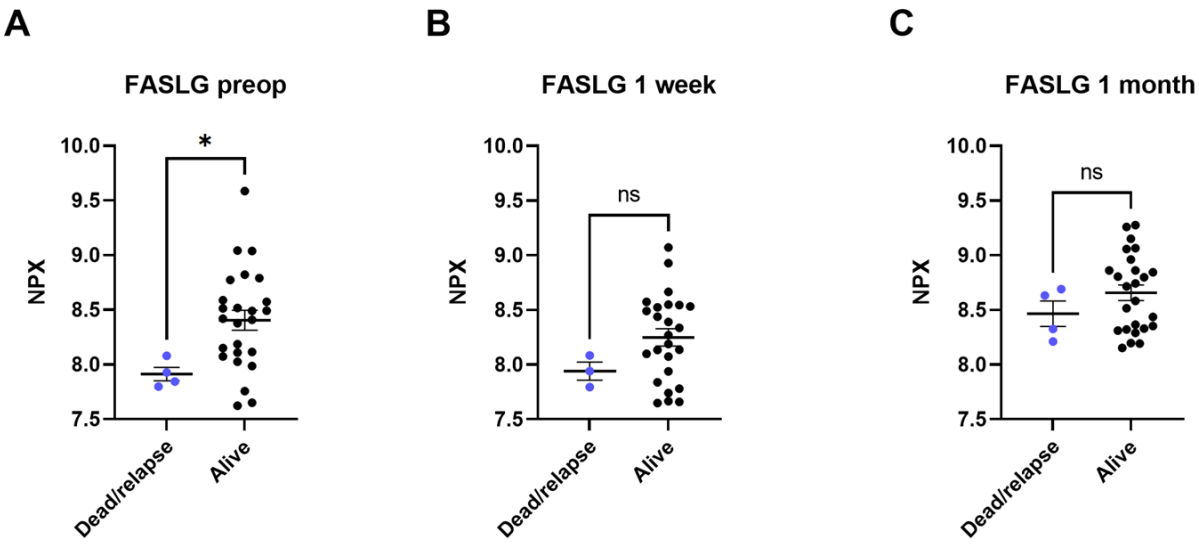

Figure 3. Plasma levels of tumor necrosis factor ligand superfamily member 6 (FASLG) compared between patients who died or had a relapse of cancer (dead/relapse) and patients still alive (alive). The comparisons were performed with Mann–Whitney tests. (**A**) comparison of preoperative samples, (**B**) comparison of 3–5 days post-surgical samples, (**C**) comparison of 1 month post-surgical samples. Protein levels are expressed as normalized protein expression (NPX), a relative protein quantification unit on a log2 scale. Statistical significance was defined as * ($p < 0.05$) and ns ($p > 0.05$).

The association of survival and death or relapse was also examined for the two proteins HGF and MIC-A/B; however, no association could be found.

3.4. Validation Using GEO DataSets Microarray Data

Microarray data from two separate NSCLC cohorts deposited at the NCBI's GEO DataSets website were used for validation of protein expression patterns found in plasma. One dataset describing gene expression in NSCLC tumor tissue and healthy lung tissue from controls (GEO: GSE10072) showed a significantly higher expression of MIC-A

(GenBank NM_000247) in healthy control subjects compared to NSCLC (MIC-A control 8.18 ± 0.04, MIC-A NSCLC 8.00 ± 0.03 [p = 0.0044]). A second dataset describing gene expression in NSCLC tissue and adjacent healthy lung tissue (GEO: GSE19804) also showed a significantly higher expression of MIC-A (GenBank NM_000247) in healthy lung tissue compared to tumor tissue (MIC-A control 8.19 ± 0.05, MIC-A NSCLC 8.00 ± 0.06 [p = 0.0166]). Additionally, in this dataset, there was a significantly higher expression of FASLG (GenBank AF288573) in healthy tissue compared to tumor tissue (FASLG control 4.56 ± 0.05, FASLG NSCLC 4.42 ± 0.04 [p = 0.0239]). The proteins HGF and GPNMB were also investigated in the datasets, but the findings of this current study could not be validated. The unit of gene expression is normalized probe intensity (Table 3).

Table 3. Gene expression of proteins MIC-A and FASLG according to separate cohorts accessed through the NCBI's GEO DataSets website. Dataset GEO: GSE10072 comparing tissue from patients with NSCLC (n = 58) and healthy control patients (n = 49). Dataset GEO: GSE19804 comparing tissue from NSCLC (n = 60) and adjacent healthy lung tissue (n = 60). Gene expression was calculated by microarray techniques and expressed as normalized probe intensity.

Protein	GenBank	GEO	Gene Expression Cancer	Gene Expression Control	Significance
MIC-A	NM_000247	GSE10072	8.00 ± 0.03	8.18 ± 0.04	p = 0.0044
MIC-A	NM_000247	GSE19804	8.00 ± 0.06	8.19 ± 0.05	p = 0.0166
FASLG	AF288573	GSE19804	4.42 ± 0.04	4.56 ± 0.05	p = 0.0239

4. Discussion

Cancer is one of modern healthcare's greatest challenges, causing millions of deaths every year. NSCLC is difficult to diagnose in its early stages and, once diagnosed, treatment of NSCLC is problematic as the disease often recurs even after initial remission [17,18]. Recently, Field et al. showed that lung cancer mortality was significantly reduced by low-dose CT screening [34]. Whilst screening does occur in many international centers, there is still a hesitation towards installing the practice, largely due to a missing organization of handling false-positive results. Screening using low-dose CT includes pre-scanning blood sampling and analyzing, as well as follow-up of kidney insufficiency, which requires additional setup and might therefore be challenging in some healthcare settings. Screening using blood samples would require less organization and would be more cost-effective than screening using low-dose CT and is therefore a highly promising field.

The present study explores the use of proteomics based on plasma to diagnose and predict the surgical outcome of NSCLC. In the current study, the patients included were sampled at three timepoints and served as their own controls. By omitting a separate control group, we minimize the risk of inherently different protein expression levels between individuals affecting the analyses. We used matched pair antibody-based PEA to analyze the incidence of 92 proteins within our patient cohort. The dual antibody binding of the method ensures a high specificity of the detected proteins, making the analytical method preferred over other antibody-based technologies that generate results in lower specificity due to the use of single antibody binding. In the present study, significant differences in plasma protein levels were found in 63 of the 92 analyzed proteins. Of those 63 proteins, the 12 proteins with the highest levels of significance were selected and presented separately.

MIC-A/B, which act as ligands to several immune cells including NK-cells, cytotoxic T-cells, and $CD8^+$ T-cells, were found to be significant and among the 12 most significant proteins in the present study. MIC-A and MIC-B are expressed by many cancers, including NSCLC, and are involved in cell-mediated antitumoral responses [35,36]. Expression of tumor-related proteases has been shown to induce the shedding of MIC-A/B in some cancers, thereby allowing the malignant cells to evade cell-mediated antitumor immunity [35,36]. Furthermore, high expression of MIC-A/B has been found to be a positive prognostic factor in patients undergoing surgery for NSCLC, and a higher expres-

sion of MIC-A specifically has been associated with significantly longer survival times in NSCLC [37,38]. The significant increase of MIC-A/B levels after surgical removal of NSCLC in the present study indicates that the suppressant of the protein has been radically removed and MIC-A/B may therefore be used as an indicator of radical removal of NSCLC. This is further validated by the findings of the microarray data (Table 3) (Figure 2). In a current study by Djureinovic et al., the authors used Olink proteomics' Oncology II panel to differentiate between NSCLC and different lung pathologies, both benign and malignant. In this study, MIC-A/B could not be used to differentiate between different lung pathologies. This is interesting but not entirely surprising as the disease areas studied are different in this publication and our current study [39].

FASLG, a member of the tumor necrosis factor ligand superfamily, was also found to be among the 12 most significant proteins in the present study. The binding of FAS to FASLG induces activation-induced cell death (AICD), cytotoxic T-cell- and NK-cell-induced cell death. The signaling pathway in which FASLG is active has a role in the apoptotic response of damaged cells, such as cancer cells [40]. The FASLG signaling pathway can be inhibited by the protein decoy receptor 3 (DcR3), which has been found to be elevated in lung and colon cancers [41,42]. DcR3 is often referred to as TNFRSF6B. TNFRSF6B is also to be found among the proteins in the Olink Target 96 Oncology II panel. Overexpression of DcR3 results in inhibited FASLG-induced cell death and cancerous cells evading the immune system [40]. In the current study, however, the plasma levels of TNFRSF6B were not higher prior to surgical treatment of NSCLC compared to samples taken at 3–5 days post-surgery and 1 month post-surgery. This could be explained by the fact that preoperative expression of TNFRSF6B was already higher than among healthy subjects, which would be in line with previous findings [41,42]. Moreover, recently Ali et al. showed that expression of FASLG is naturally higher in more differentiated, healthy tissues [43]. In the present study, plasma levels of FASLG were significantly higher 1 month after the surgical removal of NSCLC, potentially indicating that the NSCLC that had previously been suppressing the expression of FASLG has been radically removed (Figure 2). This is also validated by the patterns of gene expression in the accessed microarray data (Table 3). Interestingly, the levels of FASLG in plasma in patients who later died or had a relapse of NSCLC were lower at all three timepoints compared to the patients still alive with no relapse (Figure 3). This finding indicates that FASLG can be used as a prognostic biomarker for NSCLC as well as for the evaluation of radical surgical removal of NSCLC.

The protein HGF, a proto-oncogene that codes for a protein produced by fibroblasts in the lungs, stimulates cell motility, invasion, and morphogenesis, and acts as a potent mitogen for both healthy and cancerous cells in the bronchial epithelium [44]. Expression of HGF has been found to be elevated in tumor tissue of patients with NSCLC and especially in patients with tumor recurrence. Increased levels of HGF in plasma has been shown to correlate with poorer overall survival, and patients with stage I lung cancer with high levels of expressed HGF have a poorer prognosis than patients with stage II–III lung cancer with low expression of HGF [31]. Additionally, in a study by Masuya et al., it was shown that stromal expression of HGF in NSCLC cells correlated to a higher Ki-67 proliferation index, indicating a higher proliferation rate. It has also been shown that elevated expression of the HGF-receptor c-Met is associated with significantly lower survival [45]. In the present study, levels of HGF in plasma were initially significantly increased 3–5 days post-surgery but significantly lower between the 1 week and the 1 month timepoints, where the levels were again found to be in the same range as the pre-operative levels. Given the significant decrease in the relatively short follow-up time, a longer follow-up may have revealed a significant decrease over time compared to pre-operative levels of HGF among the surviving patients without relapse (Figure 2). In another publication using Olink's PEA technology to study protein expression in cancerous cells in a fine-needle aspirate from NSCLC patients, HGF was among the top 49 abundant proteins and could be correlated to different stages of NSCLC, in line with the current study [46].

The glycoprotein NMB, or GPNMB, has been shown to be overly expressed in several human cancers, including NSCLC [47]. In a publication by Li et al., it was shown that overexpression of GPNMB has a role in the metastasis of cancerous tumors [48]. GPNMB is known to be expressed in monocyte-derived dendritic cells (Mo-DCs), where it is involved in inhibiting T-cell activation [49]. In the present study, plasma levels of GPNMB were significantly decreased 3–5 days post-surgery, and then significantly increased 1 month post-surgery ($p < 0.0001$ and $p < 0.05$, respectively).

The plasma levels of AREG, DLL1, f"rin,'IL-6, MUC-16, TGFα, TNFRSF6B, and VEGFA were all significantly elevated after 3–5 days and 1 month aftersurgery. The increase may, in part, be explained by the inflammatory response caused by the surgical trauma itself. Due to surgical trauma, inflammatory cells including $CD4^+$ T-cells are recruited, and bradykinin is released. Elevated levels of bradykinin may explain the increased levels of AREG [50,51]. Among the cytokines released due to surgical trauma and inflammation, IL-6 and TGFα are well characterized within the process of inflammation [52–54]. DLL1 is also known to play a central role in inflammation by increased production of IFN-γ and acting as a ligand in the NOTCH signaling pathway, which plays a role in regulating macrophage-mediated inflammation [55,56]. Angiogenesis driven by VEGFA is important in wound healing and is well known to be upregulated after surgery [57]. In tissue remodeling, such as in wound healing, expression of matrix metalloproteinases (MMPs) is enhanced by furin which is also in itself enhanced in immune cells, acting to attenuate the inflammatory response that follows surgical trauma [58–60]. MUC-16, a mucin naturally expressed in airway epithelium, functions to ensure both integrity and barrier function, thus contributing to the mucosal immune defense mechanism [61,62]. Thus, all of the aforementioned proteins (AREG, DLL1, furin, IL-6, MUC-16, TGFα, TNFRSF6B, and VEGFA) have previously been shown to have a connection to inflammation after surgery, which could explain the findings of the present study. Furthermore, proteins that have been shown to have an established connection to lung cancer show a significant change in protein expression levels after surgical removal of the tumor. A summary of the 12 proteins' modes of action can be seen in Table 4.

To validate the patterns of protein expression found in plasma, the NCBI's GEO DataSets website was searched for deposited microarray data. We accessed data from lung cancer biopsies and healthy lung tissue and were able to validate MIC-A and FASLG. We accessed two datasets, in both of which the expression of MIC-A was significantly higher in healthy lung tissue compared to tumor tissue. In one of the datasets, the expression of FASLG was also significantly higher in the controls compared to the tumor tissue. These results support the findings of the current study and encourage the status of these two proteins as potential biomarkers for diagnosing and predicting the outcome of NSCLC.

Table 4. Description of the top 12 proteins with the lowest *p*-values modes of action.

Protein Abbreviation	Protein	Mode of Action
AREG	Amphiregulin	Cytokine in the epidermal growth factor family. Binds to epidermal growth factor receptors and activates signaling in inflammatory processes, cell metabolism, and the cell cycle. Produced by immune cells [63].
DLL1	Delta-like protein 1	A NOTCH ligand. Regulates immune cells. Released from T-cells and eosinophilic cells. Secretion is enhanced by interleukin 1β. Has a positive correlation to systemic inflammation [64].
Furin	Protein furin	Cleaves and activates matrix metalloproteases, integrins, and cadherins (cell adhesion molecules). Expression is upregulated by tissue hypoxia [65].

Table 4. *Cont.*

Protein Abbreviation	Protein	Mode of Action
IL-6	Interleukin-6	Involved in B-cell stimulation and induction of hepatic acute phase proteins. Increases thousand-fold in blood during inflammation. Signaling is dominated by signal transducer and activator of transcription 3 (STAT3) activation [66].
MIC-A/B	MHC class 1 polypeptide-related sequence A/B	Cancer cell-surface molecules. Activates cytolytic properties in natural killer cells and cytotoxic T-cells. Shedding of MIC-A/B by cancer cells leads to their escape from cell-mediated antitumor immunity [37].
MUC-16	Mucin-16	Glycoprotein is expressed by epithelial cells. Major component of mucus providing hydration and lubrication. Regulates mucosal defense of epithelial cells [61].
TGFα	Transforming growth factor alpha	Expressed by wound macrophages. Mediates angiogenesis, epidermal regrowth, and formation of granulation tissue [67].
TNFRSF6B	Tumor necrosis factor receptor superfamily member 6B	A soluble receptor also known as DcR3. Inhibits FASLG-induced cell death which potentially leads to the survival of malignant cells [42].
VEGFA	Vascular endothelial growth factor A	Induces angiogenesis and is important in wound healing. Plasma levels have been proven to rise post-surgery corresponding to the extent of the operative intervention [57].
FASLG	Tumor necrosis factor ligand superfamily member 6	Produced by activated T-cells and natural killer cells. Induces cell death of damaged cells. Naturally higher expression in healthy tissue. The binding of DcR3 to FASLG inhibits its function [40].
GPNMB	Transmembrane glycoprotein NMB	A transmembrane protein expressed by monocytic dendritic cells. Can inhibit T-cell activation [49]. Involved in metastasis of small-cell lung cancer [48].
HGF	Hepatocyte growth factor	A proto-oncogene, the protein stimulates cell motility, invasion, and morphogenesis. Acts as a potent mitogen [44]. High expression in NSCLC correlates with poor overall survival [31].

Limitations

Proteins found in plasma are not necessarily specific to the lung and might reflect other processes such as malignancies and inflammation in other parts of the body. Given the inflammatory response secondary to the surgical trauma itself, additional samples at later timepoints would be preferable, for example at six, twelve, and eighteen months after surgery, since they could potentially reveal additional biomarkers related to NSCLC. Because of the number of biomarker candidates, it is perhaps more realistic to envision that characterization of NSCLC would take the shape of identifying a protein pattern to use as a biomarker rather than the discovery of one single protein [24]. One of the datasets used for the validation of this study's findings consists of tumor tissue and healthy lung tissue from the same subjects. The use of a matched cohort increases the risk of selection bias which could potentially affect the differences in protein expression levels between tumor tissue and healthy tissue as the tissues are matched and the healthy lung tissue thus still originates from a patient with NSCLC.

5. Conclusions

Quantitative proteomics offers information on molecular interactions, signaling pathways, and biomarker identification by providing relative protein abundance. Using plasma as a proteomic source from patients with NSCLC, the present study implies that MIC-A/B, FASLG, and HGF are all valuable biomarkers and may not only be used as markers for radical removal of NSCLC but also to predict outcomes.

Author Contributions: Conceptualization, S.L. and J.A.; methodology, S.L. and J.A.; validation, E.B. and S.L.; formal analysis, E.B. and G.H.; investigation, E.B. and S.L.; resources, S.L. and M.M.; data curation, S.L., E.B. and G.H.; writing—original draft preparation, E.B.; writing—review and editing, S.L.; visualization, E.B.; supervision, S.L.; project administration, S.L.; funding acquisition, S.L. All authors have read and agreed to the published version of the manuscript.

Funding: This research was funded by the Sjöberg Foundation, the Region Skåne Foundation and the Knut and Alice Wallenberg Foundation.

Institutional Review Board Statement: The current study is a clinical study, performed in accordance with the Declaration of Helsinki and approved by the local ethics committee (Dnr: 2017/519).

Informed Consent Statement: Informed consent was obtained from all subjects involved in the study. All patients signed written and informed consent forms prior to enrollment.

Data Availability Statement: Data is available on request from the corresponding author. Publicly available datasets were analyzed in this study. This data can be found here: [https://www.ncbi.nlm.nih.gov/gds, accessed on 23 September 2022].

Acknowledgments: We would like to thank our fellow laboratory members in the Lindstedt laboratory group, including Franziska Olm who has been very helpful with her scientific input and support. We further would like to thank the staff on the cardiothoracic ward for their cooperativeness in working with the patients.

Conflicts of Interest: The authors declare no conflict of interest. The funders had no role in the design of the study; in the collection, analyses, or interpretation of data; in the writing of the manuscript, or in the decision to publish the results.

References

1. World Health Organization. Cancer. Available online: https://www.who.int/news-room/fact-sheets/detail/cancer (accessed on 14 April 2022).
2. World Health Organization. The Top 10 Causes of Death. Available online: https://www.who.int/news-room/fact-sheets/detail/the-top-10-causes-of-death (accessed on 14 April 2022).
3. Molina, J.R.; Yang, P.; Cassivi, S.D.; Schild, S.E.; Adjei, A.A. Non-Small Cell Lung Cancer: Epidemiology, Risk Factors, Treatment, and Survivorship. *Mayo Clin. Proc.* **2008**, *83*, 584–594. [CrossRef]
4. Herbst, R.S.; Morgensztern, D.; Boshoff, C. The biology and management of non-small cell lung cancer. *Nature* **2018**, *553*, 446–454. [CrossRef]
5. Goldstraw, P.; Crowley, J.; Chansky, K.; Giroux, D.J.; Groome, P.A.; Rami-Porta, R.; Postmus, P.E.; Rusch, V.; Sobin, L. The IASLC Lung Cancer Staging Project: Proposals for the Revision of the TNM Stage Groupings in the Forthcoming (Seventh) Edition of the TNM Classification of Malignant Tumours. *J. Thorac. Oncol.* **2007**, *2*, 706–714. [CrossRef]
6. Freedman, M.T.; Lo, S.C.; Seibel, J.C.; Bromley, C.M. Lung nodules: Improved detection with software that suppresses the rib and clavicle on chest radiographs. *Radiology* **2011**, *260*, 265–273. [CrossRef]
7. Stiles, B.M.; Mirza, F.; Towe, C.W.; Ho, V.P.; Port, J.L.; Lee, P.C.; Paul, S.; Yankelevitz, D.F.; Altorki, N.K. Cumulative Radiation Dose From Medical Imaging Procedures in Patients Undergoing Resection for Lung Cancer. *Ann. Thorac. Surg.* **2011**, *92*, 1170–1179. [CrossRef] [PubMed]
8. Herout, V.; Heroutova, M.; Merta, Z.; Jr, I.C.; Brat, K. Transbronchial biopsy from the upper pulmonary lobes is associated with increased risk of pneumothorax—A retrospective study. *BMC Pulm. Med.* **2019**, *19*, 56. [CrossRef]
9. Şahin, C.; Yılmaz, O.; Üçpınar, B.A.; Uçak, R.; Temel, U.; Başak, M.; Bayrak, A.H. Computed Tomography-guided Transthoracic Core Needle Biopsy of Lung Masses: Technique, Complications and Diagnostic Yield Rate. *Sisli Etfal Hastan. Tip Bul.* **2020**, *54*, 47–51. [CrossRef]
10. Medford, A.R.L.; Agrawal, S.; Free, C.M.; Bennett, J.A. A Prospective Study of Conventional Transbronchial Needle Aspiration: Performance and Cost Utility. *Respiration* **2010**, *79*, 482–489. [CrossRef]
11. Behjati, S.; Tarpey, P.S. What is next generation sequencing? *Arch. Dis. Child. Edu. Pract. Ed.* **2013**, *98*, 236–238. [CrossRef] [PubMed]
12. Zierhut, D.; Bettscheider, C.; Schubert, K.; Van Kampen, M.; Wannenmacher, M. Radiation therapy of stage I and II non-small cell lung cancer (NSCLC). *Lung Cancer* **2001**, *34*, 39–43. [CrossRef]
13. Howington, J.A.; Blum, M.G.; Chang, A.C.; Balekian, A.A.; Murthy, S.C. Treatment of stage I and II non-small cell lung cancer: Diagnosis and management of lung cancer, 3rd ed: American College of Chest Physicians evidence-based clinical practice guidelines. *Chest* **2013**, *143*, e278S–e313S. [CrossRef] [PubMed]
14. Galetta, D.; Solli, P.; Borri, A.; Petrella, F.; Gasparri, R.; Brambilla, D.; Spaggiari, L. Bilobectomy for Lung Cancer: Analysis of Indications, Postoperative Results, and Long-Term Outcomes. *Ann. Thorac. Surg.* **2012**, *93*, 251–258. [CrossRef]

15. Zappa, C.; Mousa, S.A. Non-small cell lung cancer: Current treatment and future advances. *Transl. Lung Cancer Res.* **2016**, *5*, 288–300. [CrossRef] [PubMed]
16. Scott, W.J.; Howington, J.; Feigenberg, S.; Movsas, B.; Pisters, K. Treatment of non-small cell lung cancer stage I and stage II: ACCP evidence-based clinical practice guidelines (2nd edition). *Chest* **2007**, *132*, 234–242. [CrossRef] [PubMed]
17. Cagle, P.T.; Allen, T.C.; Olsen, R.J. Lung Cancer Biomarkers: Present Status and Future Developments. *Arch. Pathol. Lab. Med.* **2013**, *137*, 1191–1198. [CrossRef]
18. American Cancer Society. Cancer Facts & Figures 2015. Available online: https://www.cancer.org/research/cancer-facts-statistics/all-cancer-facts-figures/cancer-facts-figures-2015.html (accessed on 17 September 2020).
19. Al-Kattan, K. Disease recurrence after resection for stage I lung cancer. *Eur. J. Cardio Thorac. Surg.* **1997**, *12*, 380–384. [CrossRef]
20. Taylor, M.D.; Nagji, A.S.; Bhamidipati, C.M.; Theodosakis, N.; Kozower, B.D.; Lau, C.L.; Jones, D.R. Tumor Recurrence After Complete Resection for Non-Small Cell Lung Cancer. *Ann. Thorac. Surg.* **2012**, *93*, 1813–1821. [CrossRef] [PubMed]
21. Blandin Knight, S.; Crosbie, P.A.; Balata, H.; Chudziak, J.; Hussell, T.; Dive, C. Progress and prospects of early detection in lung cancer. *Open Biol.* **2017**, *7*, 170070. [CrossRef]
22. Siegel, R.L.; Miller, K.D.; Jemal, A. Cancer statistics, 2020. *CA Cancer J. Clin.* **2020**, *70*, 7–30. [CrossRef]
23. Broggio, J.B.N.; Wong, K.; Poole, J.; Gildea, C.; Emmett, M.; Luchtenborg, M.; Kaur, J.; Butler, L.; Peet, M.; King, A. Cancer Survival in England: Adult, Stage at Diagnosis and Childhood—Patients Followed up to 2016. Available online: https://www.ons.gov.uk/peoplepopulationandcommunity/healthandsocialcare/conditionsanddiseases/bulletins/cancersurvivalinengland/adultstageatdiagnosisandchildhoodpatientsfollowedupto2016#cancer-survival-by-stage-at-diagnosis-for-england-adults-diagnosed-in-2015-and-followed-up-to-2016-experimental-statistics (accessed on 14 April 2022).
24. Sung, H.J.; Cho, J.Y. Biomarkers for the lung cancer diagnosis and their advances in proteomics. *BMB Rep.* **2008**, *41*, 615–625. [CrossRef]
25. Shah, R.; Sabanathan, S.; Richardson, J.; Mearns, A.J.; Goulden, C. Results of surgical treatment of stage I and II lung cancer. *J. Cardiovasc Surg.* **1996**, *37*, 169–172.
26. Van Meerbeeck, J.P.; Franck, C. Lung cancer screening in Europe: Where are we in 2021? *Transl. Lung Cancer Res.* **2021**, *10*, 2407–2417. [CrossRef]
27. Kauczor, H.-U.; Baird, A.-M.; Blum, T.G.; Bonomo, L.; Bostantzoglou, C.; Burghuber, O.; Čepická, B.; Comanescu, A.; Couraud, S.; Devaraj, A.; et al. ESR/ERS statement paper on lung cancer screening. *Eur. Radiol.* **2020**, *30*, 3277–3294. [CrossRef] [PubMed]
28. De Koning, H.J.; Van Der Aalst, C.M.; De Jong, P.A.; Scholten, E.T.; Nackaerts, K.; Heuvelmans, M.A.; Lammers, J.-W.J.; Weenink, C.; Yousaf-Khan, U.; Horeweg, N.; et al. Reduced Lung-Cancer Mortality with Volume CT Screening in a Randomized Trial. *N. Engl. J. Med.* **2020**, *382*, 503–513. [CrossRef]
29. Black, W.C.; Chiles, C.; Church, T.R.; Gareen, I.F.; Gierada, D.S.; Mahon, I.; Miller, E.A.; Pinsky, P.F.; Sicks, J.D. Lung Cancer Incidence and Mortality with Extended Follow-up in the National Lung Screening Trial. *J. Thorac. Oncol.* **2019**, *14*, 1732–1742. [CrossRef]
30. NCI. Tumor Markers. Available online: https://www.cancer.gov/about-cancer/diagnosis-staging/diagnosis/tumor-markers-fact-sheet (accessed on 14 April 2022).
31. Siegfried, J.M.; Weissfeld, L.A.; Singh-Kaw, P.; Weyant, R.J.; Testa, J.R.; Landreneau, R.J. Association of Immunoreactive Hepatocyte Growth Factor with Poor Survival in Resectable Non-Small Cell Lung Cancer. *Cancer Res.* **1997**, *57*, 433–439. [PubMed]
32. Scott, A.; Salgia, R. Biomarkers in lung cancer: From early detection to novel therapeutics and decision making. *Biomark Med.* **2008**, *2*, 577–586. [CrossRef]
33. Paruk, F.; Chausse, J.M. Monitoring the post surgery inflammatory host response. *J. Emerg. Crit. Care Med.* **2019**, *3*, 47. [CrossRef]
34. Field, J.K.; Vulkan, D.; Davies, M.P.A.; Baldwin, D.R.; Brain, K.E.; Devaraj, A.; Eisen, T.; Gosney, J.; Green, B.A.; Holemans, J.A.; et al. Lung cancer mortality reduction by LDCT screening: UKLS randomised trial results and international meta-analysis. *Lancet Reg. Health Eur.* **2021**, *10*, 100179. [CrossRef] [PubMed]
35. Ghadially, H.; Brown, L.; Lloyd, C.; Lewis, L.; Lewis, A.; Dillon, J.; Sainson, R.; Jovanovic, J.; Tigue, N.J.; Bannister, D.; et al. MHC class I chain-related protein A and B (MICA and MICB) are predominantly expressed intracellularly in tumour and normal tissue. *Br. J. Cancer* **2017**, *116*, 1208–1217. [CrossRef] [PubMed]
36. Blocking MICA/MICB Shedding Reactivates Antitumor Immunity. *Cancer Discov.* **2018**, *8*, OF20. [CrossRef]
37. Zhao, Y.; Chen, N.; Yu, Y.; Zhou, L.; Niu, C.; Liu, Y.; Tian, H.; Lv, Z.; Han, F.; Cui, J. Prognostic value of MICA/B in cancers: A systematic review and meta-analysis. *Oncotarget* **2017**, *8*, 96384–96395. [CrossRef] [PubMed]
38. Okita, R.; Yukawa, T.; Nojima, Y.; Maeda, A.; Saisho, S.; Shimizu, K.; Nakata, M. MHC class I chain-related molecule A and B expression is upregulated by cisplatin and associated with good prognosis in patients with non-small cell lung cancer. *Cancer Immunol. Immunother.* **2016**, *65*, 499–509. [CrossRef] [PubMed]
39. Djureinovic, D.; Pontén, V.; Landelius, P.; Al Sayegh, S.; Kappert, K.; Kamali-Moghaddam, M.; Micke, P.; Ståhle, E. Multiplex plasma protein profiling identifies novel markers to discriminate patients with adenocarcinoma of the lung. *BMC Cancer* **2019**, *19*, 741. [CrossRef] [PubMed]
40. Liu, W.; Ramagopal, U.; Cheng, H.; Bonanno, J.B.; Toro, R.; Bhosle, R.; Zhan, C.; Almo, S.C. Crystal Structure of the Complex of Human FasL and Its Decoy Receptor DcR3. *Structure* **2016**, *24*, 2016–2023. [CrossRef]

41. Bai, C.; Connolly, B.; Metzker, M.L.; Hilliard, C.A.; Liu, X.; Sandig, V.; Soderman, A.; Galloway, S.M.; Liu, Q.; Austin, C.P.; et al. Overexpression of M68/DcR3 in human gastrointestinal tract tumors independent of gene amplification and its location in a four-gene cluster. *Proc. Natl. Acad. Sci. USA* **2000**, *97*, 1230–1235. [CrossRef]
42. Pitti, R.M.; Marsters, S.A.; Lawrence, D.A.; Roy, M.; Kischkel, F.C.; Dowd, P.; Huang, A.; Donahue, C.J.; Sherwood, S.W.; Baldwin, D.T.; et al. Genomic amplification of a decoy receptor for Fas ligand in lung and colon cancer. *Nature* **1998**, *396*, 699–703. [CrossRef]
43. Ali, A.S.; Perren, A.; Lindskog, C.; Welin, S.; Sorbye, H.; Grönberg, M.; Janson, E.T. Candidate protein biomarkers in pancreatic neuroendocrine neoplasms grade 3. *Sci. Rep.* **2020**, *10*, 10639. [CrossRef]
44. Tsao, M.-S.; Liu, N.; Chen, J.-R.; Pappas, J.; Ho, J.; To, C.; Viallet, J.; Park, M.; Zhu, H. Differential expression of Met/hepatocyte growth factor receptor in subtypes of non-small cell lung cancers. *Lung Cancer* **1998**, *20*, 1–16. [CrossRef]
45. Masuya, D.; Huang, C.; Liu, D.; Nakashima, T.; Kameyama, K.; Haba, R.; Ueno, M.; Yokomise, H. The tumour–stromal interaction between intratumoral c-Met and stromal hepatocyte growth factor associated with tumour growth and prognosis in non-small-cell lung cancer patients. *Br. J. Cancer* **2004**, *90*, 1555–1562. [CrossRef]
46. FranzeéN, B.; Viktorsson, K.; Kamali, C.; Darai-Ramqvist, E.; Grozman, V.; Arapi, V.; Hååg, P.; Kaminskyy, V.O.; Hydbring, P.; Kanter, L.; et al. Multiplex immune protein profiling of fine-needle aspirates from patients with non-small-cell lung cancer reveals signatures associated with PD-L1 expression and tumor stage. *Mol. Oncol.* **2021**, *15*, 2941–2957. [CrossRef] [PubMed]
47. Ott, P.A.; Pavlick, A.C.; Johnson, D.B.; Hart, L.L.; Infante, J.R.; Luke, J.J.; Lutzky, J.; Rothschild, N.E.; Spitler, L.E.; Cowey, C.L.; et al. A phase 2 study of glembatumumab vedotin, an antibody-drug conjugate targeting glycoprotein NMB, in patients with advanced melanoma. *Cancer* **2019**, *125*, 1113–1123. [CrossRef] [PubMed]
48. Li, Y.N.; Zhang, L.; Li, X.L.; Cui, D.J.; Zheng, H.D.; Yang, S.Y.; Yang, W.L. Glycoprotein nonmetastatic B as a prognostic indicator in small cell lung cancer. *APMIS* **2014**, *122*, 140–146. [CrossRef] [PubMed]
49. Funk, T.; Fuchs, A.R.; Altdörfer, V.S.; Klein, R.; Autenrieth, S.E.; Müller, M.R.; Salih, H.R.; Henes, J.; Grünebach, F.; Dörfel, D. Monocyte-derived dendritic cells display a highly activated phenotype and altered function in patients with familial Mediterranean fever. *Clin. Exper. Immunol.* **2020**, *201*, 1–11. [CrossRef]
50. Deacon, K.; Knox, A.J. Human airway smooth muscle cells secrete amphiregulin via bradykinin/COX-2/PGE2, inducing COX-2, CXCL8, and VEGF expression in airway epithelial cells. *Am. J. Physiol. Lung Cell Mol. Physiol.* **2015**, *309*, L237–L249. [CrossRef]
51. Zaiss, D.M.W.; Gause, W.C.; Osborne, L.C.; Artis, D. Emerging Functions of Amphiregulin in Orchestrating Immunity, Inflammation, and Tissue Repair. *Immunity* **2015**, *42*, 216–226. [CrossRef]
52. Sakamoto, K.; Arakawa, H.; Mita, S.; Ishiko, T.; Ikei, S.; Egami, H.; Hisano, S.; Ogawa, M. Elevation of circulating interleukin 6 after surgery: Factors influencing the serum level. *Cytokine* **1994**, *6*, 181–186. [CrossRef]
53. Jones, S.A.; Jenkins, B.J. Recent insights into targeting the IL-6 cytokine family in inflammatory diseases and cancer. *Nature Rev. Immunol.* **2018**, *18*, 773–789. [CrossRef]
54. Akira, S.; Hirano, T.; Taga, T.; Kishimoto, T. Biology of multifunctional cytokines: IL 6 and related molecules (IL 1 and TNF). *FASEB J.* **1990**, *4*, 2860–2867. [CrossRef]
55. Keewan, E.A.; Naser, S.A. The Role of Notch Signaling in Macrophages during Inflammation and Infection: Implication in Rheumatoid Arthritis? *Cells* **2020**, *9*, 111. [CrossRef] [PubMed]
56. Kimball, A.S.; Joshi, A.D.; Boniakowski, A.E.; Schaller, M.; Chung, J.; Allen, R.; Bermick, J.; Carson, W.F.; Henke, P.K.; Maillard, I.; et al. Notch Regulates Macrophage-Mediated Inflammation in Diabetic Wound Healing. *Front. Immunol.* **2017**, *8*, 635. [CrossRef] [PubMed]
57. Belizon, A.; Balik, E.; Feingold, D.L.; Bessler, M.; Arnell, T.D.; Forde, K.A.; Horst, P.K.; Jain, S.; Cekic, V.; Kirman, I.; et al. Major abdominal surgery increases plasma levels of vascular endothelial growth factor: Open more so than minimally invasive methods. *Ann. Surg.* **2006**, *244*, 792–798. [CrossRef] [PubMed]
58. Pei, D.; Weiss, S.J. Furin-dependent intracellular activation of the human stromelysin-3 zymogen. *Nature* **1995**, *375*, 244–247. [CrossRef] [PubMed]
59. Guo, C.; Jiang, J.; Elliott, J.M.; Piacentini, L. Paradigmatic identification of MMP-2 and MT1-MMP activation systems in cardiac fibroblasts cultured as a monolayer. *J. Cell Biochem.* **2005**, *94*, 446–459. [CrossRef]
60. Cordova, Z.M.; Grönholm, A.; Kytölä, V.; Taverniti, V.; Hämäläinen, S.; Aittomäki, S.; Niininen, W.; Junttila, I.; Ylipää, A.; Nykter, M.; et al. Myeloid cell expressed proprotein convertase FURIN attenuates inflammation. *Oncotarget* **2016**, *7*, 54392–54404. [CrossRef]
61. Haridas, D.; Ponnusamy, M.P.; Chugh, S.; Lakshmanan, I.; Seshacharyulu, P.; Batra, S.K. MUC16: Molecular analysis and its functional implications in benign and malignant conditions. *FASEB J.* **2014**, *28*, 4183–4199. [CrossRef]
62. Kesimer, M.; Scull, M.; Brighton, B.; Demaria, G.; Burns, K.; O'Neal, W.; Pickles, R.J.; Sheehan, J.K. Characterization of exosome-like vesicles released from human tracheobronchial ciliated epithelium: A possible role in innate defense. *FASEB J.* **2009**, *23*, 1858–1868. [CrossRef]
63. Singh, S.S.; Chauhan, S.B.; Kumar, A.; Kumar, S.; Engwerda, C.R.; Sundar, S.; Kumar, R. Amphiregulin in cellular physiology, health, and disease: Potential use as a biomarker and therapeutic target. *J. Cell. Physiol.* **2022**, *237*, 1143–1156. [CrossRef]
64. Norum, H.M.; Michelsen, A.E.; Lekva, T.; Arora, S.; Otterdal, K.; Olsen, M.B.; Kong, X.Y.; Gude, E.; Andreassen, A.K.; Solbu, D.; et al. Circulating delta-like Notch ligand 1 is correlated with cardiac allograft vasculopathy and suppressed in heart transplant recipients on everolimus-based immunosuppression. *Am. J. Transplant.* **2019**, *19*, 1050–1060. [CrossRef]
65. Jaaks, P.; Bernasconi, M. The proprotein convertase furin in tumour progression. *Int. J. Cancer* **2017**, *141*, 654–663. [CrossRef]

66. Rose-John, S. Interleukin-6 Family Cytokines. *Cold Spring Harb. Perspect. Biol.* **2018**, *10*, a028415. [CrossRef] [PubMed]
67. Rappolee, D.A.; Mark, D.; Banda, M.J.; Werb, Z. Wound Macrophages Express TGF-α and Other Growth Factors in Vivo: Analysis by mRNA Phenotyping. *Science* **1988**, *241*, 708–712. [CrossRef] [PubMed]

Respiratory Research

RESEARCH

Open Access

Exhaled phospholipid transfer protein and hepatocyte growth factor receptor in lung adenocarcinoma

Jesper Andreasson[1,2], Embla Bodén[1,2], Mohammed Fakhro[3], Camilla von Wachter[4], Franziska Olm[1,2], Malin Malmsjö[2], Oskar Hallgren[2] and Sandra Lindstedt[1,2*]

Abstract

Background: Screening decreases mortality among lung cancer patients but is not widely implemented, thus there is an unmet need for an easily accessible non-invasive method to enable early diagnosis. Particles in exhaled air offer a promising such diagnostic tool. We investigated the validity of a particles in exhaled air device (PExA) to measure the particle flow rate (PFR) and collect exhaled breath particles (EBP) to diagnose primary lung adenocarcinoma (LUAD).

Methods: Seventeen patients listed for resection of LUAD stages IA–IIIA and 18 non-cancer surgical control patients were enrolled. EBP were collected before and after surgery for LUAD, and once for controls. Proteomic analysis was carried out using a proximity extension assay technology. Results were validated in both plasma from the same cohort and with microarray data from healthy lung tissue and LUAD tissue in the GSE10072 dataset.

Results: Of the 92 proteins analyzed, levels of five proteins in EBP were significantly higher in the LUAD patients compared to controls. Levels of phospholipid transfer protein (PLTP) and hepatocyte growth factor receptor (MET) decreased in LUAD patients after surgery compared to control patients. PFR was significantly higher in the LUAD cohort at all timepoints compared to the control group. MET in plasma correlated significantly with MET in EBP.

Conclusion: Collection of EBP and measuring of PFR has never been performed in patients with LUAD. In the present study PFR alone could distinguish between LUAD and patients without LUAD. PLTP and MET were identified as potential biomarkers to evaluate successful tumor excision.

Keywords: Exhaled breath particles, Hepatocyte growth factor receptor, Lung cancer, Particle flow rate, Phospholipid transfer protein, Lung adenocarcinoma

Background

Lung cancer is the leading cause of cancer mortality, causing almost 1.8 million deaths worldwide in 2020 and accounting for 18% of all cancer deaths [1]. Despite advances in treatment, 5-year survival is poor, ranging from above 25% for women with non-small cell lung cancer (NSCLC) to below 5% for men with small-cell lung cancer in the Swedish National Lung Cancer Registry [2]. Most lung cancers are detected in advanced stages when curative treatment is no longer an option. Screening with low-dose computed tomography has proven effective in two large, randomized trials, with successful early detection and reduced mortality [3, 4]. However, lung cancer screening is not widely implemented due to difficult logistics, overdiagnosis and false-positive findings [5, 6]. The addition of risk-based screening models based on sociodemographic factors, clinical symptoms and

*Correspondence: sandra.lindstedt_ingemansson@med.lu.se

[2] Department of Clinical Sciences, Lund University, Entrégatan 7, 22242 Lund, Sweden
Full list of author information is available at the end of the article

biomarkers, alone or combined, could enhance the efficacy of lung cancer screening. Biomarkers can be found in different sample types, such as blood, urine, or exhaled air, and can be based on circulating cells, nucleic acids, proteins, or other molecules. Despite great efforts to identify suitable biomarkers, no method is yet established in clinical use due to lack of significant improvement in predictive performance, and sampling procedures can be complex and costly [7]. However, there are some proteins of interest that have a known connection to LUAD. One of these is hepatocyte growth factor receptor (MET). In approximately 70% of LUAD tumor tissue the MET gene is significantly overexpressed [8], moreover, overexpression of MET in plasma of patients with LUAD is a known phenomenon [9]. Given this, we investigated the correlation between levels of MET in EBP and s-MET in plasma in this study.

Collection of exhaled air allows for investigation of exhaled breath particles (EBP) [10], volatile organic compounds [11] and exhaled breath condensate (EBC) [12, 13], offering a unique isolated matrix of the respiratory system for biomarker analysis. Volatile organic compounds might reflect the presence of neoplasms or disease processes not specific to the lungs, and EBC is hampered by salivary contamination, whereas EBP reflect the distal airways selectively [14, 15], which is why EBP have gained much interest as a potential source of biomarkers. The respiratory tract lining fluid (RTLF) covers the epithelial surfaces of the distal airways. As small airways and alveoli open and close, particles from the RTLF enter the large airways and are subsequently exhaled [16]. The particle flow from the airways is measured as the particle flow rate (PFR) of EBP, which are collected for subsequent analysis [14, 15, 17]. In this study, patients undergoing lung cancer surgery for lung adenocarcinoma (LUAD) and patients without LUAD were enrolled. We aimed to evaluate proteins in EBP as well as analyzing PFR before and 1 month after surgery and comparing the results between LUAD patients and control patients, thereby evaluating the potential to use EBP and PFR as diagnostic tools. Analyzing EBP and PFR have previously been proven useful in diagnosing and evaluating other pulmonary diseases such as asthma, acute respiratory distress syndrome (ARDS) and primary graft dysfunction (PGD) in lung transplant recipients and in patients with COVID-19 by us and other research groups [10, 14, 15, 17–19].

Patients and methods

This study is a prospective observational clinical trial with the aim to analyze exhaled breath particles from patients with LUAD and control patients to identify protein biomarkers and evaluate their potential usefulness in diagnosing and evaluating surgical resection of LUAD. We also aimed to investigate differences in particle flow rate between patients with LUAD and control patients. The study is approved by the Swedish Ethical Review Authority (Dnr. 2017/519). All patients signed a written, informed consent prior to enrollment.

Patient demographics

A total of 35 patients were included: 17 LUAD patients scheduled for resection and 18 patients without LUAD scheduled for other non-cancer surgery, referred to as the control group. Inclusion criteria were TNM staging system up to pTNM N2/IIIA (TNM 7th edition [20]). Follow-up with survival was recorded 3 years after surgery. Demographic data are shown in Table 1 and the histopathological stage of the LUAD patients is shown in Table 2. A flow chart of enrolled subjects is shown in Additional file 1: Fig. S1.

Collection of particles in exhaled air

The device to measure particles in exhaled air (PExA 2.0, PExA AB, Gothenburg, Sweden) contains an optical particle counter connected to an impactor for collection of EBP using a standardized breathing maneuver as described previously in detail [10]. Particles were quantified and divided into eight size bins ranging from 0.41 to 4.55 µm in diameter. Number of particles (count, n) and total accumulated mass (ng) were measured. PFR was described as particles per liter of exhaled air. Particles were collected onto a membrane (Millipores LCR membrane, Merck KGaA, Darmstadt, Germany) for biochemical analysis. In the LUAD group, sampling was carried out at two timepoints: the day before surgery (n = 15), and 1 month postoperatively (n = 16). Control patients were sampled at one timepoint, the day before surgery. An overview of the study is shown in Fig. 1.

Analysis of exhaled breath particles

The Olink Target 96 Cardiometabolic panel (Olink Proteomics AB, Uppsala, Sweden) was used to analyze 92 proteins with the proximity extension assay (PEA), according to the manufacturer's instructions [21]. Proteins with less than 15% detectability were excluded according to Olink's predetermined limit of detection (LOD). The analysis is based on a calculated normalized protein expression (NPX), a relative protein quantification unit on a $\log_2$ scale. This allows for identification of changes in individual protein levels across the sample set. A high NPX value indicates a high protein concentration. NPX values are relative and thus cannot be compared between proteins. All EBP samples were analyzed at the same time.

Table 1 Patient characteristics

	All patients (n = 35)	LUAD (n = 17)	Control (n = 18)	Significance
Sex				
Male	21 (60)	6 (35)	15 (83)	p = 0.0059
Female	14 (40)	11 (65)	3 (17)	p = 0.0059
Age, years	70 (43–83)	72 (59–83)	68 (43–80)	p = 0.3381
BMI, kg/m^2	27.5 (19.6–38.0)	27.4 (21.1–35.6)	27.6 (19.6–38.0)	p = 0.8799
Comorbidities				
Coronary artery disease	14 (40)	2 (12)	12 (67)	p = 0.0016
Diabetes mellitus	13 (37)	3 (18)	10 (56)	p = 0.0354
Hypertension	22 (63)	8 (47)	14 (78)	p = 0.0858
WHO performance status prior to surgery				
0	13 (37)	9 (53)	4 (22)	p = 0.0858
1	15 (43)	8 (47)	7 (39)	p = 0.7380
2	7 (20)	0 (0)	7 (39)	p = 0.0076
Smoking history				
Current	2 (6)	2 (12)	0 (0)	p = 0.2286
Former (> 6 weeks)	26 (74)	11 (65)	15 (83)	p = 0.2642
Never	7 (20)	4 (23)	3 (17)	p = 0.6906

Characteristics for patients with lung adenocarcinoma (LUAD) and non-cancer surgical control patients. All data are reported as n (%) or mean (range). *BMI* body mass index. Significance was defined as: p < 0.0001 (****), p < 0.001 (***), p < 0.01 (**), p < 0.05 (*), and p > 0.05 (not significant, ns)

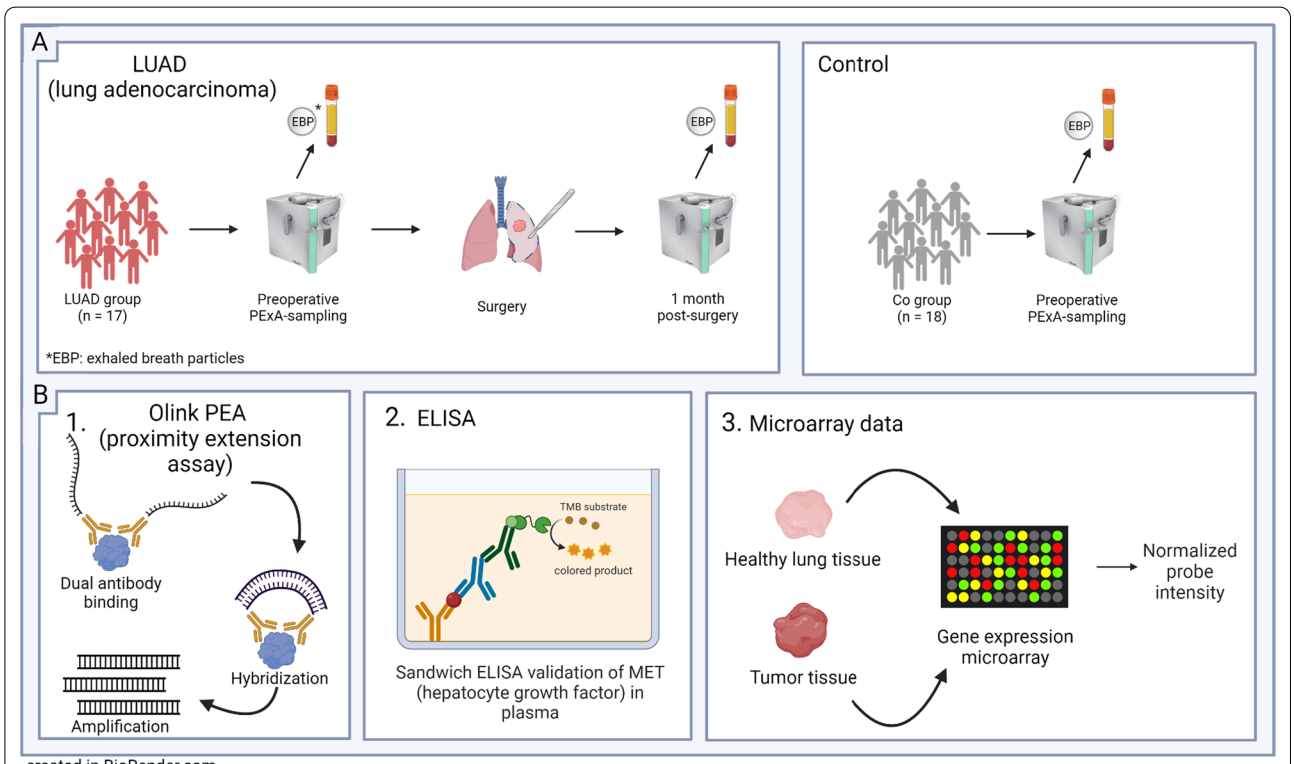

Fig. 1 Overview of workflow. **A** Patient enrollment, describes sampling of exhaled breath particles (EBP) and plasma from lung adenocarcinoma patients (LUAD) and non-cancer surgical controls (Co). Samples were collected preoperatively for both cohorts and at 1-month post-surgery for the LUAD cohort. **B** Validation, (1) Proximity extension assay (PEA) technology. (2) Standard sandwich enzyme-linked immunosorbent assay with specific antibodies for hepatocyte growth factor (MET) in plasma from all patients and timepoints (n = 49). (3) Deposited microarray data were used for validation of proteins in EBP

Table 2 Staging, resection type and radicality

Histopathological classification	n = 17
Adenocarcinoma	17 (100)
Tumor stage	
IA	10 (59)
IB	4 (24)
IIA	1 (6)
IIB	0 (0)
IIIA	2 (12)
Lung resection	
Segmental resection	2 (12)
Lobectomy	15 (88)
R0	16 (94)
R1	1 (6)

Histopathological stage, type of resection and radicality in lung adenocarcinoma patients. All data reported as n (%). *R0* microscopic radicality, *R1* microscopic margins positive for tumor

Heatmap

A heatmap was created in R version 4.1.3 using the packages "readxl" and gplots". The data were standardized to allow comparison between the proteins and the protein levels were expressed as the z-score for each sample.

Blood sampling

Blood was collected on the day before and 1 month after surgery in the LUAD group and the day before surgery in the control group. The blood was collected in ethylenediaminetetraacetic acid (EDTA) tubes (BD Vacutainer, Becton, Dickenson and company, Franklin Lakes, USA). The samples were centrifuged for 10 min at 5000 rpm, at 22 °C, within 30 min of collection, and the plasma was thereafter stored at −80 °C until analysis.

MET in plasma using ELISA

An enzyme-linked immunosorbent assay (ELISA) targeting soluble MET (s-MET) (HGFR/c-MET ELISA kit (ELH-HGFR-1), RayBiotech Life Inc., Atlanta, GA, US) was performed on plasma according to the manufacturer's instructions.

Validation of proteins

The GSE10072 dataset which contains deposited microarray data describing gene expression in biopsies from primary LUAD (n = 58) and lung biopsies from healthy controls residing in the same area (n = 49) was selected from the Gene Expression Omnibus (GEO; https://www.ncbi.nlm.nih.gov/gds) to validate protein expression in EBP [22]. Unit of gene expression was expressed as normalized probe intensity (NPI).

Statistical analysis

A power calculation with a statistical power of 87% and an effect size of 1.82 as calculated by hedges g was performed, using the results of biochemical analysis of surfactant A of a previously published study [10]. Descriptive statistics are presented as mean, range and standard error of mean (SEM). Student's t-test, simple linear regression and Pearson's correlation test were performed using GraphPad Prism version 9.2.0 for Windows (GraphPad Software, San Diego, California USA). Significance was defined as: $p < 0.0001$ (****), $p < 0.001$ (***), $p < 0.01$ (**), $p < 0.05$ (*), and $p > 0.05$ (not significant, ns).

Results

Particle flow rate from the airways was significantly higher in patients with LUAD

Particle flow rate (PFR) was measured before and 1 month after surgery and was compared to patients without LUAD. A significantly higher PFR was seen among LUAD patients before surgery compared to the control patients (18,490 ± 3306 particles/L in LUAD patients, 4021 ± 899 particles/L in the control group [$p < 0.0001$]), (Fig. 2b). The PFR was still significantly increased 1 month after surgery compared to the patients without LUAD ($p = 0.0001$). Comparing PFR in LUAD patients before and after surgery, no significant difference was found (18,490 ± 3306 particles/L before surgery and 30,210 ± 6500 particles/L 1 month after surgery ($p = 0.1142$).

Proteomic analysis of exhaled breath particles revealed differential levels between LUAD and patients without LUAD

A total of 89 unique proteins were detected using PEA technology and all were found in more than 75% of samples. A table of all 89 detected proteins can be found in Additional file 2: Table S1. Five proteins had a significantly higher protein concentration before surgery in the LUAD group compared to patients without LUAD: complement factor H-related protein 5 (CFHR5), microfibrillar-associated protein 5 (MFAP5), phospholipid transfer protein (PLTP), hepatocyte growth factor receptor/mesenchymal epithelial transition (HGF-R/MET) and carbonic anhydrase 4 (CA4), (Fig. 2a). These five proteins clustered as shown in the heatmap, the orange color representing a lower z-score (Fig. 3). One month after surgery, the three proteins, PLTP, MET and MFAP5, showed a decreasing trend, and when compared to patients

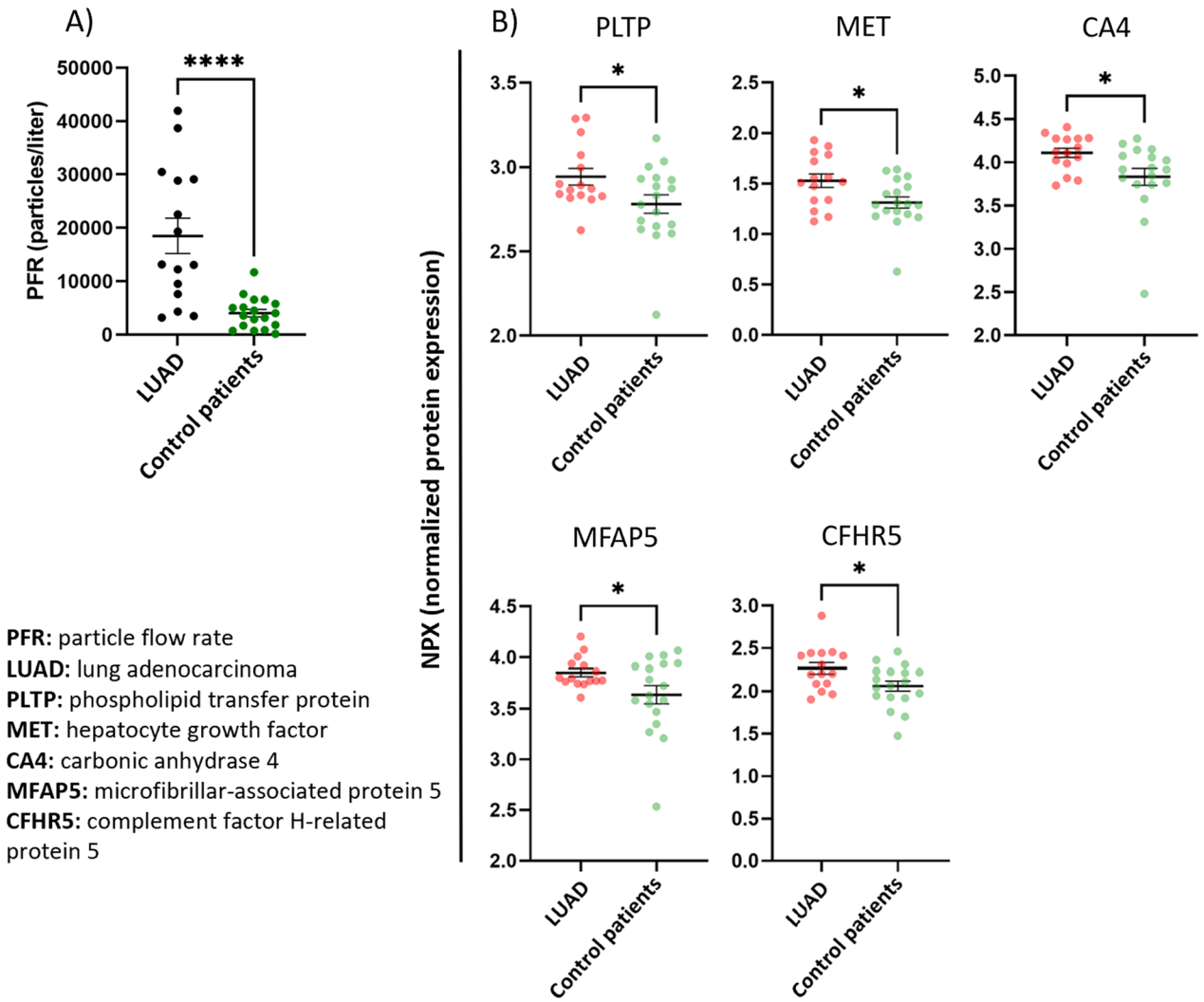

Fig. 2 Particle flow rate (PFR) from the airways as well as five proteins in exhaled breath particles (EBP) were significantly higher in patients with lung adenocarcinoma (LUAD) compared to patients without LUAD. **A** PFR was significantly higher in patients with LUAD. **B** The Figure shows normalized protein expression (NPX) of phospholipid transfer protein (PLTP), hepatocyte growth factor (MET), carbonic anhydrase 4 (CA4), microfibrillar-associated protein 5 (MFAP5) and complement factor H-related protein 5 (CFHR5) before surgical removal of LUAD compared to patients without LUAD (control patients). Data are presented as mean ± SEM. Significance was defined as: $p < 0.0001$ (****), $p < 0.001$ (***), $p < 0.01$ (**), $p < 0.05$ (*), and $p > 0.05$ (not significant, ns)

without LUAD, the significance was no longer found, possibly indicating tumor removal.

MET protein expression in plasma was elevated in LUAD patients

To further confirm if our findings in EBP also could be detected in plasma, MET in plasma was analyzed using ELISA. A significantly higher MET concentration was found before surgery in the LUAD group compared to the control group (3921 ± 144 pg/mL in LUAD patients, 2358 ± 161 pg/mL in patients without LUAD [$p < 0.0001$]), in line with the findings in EBP (Fig. 4a). There was a significant correlation of protein levels in EBP and plasma in all patients (Fig. 4b).

Survival

Postoperative 3-year survival follow-up was carried out for LUAD patients. All patients except one were still alive at 3 years.

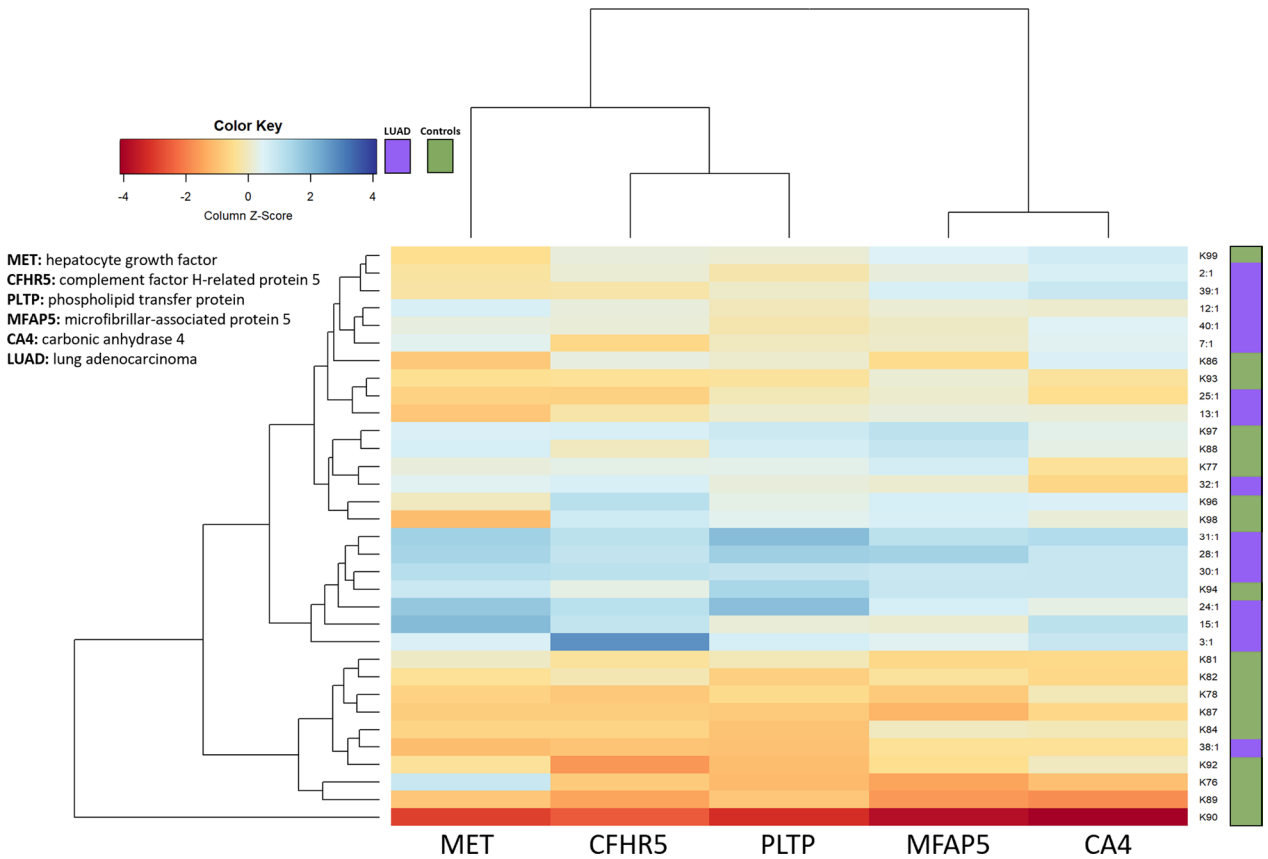

Fig. 3 Clustering of five proteins in exhaled breath particles (EBP) from lung adenocarcinoma patients compared to control patients. The heatmap displays levels of hepatocyte growth factor receptor (MET), complement factor H-related protein 5 (CFHR5), phospholipid transfer protein (PLTP), microfibrillar-associated protein 5 (MFAP5) and carbonic anhydrase 4 (CA4) expressed as z-score on the x-axis. The y-axis displays the individual sample identification codes

Validation of EBP data using dataset GSE10072 microarray data

Deposited microarray data from the dataset GSE10072 were used to validate the EBP findings. The proteins PLTP (gene ID NM_006227) and MET (gene ID BG170541 and BE870509) were significantly elevated in LUAD tissue compared to lung tissue from non-LUAD patients (PLTP: 9.66 ± 0.10 NPI in LUAD patients, 9.29 ± 0.12 NPI in non-LUAD patients [p = 0.008], MET BG170541: 9.52 ± 0.19 NPI in LUAD patients, 8.79 ± 0.07 NPI in non-LUAD patients [p = 0.0008], MET BE870509: 8.16 ± 0.07 NPI in LUAD patients, 7.88 ± 0.03 NPI in non-LUAD patients [p = 0.003]) (Table 3).

Discussion

This study explored the potential use of proteomics, based on EBP to detect possible biomarkers to diagnose patients with LUAD. In the present study patients undergoing lung cancer surgery were compared to patients without LUAD with similar age and smoking history. Using the PExA system, the PFR as well as proteins in EBP were analyzed in the two groups. The PFR reflects the number of exhaled particles and has the advantage of providing the examiner with an immediate result. The PFR was more than four times higher in the LUAD patients before the surgery compared to control patients indicating that PFR alone could be used to differentiate between patients with and without LUAD. Over the course of 1 month after surgery the PFR decreased among the LUAD patients, which might indicate tumor removal.

Given that protein content in EBP samples is considerably small, in the range of nanograms, the subsequent analysis of the EBP protein composition in the current study was performed using a unique technology, the proximity extension assay (PEA), which enables a robust high-throughput, multiplex immunoassay in very small biological samples. The technology is built upon pre-designed protein panels. Most of the PEA panels require some extent of dilution of the sample. In this early study, Olink's cardiometabolic panel, which

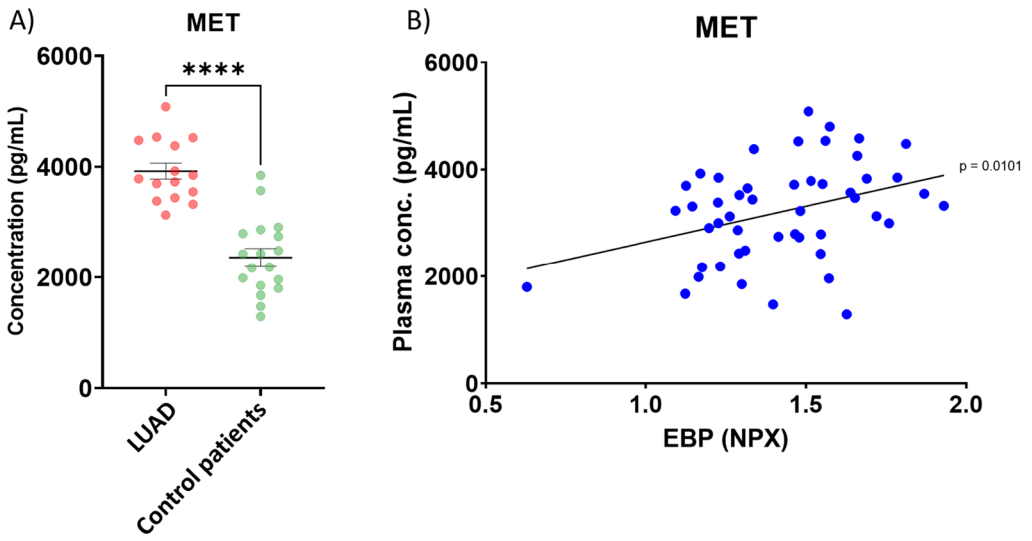

MET: hepatocyte growth factor, **LUAD:** lung adenocarcinoma, **EBP:** exhaled breath particles, **NPX:** normalized protein expression

Fig. 4 MET concentrations in plasma correlates to levels in exhaled breath particles (EBP). **A** Concentration of hepatocyte growth factor (MET) in plasma in patients with lung adenocarcinoma (LUAD) and patients without LUAD (control patients). Data are presented as mean ± SEM. **B** Correlation of MET in plasma and EBP for all patients at all timepoints (number of patients 35, number of samples 49) are shown. Protein level in EBP is expressed as normalized protein expression (NPX). Significance was defined as: $p < 0.0001$ (****), $p < 0.001$ (***), $p < 0.01$ (**), $p < 0.05$ (*), and $p > 0.05$ (not significant, ns)

Table 3 Gene expression of the proteins PLTP and MET

Protein	GenBank	Gene expression cancer	Gene expression control	Significance
PLTP	NM_006227	9.66 ± 0.10	9.29 ± 0.12	p = 0.0080
MET	BG170541	9.52 ± 0.19	8.79 ± 0.07	p = 0.0008
MET	BE870509	8.16 ± 0.07	7.88 ± 0.03	p = 0.0030

Dataset GSE10072 from Gene Expression Omnibus compares tissue from patients with LUAD (n = 58) and healthy control patients (n = 49). Gene expression was calculated by microarray techniques and expressed as normalized probe intensity

is the most sensitive panel and thus requires the least amount of biospecimen, was selected for technical reasons. The panel includes proteins involved in cellular metabolism, adhesion, and immunological processes. Patients with LUAD had significantly higher levels of PLTP, CA4, CFHR5, MFAP5, and MET compared to the control patients without LUAD, indicating that these proteins have a diagnostic potential for LUAD using EBP. One month after removal of the LUAD, expression of MET, PLTP and MFAP5 all decreased, which could be attributed to the radical tumor removal. All proteins that were found to be significantly higher expressed in EBP have a clear connection to cancer physiology, especially MET. More information on the involvement of the studied proteins is laid out in the Additional file 3.

High levels of MET in plasma have been correlated with a significantly poorer overall survival [23]. A significant correlation was found between MET in EBP and s-MET in plasma among all LUAD patients before surgery. No correlation between mortality and levels of MET could be seen in the current study. One month after surgery, both EBP and plasma levels of MET decreased but were still higher than MET in EBP and plasma in patients without LUAD. Our results are in line with previous findings of MET in LUAD tumor tissue and plasma [24]. However, this is the first time MET has been detected in EBP. MET in EBP seems to reflect MET in blood in our cohort; however, MET in plasma does not have to be disease specific whilst MET in EBP specifically comes from the RTLF and thus processes in the lung and cannot be traced to other processes or malignancies in other organs in the body [25–28].

PLTP was among the other significant proteins found in EBP, which is expressed in different types of neoplasms and is involved in cancer development [29]. In the present study, significantly higher levels of PLTP were seen in LUAD patients compared to control patients before surgical removal of the lung cancer; however, after surgery the levels of PLTP had decreased and there was no longer any significant difference when compared to the control patients, potentially indicating successful removal of the tumor. CA4 was also found to be significantly different, and low expression of CA4 can promote

proliferation of cancer cells, whereas overexpression can suppress proliferation of cancer cells [30]. Surprisingly, higher levels of CA4 were found in EBP samples in LUAD patients both preoperatively and after surgical removal of the tumor in the present study compared to control patients, indicating that CA4 might not be a good candidate for evaluating LUAD in EBP. In the current study significantly higher levels of MFAP5 were seen in EBP from LUAD patients before surgery compared to patients without LUAD; however, 1 month after surgery, the levels of MFAP5 had decreased, which might indicate that MFAP5 may be used as a biomarker in EBP to evaluate the successful surgical removal of LUAD. MFAP5 is known for signaling through the notch signaling pathway that activates cell proliferation and promotes the epithelial mesenchymal transition which leads to enhanced motility, invasion, and potential for metastasis in NSCLC [31–33]. Among the identified proteins PLTP and MET, as well as PFR were found significant, and based on the literature and support of external data these biomarkers were suggested as diagnostics in EBP for LUAD. However, some other proteins found are interesting but potentially less significant in EBP. CFHR5 is a protein in a family of 5, where CFHR1 previously been correlated to LUAD but not CFHR5. While defective CFHR5 may contribute to atypical hemolytic uremic syndrome, CFHR1 has been shown to be downregulated in tissue from LUAD tumors compared to healthy adjacent tissue. Given that CFHR1 was not included in the protein panel applied in this study, CFHR1 could not be analyzed. Given these unclarities, CFHR1 was not chosen for validation in the plasma. CA4 and MFAP5 showed reverse expression in EBP in the LUAD cohort then expected, in addition the two proteins could not be validated in any external data. Given these results CA4 and MFAP5 was seen as a less suitable biomarker in EBP.

To validate EBP findings we used microarray data from biopsies of healthy lung tissue and from LUAD tissue deposited in the dataset GSE10072. In this dataset, the gene expression of both PLTP and MET was higher in LUAD tissue compared to healthy lung tissue. These results are in line with the findings of the present study and support the use of those two biomarkers for diagnosing LUAD and to evaluate the successful surgical removal of LUAD. However, the levels of mRNA do not always correlate fully to corresponding proteins levels and tumors are very heterogeneous which indicate that further studies are of importance.

Conclusion

For the first time, PFR was measured and EBP were collected and analyzed in LUAD patients with the potential to identify novel biomarkers for the diagnosis and prognosis of LUAD. The PFR alone enabled the possibility of distinguishing between LUAD and patients without LUAD. Collection of EBP made it possible to perform a proteomic analysis of the respiratory system. Here, the proteins PLTP and MET were significantly higher in LUAD patients, which was further validated with microarray data from LUAD biopsies in a separate cohort. PLTP and MET have been identified as potential biomarkers for LUAD diagnosis and in the evaluation of successful tumor excision.

Strengths and limitations

The strength of this study is that it explores a novel technique of sampling proteins from particles in exhaled air. The technique itself has an advantage in that it samples particles exclusively from the small airways directly onto a membrane and thus dilution is avoided. Studies exploring exhaled breath proteomics in lung cancer are scarce and here we present both pre- and postoperative results. Furthermore, collection of EBPs is a completely non-invasive method, without risk to the patient. The non-invasiveness of the method makes it possible for non-clinicians to perform the sampling, which is advantageous in a screening setting. However, the current study does not explore the differences in PFR depending on the size of the tumor, nor how early one may detect lung cancer using this method. However, these questions will be further explored in future studies.

Abbreviations

CA4: Carbonic anhydrase 4; CFHR5: Complement factor H-related protein 5; EBC: Exhaled breath condensate; EBP: Exhaled breath particles; EDTA: Ethylenediaminetetraacetic acid; HGF-R/MET: Hepatocyte growth factor receptor/mesenchymal epithelial transition; HGF: Hepatocyte growth factor; LUAD: Lung adenocarcinoma; MET: Hepatocyte growth factor receptor; MFAP5: Microfibrillar-associated protein 5; NPI: Normalized probe intensity; NSCLC: Non-small cell lung cancer; PEA: Proximity extension assay; PExA: Particles in exhaled air; PFR: Particle flow rate; PLTP: Phospholipid transfer protein; RTLF: Respiratory tract lining fluid; s-MET: Soluble MET.

Supplementary Information

The online version contains supplementary material available at https://doi.org/10.1186/s12931-022-02302-4.

Additional file 1: Figure S1. Flow char tof enrolled subjects. A total of 35 patients were enrolled in the study: 17 with lung adenocarcinoma (LUAD) and 18 non-cancer surgical controls. The LUAD group was sampled at two timepoints, once before surgery and once 1 month after surgery. The control group was sampled once before surgery. Every sampling includes collection of exhaled breath particles (EBP) and blood plasma. All collected plasma samples were analyzed with an ELISA to validate the expression of the protein hepatocyte growth factor (MET).

Additional file 2: Table S1.

Additional file 3. Discussion

Acknowledgements

Gabriel Hirdman for scientific input and support.

Author contributions
JA and SL are responsible for conceptualization. JA, OH and SL came up with the methodology used in this study. EB validated the data findings. EB and OH did the formal analysis of the data. MM and SL have gathered the resources necessary for the study. MF, EB and CW are responsible for data curation. JA and EB wrote the original draft for the manuscript. JA, EB, FO and SL rewrote and edited the manuscript. EB did the visualizations. FO and SL have supervised the process. SL is in charge of project administration and has acquired the funding. All authors read and approved the final manuscript.

Funding
Open access funding provided by Lund University. The Knut and Alice Wallenberg Foundation, the Sjöberg Foundation, the National Cancer Foundation, the ALF Foundation, and the Fru Berta Kamprad Foundation.

Availability of data and materials
The dataset supporting the conclusions of this article is available in the Gene Expression Omnibus (GEO) repository, [https://www.ncbi.nlm.nih.gov/sites/GDSbrowser].

Declarations

Ethics approval and consent to participate
This study is approved by the local ethics committee (Dnr. 2017/519) (ClinicalTrials.gov NCT05395611), was performed in accordance with the Declaration of Helsinki and the STROBE statement. All patients signed informed consent forms prior to inclusion.

Consent for publication
Not applicable.

Competing interests
The authors declare that they have no competing interests.

Author details
[1]Department of Cardiothoracic Surgery, Skåne University Hospital, Lund, Sweden. [2]Department of Clinical Sciences, Lund University, Entrégatan 7, 22242 Lund, Sweden. [3]Department of Cardiothoracic Surgery, Rigshospitalet, University of Copenhagen, Copenhagen, Denmark. [4]Ludwig-Maximilians-University, Munich, Germany.

Received: 14 November 2022 Accepted: 15 December 2022
Published online: 21 December 2022

References

1. Sung H, Ferlay J, Siegel RL, Laversanne M, Soerjomataram I, Jemal A, et al. Global Cancer Statistics 2020: GLOBOCAN estimates of incidence and Mortality Worldwide for 36 cancers in 185 countries. CA Cancer J Clin. 2021;71(3):209–49.
2. Gunnar Wagenius MH, Karin Olsson, Kristina Lamberg-Lundström, Stefan Bergström. Lungcancer Nationell Kvalitetesrapport för 2020. Nationella Lungcancerregistret, NLCR. 2020. https://doi.org/https://cancercentrum.se/globalassets/cancerdiagnoser/lunga-och-lungsack/kvalitetsregister/rapport/nlcr_nationell_rapport2020.pdf. Accessed 10 Nov 2022.
3. de Koning HJ, van der Aalst CM, de Jong PA, Scholten ET, Nackaerts K, Heuvelmans MA, et al. Reduced lung-Cancer mortality with volume CT screening in a Randomized Trial. N Engl J Med. 2020;382(6):503–13.
4. National Lung Screening Trial Research Team. Lung cancer incidence and mortality with extended follow-up in the national lung screening trial. J Thorac Oncol. 2019;14(10):1732–42.
5. Mazzone PJ, Silvestri GA, Patel S, Kanne JP, Kinsinger LS, Wiener RS, et al. Screening for Lung Cancer: CHEST Guideline and Expert Panel Report. Chest. 2018;153(4):954–85.
6. Oudkerk M, Devaraj A, Vliegenthart R, Henzler T, Prosch H, Heussel CP, et al. European position statement on lung cancer screening. Lancet Oncol. 2017;18(12):e754-e66.
7. Toumazis I, Bastani M, Han SS, Plevritis SK. Risk-based lung cancer screening: a systematic review. Lung Cancer. 2020;147:154–86.
8. Salgia R. MET in Lung Cancer: Biomarker Selection based on scientific rationale. Mol Cancer Ther. 2017;16(4):555–65.
9. Drilon A, Cappuzzo F, Ou S-HI, Camidge DR. Targeting MET in Lung Cancer: will expectations finally be MET? J Thorac Oncol. 2017;12(1):15–26.
10. Broberg E, Andreasson J, Fakhro M, Olin A-C, Wagner D, Hyllén S, et al. Mechanically ventilated patients exhibit decreased particle flow in exhaled breath as compared to normal breathing patients. ERJ Open Research. 2020;6(1):00198–2019.
11. Amann A, Costello Bde L, Miekisch W, Schubert J, Buszewski B, Pleil J, et al. The human volatilome: volatile organic compounds (VOCs) in exhaled breath, skin emanations, urine, feces and saliva. J Breath Res. 2014;8(3):034001.
12. Patsiris S, Exarchos T, Vlamos P. Exhaled Breath Condensate (EBC): is it a viable source of biomarkers for Lung Diseases? Adv Exp Med Biol. 2020;1195:13–8.
13. Bajaj P, Ishmael FT. Exhaled Breath Condensates as a source for biomarkers for characterization of Inflammatory Lung Diseases. J Anal Sci Methods Instrum. 2013;03(01):17–29.
14. Broberg E, Hyllén S, Algotsson L, Wagner DE, Lindstedt S. Particle flow profiles from the airways measured by PExA Differ in lung transplant recipients who develop primary graft dysfunction. Exp Clin Transplant. 2019;17(6):803–12.
15. Stenlo M, Hyllén S, Silva IAN, Bölükbas DA, Pierre L, Hallgren O, et al. Increased particle flow rate from airways precedes clinical signs of ARDS in a porcine model of LPS-induced acute lung injury. Am J Physiol Lung Cell Mol Physiol. 2020;318(3):L510-l7.
16. Hallgren F, Stenlo M, Niroomand A, Broberg E, Hyllén S, Malmsjö M, et al. Particle flow rate from the airways as fingerprint diagnostics in mechanical ventilation in the intensive care unit: a randomised controlled study. ERJ Open Res. 2021. https://doi.org/10.1183/23120541.00961-2020.
17. Broberg E, Pierre L, Fakhro M, Algotsson L, Malmsjö M, Hyllén S, et al. Different particle flow patterns from the airways after recruitment manoeuvres using volume-controlled or pressure-controlled ventilation. Intensive Care Med Exp. 2019;7(1):16.
18. Stenlo M, Silva IAN, Hyllén S, Bölükbas DA, Niroomand A, Grins E, et al. Monitoring lung injury with particle flow rate in LPS- and COVID-19-induced ARDS. Physiol Rep. 2021;9(13):e14802.
19. Soares M, Mirgorodskaya E, Koca H, Viklund E, Richardson M, Gustafsson P, et al. Particles in exhaled air (PExA): non-invasive phenotyping of small airways disease in adult asthma. J Breath Res. 2018;12(4):046012.
20. Goldstraw P, Crowley J, Chansky K, Giroux DJ, Groome PA, Rami-Porta R, et al. The IASLC Lung Cancer Staging Project: proposals for the revision of the TNM stage groupings in the forthcoming (seventh) edition of the TNM classification of malignant tumours. J Thorac Oncol. 2007;2(8):706–14.
21. Olink Cardiometabolic Validation Data. Olink proteomics AB. 2018. https://doi.org/https://www.olink.com/content/uploads/2021/09/olink-cardiometabolic-validation-data-v2.0.pdf. Accessed 10 Nov 2022.
22. Landi MT, Dracheva T, Rotunno M, Figueroa JD, Liu H, Dasgupta A, et al. Cigarette smoking effect on lung adenocarcinoma. 2008. https://doi.org/https://www.ncbi.nlm.nih.gov/sites/GDSbrowser?acc=GDS3257#details. Accessed 10 Nov 2022.
23. Gao HF, Li AN, Yang JJ, Chen ZH, Xie Z, Zhang XC, et al. Soluble c-Met levels correlated with tissue c-Met protein expression in patients with advanced non-small-cell lung cancer. Clin Lung Cancer. 2017;18(1):85–91.
24. Lv H, Shan B, Tian Z, Li Y, Zhang Y, Wen S. Soluble c-Met is a reliable and sensitive marker to detect c-Met expression level in lung cancer. Biomed Res Int. 2015;2015:626578.
25. Bake B, Larsson P, Ljungkvist G, Ljungström E, Olin AC. Exhaled particles and small airways. Respir Res. 2019;20(1):8.
26. Lin J, Ma L, Zhang D, Gao J, Jin Y, Han Z, et al. Tumour biomarkers—tracing the molecular function and clinical implication. Cell Prolif. 2019;52(3):e12589.
27. Mayeux R. Biomarkers. Potential uses and limitations. NeuroRX. 2004;1(2):182–8.
28. Almstrand AC, Josefson M, Bredberg A, Lausmaa J, Sjovall P, Larsson P, et al. TOF-SIMS analysis of exhaled particles from patients with asthma and healthy controls. Eur Respir J. 2012;39(1):59–66.
29. Albers JJ, Vuletic S, Cheung MC. Role of plasma phospholipid transfer protein in lipid and lipoprotein metabolism. Biochim Biophys Acta. 2012;1821(3):345–57.

30. Yu DH, Huang JY, Liu XP, Ruan XL, Chen C, Hu WD, et al. Effects of hub genes on the clinicopathological and prognostic features of lung adenocarcinoma. Oncol Lett. 2020;19(2):1203–14.
31. Yuan X, Wu H, Han N, Xu H, Chu Q, Yu S, et al. Notch signaling and EMT in non-small cell lung cancer: biological significance and therapeutic application. J Hematol Oncol. 2014;7:87.
32. Sharif A, Shaji A, Chammaa M, Pawlik E, Fernandez-Valdivia R. Notch transduction in non-small cell lung cancer. Int J Mol Sci. 2020;21(16):5691.
33. Database GTHG. MFAP5 Gene Protein Coding GeneCards The Human Gene Database. https://doi.org/https://www.genecards.org/cgi-bin/carddisp.pl?gene=MFAP5. Accessed 28 Jul 2021.

Publisher's Note

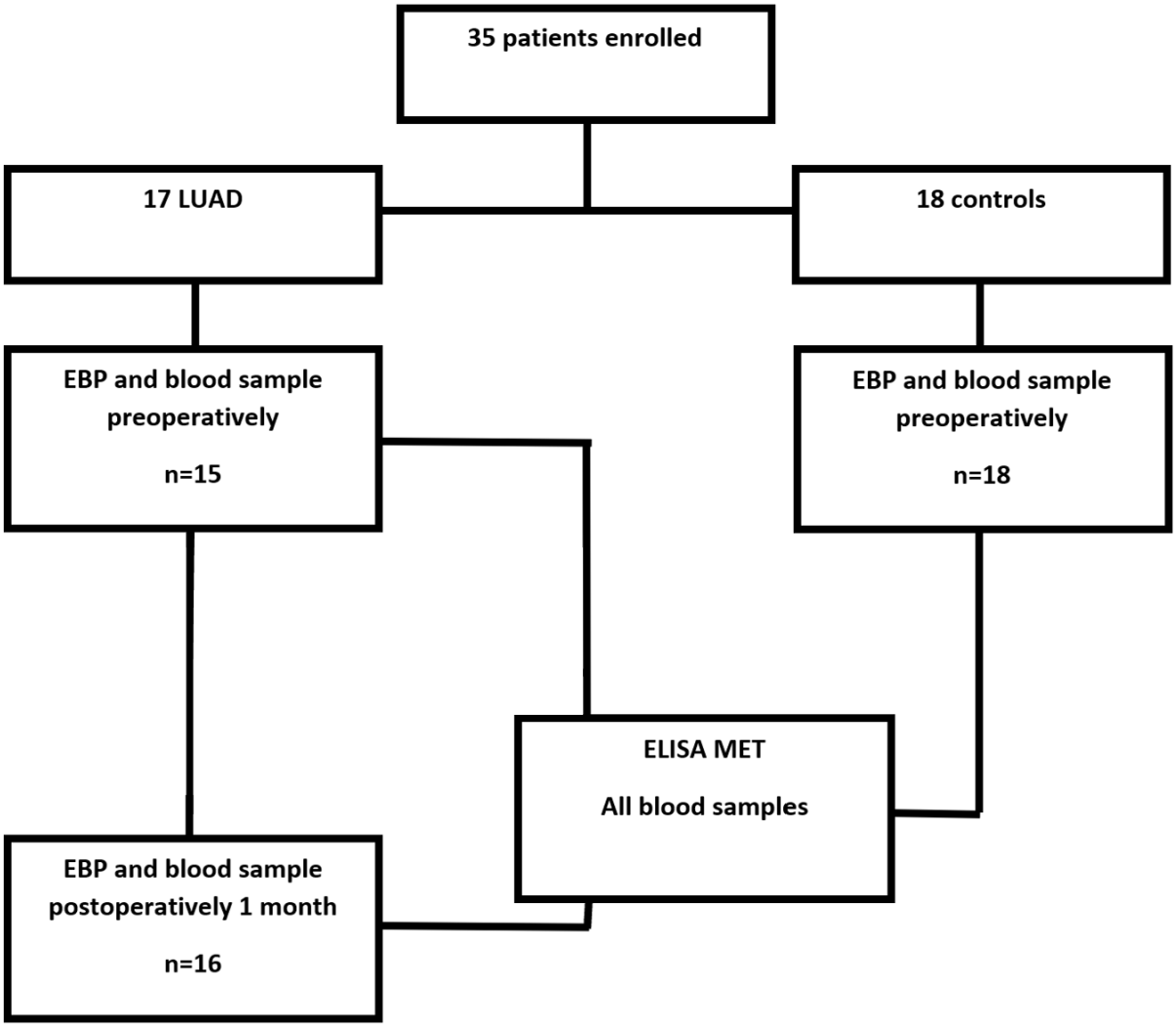

Additional file 1: Figure S1

Flow chart of enrolled subjects. A total of 35 patients were enrolled in the study: 17 with lung adenocarcinoma (LUAD) and 18 non-cancer surgical controls. The LUAD group was sampled at two timepoints, once before surgery and once 1 month after surgery. The control group was sampled once before surgery. Every sampling includes collection of exhaled breath particles (EBP) and blood plasma. All collected plasma samples were analyzed with an ELISA to validate the expression of the protein hepatocyte growth factor (MET).

Additional file 2: Table S1

	Protein	UniProt ID	Protein name
1.	PRCP	P42785	Lysosomal Pro-X carboxypeptidase
2.	CA1	P00915	Carbonic anhydrase 1
3.	ICAM1	P05362	Intercellular adhesion molecule 1
4.	CHL1	O00533	Neural cell adhesion molecule L1-like protein
5.	TGFBI	Q15582	Transforming growth factor-beta-induced protein ig-h3
6.	ENG	P17813	Endoglin
7.	PLTP	P55058	Phospholipid transfer protein
8.	SERPINA7	P05543	Thyroxine-binding globulin
9.	IGFBP3	P17936	Insulin-like growth factor-binding protein 3
10.	CR2	P20023	Complement receptor type 2
11.	SERPINA5	P05154	Plasma serine protease inhibitor
12.	FCGR3B	O75015	Low affinity immunoglobulin gamma Fc region receptor III-B
13.	IGFBP6	P24592	Insulin-like growth factor-binding protein 6
14.	CDH1	P12830	Cadherin-1
15.	CCL5	P13501	C-C motif chemokine 5
16.	CCL14	Q16627	C-C motif chemokine 14
17.	GNLY	P22749	Granulysin
18.	NOTCH1	P46531	Neurogenic locus notch homolog protein 1
19.	PAM	P19021	Peptidyl-glycine alpha-amidating monooxygenase
20.	PROC	P04070	Vitamin K-dependent protein C
21.	CST3	P01034	Cystatin-C
22.	NCAM1	P13591	Neural cell adhesion molecule 1
23.	PCOLCE	Q15113	Procollagen C-endopeptidase enhancer 1
24.	LILRB1	Q8NHL6	Leukocyte immunoglobulin-like receptor subfamily B member 1
25.	MET	P08581	Hepatocyte growth factor receptor
26.	LTBP2	Q14767	Latent-transforming growth factor beta-binding protein 2
27.	IL7R	P16871	Interleukin-7 receptor subunit alpha
28.	VCAM1	P19320	Vascular cell adhesion protein 1
29.	SELL	P14151	L-selectin
30.	F11	P03951	Coagulation factor XI
31.	COMP	P49747	Cartilage oligometric matrix protein
32.	CA4	P22748	Carbonic anhydrase 4
33.	PTPRS	Q13332	Receptor-type tyrosine-protein phosphatase S
34.	MBL2	P11226	Mannose-binding protein C
35.	TIMP1	P01033	Metalloproteinase inhibitor 1
36.	ANGPTL3	Q9Y5C1	Angiopoietin-related protein 3
37.	REG3A	Q06141	Regenerating islet-derived protein 3-alpha
38.	SOD1	P00441	Superoxide dismutase [Cu-Zn]
39.	CD46	P15529	Membrane cofactor protein
40.	ITGAM	P11215	Integrin alpha-M
41.	TNC	P24821	Tenascin
42.	NID1	P14543	Nidogen-1
43.	CFHR5	Q9BXR6	Complement factor H-related protein 5
44.	SPARCL1	Q14515	SPARC-like protein 1
45.	PLXNB2	O15031	Plexin-B2
46.	MEGF9	Q9H1U4	Multiple epidermal growth factor-like domains protein 9
47.	ANG	P03950	Angiogenin
48.	ST6GAL1	P15907	Beta-galactoside alpha-2,6-sialyltransferase 1
49.	DPP4	P27487	Dipeptidyl peptidase 4
50.	FCN2	Q15485	Ficolin-2
51.	FETUB	Q9UGM5	Fetuin-B
52.	CES1	P23141	Liver carboxylesterase 1
53.	CRTAC1	Q9NQ79	Cartilage acidic protein 1
54.	TCN2	P20062	Transcobalamin-2

55.	PRSS2	P07478	Trypsin-2
56.	ICAM3	P32942	Intercellular adhesion molecule 3
57.	SAA4	P35542	Serum amyloid A-4 protein
58.	CNDP1	Q96KN2	Beta-Ala-His dipeptidase
59.	FCGR2A	P12318	Low affinity immunoglobulin gamma Fc region receptor II-a
60.	NRP1	O14786	Neuropilin-1
61.	EFEMP1	Q12805	EGF-containing fibulin-like extracellular matrix protein 1
62.	TIMD4	Q96H15	T-cell immunoglobulin and mucin domain-containing protein 4
63.	FAP	Q12884	Prolyl endopeptidase FAP
64.	TIE1	P35590	Tyrosine-protein kinase receptor Tie-1
65.	THBS4	P35443	Thrombospondin-4
66.	F7	P08709	Coagulation factor VII
67.	GP1BA	P07359	Platelet glycoprotein Ib alpha chain
68.	LYVE1	Q9Y5Y7	Lymphatic vessel endothelial hyaluronic acid receptor 1
69.	CA3	P07451	Carbonic anhydrase 3
70.	TGFBR3	Q03167	Transforming growth factor beta receptor type 3
71.	DEFA1	P59655	Neutrophil defensin 1
72.	CD59	P13987	CD59 glycoprotein
73.	APOM	O95445	Apolipoprotein M
74.	OSMR	Q99650	Oncostatin-M-specific receptor subunit beta
75.	LILRB2	Q8N423	Leukocyte immunoglobulin-like receptor subfamily B member 2
76.	UMOD	P07911	Uromodulin
77.	CCL18	P55774	C-C motif chemokine 18
78.	COL18A1	P39060	Collagen alpha-1(XVIII) chain
79.	LCN2	P80188	Neutrophil gelatinase-associated lipocalin
80.	KIT	P10721	Mast/stem cell growth factor receptor Kit
81.	C1QTNF1	Q9BXJ1	Complement C1q tumor necrosis factor-related protein 1
82.	GAS6	Q14393	Growth arrest-specific protein 6
83.	IGLC2	P0DOY2	Ig lambda-2 chain C regions
84.	PLA2G7	Q13093	Platelet-activating factor acetylhydrolase
85.	TNXB	P22105	Tenascin-X
86.	MFAP5	Q13361	Microfibrillar-associated protein 5
87.	VASN	Q6EMK4	Vasorin
88.	LILRB5	O75023	Leukocyte immunoglobulin-like receptor subfamily B member 5
89.	C2	P06681	Complement C2

Proteins detected in EBP (n = 89) using Olink proteomics Cardiometabolic protein panel.

Exhaled phospholipid transfer protein and hepatocyte growth factor receptor in lung adenocarcinoma

Jesper Andreasson, MD[1,2], Embla Bodén, MD[1,2], Mohammed Fakhro, MD, PhD[3], Camilla von Wachter[4], Franziska Olm, PhD[1,2] Malin Malmsjö, MD, PhD[2], Oskar Hallgren, PhD[2], Sandra Lindstedt, MD, PhD[1, 2]

[1]Department of Cardiothoracic Surgery, Skåne University Hospital, Sweden

[2]Lund University, Department of Clinical Sciences, Sweden

[3]Department of Cardiothoracic Surgery, Rigshospitalet, University of Copenhagen, Denmark

[4]Ludwig-Maximilians-University, Munich, Germany

Corresponding author:

Sandra Lindstedt
Entrégatan 7, 22242, Lund, Sweden
sandra.lindstedt_ingemansson@med.lu.se

Additional file 3: Discussion

The proteins studied in this paper are all linked to processes central to cancer such as inflammation, cell proliferation, metastasis or anti-tumor immune mediated responses. The over- or under expression of these protein biomarkers impacts upon cancer development and progression in different ways. A literature search was conducted to gain understanding of how each protein functions within this field. PLTP (phospholipid transfer protein) is a glycoprotein that regulates transportation of phospholipids, and is highly expressed in pulmonary epithelial cells. PLTP is expressed in different types of neoplasms and is involved in cancer development (1). Silencing of PLTP in a murine model has been shown to result in increased inflammation, suggesting an anti-inflammatory role for PLTP. Expression of PLTP is elevated in patients with chronic obstructive pulmonary disease (COPD) and the activity of the protein correlates negatively with lung function as determined by forced expiratory volume in the first second (FEV1) (2).

CA4 (carbonic anhydrase 4) is a zinc membrane-associated metalloenzyme which catalyzes the interconversion of water and carbon dioxide into ions of carbonic acid and was also found in exhaled breath particles (EBP). CA4 is normally found in healthy lung tissue and has a role in regulating the local pH of the lung, but it is expressed in lower levels in lung cancer patients in general and in those with lung adenocarcinoma (LUAD) specifically (3-5). Lower levels have also been linked to lymph node metastasis and a shorter overall survival in lung cancer (5).

MFAP5 (microfibrillar-associated protein 5) is an extracellular microfibril-associated glycoprotein, upregulated in cancer-associated fibroblasts in multiple malignancies, including non-small cell lung cancer (NSCLC) (6, 7). Among others, MFAP5 is central to cancer-associated fibroblast differentiation and epithelial mesenchymal transition (7, 8). MFAP5 signals through the Notch signaling pathway that activates cell proliferation and promotes the epithelial mesenchymal transition which leads to enhanced motility, invasion, and potential for metastasis in NSCLC (8-10).
CFHR (complement factor H-related protein 5) is a family of five proteins, CFHR1–5, which can each bind to the complement component C3b. While defective CFHR5 may contribute to atypical

hemolytic uremic syndrome, CFHR1 has been shown to be downregulated in tissue from LUAD tumors compared to healthy adjacent tissue. Patients with lower expressed levels of CFHR1 were found to have a significantly shorter overall survival (11).

MET (hepatocyte growth factor receptor) is a transmembrane receptor tyrosine kinase for hepatocyte growth factor (HGF) involved in epithelial cellular migration, proliferation, morphogenesis, and survival. Mutation of MET is linked to several forms of cancer, including NSCLC (12). Studies have shown that patients with elevated expression of MET intratumorally have significantly lower survival compared to patients with MET-negative tumors (13). Furthermore, MET amplification is involved in the acquired resistance that develops in many patients treated with epidermal growth factor receptor (EGFR) inhibitor (14).

References

1. Albers JJ, Vuletic S, Cheung MC. Role of plasma phospholipid transfer protein in lipid and lipoprotein metabolism. Biochim Biophys Acta. 2012;1821(3):345-57.

2. Brehm A, Geraghty P, Campos M, Garcia-Arcos I, Dabo AJ, Gaffney A, et al. Cathepsin G degradation of phospholipid transfer protein (PLTP) augments pulmonary inflammation. Faseb j. 2014;28(5):2318-31.

3. Xu Y, Xu WH, Shi SN, Yang XL, Ren YR, Zhuang XY, et al. Carbonic Anhydrase 4 serves as a Clinicopathological Biomarker for Outcomes and Immune Infiltration in Renal Cell Carcinoma, Lower Grade Glioma, Lung Adenocarcinoma and Uveal Melanoma. J Cancer. 2020;11(20):6101-13.

4. Yu DH, Huang JY, Liu XP, Ruan XL, Chen C, Hu WD, et al. Effects of hub genes on the clinicopathological and prognostic features of lung adenocarcinoma. Oncol Lett. 2020;19(2):1203-14.

5. Chen J, Hu L, Zhang F, Wang J, Chen J, Wang Y. Downregulation of carbonic anhydrase IV contributes to promotion of cell proliferation and is associated with poor prognosis in non-small cell lung cancer. Oncol Lett. 2017;14(4):5046-50.

6. Yeung TL, Leung CS, Yip KP, Sheng J, Vien L, Bover LC, et al. Anticancer Immunotherapy by MFAP5 Blockade Inhibits Fibrosis and Enhances Chemosensitivity in Ovarian and Pancreatic Cancer. Clin Cancer Res. 2019;25(21):6417-28.

7. Navab R, Strumpf D, Bandarchi B, Zhu CQ, Pintilie M, Ramnarine VR, et al. Prognostic gene-expression signature of carcinoma-associated fibroblasts in non-small cell lung cancer. Proc Natl Acad Sci U S A. 2011;108(17):7160-5.

8. Yuan X, Wu H, Han N, Xu H, Chu Q, Yu S, et al. Notch signaling and EMT in non-small cell lung cancer: biological significance and therapeutic application. J Hematol Oncol. 2014;7:87.

9. Sharif A, Shaji A, Chammaa M, Pawlik E, Fernandez-Valdivia R. Notch Transduction in Non-Small Cell Lung Cancer. Int J Mol Sci. 2020;21(16).

10. Database GTHG. MFAP5 Gene Protein Coding GeneCards The Human Gene Database [cited 2021 28/7]. Available from: https://www.genecards.org/cgi-bin/carddisp.pl?gene=MFAP5.

11. Wu G, Yan Y, Wang X, Ren X, Chen X, Zeng S, et al. CFHR1 is a potentially downregulated gene in lung adenocarcinoma. Mol Med Rep. 2019;20(4):3642-8.

12. Matsumoto K, Umitsu M, De Silva DM, Roy A, Bottaro DP. Hepatocyte growth factor/MET in cancer progression and biomarker discovery. Cancer Sci. 2017;108(3):296-307.

13. Masuya D, Huang C, Liu D, Nakashima T, Kameyama K, Haba R, et al. The tumour-stromal interaction between intratumoral c-Met and stromal hepatocyte growth factor associated with tumour growth and prognosis in non-small-cell lung cancer patients. Br J Cancer. 2004;90(8):1555-62.

14. Bean J, Brennan C, Shih JY, Riely G, Viale A, Wang L, et al. MET amplification occurs with or without T790M mutations in EGFR mutant lung tumors with acquired resistance to gefitinib or erlotinib. Proc Natl Acad Sci U S A. 2007;104(52):20932-7.

Clinical Proteomics

RESEARCH

Open Access

Proteomic characteristics and diagnostic potential of exhaled breath particles in patients with COVID-19

Gabriel Hirdman[1,2,3], Embla Bodén[1,2,3], Sven Kjellström[4], Carl-Johan Fraenkel[5,6], Franziska Olm[1,2,3], Oskar Hallgren[1,2,3] and Sandra Lindstedt[1,2,3,7*]

Abstract

Background SARS-CoV-2 has been shown to predominantly infect the airways and the respiratory tract and too often have an unpredictable and different pathologic pattern compared to other respiratory diseases. Current clinical diagnostical tools in pulmonary medicine expose patients to harmful radiation, are too unspecific or even invasive. Proteomic analysis of exhaled breath particles (EBPs) in contrast, are non-invasive, sample directly from the pathological source and presents as a novel explorative and diagnostical tool.

Methods Patients with PCR-verified COVID-19 infection (COV-POS, n = 20), and patients with respiratory symptoms but with > 2 negative polymerase chain reaction (PCR) tests (COV-NEG, n = 16) and healthy controls (HCO, n = 12) were prospectively recruited. EBPs were collected using a "particles in exhaled air" (PExA 2.0) device. Particle per exhaled volume (PEV) and size distribution profiles were compared. Proteins were analyzed using liquid chromatography-mass spectrometry. A random forest machine learning classification model was then trained and validated on EBP data achieving an accuracy of 0.92.

Results Significant increases in PEV and changes in size distribution profiles of EBPs was seen in COV-POS and COV-NEG compared to healthy controls. We achieved a deep proteome profiling of EBP across the three groups with proteins involved in immune activation, acute phase response, cell adhesion, blood coagulation, and known components of the respiratory tract lining fluid, among others. We demonstrated promising results for the use of an integrated EBP biomarker panel together with particle concentration for diagnosis of COVID-19 as well as a robust method for protein identification in EBPs.

Conclusion Our results demonstrate the promising potential for the use of EBP fingerprints in biomarker discovery and for diagnosing pulmonary diseases, rapidly and non-invasively with minimal patient discomfort.

Keywords Exhaled breath particles, Proteomics, COVID-19, LC–MS/MS, Breath analysis

*Correspondence:
Sandra Lindstedt
sandra.lindstedt_ingemansson@med.lu.se
Full list of author information is available at the end of the article

Introduction

In late December 2019, doctors in Wuhan, China, notified the world of a new cluster of patients with pneumonia of unknown origin [1]. A novel virus, originating from the betacoronavirus family was rapidly sequenced and identified and named severe acute respiratory coronavirus 2 (SARS-CoV-2) causative of the respiratory disease, coronavirus disease 2019 (COVID-19) [2]. The specifics of the pathophysiology of SARS-CoV-2 infection remain poorly understood. Individuals are primarily infected via the airways, where SARS-CoV-2 binds with host angiotensin-converting enzyme 2 (ACE2) via its receptor-binding domain on the spike protein resulting in internalization of the virus into host cells [3]. The subsequent imbalance between the protective and adverse axis of the RAS pathway causes decreased stability of the pulmonary endothelium, inflammatory and thrombotic processes causing respiratory distress [4].

The COVID-19 pandemic highlighted many of the diagnostical challenges of pulmonary disease. Common diagnostical techniques include RT-PCR swabs for viral detection, auscultation, blood work, chest x-ray and computer tomography scans (CT-scans) [5]. However, only bronchoalveolar lavage (BAL) performed during bronchoscopy under sedation can properly detect pathological changes in the otherwise unreachable small airways. Furthermore, all current diagnostical methods have their weaknesses regarding sensitivity, specificity, or potential harm to patients. Novel diagnostical methods in pulmonary medicine are therefore urgently needed.

Exhaled breath is a carrier of valuable information from the respiratory system and analysis of particles and biomarkers provides an attractive such approach. Samples are collected non-invasively and provide a localized sample of the most distal parts of human lungs. Currently two such approaches are actively being researched. Measurements of the volatile compounds in breath, an alcohol breath analyzer being a common example, or the detection and analysis of exhaled breath particles (EBP). Compared with volatile compounds, EBPs can offer more specific insights into disease processes because an array of molecules can be measured. EBPs originate from the respiratory tract lining fluid that covers the epithelial surface of the distal parts of the lung. EBPs are thought to be generated during opening and closing of the distal airways but can also be generated through shear stress [6]. The protein composition of EBPs closely resembles that of BAL fluid of which changes in the proteomic composition have been connected to different pulmonary diseases [7].

A few studies have investigated the proteomic characteristics and changes in COVID-19 patients in plasma, BAL, sputum and pulmonary tissue [8–11]. Yet, none have yet investigated the proteomic profile of COVID-19 in EBPs. Furthermore, the proteomic composition of EBPs and alterations in human disease are still poorly understood. We therefore investigated the proteomic composition of EBPs in healthy subjects, in patients with respiratory symptoms but with repeated negative PCR test for COVID-19 infection and in COVID-19 infected patients through high-performance liquid chromatography-mass spectrometry (HPLC–MS/MS) to identify potential biomarkers in exhaled breath for rapid, non-invasive diagnosis and evaluation of pulmonary disease status.

Methods

Patients

Patients were recruited prospectively between the 14th of May and 14th of November 2020. A total of 48 patients participated in the study and split into two groups: PCR-verified COVID-19 infection (COV-POS, n = 20), repeat PCR-negative but COVID-19 symptomatic patients (COV-NEG, n = 16) and additionally healthy volunteers were included as controls (HCO, n = 12). Patients were recruited as either inpatients at the infectious disease wards or the emergency department at Skåne university hospital in Sweden. Mean age was 57 years (range 21–70). All patients signed an informed consent form before taking part in the study. The study was approved by the Swedish Ethical Review Authority EPN Dur 2018/129, 2020–018640427 and registered at ClinicalTrials.gov with the trial register number NCT04503057.

Particle collection

Particles were collected using a PExA 2.0 device (PExA, Gothenburg, Sweden). The instrument uses a two-way valve that allows participants to inhale particle-free air through a HEPA filter and exhale into the instrument. Particles are measured by their size and quantity by an optical particle counter and sized into 16 size bins and collected on a membrane by an inertial impactor within the device. The bin sizes averages ranges from 0.33 µm to 3.67 µm. Exhaled flow and volume are measured by an ultrasonic flow meter. A breathing maneuver, previously described, was used for the EBP collection until a goal amount of 120 ng of sampled particles had been collected [6, 12]. The particles are measured and expressed as number of particles per volume (PEV) and relative counts per particle size. All samples were immediately transferred after collection and stored at − 80 °C for later analysis. No participants reported any adverse events in connection to EBP sampling.

Statistical analysis of particle data

All statistical test related with PEV were done using Graphpad Prism 9 (Graphpad Software, San Diego, CA). Descriptive statistics in the form of median and interquartile range was used for particle and patient data. Kruskal–Wallis test with Dunn's post hoc test was used to compare PEV between groups. For statistical analysis between correlation of PEV to age the data were first transformed into its natural logarithms and then analyzed using Pearson parametric correlation coefficients and reported as R2. For comparison of PEV between sexes Mann–Whitney-U was used. For comparison of relative particle sizes between groups log transformed particle data was analyzed with a mixed effects model REML and Tukey's multiple comparisons test. Statistical significance was defined as ****$p < 0.0001$, ***$p < 0.001$, **$p < 0.01$, *$p < 0.05$ and NS ($p > 0.05$).

Sample preparation for LC–MS/MS

EBP samples were incubated in 2% sodium dodecyl sulfate (SDS, Sigma-Aldrich, St. Louis, USA) in 50 mM Triethylammonium bicarbonate (TEAB, Thermo Fisher Scientific) at 37 °C for 2 h with subsequent addition of 400 mM dithiothreitol (Sigma-Aldrich) and further incubation for 45 min.. Alkylation was performed in the dark for 30 min with the addition of 800 mM iodacetamide (Sigma-Aldrich) after which 12% aqueous phosphoric acid was added to a final concentration of 1.2%. Proteins were collected onto S-TRAP columns (Protifi, Farmingdale, USA) with a mixture of 90% methanol and 100 mM TEAB. Digestion of proteins was performed with 1 µg of Lys-C (Lys-C, Mass Spec Grade, Promega, Fitchburg, USA) incubated at 37 °C for 2 h after which 1 µg of trypsin (Promega sequence grade) was added overnight with addition of 0.45 µg Trypsin after 12 h. Peptides were then eluted with 50 mM TEAB, 0.2% formic acid (FA, Sigma-Aldrich) and 50% acetonitrile (ACN, Sigma-Aldrich) with 0.2% formic acid and dried by speedvac (Eppendorf, Hamburg, Germany) at 45 °C and re-dissolved in 20 uL of 0.1% FA and 2% ACN solution.

LC–MS/MS

Digested peptides were separated with nanoflow reversed-phase chromatography with an Evosep One liquid chromatography (LC) system (Evosep One, Odense, Denmark) after loading the samples on Evosep tips. Separation was performed with the 60 SPD method (gradient length 21 min) using an 8 cm × 150 µm Evosep column packed with 1.5 µm ReproSil-Pur C18-AQ particles. The Evosep One was coupled to a captive source mounted on a timsTOF Pro mass spectrometer from Bruker Daltonics (Billerica, Massachusetts, USA). The instrument was operated in the DDA PASEF mode with 10 PASEF scans per acquisition cycle and accumulation and ramp times of 100 ms each. Singly charged precursors were excluded, the 'target value' was set to 20,000 and dynamic exclusion was activated and set to 0.4 min. The quadrupole isolation width was set to 2 Th for $m/z < 700$ and 3 Th for $m/z > 800$.

LC–MS/MS data analysis

MaxQuant (v2.0.20, Max Planck institute of biochemistry, Munich, Germany) using the Andromeda database search algorithm was used to analyze raw MS data [13]. Spectra files were searched against the UniProt filtered and reviewed human protein database using the following parameters: Type: TIMS-DDA LFQ, Variable modifications: Oxidation (M), Acetyl (Protein N-term) and Fixed modifications: Carbamidomethyl (C). Digestion, Trypsin/P, Match between runs: False. FDR was set at 1% for both protein and peptide levels. MS1 match tolerance was set as 20 ppm for the first search and 40 ppm for the main search. Missed cleavages allowed was set to 2. Subsequently the Spectra files were searched against the UniProt SARS-CoV-2 proteome database (Proteome ID: UP000464024) using the same parameters. Data was first normalized with NormalyzerDE using robust linear regression normalization [14]. Perseus (v2.0.5.0, Max Planck institute of biochemistry, Germany) and RStudio (v4.2.0, RStudio, Boston, MA, US) were used for downstream analysis of proteomics data. Proteins denoted as decoy hits, contaminants, only identified by site were removed. Next proteins identified in less than 45% of samples in at least one group were removed. Significant differences in protein intensities between groups were determined with an ANOVA q-value of < 0.05 and post hoc Tukey's test of the log2-transformed LFQ intensities. Differentially expressed proteins were determined using and s0 of 0.1 and FDR of 0.05. For the heatmap LFQ values were normalized with a Z-score and rendered in RStudio using the pheatmap package using euclidean clustering. Protein–protein interaction and Reactome Pathways were analyzed using STRING v11.5 using the stringApp within Cytoscape v3.9.1. Subcellular location determined with CellWhere v.1.1 [15]. Statistical significance was defined as ****$p < 0.0001$, ***$p < 0.001$, **$p < 0.01$, *$p < 0.05$ and NS ($p > 0.05$).

Machine learning classification model

A diagnostic classification model was built using the R CARET package (version 6.0–93). For the machine learning analysis, missing values were first imputed in Perseus with a width of 0.3 and a down shift of 1.3. Independent feature selection was used within Perseus and based on ANOVA scores and least number of missing values. The

top 11 proteins as well as each subject´s PEV count was determined to give the smallest error percentage. The following biomarker panel was selected: ORM1, IGHG1, CAPN1, CASP14, PEV, IGLC6, APOA1, TF, IGKC, EPPK1, SFTPB and IGHA1 and the data subsequently exported into R. The cohort was split randomly in a 60/40 split for training (n = 22) and testing (n = 12) respectively with subjects classified as either positive (COV-POS, n = 12) or negative (COV-NEG and HCO, n = 22). A random forest model was trained on the training set with tenfold cross validation repeated 100 times and using 1000 trees. Receiver operating characteristic (ROC) was used to select the optimal number of randomly drawn candidate variables (mtry) and set at 2. The results of the model are based on application of the model on the test set and reported as accuracy, sensitivity and specificity and area under the ROC curve (AUC-ROC).

Results

Patient demographics

Median age and sex were similar between COV-POS and COV-NEG with median age being lower in HCO. COV-POS patients had a higher incidence of obesity and asthma in comparison to COV-NEG and HCO. Symptomatology were similar between COV-POS and COV-NEG regarding fever, throat pain, stomach pain and myalgia but differed significantly regarding dyspnea with 95% of COV-POS patients reporting it as a symptom. No symptoms were reported in the HCO group. EBP measurements were on average sampled on day 7 post COVID-19 positive test but ranged between 1 and 9 days. A summary of participant information can be found in Table 1.

Analysis of exhaled particle data

EBPs were collected and particles per exhaled volume (PEV) were measured over time, summed, and compared between groups. There was a significant increase in PEV in COV-POS and COV-NEG patients compared to HCO. COV-POS exhaled a median of 11,902 particles (Interquartile range (IQR): 6119–17,893) and COV-NEG a median of 8,159 (IQR: 5406–12,000) compared to a median of 3,622 (IQR: 2506–5790) in the HCO group. Figure 1A demonstrates this large intra-group variation in IQR range in PEV in COV-POS and COV-NEG.

Table 1 Patient characteristics

Characteristics	COV-POS	COV-NEG	HCO
Number of participants	20	16	12
Sex: Male	10 (50%)	8 (50%)	4 (44%)
Age (Median)	56 (IQR: 53–64)	69 (IQR: (53–80)	44 (IQR: 29–46)
Days since symptom debut*	8 (IQR: 3.75–10)	2 (IQR: 1–4.75)	0
Clinical diagnosis			
Infectious etiology			
Viral	20 (100%)	5 (31.3%)	0 (0%)
Bacterial	0 (0%)	4 (25%)	0 (0%)
Unknown	0 (0%)	5 (31,3%)	0 (0%)
Non-infectious respiratory symptoms	0 (0%)	2 (12.5%)	0 (0%)
Comorbidities			
Asthma	1 (5%)	0 (0%)	0 (0%)
COPD	3 (15%)	1 (6.25%)	0 (0%)
Obesity	10 (50%)	4 (25%)	1 (8.3%)
Symptoms			
Coughing	14 (70%)	8 (50%)	0 (0%)
Fever	11 (55%)	6 (38%)	0 (0%)
Throat pain	2 (10%)	3 (19%)	0 (0%)
Stomach pain	4 (20%)	4 (25%)	0 (0%)
Dyspnea	19 (95%)	9 (56%)	0 (0%)
Myalgia	3 (15%)	1 (6%)	0 (0%)
Hospitalized	20 (100%)	7 (44%)	0 (0%)

Characteristics for patients with PCR-verified COVID-19 infection (COV-POS), COVID-19 PCR-negative patients with respiratory symptoms (COV-NEG) and healthy controls (HCO)

IQR Interquartile rang**e**

*Or days since seeking medical care if unknown. Descriptive statistics presented as number of patients and percentage

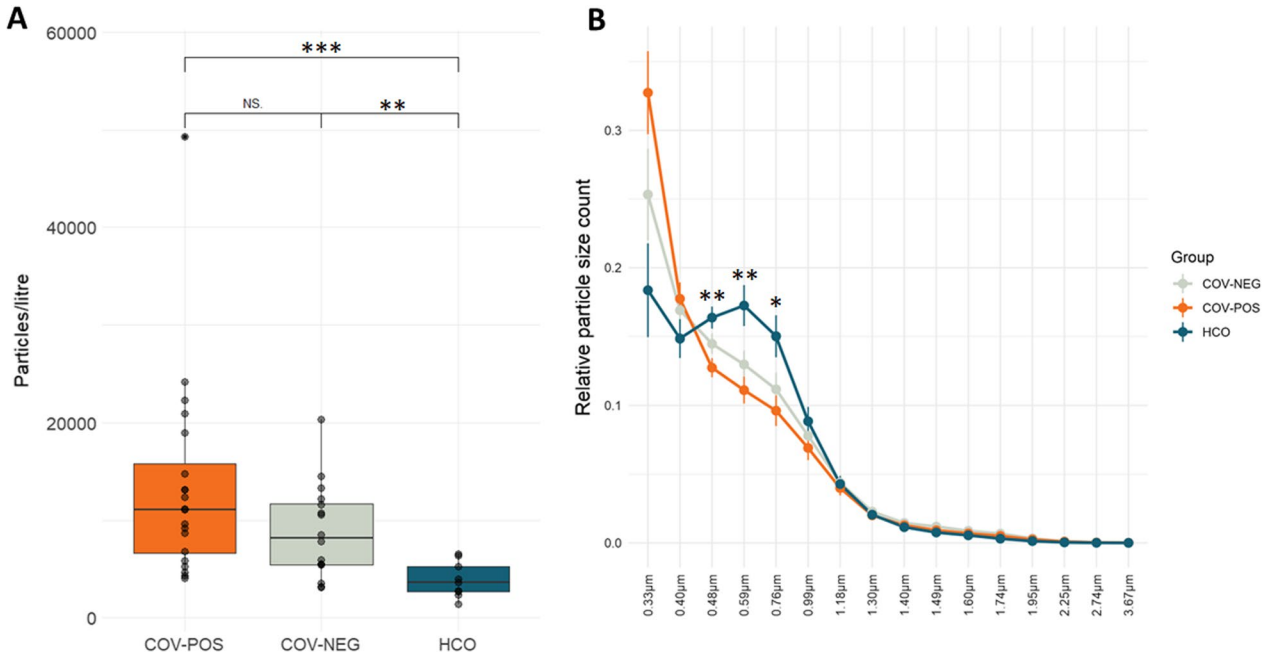

Fig. 1 Exhaled breath particle concentrations and particle size distributions differed significantly between symptomatic and healthy patients. Particles in exhaled air were measured using an optical particle counter. **A** Particles per exhaled volumes (PEV) for patients with PCR-verified COVID-19 infection (COV-POS), patients with respiratory symptoms but with > 2 negative polymerase chain reaction (PCR) tests for COVID-19 (COV-NEG) and healthy controls (HCO) Data shown as individual values (black dots) with lower and upper boundary of boxplots representing 25th and 75th percentile. Statistical significance was tested with Kruskal–Wallis test with Dunn's multiple hypothesis testing correction. **B** Relative particle size counts per particle size bin for COV-POS, COV-NEG and HCO. Data are shown as mean ± standard error of mean. Statistical significance was tested using ANOVA with Tukey's multiple comparisons correction and significance values are shown between COV-POS and HCO. Statistical significance was defined as ****$p < 0.0001$, ***$p < 0.001$, **$p < 0.01$, *$p < 0.05$ and NS ($p > 0.05$)

Furthermore, there was no correlation between PEV and age ($r^2 = 0.06954$) or between sexes in PEV ($p = 0.3254$).

Patients with respiratory symptoms (COV-POS and COV-NEG) skewed towards exhaling smaller particles in comparison to the HCO group. In these patients, particle bin size 1, accounting for particles with a median diameter of 0.33 µm constituted on average 33% of total exhaled particles compared to just 18% for the same particle bin size in HCO. The HCO group presented with a bimodal distribution of relative particle size distribution in comparison with the right skewed distribution in the symptomatic groups. Figure 1B presents particle size distributions between the three groups.

LC–MS/MS based protein identification of exhaled particles

Patient samples with 100 ng or more collected particles were selected for LC–MS/MS protein identification yielding a total of 34 samples for further analysis. 12 samples each from the COV-POS and COV-NEG groups were analyzed and 10 samples from the HCO group. A flow chart summarizing sample exclusion can be seen in Additional file 1: Fig. S1. In total 267 unique proteins could be identified across all three groups after exclusion of potential contaminants. 146 proteins were present in 45% of samples in at least one group, identifying immunoglobulin heavy constant gamma 3 (IGHG33) as the only unique protein found in the COV-POS group, identified in 50% (n = 6) of all samples in the group. Mean number of proteins identified per sample was 110.1 (SD: 15.8). No viral SARS-CoV-2 proteins could reliably be detected in any of the samples.

LC–MS/MS quantitative proteomics of exhaled particles

Subsequently, identified proteins were quantified with label free quantification (LFQ) of exhaled particles. In total 26 proteins were identified as significantly differentially expressed and summarized in Table 2. Significantly differentiated proteins were mainly extracellular proteins, as shown in Fig. 2, but included proteins localized to the cell membrane and intracellular proteins. Reactome pathway analysis revealed differentially expressed proteins related to, among other things, the innate immune system as well as neutrophil and platelet degranulation. Clustering analysis of significantly differentiated proteins among groups revealed three distinct groups, of which 67% (n = 8) of COV-POS patients compromised one cluster as shown in Fig. 3. A second cluster was comprised of three COV-NEG

Table 2 Significantly differentially expressed proteins

Gene names	Protein names	ANOVA	q-value	Mean difference		Andromeda score
				COV-POS	COV-NEG	HCO
IGHG1	Ig gamma-1 chain C region	0.004	4.4	-3.0	-4.4	323
IGKC	Ig kappa chain C region	0.011	3.1	-3.1	2.2	323
ORM1	Alpha-1-acid glycoprotein 1	0.012	2.8	− 2.8	− 2.6	165
SFTPB	Pulmonary surfactant-associated protein B	0.016	− 2.7	− 2.2	2.7	69
TF	Serotransferrin	0.021	2.9	− 2.9	0.0	323
IGHA1	Ig alpha-1 chain C region	0.022	1.3	− 2.9	2.9	323
CASP14	Caspase-14	0.027	− 2.6	2.6	1.5	323
EPPK1	Epiplakin	0.029	2.6	− 1.4	− 2.6	292
CAPN1	Calpain-1 catalytic subunit	0.033	− 2.3	2.3	1.4	61
IGLC6	Ig lambda-6 chain C region	0.034	2.5	− 2.5	1.4	229
APOA1	Apolipoprotein A-I	0.036	2.4	− 2.4	0.0	308
CAT	Catalase	0.036	− 1.4	2.2	− 2.2	323
DSC3	Desmocollin-3	0.037	− 2.2	2.2	− 1.7	270
VCL	Vinculin	0.040	− 1.8	− 1.8	1.8	52
PKP1	Plakophilin-1	0.041	− 2.1	2.1	0.0	323
TGM1	Protein-glutamine gamma-glutamyltransferase K	0.043	− 1.8	1.8	− 1.5	261
PSMA3	Proteasome subunit alpha type-3	0.043	− 2.1	2.1	1.7	88
ZG16B	Zymogen granule protein 16 homolog B	0.043	0.0	− 2.2	2.2	323
ARG1	Arginase-1	0.044	− 2.1	2.1	0.0	323
SERPINA1	Alpha-1-antitrypsin	0.044	2.2	− 2.2	0.0	323
ACTN4	Alpha-actinin-4	0.046	2.0	− 1.3	− 2.0	65
S100A14	Protein S100-A14	0.047	− 1.9	1.9	0.0	227
TXN	Thioredoxin	0.048	− 1.3	− 1.8	1.8	84
PIGR	Polymeric immunoglobulin receptor	0.048	− 1.6	− 1.6	1.6	109
HP	Haptoglobin	0.049	2.0	0.0	− 2.0	188
PLBD1	Phospholipase B-like 1	0.049	− 1.9	1.9	0.0	76

Summary of significantly differentially expressed proteins between PCR-verified COVID-19 infection (COV-POS), COVID-19 PCR-negative patients with respiratory symptoms (COV-NEG) and healthy controls (HCO) and their adjusted p-value (ANOVA q-value) and Andromeda score from the MaxQuant search engine

samples and the last cluster of the remaining samples, including four COV-POS samples. Nine proteins were significantly upregulated in COV-POS patients in comparison to the COV-NEG and HCO groups and are shown in Fig. 4A, B. In comparing COV-NEG to HCO, eight proteins were found to be significantly downregulated as shown in Fig. 4C. The upregulated proteins included three immunoglobulins: Immunoglobin kappa constant (IGKC), Immunoglobulin heavy constant gamma 1 (IGHG1) and immunoglobin lambda constant 3 (IGLC3) as well as Epiplakin (EPPK1), a protein involved in wound healing. Figure 5 presents boxplots of proteins significantly differentially expressed of particular interest in COV-POS patients and include Serotransferrin (TF, F), Apolipoprotein A-I (APOA1, C), Caspase-14 (CASP14, B), Calpain-1 (CAPN1, D), and Alpha-1-acid glycoprotein 1 (ORM1 1, A), a modulator of the immune system during the acute-phase reaction. Pulmonary surfactant-associated protein B (SFTPB, E) was significantly downregulated in COV-POS and COV-NEG patients versus the HCO group.

Machine learning classification of samples

A machine learning (ML) random forest classification model was built using 11 proteins found in all groups and subjects PEV counts. For training, 22 samples were randomly selected, and variables ranked by the ML model according to importance (Fig. 6A). The ROC-AUC for the training data was determined to be 0.97 (CI 0.88–1.06). Next the model was tested on the remaining 12 samples and achieved an accuracy of 0.92 (CI 0.62–0.99), with only one COVID-19 positive sample misclassified as negative, in the testing cohort. The misclassified sample belonged to a 51-year-old female that had tested positive 8-days prior to particle collection and was subsequently discharged from the hospital the following day, possibly affecting the classification. Sensitivity for the model was determined as 75% and specificity as 100%. AUC-ROC in

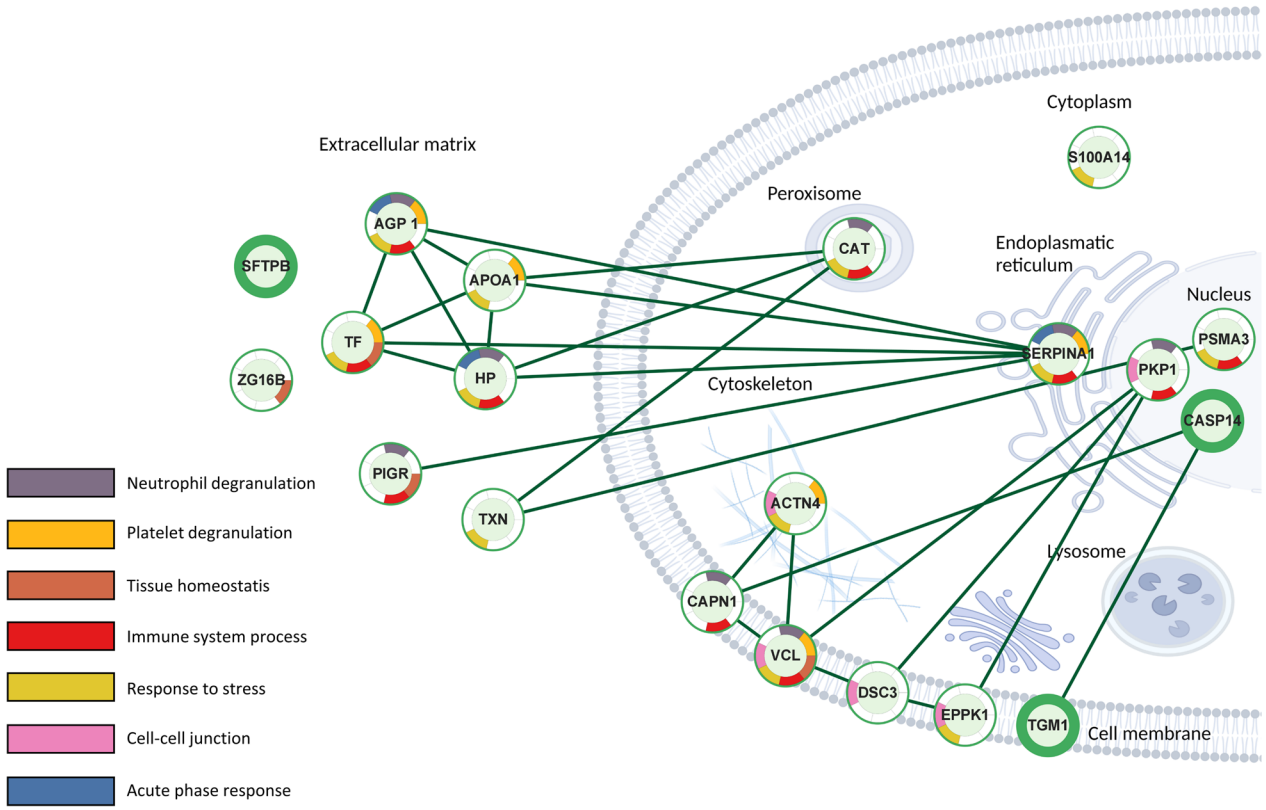

Fig. 2 Schematic of protein–protein interaction network with subcellular location and Reactome Pathways for significantly differentiated proteins. Protein–protein interaction and Reactome Pathways created with STRING v11.5 inside Cytoscape v3.9.1 and subcellular location determined with CellWhere v1.1. Only significantly differentiated proteins found within the STRING database are mapped. Image created with biorender

the training data was 0.97 (CI 0.88–1.06) and AUC-ROC of the test data 0.81 (CI 0.52–1.1).

Discussion

This study presents a novel method for analyzing the proteome of exhaled breath particles for diagnosis and characterization of disease. Sampling of approximately 100 ng of exhaled particles allowed for detection of an average of 110 proteins per sample. This is in stark comparison to the commonly used exhaled breath condensate (EBC) analysis, where the low protein concentrations often require pooling of samples to identify similar numbers of proteins [16, 17]. We achieved a deep proteomic profiling of EBP across the three groups with proteins involved in immune activation, acute phase response, cell adhesion, blood coagulation, and known components of the respiratory tract lining fluid (RTLF), among others. EBP sampling moreover allowed for the analysis of the respiratory tract health status in two-dimensions. Both in terms of the proteome of the exhaled particles as well as the particle concentrations and size distributions, which in turn have previously been implicated in respiratory disease [18].

In accordance with other published work, we identified an increase in particle production in patients with respiratory symptoms [18, 22, 23]. Particle production is thought to depend on the bulk rheological properties of RTLF. Studies have shown that modifications to the viscoelastic properties of RTLF, such as inhalation of isotonic saline, significantly change particle production, possibly explaining the increases in particle production found in our study [24]. COVID-19 patients exhibited a significant increase in particle production with a tendency towards the smaller particles. Similarly, COV-NEG patients, meaning patients with respiratory symptoms, likewise presented with a slightly lower increase in particle concentrations suggestive of a disease-dependent variation in surfactant composition. Thus, EBP collection is a promising new method for monitoring pulmonary health status over the course of an infection and has previously been investigated in other diseases [25, 26].

Proteins in the RTLF originate from various sources, including respiratory epithelial cells, resident inflammatory cells, and plasma proteins that leak from the capillary membrane. Proteins in the RTLF have broad mechanistic roles, including microbial defence, wound healing,

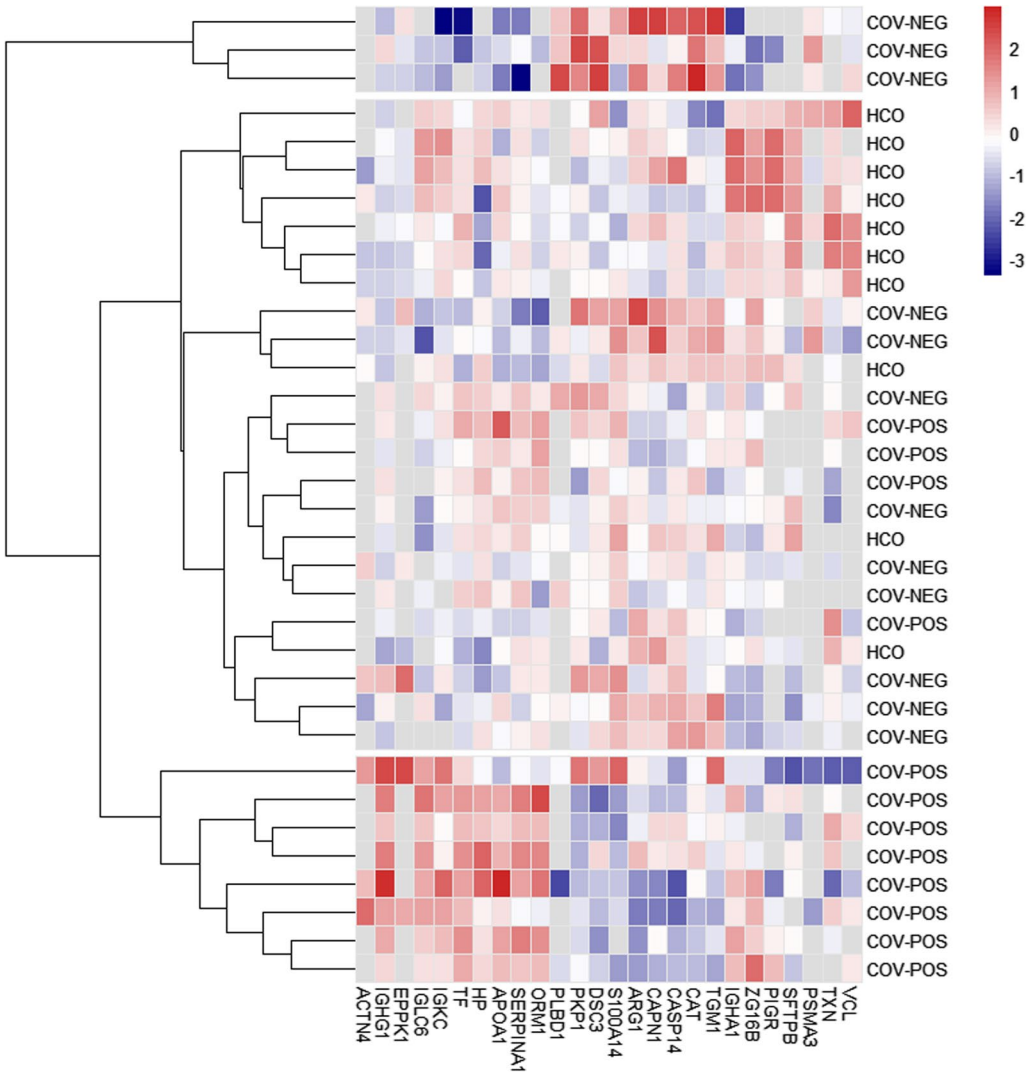

Fig. 3 COVID-19 positive patients exhibited a clustered expression profile of exhaled breath proteins. Protein intensities of the 27 differentially expressed proteins were log10 transformed, normalized with a Z-score and displayed as colors ranging from blue to red with white boxes indicating missing values. Rows are clustered using Euclidean distance and cluster into three distinct expression profiles indicated by gap between rows. Samples are grouped into patients with PCR-verified COVID-19 infection (COV-POS), patients with respiratory symptoms but with > 2 negative polymerase chain reaction (PCR) tests for COVID-19 (COV-NEG) and healthy controls (HCO)

maintaining the viscoelastic properties of the fluid, and nutrient transport, among others. Understanding and being able to monitor the proteomic changes would therefore be an attractive approach for diagnosis and disease monitoring directly from the infection or pathological focus. Proteomic analysis of BALF is one such approach and allows direct sampling of the RTLF, yet it is highly invasive and can only be performed on a limited scale in the clinic and for biomarker research. Previously reported overexpressed proteins in BALF in COVID-19 patients, correspond well to our findings, particularly for the six most abundant proteins in all samples [27]. Of particular interest in biomarker research for infectious diseases are acute phase proteins, which increase in expression in response to inflammation. Three acute phase proteins were significantly overexpressed in EBP in COVID-19 patients compared to COV-NEG and HCO. These proteins were ORM1, alpha 1 antitrypsin, and haptoglobin. Of these three, ORM1 was identified in almost all samples and significantly increased in the COV-POS group compared with both COV-NEG and HCO in EBP. ORM1 is mainly excreted from hepatic cells in response to various stress-related stimuli, but extrahepatic production has been reported, such as from alveolar type

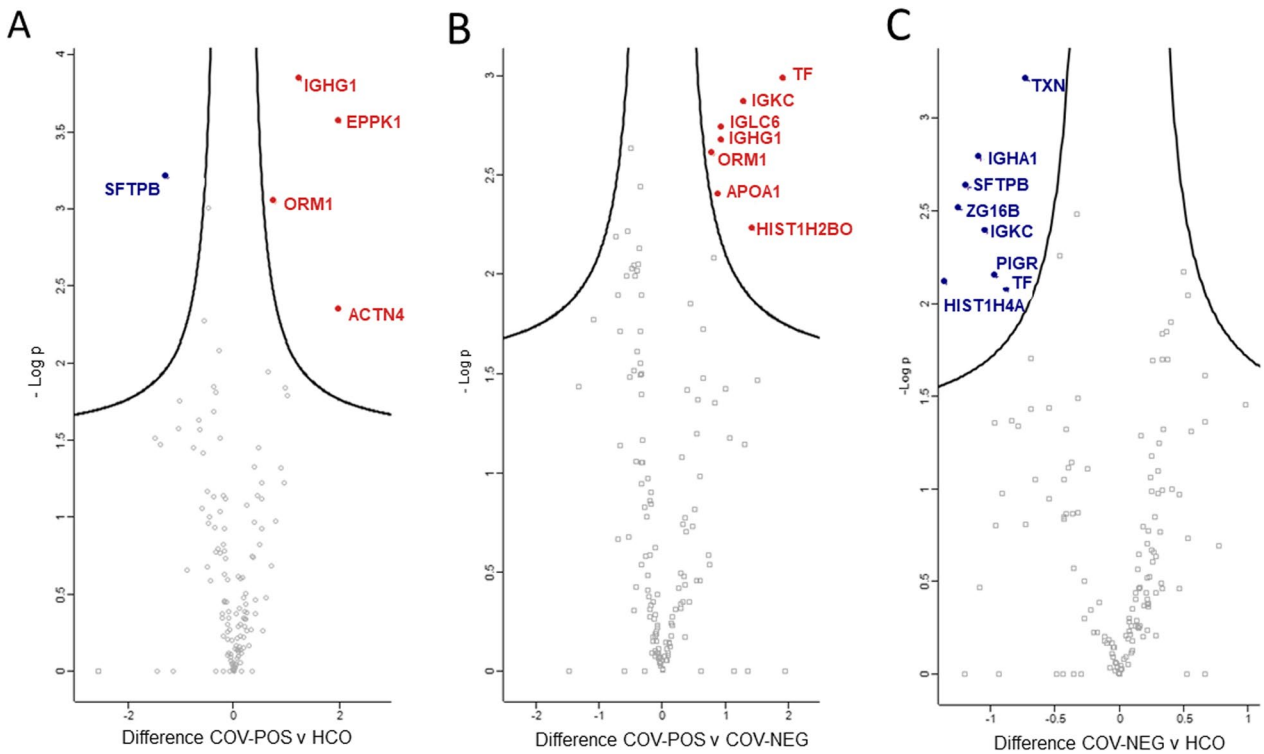

Fig. 4 COVID-19 positive patients showed statistically significant differentially expressed proteins in exhaled breath. X-axis show difference in intensities and y-axis negative log p-value calculated using a student's *t*-test. Significantly differentially expressed upregulated proteins are highlighted in red and downregulated proteins are highlighted in blue. **A** Volcano plot of differentially expressed proteins between PCR-verified COVID-19 infection (COV-POS) and healthy controls (HCO). **B** Volcano plot of differentially expressed proteins between COV-POS and patients with respiratory symptoms but with > 2 negative polymerase chain reaction (PCR) tests for COVID-19 (COV-NEG). **C** Volcano plot of differentially expressed proteins between patients with respiratory symptoms but with > 2 negative polymerase chain reaction (PCR) tests for COVID-19 (COV-NEG) and healthy controls (HCO)

II cells upon lipopolysaccharide (LPS) induction in rats [28]. ORM1 has previously been of interest for pulmonary infections. Hamid et al. found that ORM1 plasma levels were a sensitive and specific biomarker for mortality prediction in children with pneumonia [29]. Plasma proteomic studies in COVID-19 patients, have similarly found increased expression levels, and correlations to disease severity have been reported [27]. Sampling of ORM1 from the RTLF using EPB collection, therefore, presents an opportunity for direct detection of stress-related changes in the lungs, possibly long before such changes can be seen in plasma or detected through physiological changes (see Additional file 2).

Of further interest in biomarker discovery in COVID-19 are stress response proteins. APOA1 is such a marker and was found to be significantly increased between COV-POS and COV-NEG. It has previously been implicated in the inflammatory response and immune regulation, including antioxidative and antiviral properties and is expressed in the lung epithelium [30–33]. Recently published plasma proteomic studies of COVID-19, in contrast, report finding decreased levels of APOA1 [9, 34]. However, in BAL, increases in concentrations have been reported correlating with lymphocyte concentrations or severity of lung injury [35, 36]. APOA1 might therefore be a highly specific diagnostic protein for lung injury with upregulation localized to the RTLF and, together with ORM1 forms a signature of an early response to pulmonary infection. Other stress response proteins include serotransferrin (TF). It is an iron-binding transported glycoprotein mainly synthesized by hepatocytes and, to a certain degree, in lymphocytes [37, 38]. In the human lung, TF is primarily synthesized and excreted by pulmonary epithelial cells and submucosal glands, and alveolar macrophages [39]. TF in BAL have been reported to be present in much higher concentrations in comparison with plasma, making it a particularly interesting protein in EBP research [40]. TF is mainly known for the iron-binding activity. However, new evidence points to its activity within the coagulation cascade, interfering with antithrombin/SERPINC1 and factor XIIa leading to increased coagulation

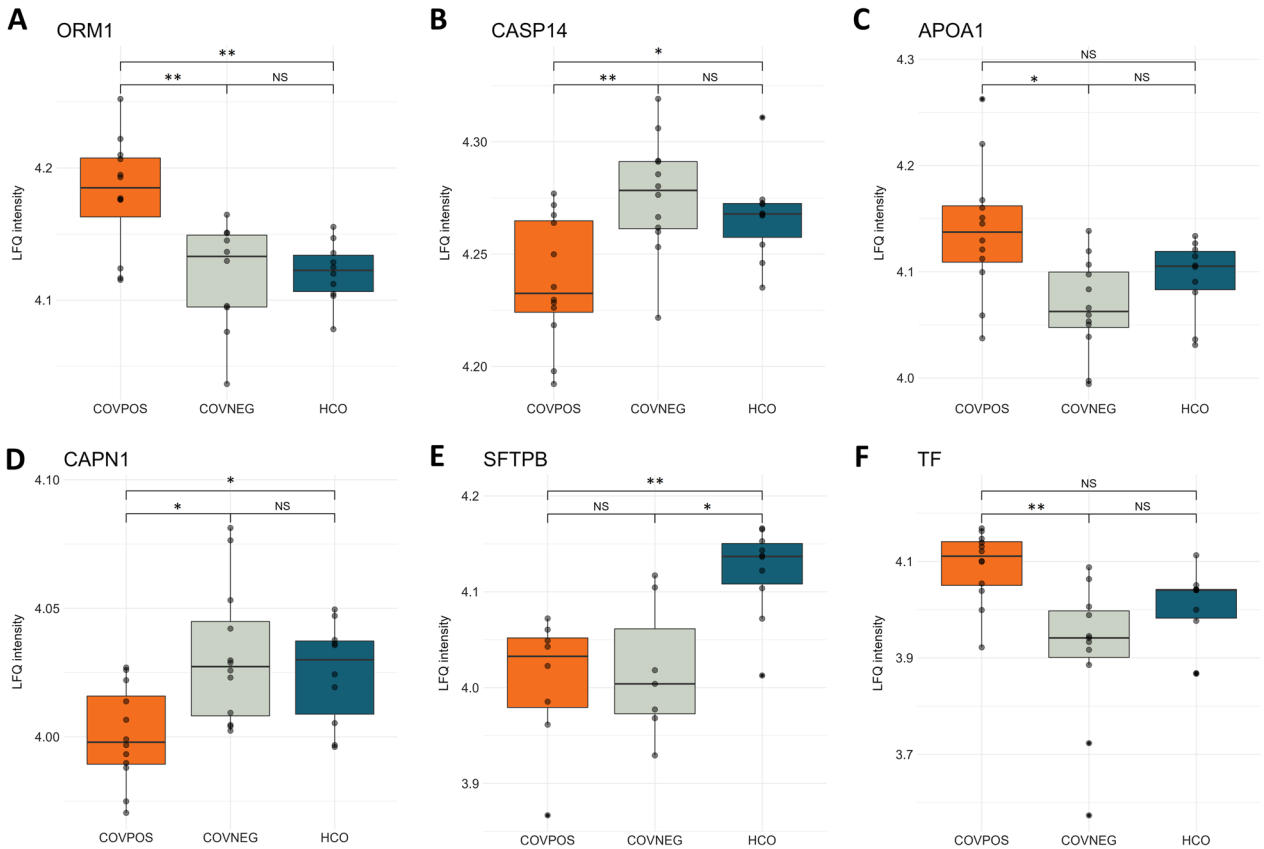

Fig. 5 The six most abundant differentially expressed proteins between groups. Differences in protein expression between PCR-verified COVID-19 infection (COV-POS), patients with respiratory symptoms but with > 2 negative polymerase chain reaction (PCR) tests for COVID-19 (COV-NEG) and healthy controls (HCO). Boxplots of COV-POS (orange), COV-NEG (grey) and HCO (blue) for **A** Alpha-1-acid glycoprotein 1 (ORM1), **B** Caspase-14 (CASP14), **C** Apolipoprotein 1 (APOA1), **D** Calpain 1 (CAPN1), **E** Pulmonary surfactant associated protein B (SFTPB), and **F** Transferrin (TF). Data are presented as individual values (black dots). Line in boxplots represents mean and the lower and upper boundary of boxplots representing 25th and 75th percentile with whiskers below and above boxes representing 10th and 90th percentile, respectively. Statistical significance was tested with ANOVA and Tukey's honest significance test and defined as ****$p < 0.0001$, ***$p < 0.001$, **$p < 0.01$, *$p < 0.05$ and NS ($p > 0.05$)

indicating an increased tendency for procoagulant disorders in COVID-19 patients [41]. Increased levels of TF have been reported in BAL fluid in patients with ARDS and patients at risk of ARDS while simultaneously being downregulated in plasma, presenting it as an exciting biomarker candidate in EBP [42]. Furthermore, TF abundance was discordantly downregulated in COV-NEG patients in comparison to HCO, suggestive of a COVID-19 causative specific increase in EBP.

COVID-19 utilizes ACE2 receptors to access and infect pulmonary surfactant-producing alveolar type II (ATII) cells [43]. Subsequent viral-induced lysis and apoptosis of ATII cells and consequent loss of surfactant in COVID-19 patients are an important part of the pathology and are linked to diffuse alveolar damage, protein leakage and hyaline membrane formation [44]. In accordance, levels of SFTPB were significantly decreased in the EBP of diseased lungs, indicating that EBP collection and analysis could offer a simple and effective way of sampling the health status of the distal parts of the lungs, which has not been possible in the clinic before. Reduction of SFTPB levels in the alveolar space has been shown to precede the clinical development of ARDS and decrease the surface tension, perhaps an important mechanism for increased particle production in these individuals [45, 46]. Surfactant is mainly composed of Dipalmitoylphosphatidylcholine and has previously been studied in EBP, showing decreases in smokers' lungs [47]. Exogenous administrated surfactant has been shown to improve oxygenation in COVID-19 ARDS, and early administration could provide a benefit, showing the potential for EBP collection and analysis in rapidly aiding clinicians in driving therapeutic decisions. [48].

No viral proteins were identified in any of the samples by LC–MS/MS analysis. Previous attempts at detecting viral SARS-CoV-2 proteins using the more sensitive PCR analysis corroborate these results with detection of SARS-CoV-2 in only 3 of 25 samples using

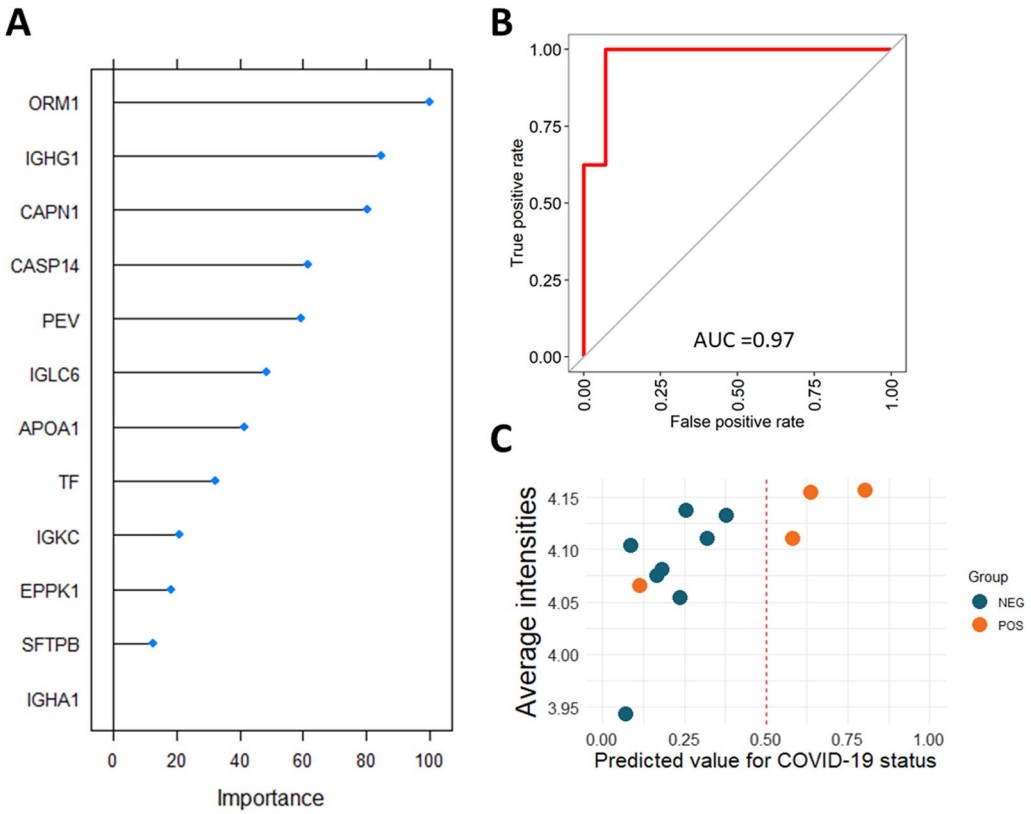

Fig. 6 Random forest machine learning model classification of EBP data to predict COVID-19 disease status. **A** Scaled variable importance for the classification model ranked by mean decrease in accuracy of the model. **B** Receiver operating characteristics of the random forest model in the training cohort. **C** Outcome of the model on the test cohort shown as predicted value for COVID-19 status with 1.0 as certain and < 0.5 as negative for COVID-19. Only one sample was misclassified by the model

the standardize breathing maneuver [19]. Although attempts at identifying SARS-CoV-2 proteins by LC–MS/MS methods have been successful, for example in gargle solution and nasopharyngeal nose swaps, these represent samples from the upper respiratory tract, which may explain the lack of detection in the lower tract sampling method of EBP [20, 21].

In order to examine the diagnostic potential of EBP for lung diseases we composed an integrated proteomic biomarker panel with particle production counts for a machine learning algorithm. The classifier consequentially achieved an overall accuracy of 92% in our test data illustrating the robust potential for future protein and particle production fingerprints in diagnosing pulmonary disease, rapidly and non-invasively with minimal patient discomfort.

While this study shows promising results for the use of EBP it includes a few limitations. Firstly, the study includes a relatively small sample size. Correct sensitivity and specificity values for the machine classifier are therefore difficult to accurately quantify and more differences in EBP expression could be undetected due to low power. Furthermore, days since symptom onset were unmatched between groups, possibly affecting PCR readout accuracy of COVID-19 and proteomic changes in EBP. All patients with negative COVID-19 PCR tests have therefore been reviewed for the presence of a positive COVID-19 tests in the days during the patients entire hospital stay in the days following EBP sampling. Future studies of EBP in COVID-19 and similar diseases will be needed to improve and further evaluate the diagnostical accuracy.

EBP collection allows for the detection of upregulated proteins localized to the lung milieu and enables clinicians to obtain direct insight into disease-related activity at the source. Our data show promising results to stratify protein expression patterns to distinguishing healthy RTLF from diseased. Together with particle production data, a complete picture of RTLF composition and viscoelastic function can be discerned and used to drive clinical decision-making.

Conclusion

Mass-spectrometry-based proteomic analysis of exhaled breath particles enables exciting new possibilities for pulmonary diagnostics and biomarker discovery. Particle production is indicative of pulmonary disease status, and protein composition differs significantly between healthy and infected patients. Potential biomarkers in EBP include extracellular acute-phase proteins, decreases in surfactant-associated proteins, and intracellular proteins. Furthermore, we have shown promising potential for the use of an EBP biomarker panel together with particle concentration for diagnosis of COVID-19 as well as a robust method for protein identification in EBP.

Abbreviations

SARS-CoV-2	Severe acute respiratory syndrome coronavirus 2
ACE2	Angiotensin-converting enzyme 2
CT-scans	Computer tomography scans
BAL	Bronchoalveolar lavage
EBP	Exhaled breath particles
HPLC–MS/MS	High-performance liquid chromatography-mass spectrometry
PEV	Particles per volume
LFQ	Label free quantification
IGKC	Immunoglobin kappa constant
IGHG1	Immunoglobin heavy constant gamma 1
IGLC2	Immunoglobin lambda constant 3
EPPK1	Epiplakin 1
TF	Serotransferrin
APOA1	Apolipoprotein A-1
CASP14	Caspase-14
CAPN1	Calpain-1
ORM1	Alpha-1-acid glycoprotein 1
SFTPB	Pulmonary surfactant associated protein B
ML	Machine learning
RTLF	Respiratory tract lining fluid
ARDS	Acute respiratory distress syndrome

Supplementary Information

The online version contains supplementary material available at https://doi.org/10.1186/s12014-023-09403-2.

Additional file 1: Figure S1. Flow chart of patient inclusion and sample exclusion. In total 48 subjects were recruited and split into three groups based on symptoms and COVID-19 PCR test results. Subsequently 13 samples were excluded due to insufficient particle collection (< 100 ng of sampled material). One sample in the Healthy control group further failed the mass spectrometry analysis due to technical reasons. The remaining samples where then used for training and testing a machine learning classifier.

Additional file 2: Table S1. LC-MS/MS identified proteins with their statistical differences. Summary of all comparisons between PCR-verified COVID-19 infection (COV-POS), PCR-negative patients with respiratory symptoms (COV-NEG) and healthy controls (HCO) and their adjusted p-value (ANOVA q-value) and Andromeda score from the MaxQuant search engine.

Acknowledgements

Support from the Swedish National Infrastructure for Biological Mass Spectrometry is gratefully acknowledged.

Author contributions

GH and EB conducted the EBP sampling with extensive help from CJF. OH and SK developed the MS protocol. GH conducted all analysis and writing of the manuscript. SL, FO and CJF conceptualized, planned the study design, and revised the manuscript. All authors read and approved the final manuscript.

Funding

Open access funding provided by Lund University. Region Skåne, Lund, Sweden.

Availability of data and materials

The datasets supporting the conclusions of this article are available at the ProteomeXchange Consortium via the PRIDE partner repository with the dataset identifier PXD039058.

Declarations

Ethics approval and consent to participate

All patients signed an informed consent form before taking part in the study. The study was approved by the Swedish Ethical Review Authority EPN Dur 2018/129, 2020-018640427.

Consent for publication

Not applicable.

Competing interests

All authors have completed the ICMJE uniform disclosure form at http://www.icmje.org/disclosure-of-interest/ and declare: no support from any organization for the submitted work; no financial relationships with any organizations that might have an interest in the submitted work in the previous three years; no other relationships or activities that could appear to have influenced the submitted work.

Author details

[1]Dept. of Clinical Sciences, Lund University, Lund, Sweden. [2]Wallenberg Center for Molecular Medicine, Lund University, Lund, Sweden. [3]Lund Stem Cell Center, Lund University, Lund, Sweden. [4]BioMS - Swedish National Infrastructure for Biological Mass Spectrometry, Lund University, Lund, Sweden. [5]Department of Infection Control, Region Skåne, Lund, Sweden. [6]Division of Infection Medicine, Department of Clinical Sciences, Lund University, Lund, Sweden. [7]Dept. of Cardiothoracic Surgery and Transplantation, Skåne University Hospital, SE-221 85 Lund, Sweden.

Received: 21 December 2022 Accepted: 13 March 2023
Published online: 27 March 2023

References

1. WHO, Pneumonia of unknown cause—China. WHO. World Health Organization. 2020. http://www.who.int/csr/don/05-january-2020-pneumonia-of-unkown-cause-china/en/. Accessed 10 Nov 2020.
2. Zhu N, Zhang D, Wang W, Li X, Yang B, Song J, et al. A novel coronavirus from patients with pneumonia in China, 2019. N Engl J Med. 2020;382(8):727–33.
3. Yang J, Petitjean SJL, Koehler M, Zhang Q, Dumitru AC, Chen W, et al. Molecular interaction and inhibition of SARS-CoV-2 binding to the ACE2 receptor. Nat Commun. 2020;11(1):4541.
4. Farahani M, Niknam Z, Mohammadi Amirabad L, Amiri-Dashatan N, Koushki M, Nemati M, et al. Molecular pathways involved in COVID-19 and potential pathway-based therapeutic targets. Biomed Pharmacother. 2022;1(145): 112420.
5. Filchakova O, Dossym D, Ilyas A, Kuanysheva T, Abdizhamil A, Bukasov R. Review of COVID-19 testing and diagnostic methods. Talanta. 2022;1(244): 123409.
6. Almstrand AC, Bake B, Ljungström E, Larsson P, Bredberg A, Mirgorodskaya E, et al. Effect of airway opening on production of exhaled particles. J Appl Physiol. 2010;108(3):584–8.

7. Carvalho AS, Matthiesen R. Bronchoalveolar lavage: quantitative mass spectrometry-based proteomics analysis in lung diseases. Methods Mol Biol. 2017;1619:487–94.
8. Wang S, Yao X, Ma S, Ping Y, Fan Y, Sun S, et al. A single-cell transcriptomic landscape of the lungs of patients with COVID-19. Nat Cell Biol. 2021;23(12):1314–28.
9. Shen B, Yi X, Sun Y, Bi X, Du J, Zhang C, et al. Proteomic and metabolomic characterization of COVID-19 patient Sera. Cell. 2020;182(1):59-72.e15.
10. Zeng HL, Chen D, Yan J, Yang Q, Han QQ, Li SS, et al. Proteomic characteristics of bronchoalveolar lavage fluid in critical COVID-19 patients. FEBS J. 2021;288(17):5190–200.
11. Liu JF, Zhou YN, Lu SY, Yang YH, Wu SF, Liu DP, et al. Proteomic and phosphoproteomic profiling of COVID-19-associated lung and liver injury: a report based on rhesus macaques. Signal Transduct Target Ther. 2022;7(1):27.
12. Broberg E, Andreasson J, Fakhro M, Olin AC, Wagner D, Hyllén S, et al. Mechanically ventilated patients exhibit decreased particle flow in exhaled breath as compared to normal breathing patients. ERJ Open Res. 2020;6(1):00198–2019.
13. Tyanova S, Temu T, Cox J. The MaxQuant computational platform for mass spectrometry-based shotgun proteomics. Nat Protoc. 2016;11(12):2301–19.
14. Willforss J, Chawade A, Levander F. NormalyzerDE: online tool for improved normalization of omics expression data and high-sensitivity differential expression analysis. J Proteome Res. 2019;18(2):732–40.
15. Zhu L, Malatras A, Thorley M, Aghoghogbe I, Mer A, Duguez S, et al. Cell Where: graphical display of interaction networks organized on subcellular localizations. Nucleic Acids Res. 2015;43(W1):W571-575.
16. Lacombe M, Marie-Desvergne C, Combes F, Kraut A, Bruley C, Vandenbrouck Y, et al. Proteomic characterization of human exhaled breath condensate. J Breath Res. 2018;12(2): 021001.
17. Muccilli V, Saletti R, Cunsolo V, Ho J, Gili E, Conte E, et al. Protein profile of exhaled breath condensate determined by high resolution mass spectrometry. J Pharm Biomed Anal. 2015;25(105):134–49.
18. Stenlo M, Hyllén S, Silva IAN, Bölükbas DA, Pierre L, Hallgren O, et al. Increased particle flow rate from airways precedes clinical signs of ARDS in a porcine model of LPS-induced acute lung injury. Am J Physiol Lung Cell Mol Physiol. 2020;318(3):L510–7.
19. Viklund E, Kokelj S, Larsson P, Nordén R, Andersson M, Beck O, et al. Severe acute respiratory syndrome coronavirus 2 can be detected in exhaled aerosol sampled during a few minutes of breathing or coughing. Influenza Other Respir Viruses. 2022;16(3):402–10.
20. Ihling C, Tänzler D, Hagemann S, Kehlen A, Hüttelmaier S, Arlt C, et al. Mass spectrometric identification of SARS-CoV-2 proteins from gargle solution samples of COVID-19 patients. J Proteome Res. 2020;19(11):4389–92.
21. Zakharova N, Kozyr A, Ryabokon AM, Indeykina M, Strelnikova P, Bugrova A, et al. Mass spectrometry based proteome profiling of the exhaled breath condensate for lung cancer biomarkers search. Expert Rev Proteomics. 2021;18(8):637–42.
22. Stenlo M, Silva IAN, Hyllén S, Bölükbas DA, Niroomand A, Grins E, et al. Monitoring lung injury with particle flow rate in LPS- and COVID-19-induced ARDS. Physiol Rep. 2021;9(13): e14802.
23. Edwards DA, Ausiello D, Salzman J, Devlin T, Langer R, Beddingfield BJ, et al. Exhaled aerosol increases with COVID-19 infection, age, and obesity. Proc Natl Acad Sci. 2021;118(8): e2021830118.
24. Edwards DA, Man JC, Brand P, Katstra JP, Sommerer K, Stone HA, et al. Inhaling to mitigate exhaled bioaerosols. Proc Natl Acad Sci USA. 2004;101(50):17383–8.
25. Hallgren F, Stenlo M, Niroomand A, Broberg E, Hyllén S, Malmsjö M, et al. Particle flow rate from the airways as fingerprint diagnostics in mechanical ventilation in the intensive care unit: a randomised controlled study. ERJ Open Res. 2021;7(3):00961–2020.
26. Broberg E, Wlosinska M, Algotsson L, Olin AC, Wagner D, Pierre L, et al. A new way of monitoring mechanical ventilation by measurement of particle flow from the airways using Pexa method in vivo and during ex vivo lung perfusion in DCD lung transplantation. Intensive Care Med Exp. 2018;6(1):18.
27. Shu T, Ning W, Wu D, Xu J, Han Q, Huang M, et al. Plasma proteomics identify biomarkers and pathogenesis of COVID-19. Immunity. 2020. https://doi.org/10.1016/j.immuni.2020.10.008.
28. Crestani B, Rolland C, Lardeux B, Fournier T, Bernuau D, Poüs C, et al. Inducible expression of the alpha1-acid glycoprotein by rat and human type II alveolar epithelial cells. J Immunol. 1998;160(9):4596–605.
29. Hamid EA, Ali W, Ahmed H, Megawer A, Osman W. Significance of acute phase reactants as prognostic biomarkers for pneumonia in children. Biomed Pharmacol J. 2021;14(3):1309–21.
30. Gordon SM, Hofmann S, Askew DS, Davidson WS. High density lipoprotein: it's not just about lipid transport anymore. Trends Endocrinol Metab TEM. 2011;22(1):9–15.
31. Georgila K, Vyrla D, Drakos E. Apolipoprotein A-I (ApoA-I), immunity, inflammation and cancer. Cancers. 2019;11(8):E1097.
32. Catapano AL, Pirillo A, Bonacina F, Norata GD. HDL in innate and adaptive immunity. Cardiovasc Res. 2014;103(3):372–83.
33. Lee EH, Lee EJ, Kim HJ, Jang AS, Koh ES, Uh ST, et al. Overexpression of apolipoprotein A1 in the lung abrogates fibrosis in experimental silicosis. PloS ONE. 2013;8(2): e55827.
34. Schmelter F, Föh B, Mallagaray A, Rahmöller J, Ehlers M, Lehrian S, et al. Metabolic and lipidomic markers differentiate COVID-19 from non-hospitalized and other intensive care patients. Front Mol Biosci. 2021;8: 737039.
35. Nukui Y, Miyazaki Y, Suhara K, Okamoto T, Furusawa H, Inase N. Identification of apolipoprotein A-I in BALF as a biomarker of sarcoidosis. Sarcoidosis Vasc Diffuse Lung Dis. 2018;35(1):5–15.
36. Mehrani H, Ghanei M, Aslani J, Golmanesh L. Bronchoalveolar lavage fluid proteomic patterns of sulfur mustard-exposed patients. Proteomics Clin Appl. 2009;3(10):1191–200.
37. Gomme PT, McCann KB, Bertolini J. Transferrin: structure, function and potential therapeutic actions. Drug Discov Today. 2005;10(4):267–73.
38. Lum JB, Infante AJ, Makker DM, Yang F, Bowman BH. Transferrin synthesis by inducer T lymphocytes. J Clin Invest. 1986;77(3):841–9.
39. Yang F, Friedrichs WE, Coalson JJ. Regulation of transferrin gene expression during lung development and injury. Am J Physiol. 1997;273(2 Pt 1):L417-426.
40. Mateos F, Brock JH, Pérez-Arellano JL. Iron metabolism in the lower respiratory tract. Thorax. 1998;53(7):594–600.
41. Tang X, Zhang Z, Fang M, Han Y, Wang G, Wang S, et al. Transferrin plays a central role in coagulation balance by interacting with clotting factors. Cell Res. 2020;30(2):119–32.
42. Krsek-Staples JA, Kew RR, Webster RO. Ceruloplasmin and transferrin levels are altered in serum and bronchoalveolar lavage fluid of patients with the adult respiratory distress syndrome. Am Rev Respir Dis. 1992;145(5):1009–15.
43. Lan J, Ge J, Yu J, Shan S, Zhou H, Fan S, et al. Structure of the SARS-CoV-2 spike receptor-binding domain bound to the ACE2 receptor. Nature. 2020;581(7807):215–20.
44. Xu Z, Shi L, Wang Y, Zhang J, Huang L, Zhang C, et al. Pathological findings of COVID-19 associated with acute respiratory distress syndrome. Lancet Respir Med. 2020;8(4):420–2.
45. Rühl N, Lopez-Rodriguez E, Albert K, Smith BJ, Weaver TE, Ochs M, et al. Surfactant protein B deficiency induced high surface tension: relationship between alveolar micromechanics, alveolar fluid properties and alveolar epithelial cell injury. Int J Mol Sci. 2019;20(17):E4243.
46. Oratis AT, Bush JWM, Stone HA, Bird JC. A new wrinkle on liquid sheets: turning the mechanism of viscous bubble collapse upside down. Science. 2020;369(6504):685–8.
47. Bredberg A, Josefson M, Almstrand AC, Lausmaa J, Sjövall P, Levinsson A, et al. Comparison of exhaled endogenous particles from smokers and non-smokers using multivariate analysis. Respir Int Rev Thorac Dis. 2013;86(2):135–42.
48. Heching M, Lev S, Shitenberg D, Dicker D, Kramer MR. Surfactant for the Treatment of ARDS in a Patient With COVID-19. Chest. 2021;160(1):e9-12.

Publisher's Note

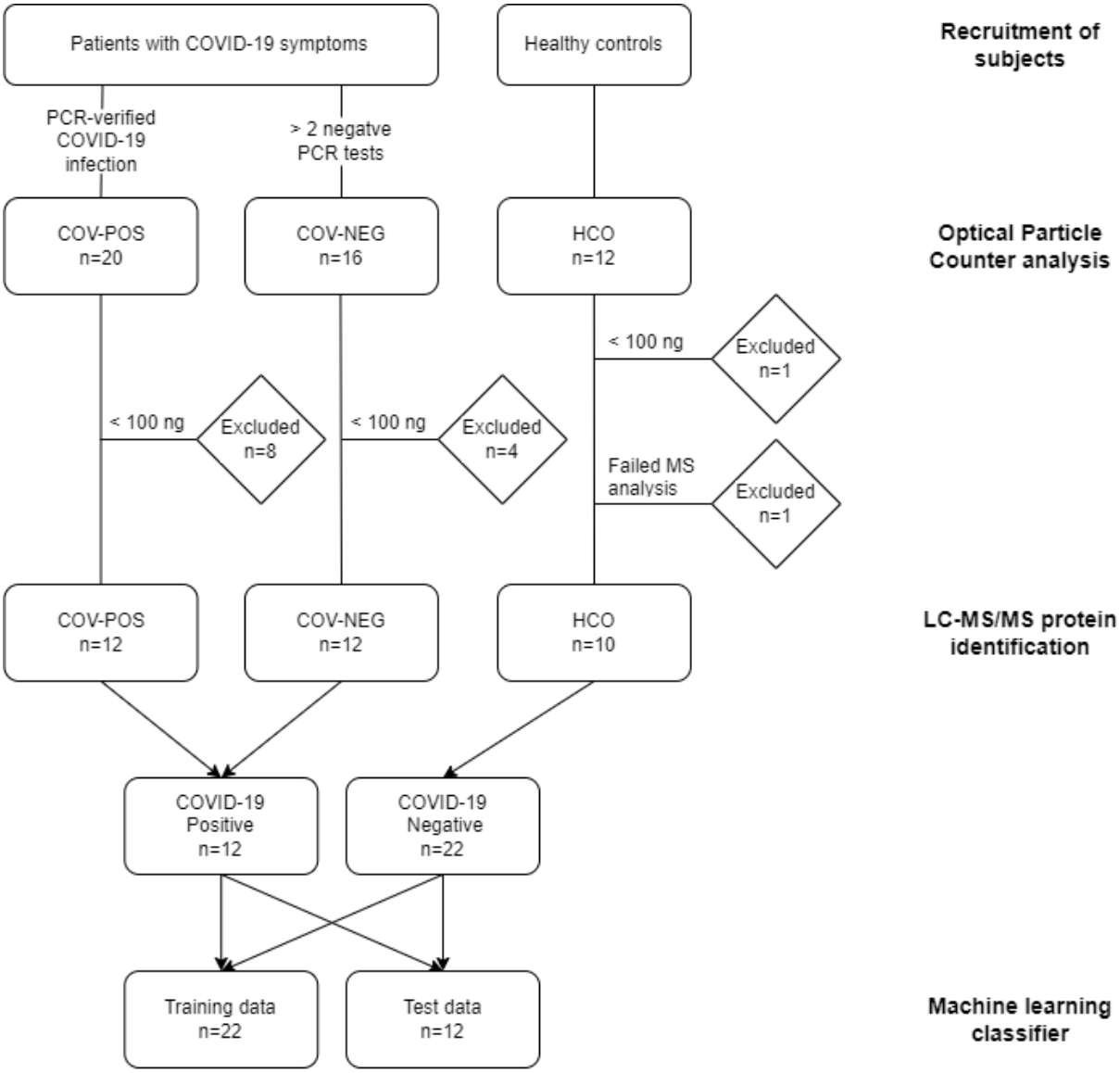

Figure S1. Flow chart of patient inclusion and sample exclusion. In total 48 subjects were recruited and split into three groups based on symptoms and COVID-19 PCR test results. Subsequently 13 samples were excluded due to insufficient particle collection (< 100 ng of sampled material). One sample in the Healthy control group further failed the mass spectrometry analysis due to technical reasons. The remaining samples were then used for training and testing a machine learning classifier.

Supplementary Table 1 – LC-MS/MS identified proteins with their statistical differences.

Summary of all comparisons between PCR-verified COVID-19 infection (COV-POS), PCR-negative patients with respiratory symptoms (COV-NEG) and healthy controls (HCO) and their adjusted p-value (ANOVA q-value) and Andromeda score from the MaxQuant search engine.

Gene names	Protein names	ANOVA q-value	Mean difference			Andromeda Score
A2M	Alpha-2-macroglobulin	0,194	0.0	0.0	0.0	107
A2ML1	Alpha-2-macroglobulin-like protein 1	0,962	0.0	0.0	0.0	323
ACPP	Prostatic acid phosphatase	0,920	0.0	0.0	0.0	50
ACTB	Actin, cytoplasmic 1	0,157	0.0	0.0	0.0	323
ACTC1	Actin, alpha cardiac muscle 1	0,862	0.0	0.0	0.0	42
ACTG1	Actin, cytoplasmic 2	0,448	0.0	0.0	0.0	54
ACTN4	Alpha-actinin-4	0,046	2.0	-1.3	-2.0	65
AHNAK	Neuroblast differentiation-associated protein AHNAK	0,455	0.0	0.0	0.0	37
ALDOA	Fructose-bisphosphate aldolase A	0,864	0.0	0.0	0.0	49
ALOX12B	Arachidonate 12-lipoxygenase, 12R-type	0,125	0.0	0.0	0.0	309
AMY2B	Alpha-amylase 2B	0,685	0.0	0.0	0.0	323
ANXA1	Annexin A1	0,862	0.0	0.0	0.0	323
ANXA2	Annexin A2	0,243	0.0	0.0	0.0	323
APOA1	Apolipoprotein A-I	0,036	2.4	-2.4	0.0	308
ARG1	Arginase-1	0,044	-2.1	2.1	0.0	323
ASAH1	Acid ceramidase	0,061	-1.8	0.0	1.8	65
ASPRV1	Retroviral-like aspartic protease 1	0,097	-1.5	1.5	0.0	292
AZGP1	Zinc-alpha-2-glycoprotein	0,541	0.0	0.0	0.0	323
BLMH	Bleomycin hydrolase	0,071	-1.7	1.7	0.0	201
BPIFA1	BPI fold-containing family A member 1	0,135	0.0	0.0	0.0	323
BPIFB1	BPI fold-containing family B member 1	0,558	0.0	0.0	0.0	206
C3	Complement C3	0,202	0.0	0.0	0.0	95
CALML3	Calmodulin-like protein 3	0,291	0.0	0.0	0.0	77
CALML5	Calmodulin-like protein 5	0,961	0.0	0.0	0.0	323
CAPN1	Calpain-1 catalytic subunit	0,033	-2.3	2.3	1.4	61
CASP14	Caspase-14	0,027	-2.6	2.6	1.5	323
CAT	Catalase	0,036	-1.4	2.2	-2.2	323
CDSN	Corneodesmosin	0,308	0.0	0.0	0.0	60
CFL1	Cofilin-1	0,307	0.0	0.0	0.0	99
CLU	Clusterin	0,810	0.0	0.0	0.0	69
CPA4	Carboxypeptidase A4	0,965	0.0	0.0	0.0	72
CRNN	Cornulin	0,307	0.0	0.0	0.0	55
CSTA	Cystatin-A	0,822	0.0	0.0	0.0	323
CTSD	Cathepsin D	0,995	0.0	0.0	0.0	224
DCD	Dermcidin	0,369	0.0	0.0	0.0	164
DMBT1	Deleted in malignant brain tumors 1 protein	1,000	0.0	0.0	0.0	167
DSC1	Desmocollin-1	0,314	0.0	0.0	0.0	323
DSC3	Desmocollin-3	0,037	-2.2	2.2	-1.7	270
DSG1	Desmoglein-1	0,163	0.0	0.0	0.0	323

DSP	Desmoplakin	0,102	0.0	1.4	-1.4	323
ECM1	Extracellular matrix protein 1	0,452	0.0	0.0	0.0	116
EEF1A1	Elongation factor 1-alpha 1	0,893	0.0	0.0	0.0	50
EEF2	Elongation factor 2	0,750	0.0	0.0	0.0	85
EIF6	Eukaryotic translation initiation factor 6	0,370	0.0	0.0	0.0	41
ENO1	Alpha-enolase	0,997	0.0	0.0	0.0	323
EPPK1	Epiplakin	0,029	2.6	-1.4	-2.6	292
FABP5	Fatty acid-binding protein,. epidermal	0,703	0.0	0.0	0.0	219
FGA	Fibrinogen alpha chain	0,160	0.0	0.0	0.0	126
FGB	Fibrinogen beta chain	0,062	1.4	-1.4	0.0	125
FGG	Fibrinogen gamma chain	0,097	1.4	-1.4	0.0	164
GAPDH	Glyceraldehyde-3-phosphate dehydrogenase	0,064	0.0	1.6	-1.6	323
GGCT	Gamma-glutamylcyclotransferase	0,134	0.0	0.0	0.0	323
GGH	Gamma-glutamyl hydrolase	0,100	-1.4	1.4	0.0	32
GSDMA	Gasdermin-A	0,063	-1.8	1.8	0.0	215
GSTP1	Glutathione S-transferase P	0,822	0.0	0.0	0.0	38
HAL	Histidine ammonia-lyase	0,281	0.0	0.0	0.0	109
HBA1	Hemoglobin subunit alpha	0,961	0.0	0.0	0.0	323
HBB	Hemoglobin subunit beta	0,812	0.0	0.0	0.0	323
HIST1H2AJ	Histone H2A type 1-J	0,484	0.0	0.0	0.0	72
HIST1H2BO	Histone H2B type 1-O	0,066	1.5	-1.5	0.0	132
HIST1H4A	Histone H4	0,063	-1.4	-1.5	1.5	15
HP	Haptoglobin	0,049	2.0	0.0	-2.0	188
HPX	Hemopexin	0,355	0.0	0.0	0.0	84
HSPA1B	Heat shock 70 kDa protein 1B	0,325	0.0	0.0	0.0	22
HSPA5	78 kDa glucose-regulated protein	0,063	-1.8	0.0	1.8	137
HSPB1	Heat shock protein beta-1	1,000	0.0	0.0	0.0	323
IDE	Insulin-degrading enzyme	0,811	0.0	0.0	0.0	29
IGHA1	Ig alpha-1 chain C region	0,022	1.3	-2.9	2.9	323
IGHG1	Ig gamma-1 chain C region	0,004	4.4	-3.0	-4.4	323
IGHG2	Ig gamma-2 chain C region	1,000	0.0	0.0	0.0	165
IGHG3	Ig gamma-3 chain C region	1,000	0.0	0.0	0.0	7
IGJ	Immunoglobulin J chain	0,267	0.0	0.0	0.0	34
IGKC	Ig kappa chain C region	0,011	3.1	-3.1	2.2	323
IGLC6	Ig lambda-6 chain C region	0,034	2.5	-2.5	1.4	229
IL36G	Interleukin-36 gamma	0,361	0.0	0.0	0.0	181
JUP	Junction plakoglobin	0,061	-1.7	1.7	0.0	323
KLK7	Kallikrein-7	0,122	0.0	0.0	0.0	20
KPRP	Keratinocyte proline-rich protein	0,063	-1.6	1.6	0.0	323
LCN1	Lipocalin-1	0,160	0.0	0.0	0.0	65
LDHA	L-lactate dehydrogenase A chain	0,225	0.0	0.0	0.0	64
LGALS7	Galectin-7	0,818	0.0	0.0	0.0	107
LMNA	Prelamin-A/C	0,992	0.0	0.0	0.0	125
LTF	Lactotransferrin	0,072	0.0	-1.7	1.7	323
LYZ	Lysozyme C	0,067	-1.7	0.0	1.7	103

MUC5B	Mucin-5B	0,277	0.0	0.0	0.0	70
MYH9	Myosin-9	0,617	0.0	0.0	0.0	323
NCCRP1	F-box only protein 50	0,813	0.0	0.0	0.0	41
ORM1	Alpha-1-acid glycoprotein 1	0,012	2.8	-2.8	-2.6	165
PEBP1	Phosphatidylethanolamine-binding protein 1	1,000	0.0	0.0	0.0	39
PIGR	Polymeric immunoglobulin receptor	0,048	-1.6	-1.6	1.6	109
PIP	Prolactin-inducible protein	0,610	0.0	0.0	0.0	219
PKM	Pyruvate kinase PKM	0,991	0.0	0.0	0.0	94
PKP1	Plakophilin-1	0,041	-2.1	2.1	0.0	323
PLBD1	Phospholipase B-like 1	0,049	-1.9	1.9	0.0	76
PNP	Purine nucleoside phosphorylase	0,588	0.0	0.0	0.0	159
POF1B	Protein POF1B	0,153	0.0	0.0	0.0	184
PRDX1	Peroxiredoxin-1	0,792	0.0	0.0	0.0	174
PRDX2	Peroxiredoxin-2	0,746	0.0	0.0	0.0	113
PRH1	Salivary acidic proline-rich phosphoprotein 1/2	0,359	0.0	0.0	0.0	133
PSMA2	Proteasome subunit alpha type-2	0,269	0.0	0.0	0.0	109
PSMA3	Proteasome subunit alpha type-3	0,043	-2.1	2.1	1.7	88
PSMA5	Proteasome subunit alpha type-5	0,062	-1.6	1.6	1.3	53
PSMA6	Proteasome subunit alpha type-6	0,717	0.0	0.0	0.0	32
PSMA7	Proteasome subunit alpha type-7	0,118	0.0	-1.3	1.3	64
PSMB1	Proteasome subunit beta type-1	0,925	0.0	0.0	0.0	14
PSMB3	Proteasome subunit beta type-3	0,997	0.0	0.0	0.0	82
PSMB5	Proteasome subunit beta type-5	0,101	-1.4	0.0	1.4	36
RNASE7	Ribonuclease 7	0,814	0.0	0.0	0.0	31
S100A14	Protein S100-A14	0,047	-1.9	1.9	0.0	227
S100A16	Protein S100-A16	0,384	0.0	0.0	0.0	10
S100A7	Protein S100-A7	0,780	0.0	0.0	0.0	323
S100A8	Protein S100-A8	0,722	0.0	0.0	0.0	298
S100A9	Protein S100-A9	0,851	0.0	0.0	0.0	323
SBSN	Suprabasin	0,897	0.0	0.0	0.0	323
SCGB2A1	Mammaglobin-B	0,955	0.0	0.0	0.0	31
SDR9C7	Short-chain dehydrogenase/reductase family 9C member 7	0,848	0.0	0.0	0.0	11
SERPINA1	Alpha-1-antitrypsin	0,044	2.2	-2.2	0.0	323
SERPINA12	Serpin A12	0,096	-1.5	1.5	0.0	173
SERPINA3	Alpha-1-antichymotrypsin	0,625	0.0	0.0	0.0	49
SERPINB12	Serpin B12	0,310	0.0	0.0	0.0	323
SERPINB13	Serpin B13	0,143	0.0	0.0	0.0	115
SERPINB2	Plasminogen activator inhibitor 2	0,875	0.0	0.0	0.0	75
SERPINB3	Serpin B3	0,200	0.0	0.0	0.0	323
SERPINB4	Serpin B4	0,560	0.0	0.0	0.0	281
SERPINB7	Serpin B7	0,312	0.0	0.0	0.0	40
SFTPA1	Pulmonary surfactant-associated protein A1	0,145	0.0	0.0	0.0	323
SFTPB	Pulmonary surfactant-associated protein B	0,016	-2.7	-2.2	2.7	69
TAGAP	T-cell activation Rho GTPase-activating protein	0,436	0.0	0.0	0.0	2

TF	Serotransferrin	0,021	2.9	-2.9	0.0	323
TGM1	Protein-glutamine gamma-glutamyltransferase K	0,043	-1.8	1.8	-1.5	261
TGM3	Protein-glutamine gamma-glutamyltransferase E	0,821	0.0	0.0	0.0	323
TGM5	Protein-glutamine gamma-glutamyltransferase 5	0,864	0.0	0.0	0.0	310
TKT	Transketolase	0,140	0.0	0.0	0.0	142
TOLLIP	Toll-interacting protein	1,000	0.0	0.0	0.0	11
TPI1	Triosephosphate isomerase	0,239	0.0	0.0	0.0	36
TPM3	Tropomyosin alpha-3 chain	0,998	0.0	0.0	0.0	39
TPP1	Tripeptidyl-peptidase 1	0,996	0.0	0.0	0.0	102
TTR	Transthyretin	0,291	0.0	0.0	0.0	245
TUBA1C	Tubulin alpha-1C chain	0,856	0.0	0.0	0.0	62
TUBB2B	Tubulin beta-2B chain	1,000	0.0	0.0	0.0	105
TXN	Thioredoxin	0,048	-1.3	-1.8	1.8	84
UBA52	Ubiquitin-60S ribosomal protein L40	0,065	-1.8	1.8	0.0	323
VCL	Vinculin	0,040	-1.8	-1.8	1.8	52
YOD1	Ubiquitin thioesterase OTU1	0,448	0.0	0.0	0.0	35
YWHAZ	14-3-3 protein zeta/delta	0,956	0.0	0.0	0.0	141
ZG16B	Zymogen granule protein 16 homolog B	0,043	0.0	-2.2	2.2	323